Division of Pharmaceutical Sciences
Strathclyde Institute of Pharmacy and Biomedical Sciences
University of Strathclyde, Glasgow

INVESTIGATION INTO THE USE OF SYNTHETIC MEMBRANES FOR DRUG DIFFUSION IN FRANZ CELLS

Ng Shiow Fern

A thesis presented in fulfilment of the requirements for the degree of

Doctor of Philosophy

April 2007

Declaration of Author's Rights

'The copyright of this thesis belongs to the author under the terms of the United Kingdom Copyright Acts as qualified by University of Strathclyde Regulation 3.51. Due acknowledgement must always be made of the use of any material contained in, or derived from, this thesis.'

Dedication

To my late sister, Ng Wei Fern

Acknowledgements

Firstly, I would like to express my deepest gratitude to Professor Gillian M. Eccleston for supervising my very first undertaking in research. It was truly an invaluable experience working with Prof. Eccleston. She not only taught me ways to become an effective researcher, but also bring out the best potential in me. I would also like to make a special note to Dr. Jennifer J. Rouse, who always stands alongside and made an effort to understand the difficulties I faced, especially in the practical work. I truly appreciate all her time and assistance.

I want to express my appreciation Dr. F. Dominic Sanderson from GlaxoSmithKline, for being my industrial supervisor and his enormous help especially during my one-month industrial attachment in Harlow. I also thank him for sharing his knowledge, and teaching me that 'perseverance' is the key for becoming a successful scientist.

I also thank the University of Strathclyde and GlaxoSmithKline for funding this project, and also sponsoring my trips to various conferences during the course of study.

Next, I would like to thank to all my colleagues who work in SIBS 212, 215/217, 218 for creating a friendly working environment, as well as to the technical staff of the Department of Pharmaceutical Sciences for all their laboratory assistance.

Finally, my special appreciation to my family: my parents, Ng Kuek New and Lai Yoon Ying; my brother, Kevin Ng Wei Loong and sister-in-law Cindy Lim, for their love and always understands the demands placed upon me by my work. And last but not least, Dr. Siow Lee Roy, Uncle and Auntie Siow, who never stop believing in me.

Table of Contents

CHAPTER II Materials and Methods

CHAPTER III Validation of Franz diffusion cells experiment

Abstract

Franz diffusion cells employ synthetic membranes because of membrane simplicity and supposed good reproducibility. For topical product assessment, the synthetic membrane should provide no diffusional resistance to drug diffusion. However, different synthetic membranes do show rate-limiting effects. The aims of this study were to validate and minimise errors that occur in Franz cell experiments, to examine the effect of different types of synthetic membrane on drug diffusion and to test the suitability of Franz cell experiments for drug release from a freeze-dried sodium alginate wafer and a sodium alginate gel.

Franz cell experimental variables were validated using physical and visual tests, a plasticiser assay and incorporation of tonicity agents. The drug flux from a commercial gel was compared before and after validation. Thirteen types of synthetic membranes were screened using ibuprofen saturated solution. The impact of drug log P on flux was evaluated using ibuprofen (hydrophobic drug), riboflavin (hydrophilic drug) and four parabens of increasing hydrophobicity. The physical characteristics of sodium alginate gel and its lyophilised wafer were characterised by rheology, thermal analysis, microscopy and their drug release profiles compared.

The coefficient of variation (CV) for drug flux was reduced from 26% to 4% (n=6) after validation of the Franz cells. The membranes were grouped into two categories, high-flux (8 – 18 mg/cm^2/h) and low-flux (0.1 – 3 mg/cm^2/h) depending on ibuprofen flux. The riboflavin and paraben drug fluxes showed similar membrane groupings to ibuprofen. However butylparaben showed a possible drug-membrane interaction. Rheology, thermal and microscopic data showed that sodium alginate formed stable gels in ibuprofen saturated solution (pH 7.2). Using the validated Franz cells, the ibuprofen flux from sodium alginate gel and wafer were 2.55 mg/cm^2/h and 1.54 mg/cm^2/h respectively.

This study demonstrated that the validation of Franz cells is mandatory to ensure that drug release results are solely due to the properties of the membrane and the formulation. The high flux membranes were mainly synthetic microfiltration membranes, while the low flux membranes were mostly semi-synthetic (cellulose-based) membranes. The membrane choice for quality control should be selected from the high-flux group because these membranes offer the least drug diffusional resistance. The tight CV of flux obtained demonstrated that Franz cell is a robust method for wafer and gel drug release measurement. The slower release of drug from sodium alginate wafers suggests that wafers have potential for a controlled release dressing for wound healing.

CHAPTER I

GENERAL INTRODUCTION

1.1 Skin as a route for drug delivery

Over the years, the skin has been explored as a useful route for drug delivery as it offers easy access and a painless route for drug application. This in turn leads to increased patient compliance for both local and systemic action. Dermatological formulations have been developed to carry active substances into and across the skin for their therapeutic effect. Conventional topical semisolid formulations such as creams, ointments and gels are widely used for local delivery, whereas novel vehicles such as transdermal patches have been successfully developed as a time-controlled release vehicle for skin delivery.

Drug permeation across the stratum corneum depends upon the interaction between the skin, the drug and the components in the formulation vehicle. Several *in vitro* methods have been developed for the evaluation of drug permeation with excised skin. The use of Franz-type diffusion cells [Franz, 1975] is one of the most popular *in vitro* models for the study of percutaneous absorption. This method is popular due to its simplicity, cost effectiveness, and the fact that the experimental conditions can be easily controlled by the investigator according to the purpose of investigation. Apart from skin, the Franz diffusion cell is used with synthetic membranes, either for skin simulation or as a topical product quality control tool, mainly because synthetic membranes, unlike skin, do not provide biological variations and are inert. Although both applications utilise synthetic membranes, the criteria for membrane selection are vastly different. The synthetic membrane for skin mimicry is usually hydrophobic and rate-limiting to mirror the stratum corneum; in contrast, the synthetic membrane for quality control must not provide diffusional resistance to drug diffusion, and should only act as a support to separate the drug dosage form from the dissolution medium.

The significance of Franz diffusion studies and synthetic membranes in skin simulation and quality control studies involves an understanding of the fundamentals of skin and synthetic membranes. This chapter explores skin properties, the transport mechanisms across natural and artificial membranes, diffusion cells characteristics and synthetic membranes in general, as well as in relation to Franz diffusion cell studies.

1.1.1 Human skin – the ultimate biological shield

The skin is the largest organ in the body, occupied 10% of body mass with a large surface area, covering ~2 m^2 for an average person. The skin effectively protects the body from ultraviolet radiation, chemicals, micro-organisms and free radicals. The water resistant outermost layer (the stratum corneum) prevents dehydration and maintains the electrolyte level in the body. It serves as a mechanical as well as chemical barrier for the protection of our body from external environment. The structure of skin is shown in Figure 1.1.

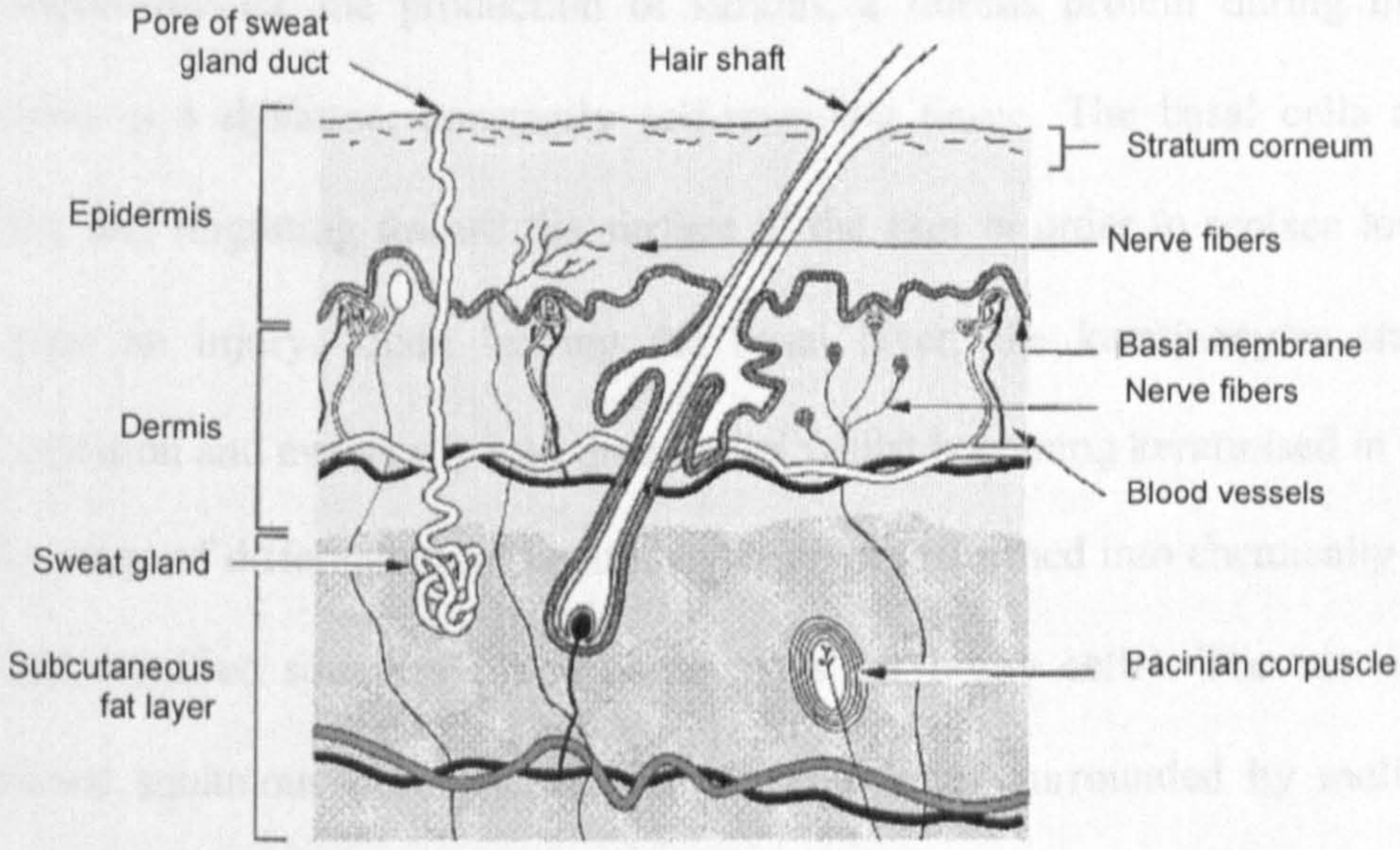

Figure 1.1: A sketch of a cross section of the skin [adapted from The Pharmaceutical Codex, 1994].

The skin is essentially divided into three major layers: the epidermis, the dermis and the subcutaneous fat. The subcutaneous fat layer, sometimes referred to as the hypodermis,

contains adipose fat tissues and connective tissue which attaches the skin to underlying bone. Immediately adjacent to the subcutaneous fat is the dermis. The dermis consists of a superficial papillary layer and a deeper reticular layer. The superficial papillary layer forms ripple-like ridges extended into the epidermis and this layer contains loose connective tissue with rich capillaries and nerves supplying the surface of the skin where as the deeper reticular layer has dense connective tissues which provide support and attachment for the dermis. The hair follicles are situated here with the erector pili muscle that attaches to each follicle. Sebaceous (oil) glands and apocrine (scent) glands are associated with the follicle. This layer also contains eccrine (sweat) glands, but they are not associated with hair follicles.

The epidermis is the outermost layer of skin, separated from the dermis by a basement membrane. It contains no blood vessels but is nourished by nutrients that diffuse from capillaries of the papillary layer. Most of the cells in the epidermis are keratinocytes, which are responsible for the production of keratin, a fibrous protein during maturation. The epidermis is a dynamic, constantly self-renewing tissue. The basal cells are continually dividing and migrating toward the surface of the skin in order to replace lost surface cells e.g. after an injury. Upon leaving the basal layer, the keratinocytes start to undergo differentiation and eventually loss their nuclei whilst becoming keratinised in the process. At the last stage of differentiation, keratinocytes are transformed into chemically and physically resistant cornified squames called corneocytes (or horny cells). The corneocytes are flat anucleated squamous cells packed with keratin fibres surrounded by multilamellar lipid bilayers. When the differentiation process is completed, the phospholipids are degraded enzymatically and transformed into ceramides, which formed a flat horny layer called the stratum corneum. The transition from basal to horny cells is illustrated in a schematic diagram in Figure 1.2. It takes approximately 14 days for a basal cell to differentiate into a

stratum corneum horny cell, and the stratum corneum cells are typically retained for a further of 14 days prior to shedding.

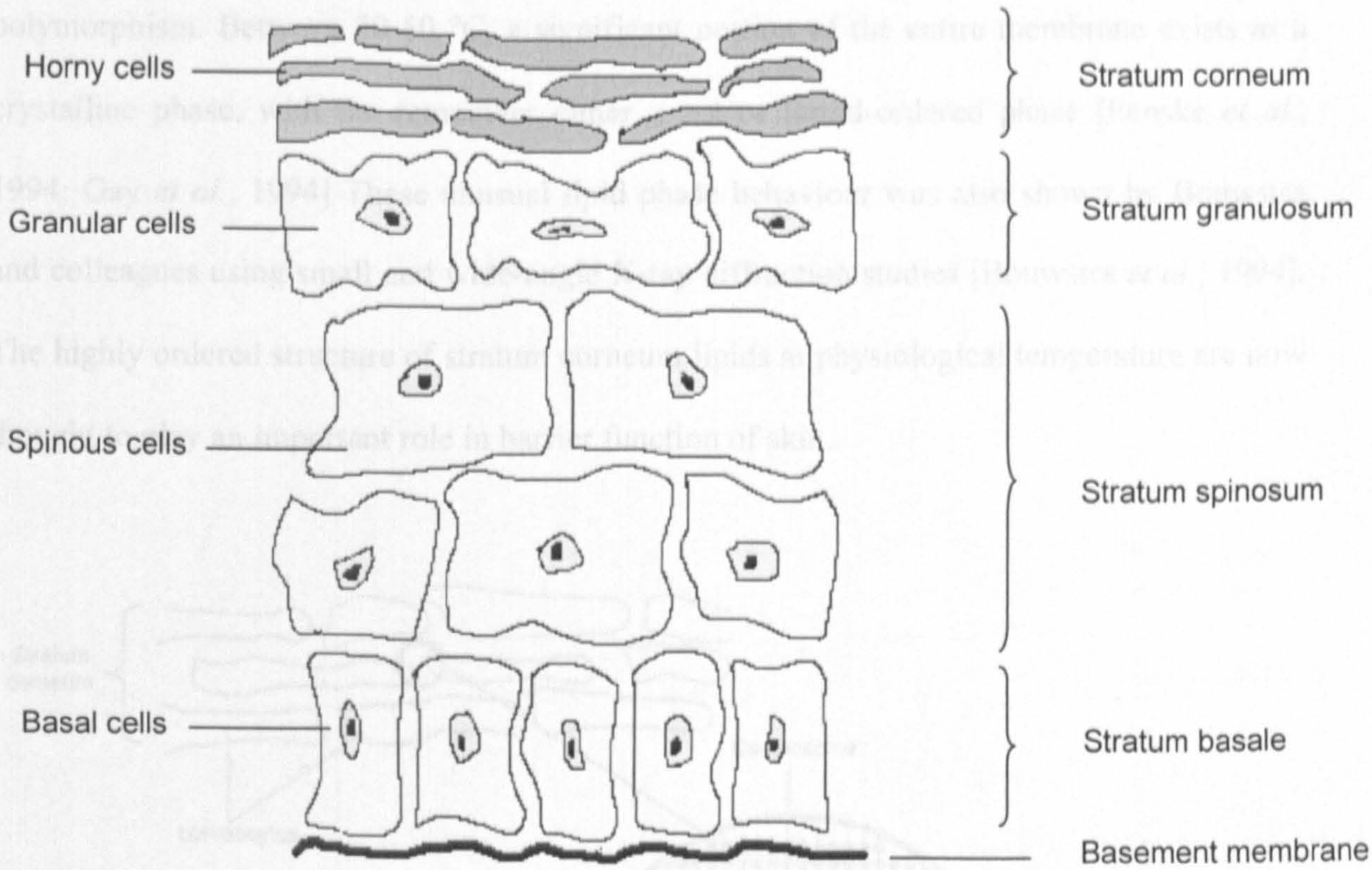

Figure 1.2: Schematic diagram of skin regeneration [adapted from Williams, 2003b].

1.1.2 The barrier - stratum corneum

Only a limited number of materials can pass through the stratum corneum. With a thickness of less than 20μm, the stratum corneum effectively protects our body from desiccation. The properties of the stratum corneum are primarily due to the unique and well-organised structure arrangements of the lipid matrix and the lipid envelop surrounding the cells. About 90% of the cells in stratum corneum are corneocytes entirely surrounded by crystalline lamellar lipid regions. The cell boundary is a very densely crosslinked protein structure, which reduces absorption of drugs into the cells. The intercellular lipids are formed, in part, by small ovoid vesicles located in the cells of the stratum granulosum layer: the lamellar bodies [Swartzendruber *et al.*, 1989]. The lipids form bilayers around the corneocytes,

creating a 'brick-and-mortar' model (Figure 1.3) with the corneocytes as the bricks and the intercellular lipids providing the mortar [Elias, 1983]. Fourier transform infrared (FTIR) spectroscopy and deuterium NMR studies show that lipid mixtures exhibited a complex polymorphism. Between 20-50 °C, a significant portion of the entire membrane exists as a crystalline phase, with the remainder either a gel or liquid-ordered phase [Fenske *et al.*, 1994; Gay *et al.*, 1994] These unusual lipid phase behaviour was also shown by Bouwstra and colleagues using small and wide-angle X-ray diffraction studies [Bouwstra *et al.*, 1994]. The highly ordered structure of stratum corneum lipids at physiological temperature are now thought to play an important role in barrier function of skin.

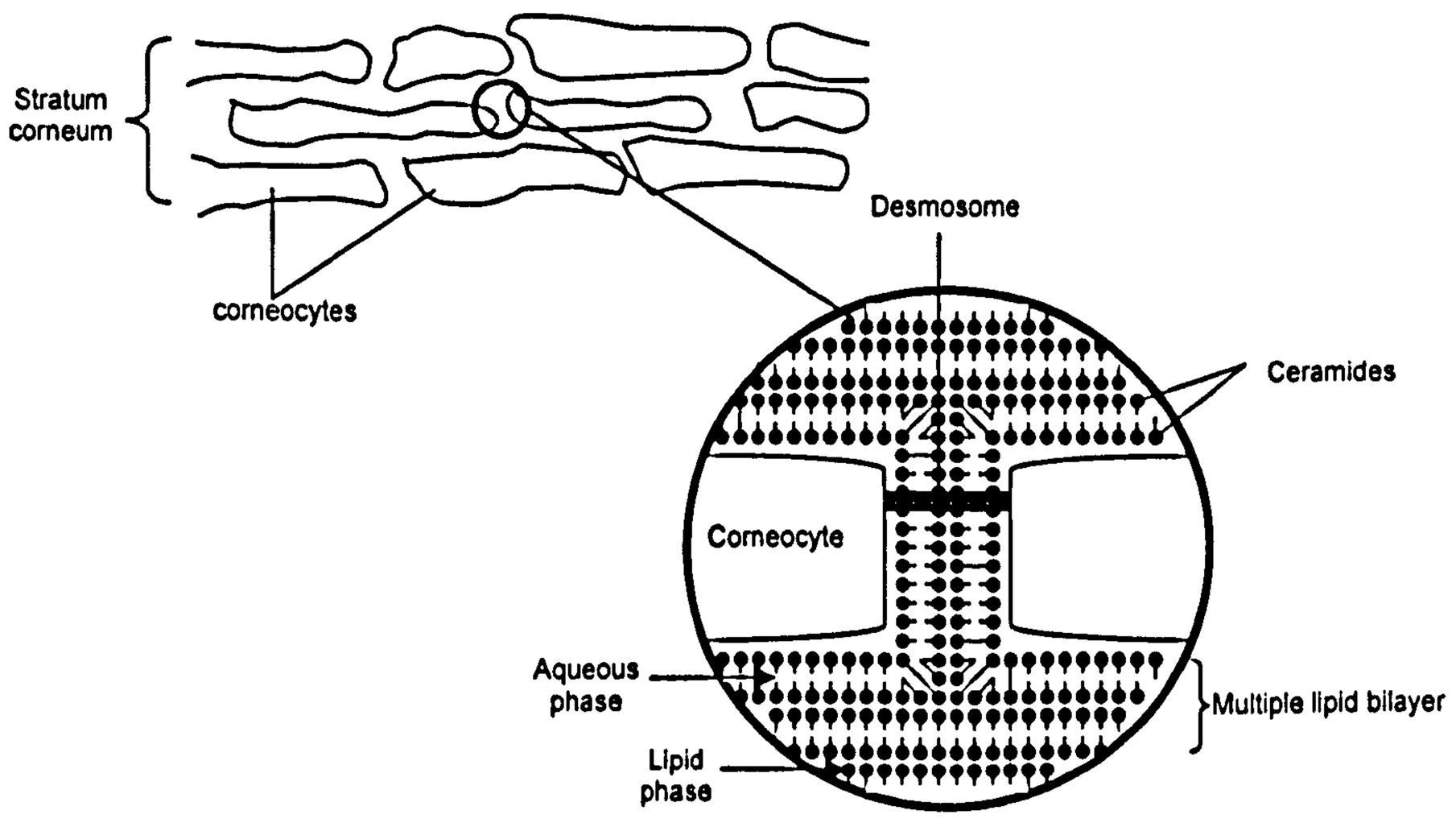

Figure 1.3: A schematic of the 'brick-and-mortar' model of human stratum corneum [adapted from Williams, 2003b].

As far as the drug delivery is concerned, the stratum corneum is the rate-limiting layer which restricts the ingress of topically applied agents.

1.1.3 Routes and mechanism of skin permeation

The percutaeneous absorption of a drug involves diffusion through the stratum corneum and the viable cell layers of epidermis, finally through the upper layers of dermis into the systemic circulation. This is a passive process which does not require input of energy [Scheuplein, 1978]. There are a number of possible ways in which molecule can cross stratum corneum, including intercellular, intracellular and appendageal (through either the eccrine (sweat) glands or hair follicles) [Scheuplein and Blank, 1971], illustrated in Figure 1.4.

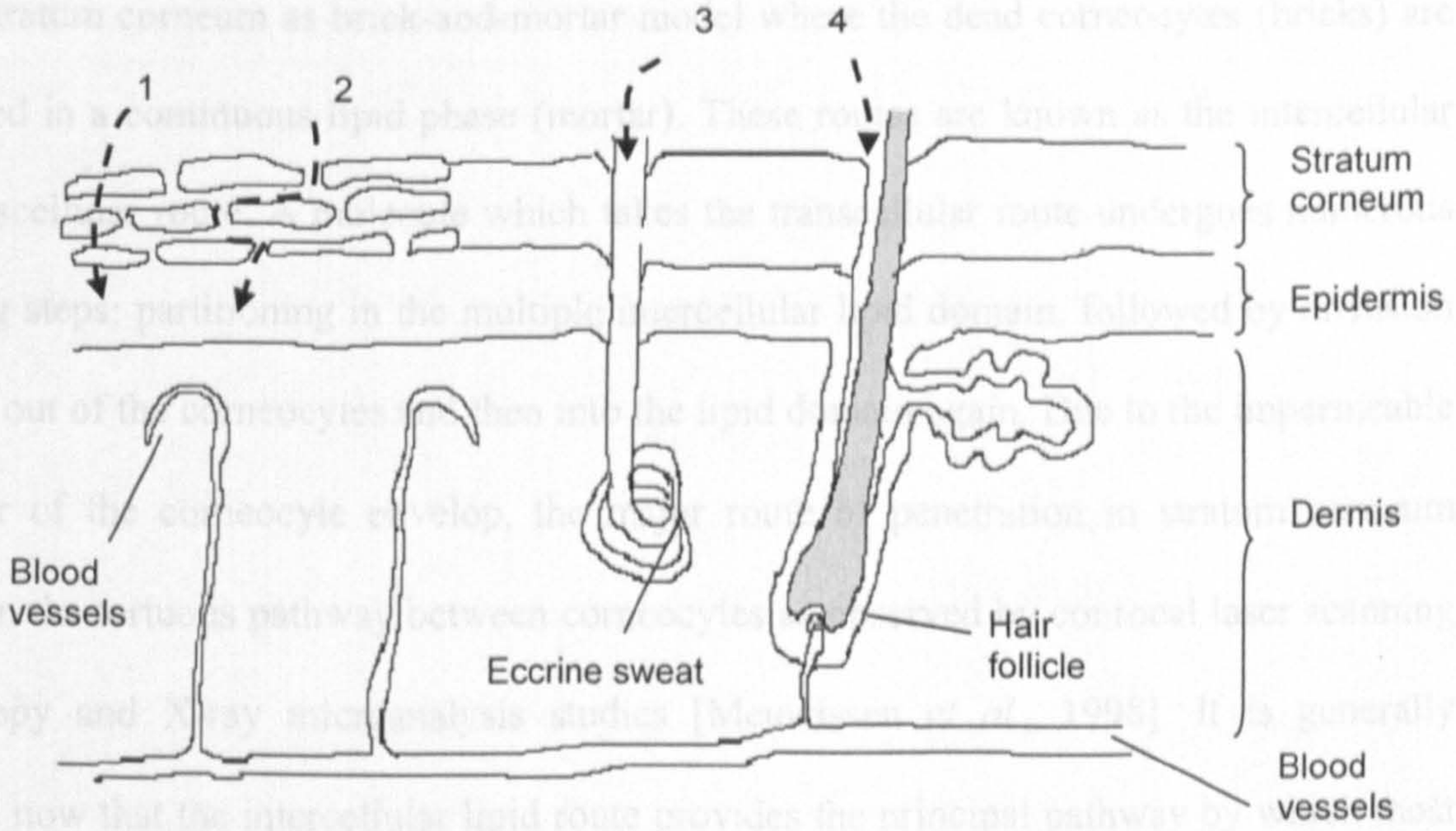

Figure 1.4: A schematic presentation of the skin showing the different possible routes of penetration. 1. Intracellular route; 2. intercellular route; and shunt routes via 3. sweat glands and 4. hair follicles. [adapted from Hadgraft, 2001]

The skin is pierced by a variety of appendages (route 3 and 4 in Figure 1.4) which offer a direct route of penetration by bypassing the stratum corneum. Skin appendages are not thought to be the very important route owing to the relatively small total surface area (0.1% for follicular and 0.001% for eccrine) [Scheuplein, 1967]. But much research had been done to show the importance of this pathway for ions and large polar molecules that transport to

cross intact stratum corneum [Illel *et al.*, 1991; Kao *et al.*, 1988; Tregear, 1966]. Recently, a novel 'skin sandwich system' was shown to be a useful model for the investigation of follicular penetration in vitro [Barry, 2002]. Frum and co-workers tested a series of drugs varying in lipophilicity (log P) of similar molecular weight on this model and they reported that lipophilic drugs may participate in transfollicular route but only up to a critical log P value did the follicular route was shown to be apparent [Frum *et al.*, 2007].

The interpretation of the two other routes (route 1 and 2 in Figure 1.4) of penetration is based on the stratum corneum as brick-and-mortar model where the dead corneocytes (bricks) are embedded in a continuous lipid phase (mortar). These routes are known as the intercellular and transcellular route. A molecule which takes the transcellular route undergoes numerous repeating steps: partitioning in the multiple intercellular lipid domain, followed by diffusion into and out of the corneocytes and then into the lipid domain again. Due to the impermeable character of the corneocyte envelop, the major route of penetration in stratum corneum resides in the tortuous pathway between corneocytes as observed by confocal laser scanning microscopy and X-ray microanalysis studies [Meuwissen *et al.*, 1998]. It is generally accepted now that the intercellular lipid route provides the principal pathway by which most small, uncharged molecules traverse stratum corneum. And the composition and organisation of the lipids (ceramides) plays an important role in determining the rate of permeation [Grubauer *et al.*, 1989].

1.1.4 Topical formulations

Drug delivery to or through the skin is aimed at targeting the drug to three anatomical sites, namely (1) the skin itself (local delivery), (2) the deeper tissues such as joints or musculature (regional delivery), and (3) the blood circulation (systemic delivery). For drug delivery, the drugs are prepared in carriers or vehicles before being applied to the skin. Conventional

dermatological vehicles ranging from powders through semisolids and liquids have been employed as topical drug carriers for decades. Of the various dosage forms, semisolids such as creams, ointments and gels are the most common. Semisolids are dispersions that have two immiscible phases where one phase (the dispersed phase) is dispersed as particles throughout another phase (continuous medium). The common topical dispersion system preparations are shown in Table 1.1, with their respective dispersed and continuous phase.

Table 1.1: Examples of common pharmaceutical topical dispersion systems

Dispersion type	Dispersed phase	Continuous phase	Examples
Emulsion (oil-in-water, water-in oil)	Liquid	Liquid	Aqueous cream BP, Calamine lotion
Suspension	Solid	Liquid	Ophthalmic suspension e.g. betaxolol eye drops.
Paste	Solid	Semisolid	Zinc and salicylic paste, coal tar paste
Spray/aeroaol	Gas	Liquid	Beclomethasone nasal spray
Gel	Solid	Liquid	Carbomer, hypromellose eye gels

Usually topical preparations are prepared in terms of storage stability, compatibility with drugs and excipients, and patient acceptability. The problems in formulating disperse system are mostly associated with instability due to their non-equilibrium state. This is because the dispersion is a thermodynamically unfavourable system. The product will tend to revert back into its original state, i.e. phase separation occurs due to the immiscibility of the two phases. These dispersions are called 'lyophobic', or 'solvent hating' dispersions. Formulators therefore must seek the necessary energy barriers to delay the thermodynamically driven changes during the shelf life of the product.

One typical example of a topical lyophobic dispersion is an emulsion. An emulsion is a system containing two immiscible liquid phases, usually oil and water, one of which is dispersed in the other as droplets varying between 0.1 and 50 μm in diameter. A stable emulsion is where the dispersed droplets retained their original state and remained uniformly distributed in the continuous phase for the desired shelf life. An emulsion without emulsifiers is a thermodynamically unfavourable system and its instability is because the system possesses high free energy. The physical changes in emulsions occur as separation of the dispersed and the continuous phase into two layers. Emulsion instability can occur via several ways (Figure 1.5), but mainly through flocculation, i.e. clusters of dispersed droplets, which then slowly leads to coalescence and creaming. Eventually the emulsion will break into two phase in order to decrease its overall free energy.

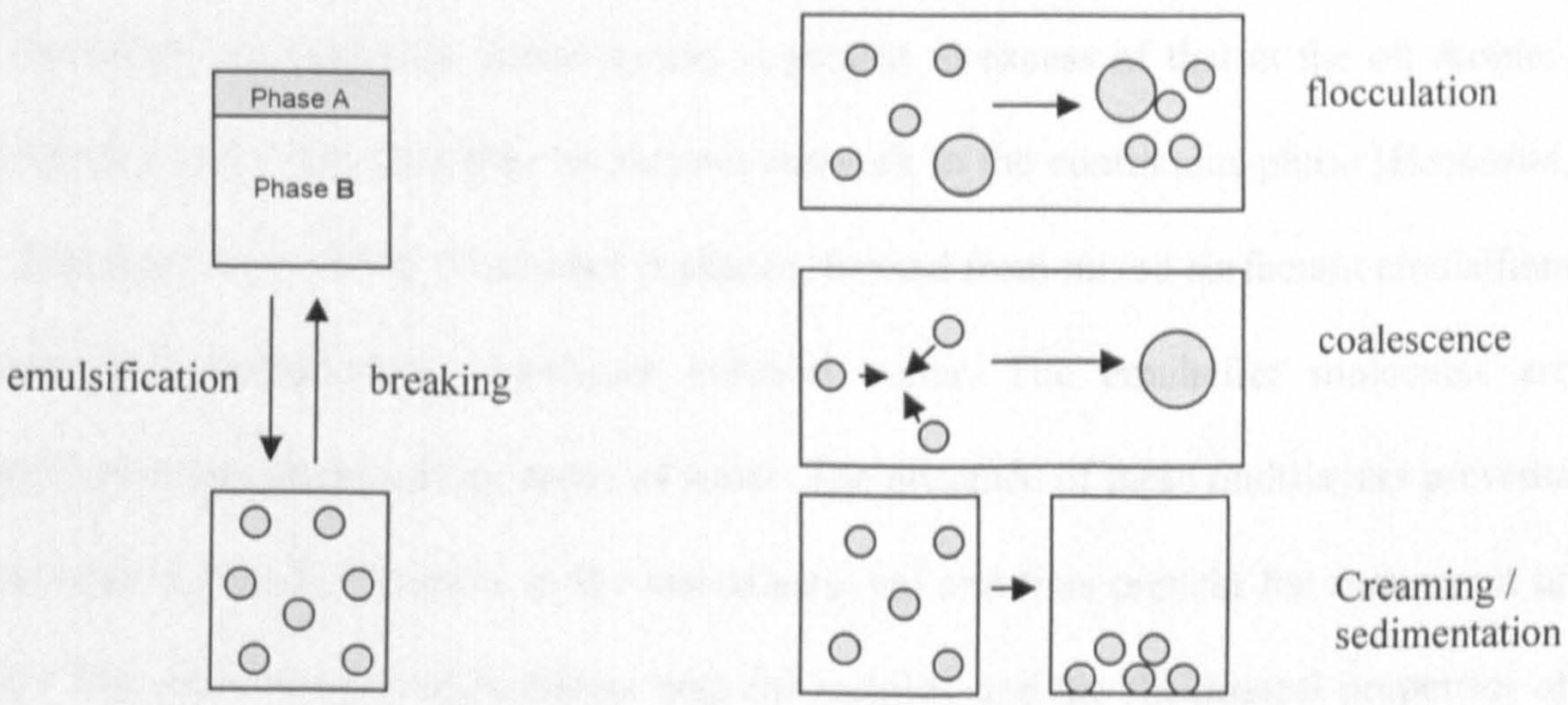

Figure 1.5: Illustration of various emulsion destabilisation processes.

Emulsifiers have a vital role in promoting emulsification. They prevent the closeness of the droplets by adsorbing on the droplet surface thus decreasing the interfacial tensions and providing electrostatic or steric repulsion, thus reducing the tendency of droplet recombination. In practice, combinations of emulsifiers are employed rather than just single agents. Table 1.2 shows the common pharmaceutical emulsifiers. They are generally

classified into three groups: 1) natural or synthetic surface-active agents, 2) macromolecular (polymer) materials, and 3) finely divided solids.

Table 1.2: Commonly used pharmaceutical emulsifying agents and some examples

Class	Examples
Surface-active agents	Sodium lauryl sulphate, cetrimonium cromide, cetyl alcohol, polysorbate 80
Macromolecular polymer	Acacia, carogeen, methylcellulose
Finely divided solids	Bentonite, veegum, aluminium hydroxide

Nevertheless, it is now known that emulsifiers do not just formed monolayers around droplets to reduce surface tension, but they also influence on the microstructure and control the consistency of the emulsion. Intensive investigation had been carried out by Eccleston to show that when the emulsifier concentration is present in excess of that at the oil droplet-water interface, they formed stable viscoelastic network in the continuous phase [Eccleston, 1990; Eccleston *et al.*, 2000]. The lamellar phases, formed from mixed surfactant emulsifiers can swell and incorporating significant volumes water. The emulsifier molecules are arranged in bilayers alternated by layers of water. The presence of these multilayers prevents the coalescence trapping droplets in the viscoelastic gel and thus prevent the movement of droplets. The emulsifying system affects both the stability and the rheological properties of an emulsion. The viscosity of the emulsion will only be affected when the emulsion concentration is sufficient to cause the formation, in the external phase of the emulsion, aggregations, micelles or network gels [Eccleston, 1997].

Gels or jellies are another form of commonly used dermatological base for topical drug delivery. Gels are an example of 'lyophilic' dispersed system in which the polymer is dispersed readily in liquid media forming a three-dimensional semisolid swollen network. When the continuous phase is aqueous media, the gel is called hydrogel. Hydrogel polymers

are hydrophilic and may absorb water up to thousand fold of their original dry mass. The swollen three-dimensional network in hydrogels is produced through the cross-linking of polymer chains. The cross linking can be of physical or chemical in nature. The former is known as a physical gel where the networks are held together by only molecular entanglements and/or secondary forces including ionic, H-bond or hydrophobic forces. Pluronic, alginate, gelatin gel are examples of physical hydrogels. On the other hand, chemical gels are generated when they are covalently-crosslinked, and usually they can be formed with or without the addition of crosslinkers. Synthetic hydrogels of copolymerization of hydroxyethylmetacrylate with crosslinker ethylene glycol dimethacrylate (EDGMA) is an example of a chemical gel. Figure 1.6 illustrates the formation of physical and chemical gels.

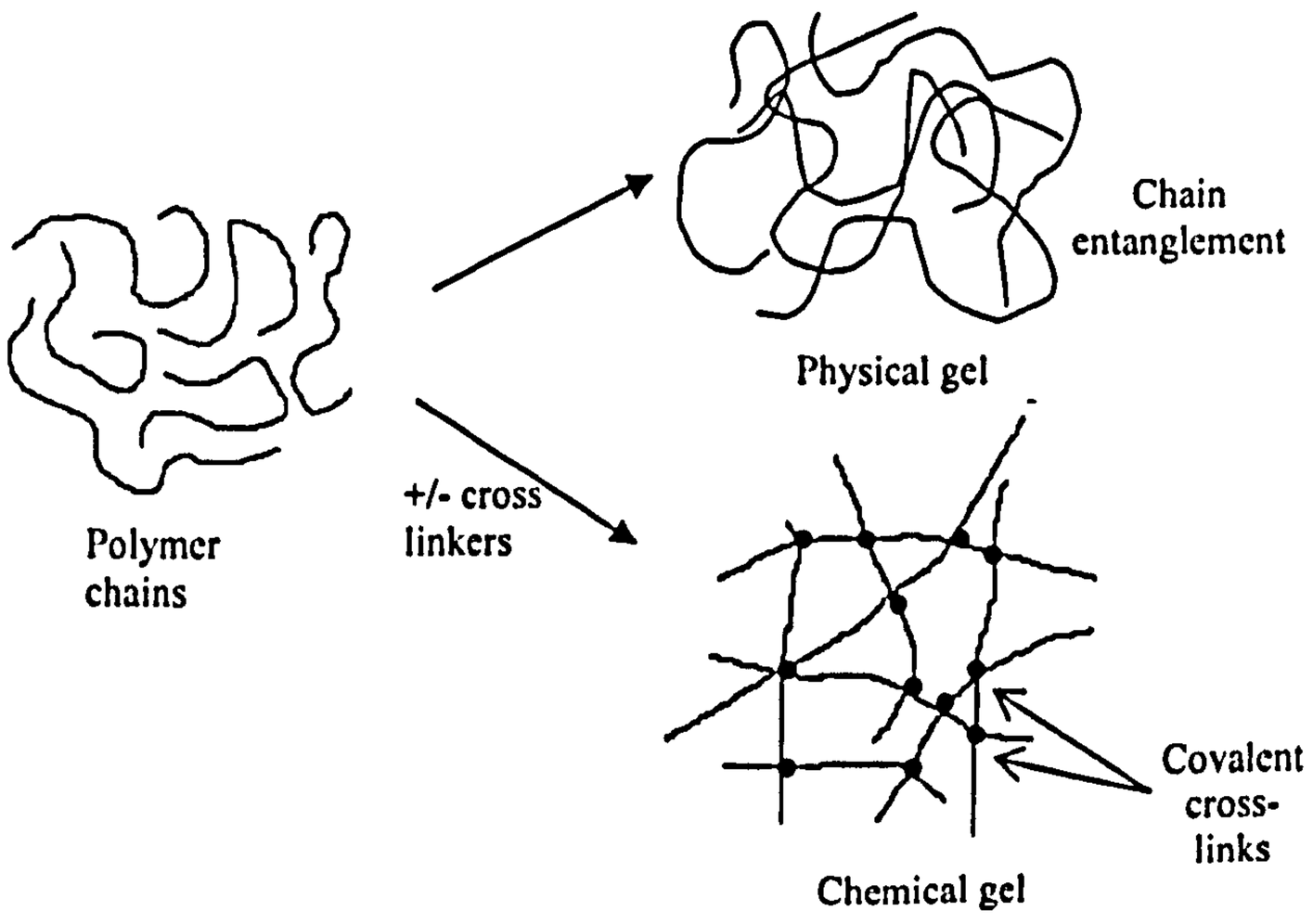

Figure 1.6: Formation of chemical and physical gels [adapted from Hoffman, 2002].

Typical polymers used to formulate pharmaceuticals gels include the natural gums alginates, tragacanth, carrageen, pectin, agar, and alginic acid; semi-synthetic materials such as methylcellulose (MC), hydroxylethycellulose (HEC), hydroxylpropylmethylcellulose (HPMC), and carboxymethylcellulose (CMC) and synthetic polymers such as Carbopol or carbomers. Novel drug delivery vehicles, e.g. sponges or wafers, for wound suppuration can

be achieved via lyophilisation of gel. In our work, wafers were produced using sodium alginate gels.

1.1.5 Transdermal patches

A transdermal patch is a medicated adhesive patch that is placed on the skin to deliver a time-released dose of medication through the skin and into the systemic bloodstream. The controlled release manner of drug release is aimed to reduce the dosing frequency. Transdermal patches are usually polymeric multi-layered devices. A drug reservoir or a drug polymer matrix is fixed in between two laminated layers of polymer. One layer is the backing layer, which is impermeable to the drug in order to prevent loss of drug as well as to protect the matrix or reservoir; while the other polymeric layer is the adhesive of rate controlling drug membrane for the drug. There are several transdermal patch designs but are generally categorised into 'membrane-controlled' and 'matrix-controlled' systems (Figure 1.7). The drug in the former is dissolved in an appropriate solvent or distributed uniformly in a solid polymer matrix such as polyisobutylene, which is suspended in a viscous liquid such as silicone oil. The drug release from the reservoir into the skin is controlled by the diffusional resistance across a polymeric membrane. Polyethylene vinylacetate (EVA) is often employed as the rate-controlling membrane. One example is Estraderm® which delivers 17β-estradiol to women at rates of 0.05 - 0.1 mg/day for 3-4 days. Nicoderm®CQ™ and Transderm-Scop® use microporous membrane (polyethylene and polypropylene respectively) by the means of controlling the rate of drug release. In matrix-controlled system, the drug is dissolved in a hydrophilic or hydrophobic polymer matrix reservoir, which is mounted on an impermeable backing membrane. In some cases, the system contains only the backing layer and the drug in the adhesive, which is covered by a peelable liner. An example of a matrix system currently marketed is Alza Testoderm® patch for the treatment of testosterone deficiency, which consists of three layers: backing layer of polyethylene

terephthalate, matrix film layer of testosterone and EVA copolymer and adhesive strips of polyisobutylene and colloidal silicone dioxide. The testosterone releases from the matrix in a controlled manner into the body at a rate of 4-6 mg/day and treatment continues for 3-4 weeks.

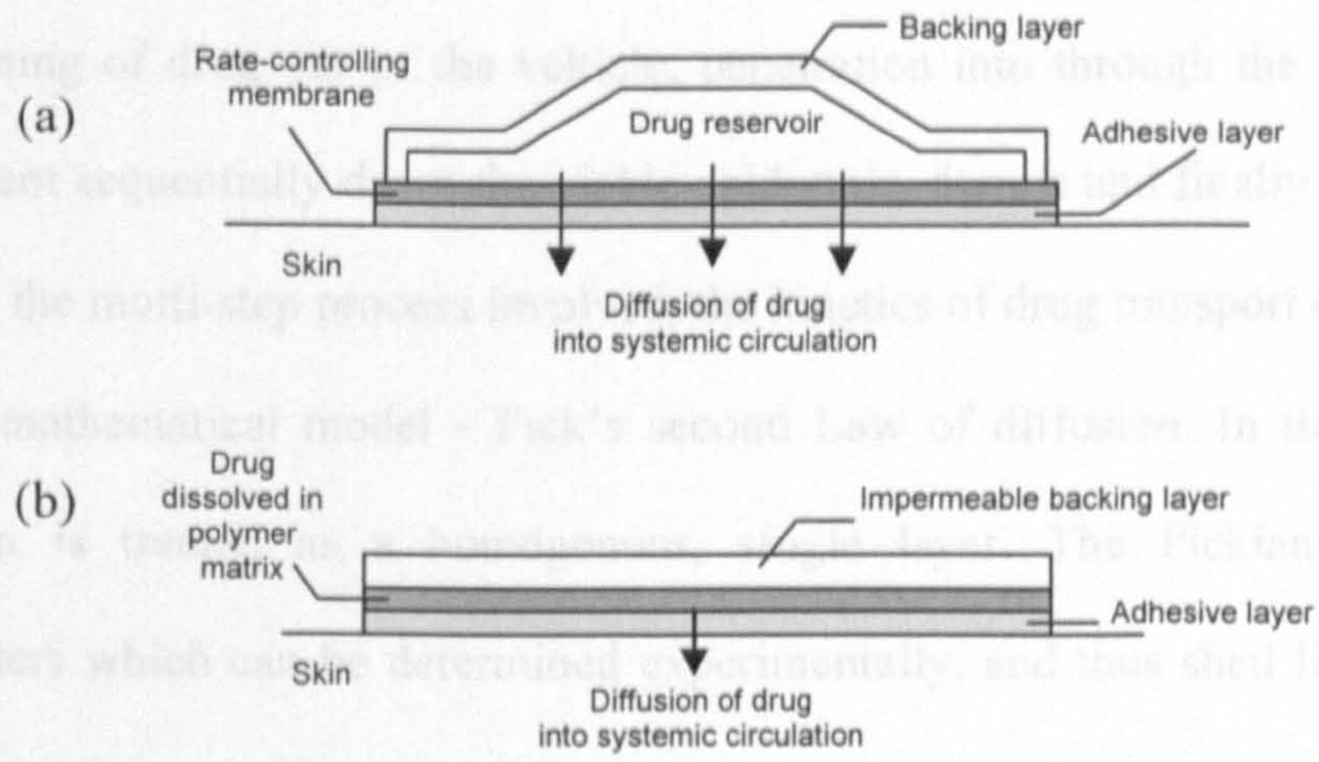

Figure 1.7: Schematic of two types of transdermal patches (a) membrane controlled system (b) matrix-controlled system [adapted from Pharmaceutical Codex, 1994].

1.2 Skin permeation of drugs

Only selective drug substances (hydrophobic, MW<500 Da) can pass through the skin effectively [Williams, 2003]. This is primarily due to the impermeable outermost layer of skin, i.e. the stratum corneum, which is the rate limiting barrier to most of the topical agents.

In percutaneous drug delivery context, the terms 'percutaneous absorption' and 'skin permeation' are often used. It is crucial to differentiate between them because these two terms are subtly different. An *in vitro* percutaneous penetration workshop led by FDA and AAPS [Skelly et al., 1987] defined percutaneous absorption as "a process pertaining to the permeation of solute through the epidermis and into the deep layers of skin and finally the general circulation, a process total of transport through the skin and local clearance"; whilst

skin permeation refers to only the initial part of the process, i.e. just the diffusion across the stratum corneum. These terms are sometimes use interchangeably.

1.2.1 Theoretical considerations of drug permeation

Percutaneous absorption of drugs is not a straight forward process. It begins with the partitioning of drug out of the vehicle, penetration into through the stratum corneum, and movement sequentially down the viable epidermis, dermis and finally into the blood stream. Despite the multi-step process involved, the kinetics of drug transport can be described using simple mathematical model - Fick's second Law of diffusion. In this model, the stratum corneum is treated as a homogenous, single layer. The Fickian Law contains basic parameters which can be determined experimentally, and thus shed light onto investigating the factors that can affect drug flux.

The drug formulated in a vehicle with a concentration (Cv) diffuses across the membrane or skin, in which the drug concentration is zero (sink condition). The skin or membrane is the isotropic barrier controlling the rate of drug diffusion. The first step of diffusion requires the drug to partition into the skin. This parameter is expressed as the 'partition coefficient', which measures the distribution of drug between the first layer of the membrane (skin) and the vehicle. The ability of a drug molecule to leave the vehicle and into the skin is dependent on the solubility of drug between vehicle and the skin. This is the partition coefficient (K) and can be written as

$$K = \frac{Cs}{Cv} \qquad \text{Eq. 1.1}$$

where Cs is the drug concentration in the first layer of skin. Once absorbed into the membrane, the drug is transported across the membrane via passive diffusion. For steady

state drug diffusion, the parameters above are expressed in a modified Fick's Law expression:

$$J = \frac{D.Cs}{h} \qquad \text{Eq. 1.2}$$

The flux, J, is the rate of drug transport per unit area of surface, and h is thickness of the skin or membrane (actually tortuous diffusional pathlength of the skin or membrane) and D is the diffusional coefficient. The diffusion coefficient measures how easily it will traverse through the skin tissue. When combined equation 1.1 and 1.2, the drug diffusion steady state can be rewritten as

$$J = \frac{D.K.Cv}{h} \qquad \text{Eq. 1.3}$$

The full derivative of this equation can be obtained from [Watkinson and Brain, 2002]. The term permeability coefficient (Kp) described the rate of permeant transport per unit concentration, it is defined as

$$Kp = \frac{K.D}{h} \qquad \text{Eq. 1.4}$$

thus the Eq. 1.3 can re-written as

$$J = Kp.Cv \qquad \text{Eq. 1.5}$$

Kp is useful when the relative permeabilities of a series of compounds under conditions where only the Kp can be measured (e.g. *in vitro* study), and not D and K alone. The true driving force for percutaneous absorption is the thermodynamic activity (α) of the permeant in the vehicle. Thermodynamic activity measures the 'escape tendency' of a molecule from its formulation. An alternative form of Equation 1.3 uses thermodynamic activities [Higuchi, 1960], expressed as

$$J = \frac{D}{h} \times \frac{\alpha}{\gamma} \qquad \text{Eq. 1.6}$$

where α is the thermodynamic activity of drug in its vehicle and γ is the effective activity coefficient in the skin barrier. The thermodynamic activity of the drug in the vehicle is the true driving force for drug permeation into skin. For maximum penetration rate, the drug should be at its highest thermodynamic activity. The thermodynamic activity of drug in the vehicle α, is defined the ratio of the drug concentration in the vehicle Cv, to the saturation solubility of the drug in the base C_{sat}, or $\alpha = Cv/C_{sat}$. Generally, the maximum flux is obtained when the drug is saturated in the vehicle, i.e. the thermodynamic activity is at unity. However, activity can exceed unity when supersaturated states are formed. So, the theoretical flux may thus increase as $\alpha > 1$, i.e. supersaturation. Supersaturation in a topical dosage form can be achieved by evaporation of a solvent from the system. Some authors employed co-solvent system [Megrab *et al.*, 1995] or anti-nucleating agents [Pellett *et al.*, 1997] and using the *in vitro* model for the maintenance of the supersaturated state, they managed to show enhanced drug diffusion. However, Schwarb and co-workers were unable to show an effect of supersaturation in increasing the delivery of fluocinonide *in vivo*, as assessed by the vasoconstrictor assay [Schwarb *et al.*, 1999].

The parameters in equation 1.3 can be derived experimentally using a diffusion cell such as the Franz cell. A diffusion cell consists of two compartments. One compartment (donor) contains the drug formulation of interest; while the other compartment (receptor) is filled with solvent in which the drug can be solubilised in. A skin or synthetic membrane is placed in between separating the two compartments (see details later in section 1.2.2). The cumulative drug release versus time plot can then be constructed by withdrawing sample of fluid from the receptor compartment and analysed. Typical drug release graphs are shown in Figure 1.8.

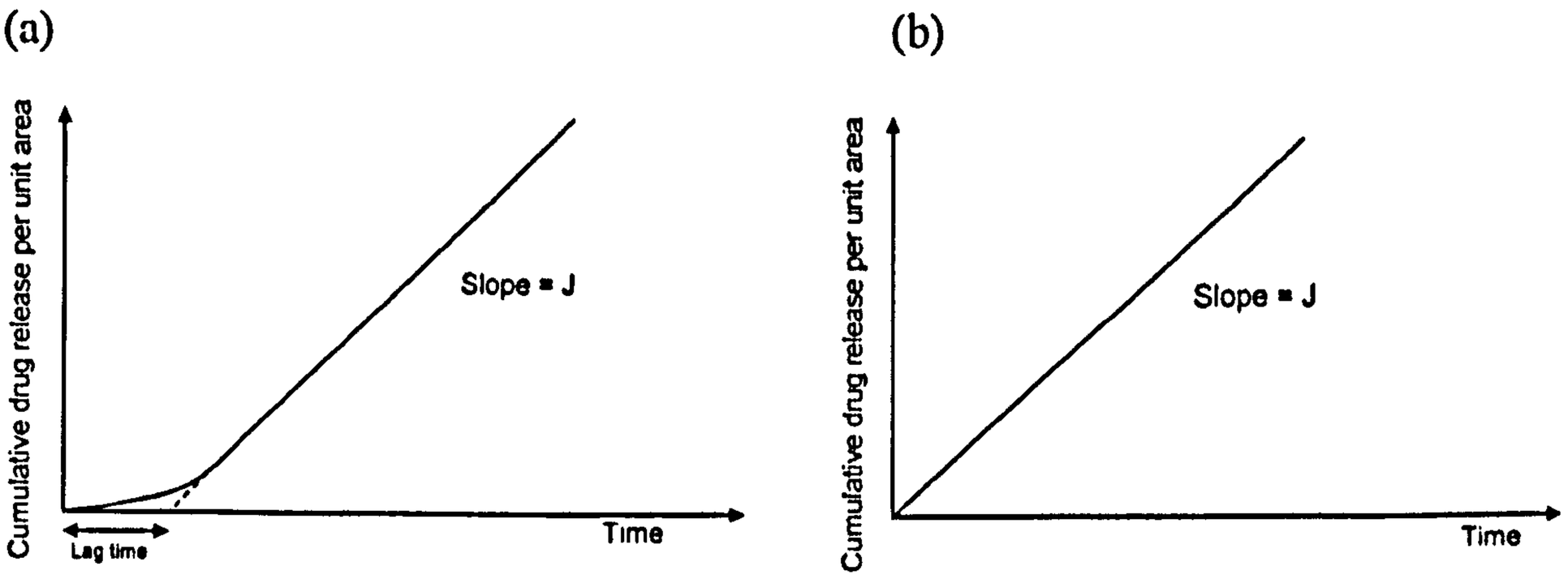

Figure 1.8: A typical cumulative drug release vs. time graph obtained from Franz diffusion cell drug release experiment. The present of lag time indicates that the membrane (e.g. skin) is limiting the drug diffusion (a); whereas if a synthetic membrane with no diffusional resistance is employed, no lag time would be observed (b).

If there is no interaction between the vehicle and the skin, the cumulative drug release per unit area of drug diffusion increases linearly with time until the drug in the donor becomes exhausted. The drug flux, J, is measured from the linear part of the plot. The permeability coefficient, Kp, can be calculated from flux (J) divided by drug concentration in the vehicle (Cv) such as in equation 1.5. The diffusion coefficient D can be estimated from $L= h^2/6D$ where L is the lag time and h is the thickness of the barrier (skin).

1.2.2 Diffusion cells for topical drug delivery

The *in vitro* test for percutaneous absorption studies is an essential tool in topical drug delivery. The *in vitro* tests are not only useful for the development of new dosage forms or the evaluation of pharmaceutical and cosmeceutical products [Cooper *et al.*, 2004; Huang *et al.*, 2005], but also to obtain information about the effects of drug and/or excipients on the

barrier function of the skin [Auner and Valenta, 2004; Brown *et al.*, 2000; Cho and Choi, 1998]. Furthermore, they can also be used in the evaluation of the risk associated with dermal contacts with toxic substances. [Adami *et al.*, 2006; Walter *et al.*, 1998; Zorin *et al.*, 1999]. The use of excised animal or human skin mounted on suitable *in vitro* test systems is an alternative for the *in vivo* study of percutaneous absorption. Apart from reducing the number of *in vivo* tests, the *in vitro* model is recommended as cheaper option as well as easier to set up. The investigator is able to control the experimental conditions and large amount of data can be obtained in a short period. Conventionally, the *in vitro* model with excised skin is employed to predict the drug release kinetics in relevant to *in vivo* situation. Nevertheless, synthetic membranes have also been used in the place of skin either for skin simulation or the topical product quality control purposes [Shah *et al.*, 1989].

Diffusion cells have been widely adopted as the *in vitro* model for percutaneous study, particularly Franz-type diffusion cells [Franz, 1975; 1978]. The diffusion cells generally have common elements: two chambers, one containing the active agent (donor) and the other containing a stirred receiver solution (receptor), separated by a skin or synthetic membrane. A countless of cell designs have evolved over the last three decades. However, most designs fall into two main categories: side-by-side and vertical diffusion cells.

Examples of side-by-side cells are shown in Figure 1.9 below. Typically, the two glass chambers are arranged horizontally and immersed in a water bath for temperature regulation. The membrane is supported in between the chambers with a stainless steel mesh, and the sampling is accomplished through sampling ports located on each chamber. Since the donor chamber of side-by-side diffusion cells is usually filled with liquid formulation, so both chambers are usually stirred to ensure the uniformity of the drug molecules in the solution.

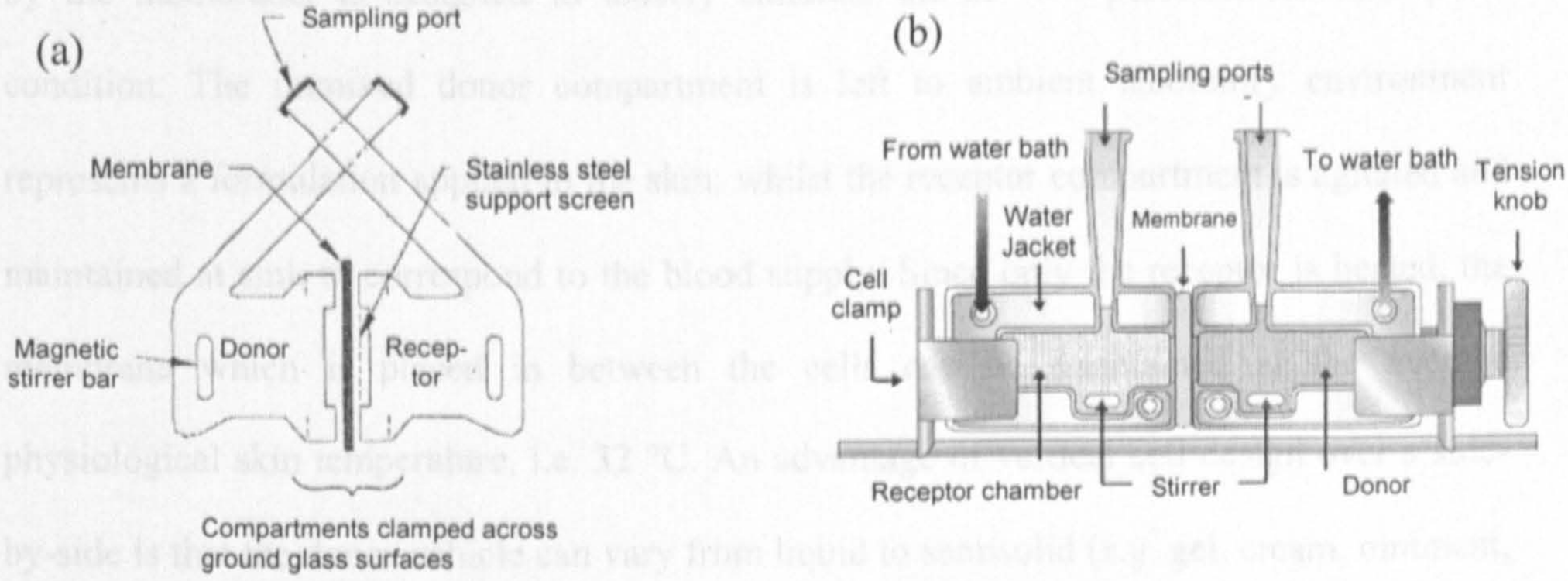

Figure 1.9: (a) Typical side-by-side diffusion cell [redrawn from Southwell and Barry, 1983], (b) Side-by-side cell designed by PermeGear, Inc.

In the past, much skin permeation data has been collected using the side-by-side cells [Astley and Levine, 1976; Barry *et al.*, 1985; Jetzer *et al.*, 1986; Scheuplein and Ross, 1974; Southwell and Barry, 1983; Tojo *et al.*, 1967; Tojo *et al.*, 1984]. Such diffusion cell designs have several advantages including the fact that air bubbles do not readily lodge under the membrane which could affect drug flux. Both compartments are constantly stirred to ensure homogeneity of the solutions and minimise stagnant layers next to the membrane. The limitation of the side-by-side design is that both sides of the skin or the synthetic membrane are constantly bathed with solution throughout the experiment leading to potential hydration of the skin or membrane which may disrupt membrane integrity [Friend, 1992]. The side-by-side diffusion cell is useful in predicting the steady state diffusion or zero-order flux of a drug from a solution across a skin or synthetic membrane [Barry, 1983]; nevertheless, measurement of permeation rates under simulated *in vivo* condition requires a different cell design, known as the vertical diffusion cell.

The vertical diffusion cell, consisting of donor cell at the top and receptor below separated by the membrane, is designed to closely simulate the *in vivo* percutaneous absorption condition. The unmixed donor compartment is left to ambient laboratory environment represents a formulation applied to the skin; whilst the receptor compartment is agitated and maintained at sink to correspond to the blood supply. Since only the receptor is heated, the membrane which is placed in between the cells can be maintained at the average physiological skin temperature, i.e. 32 °C. An advantage of vertical cell design over a side-by-side is that the donor vehicle can vary from liquid to semisolid (e.g. gel, cream, ointment, paste). Figure 1.10 shows various designs of vertical diffusion cells.

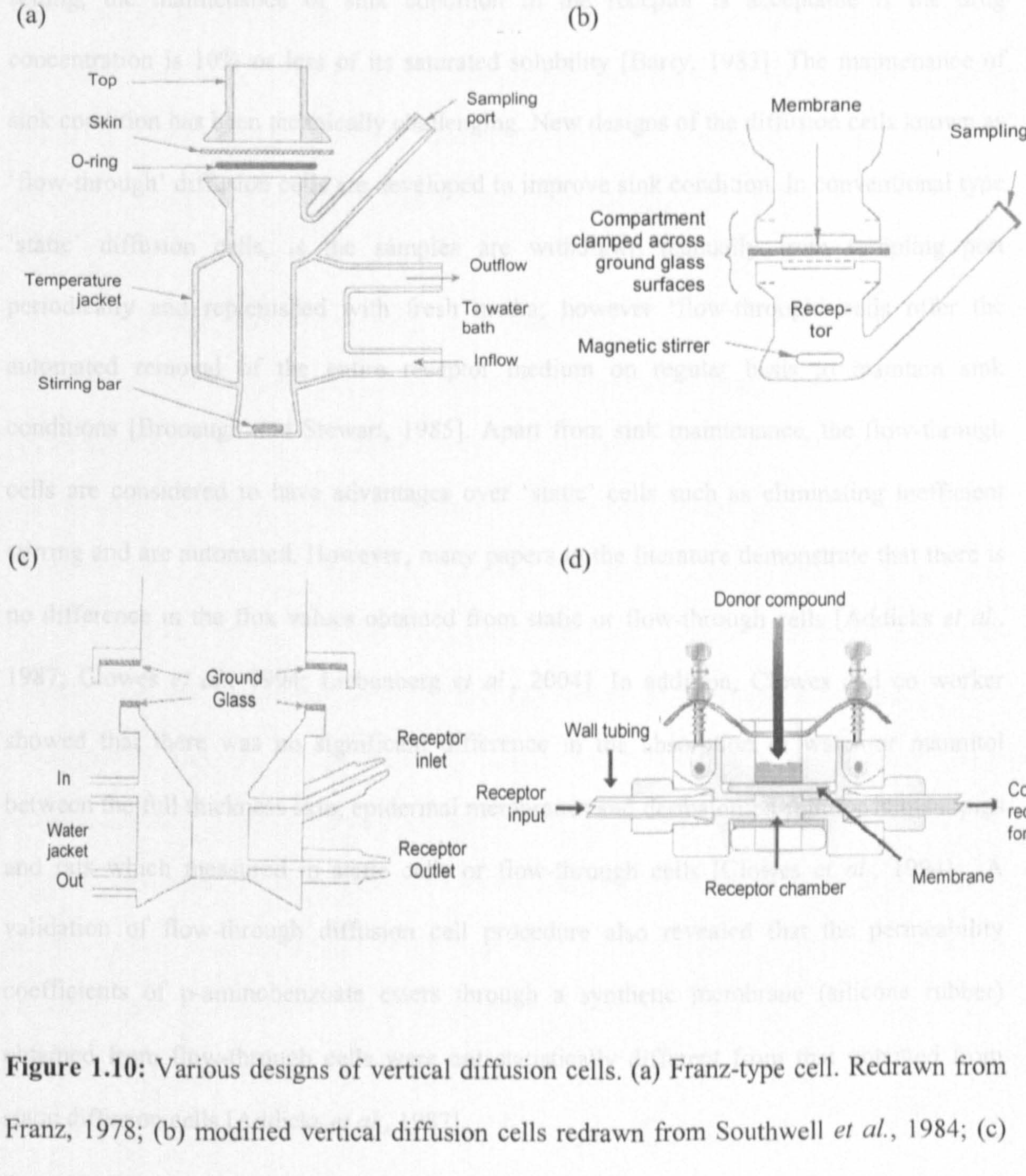

Figure 1.10: Various designs of vertical diffusion cells. (a) Franz-type cell. Redrawn from Franz, 1978; (b) modified vertical diffusion cells redrawn from Southwell *et al.*, 1984; (c) flow-through diffusion cells redrawn from Gummer *et al.*, 1987; (d) Flow through cell designed by PermeGear, Inc.

In skin, a sink condition ('zero' concentration) occurs below the skin because the drug which diffuses through is constantly removed by systemic circulation. In the *in vitro* laboratory setting, the maintenance of sink condition in the receptor is acceptable if the drug concentration is 10% or less of its saturated solubility [Barry, 1983]. The maintenance of sink condition has been technically challenging. New designs of the diffusion cells known as 'flow-through' diffusion cells are developed to improve sink condition. In conventional type 'static' diffusion cells, is the samples are withdrawn manually from sampling port periodically and replenished with fresh media; however 'flow-through' cells offer the automated removal of the entire receptor medium on regular basis to maintain sink conditions [Bronaugh and Stewart, 1985]. Apart from sink maintenance, the flow-through cells are considered to have advantages over 'static' cells such as eliminating inefficient stirring and are automated. However, many papers in the literature demonstrate that there is no difference in the flux values obtained from static or flow-through cells [Addicks *et al.*, 1987; Clowes *et al.*, 1994; Liebenberg *et al.*, 2004]. In addition, Clowes and co worker showed that there was no significant difference in the absorption of water or mannitol between the full thickness skin, epidermal membranes and dermatomed skin for human, pigs and rats which measured in static cells or flow-through cells [Clowes *et al.*, 1994]. A validation of flow-through diffusion cell procedure also revealed that the permeability coefficients of p-aminobenzoate esters through a synthetic membrane (silicone rubber) obtained from flow-through cells were not statistically different from that obtained from static diffusion cells [Addicks *et al.*, 1987].

Despite the diverse range of diffusion cells exist, the static Franz-type cell [Franz, 1975] is still the most widely used to determine the diffusion and penetration properties of drug compounds through skin [Friend *et al.*, 1989; Gallagher *et al.*, 2003b; Pellett *et al.*, 1997;

Vincent *et al.*, 1999; Watkinson *et al.*, 1995; Akomeah *et al.*, 2004; Brown *et al.*, 2000; Heard *et al.*, 2006; Santhanam *et al.*, 2004]. The use of the Franz cell to correlate with *in vivo* permeation is important in topical drug delivery. In fact, the use of vertical diffusion cells for measuring the percutaneous absorption in relation to *in vivo* permeation was first carried out by Thomas J. Franz in 1970s (hence the name 'Franz cell'). He showed that the absorption pattern of twelve organic compounds determined *in vitro* rather precisely paralleled the pattern which was obtained *in vivo*. However, the correlation was more of a qualitative relationship rather than a quantitative relationship [Franz, 1975].

1.3 Synthetic and semi-synthetic membranes

Generally, the synthetic membranes employed in drug diffusion studies have one of the two functions: skin simulation or quality control. The synthetic membranes for skin simulation are generally hydrophobic and rate-limiting to imitate the stratum corneum (silicone-based membrane e.g. polydimethylsiloxane, carbosil). In contrast, unlike membranes for skin mimicry, synthetic membranes for quality control are required to act as a support rather than a barrier (e.g. cellulose esters, polysulfone). The finding of a suitable membrane for such investigations had led to an increased search for synthetic membranes from other applications such as the separation industry and filtration application. The properties of a synthetic membrane can vary greatly from one application to another because to a certain extent they are 'tailor-made' so that their separation properties can be adjusted to a specific separation task. In this thesis, we also employed membranes from other applications. The following section gives a general overview of synthetic membranes, which encompasses the brief background history, the use of synthetic membranes for various applications, as well as the characteristics of different type of synthetic membranes employed in each application.

1.3.1 Background history of synthetic membranes

The history of synthetic membranes is extensively reviewed in many textbooks [Bungay, et al., 1986; Matsuura, 1993; Mulder, 1996]. The first use of synthetic membranes can be traced back as early as the 19th century. Since its discovery of in 1846, the cellulose nitrate polymer became one of the most widely used membranes in the 19th century as a laboratory tool for the development of physical/chemical theory. Cellulose nitrate membranes were first used for the study of molecular diffusion processes in 1855. In 1887, a Dutch chemist Jacobus van't Hoff used artificial membranes to develop the concept of osmotic pressure in solution and this led to the derivation of van't Hoff equation. The development of synthetic membranes did not begin till early 20th century when Bechhold successfully devised a series of nitrocellulose microporous membranes of various pore sizes using a bubble test. The Bechhold technique was improvised and microporous cellulose nitrate membranes became commercially available by 1930s [Ferry, 1936]. At about the same time, an independent development of membranes for medical separation, i.e. the artificial kidneys using cellulose membranes emerged. This was a major breakthrough for the use of artificial membranes in medical applications and this became a major life-saving procedure today. In the early 1960s, Loeb and Sourirajan developed asymmetric cellulose acetate membranes with relatively high water fluxes and separations [Loeb and Sourirajan, 1963]. This development stimulated both commercial and academic interest, first in desalination by hyperfiltration and then in other membrane processes and applications. The rapid expansion of membrane industry has brought significant progress in membrane development for the next two decades. Such development includes applications, research tools, membrane formation processes, chemical structure, physical structures, and packaging.

1.3.2 Synthetic membranes and their applications

Synthetic membranes are composed of thin sheets of polymeric macromolecules that can control the passage of components. They may be made of synthetic polymers e.g.

polysulfone, polycarbonate, polyacrylonitrile and polypropylene, or semi-synthetic cellulose polymers e.g. cellulose acetate, cellulose nitrate and regenerated cellulose. Sometimes, additional compounds to provide mechanical support, drainage or adhesion (for example a transdermal patch) may also be present in a synthetic membrane. Synthetic membranes have gained an important place in chemical technology and are manufactured for various separation processes undertaken in the industry and laboratory such as microfiltration, ultrafiltration, reverse osmosis, electrodialysis, pervaporation and gas separation. The transport of solutes across a synthetic membrane is driven by the force acted upon the membrane, which may be due to concentration gradient, chemical potential, temperature gradient, electrical potential or pressure. Each separation process is driven by different driving forces and the summary between the two factors are shown in Table 1.3.

Table 1.3: Membrane separation processes and driving forces [Mulder, 1996].

Pressure gradient	Concentration gradient	Electrical potential gradient	Temperature gradient
Microfiltration	Dialysis	Electrodialysis	Membrane distillation
Ultrafiltration	Pervaporation	Electro-osmosis	
Reverse osmosis	Gas Separation		

The ability of synthetic membranes to control permeation rate and allow only selective species to pass through has led to the emergence of a relatively new branch of chemical technology called 'separation and filtration technology' where all the processes use synthetic membranes to separate or filter particulate of size less than a micron. Figure 1.11 below is a schematic representation of the relative particle size (in micron, nanometer and molecular-weight cut off (MWCO)) and the membrane separation processes involved.

The application of synthetic membranes has expanded tremendously over the years, from small laboratory scale to large industrial setting. The membrane applications in Figure 1.11 are broadly characterised according to the size of the particle separated. Microfiltration, ultrafiltration, electrodialysis and reverse osmosis are well-established processes; gas separation and pervaporation are still in the developing stage. Table 1.4 summarises the common membrane applications and types of synthetic membrane involved.

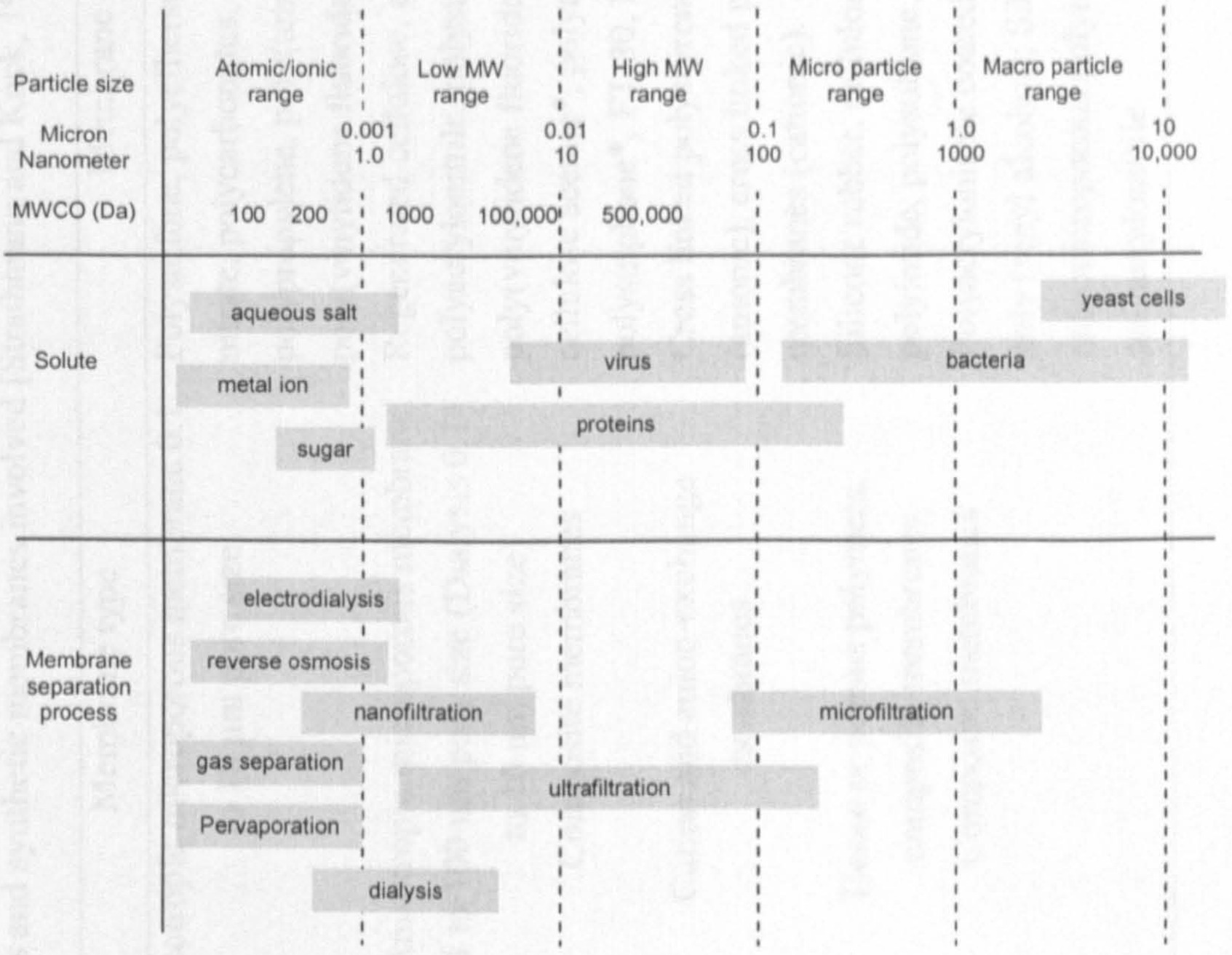

Figure 1.11: Schematic summary of particle sizes and membrane separation processes. [adapted from Mulder, 1996].

Table 1.4: Summary of various membrane processes and synthetic membranes involved [Strathmann and Kock, 1977].

Separation process	Description	Membrane type	Membrane examples
Microfiltration[a]	Sterile filtration	Isotropic microporous membrane 0.1 to 10 μm pore size	Polysulfone, polyethersulfone, cellulose nitrate, polycarbonates, polyamides, polypropylene, poly(tetrafluoroethylene), poly(vinylidene fluoride).
Ultrafiltration[a]	Separation of salts and microsolutes from macromolecules solution	Anisotropic microporous membrane 1 to 100 nm pore size (Dialysis 0.1 to 10 nm pore size)	Regenerated cellulose, cellulose acetate, polyacrylonitrile, polysulfone, poly(vinylidene fluoride).
Reverse osmosis[b]	Separation of salt from solutions	Composite membranes	cellulose acetate*, polyamide*, polysulphone*, FT-30, NF-40
Electrodialysis[b]	Desalting of ionic solution	Cation and anion-exchange membranes	Cross linked polystyrene membrane (anionic), cross linked perfluorocarbon membranes (cationic).
Gas separation[b]	Separation of gas mixture	Dense or porous polymers, composite membranes	Silicone rubber, cellulose acetate*, polyimide, polysulfone.
Pervaporation[b]	Separation of liquid mixture by partial evaporation	Composite membranes	Polyacrylonitrile coated with a thin layer of poly (vinyl alcohol); Silicone rubber coated onto microporous polyimides or polyacrylonitrile

[a]small scale [b]industrial scale *less widely use

Some of the membranes listed in Table 1.4 are utilised in Franz cell experiments in the literature, for example, the silicone rubber of gas separation, the regenerated celluloses of ultrafiltration. These membranes are manufactured for specific application but also consist of certain features which are desirable for the Franz cell investigations. However, not all the applications are suitable for the drug diffusion studies. In the following section, each synthetic membrane process is described in general, then their synthetic membrane characteristics in relation to Franz cell investigations are highlighted.

1.3.2.1 Reverse osmosis

Reverse osmosis is a method of de-salting water using synthetic membrane and the method had been known since the 1930s. Today, the process is often carried out to obtain fresh water from brackish water and seawater. Salt rejection of 99.3% is required to produce an acceptable solution consisting less than 550 ppm salt. Reverse osmosis and normal osmosis are directly related processes. If a semipermeable membrane (permeable to water only) separates a salt solution from pure water, water will pass through the membrane from the pure water side into the salt solution. This is the normal osmosis shown in Figure 1.12.

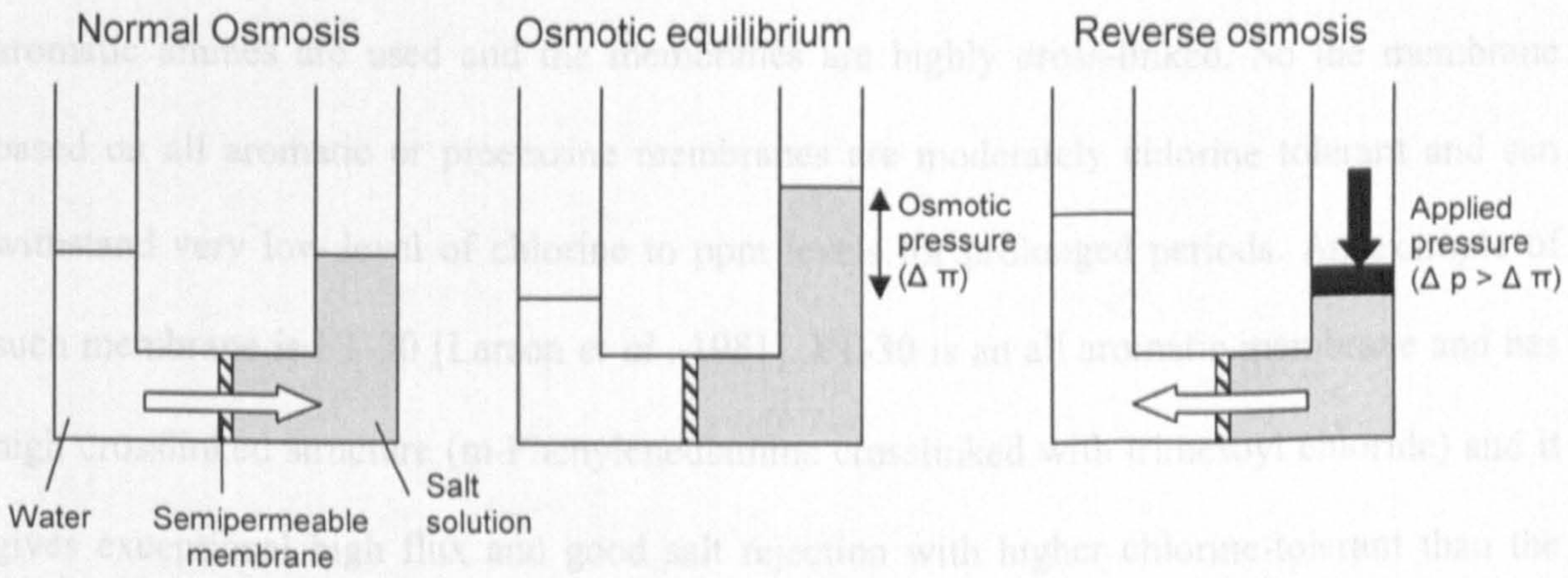

Figure 1.12: A Schematic illustration of the relationship between osmosis, osmotic equilibrium and reverse osmosis.

Osmosis ceases when the hydrostatic pressure applied at the salt side of the membrane is equivalent to the osmotic pressure. If a hydrostatic pressure exceeding the osmotic pressure is applied to the salt solution side of the membrane, the flow of water is reversed. The water will now flow from the salt solution to the pure water side of the membrane. This process is called reverse osmosis or desalination.

The synthetic membranes in reverse osmosis are aimed to produce high water flux (30 gal/ft^2 per day), high salt rejection (>99%) as well as with-stand pressure of 800-1000 psi [Baker, 2004c]. Anisotropic Loeb-Sourirajan cellulose acetate was one of the earliest membranes used for reverse osmosis because it is cheap, easy to manufacture and produces relatively good salt rejection. However, the water permeability of the cellulose acetate is low, producing low water flux [Lonsdale *et al.*, 1965]. Cellulose membranes were later surpassed by polymeric interfacial anisotropic composite membranes by Cadotte which generally give high flux and good salt rejection. In the reverse osmosis process, chlorination is often used for water sterilisation. The major drawback of the interfacial composite membrane is that the amine portions of the membrane chemistry are loss in degradation resulting from exposure to even ppb levels of chlorine. But this has improved if the tertiary aromatic amines are used and the membranes are highly cross-linked. So the membrane based on all aromatic or piperazine membranes are moderately chlorine tolerant and can withstand very low level of chlorine to ppm levels for prolonged periods. An example of such membrane is FT-30 [Larson *et al.*, 1981]. FT-30 is an all aromatic membrane and has high crosslinked structure (m-Phenylenediamine crosslinked with trimesoyl chloride) and it gives exceptional high flux and good salt rejection with higher chlorine-tolerant than the early composite membranes.

Reverse osmosis membrane allows only water molecules but rejects salt solutes, which imply that only small molecular weight solute (MW <50) can passes through. This indicates that the membranes are not useful for diffusion studies using drugs of high MW.

Furthermore, these composite membranes are sensitive to chlorine degradation, which is not a desirable feature if one of the components in the donor or receptor phase contained chlorides (e.g. saline) or similar halides. Thus the reverse osmosis membrane was not considered for Franz cell studies in this work.

1.3.2.2 Electrodialysis

Electrodialysis is a separation of salts from one solution to another solution by applying an electric current. It uses ion-exchanged membranes (also known as ion-selective membrane) which are normally thin films of polymeric chains containing electrically charged functional groups. The transport of the components occurs under the driving forces of both concentration and electric potentical gradients. These selectively charged membranes can separate ions: if the membrane is positively charged (e.g. with quartenary ammonium groups) only anions will be allowed through it and it is called an anion-exchange membrane. Similarly, negatively charged membranes (i.e. with sulfonate groups) are called cation-exchange membranes. In the elctrodialysis system, a cation and anion exchange membrane forms a cell pair and these cell pairs are arranged in stacks in between the anode and cathode (see Figure 1.13 below for electrodialysis illustration). The salt solution is passed through the cells while an electrical potential is generated across the electrodes. Separation occurs as the electrical potential applied.

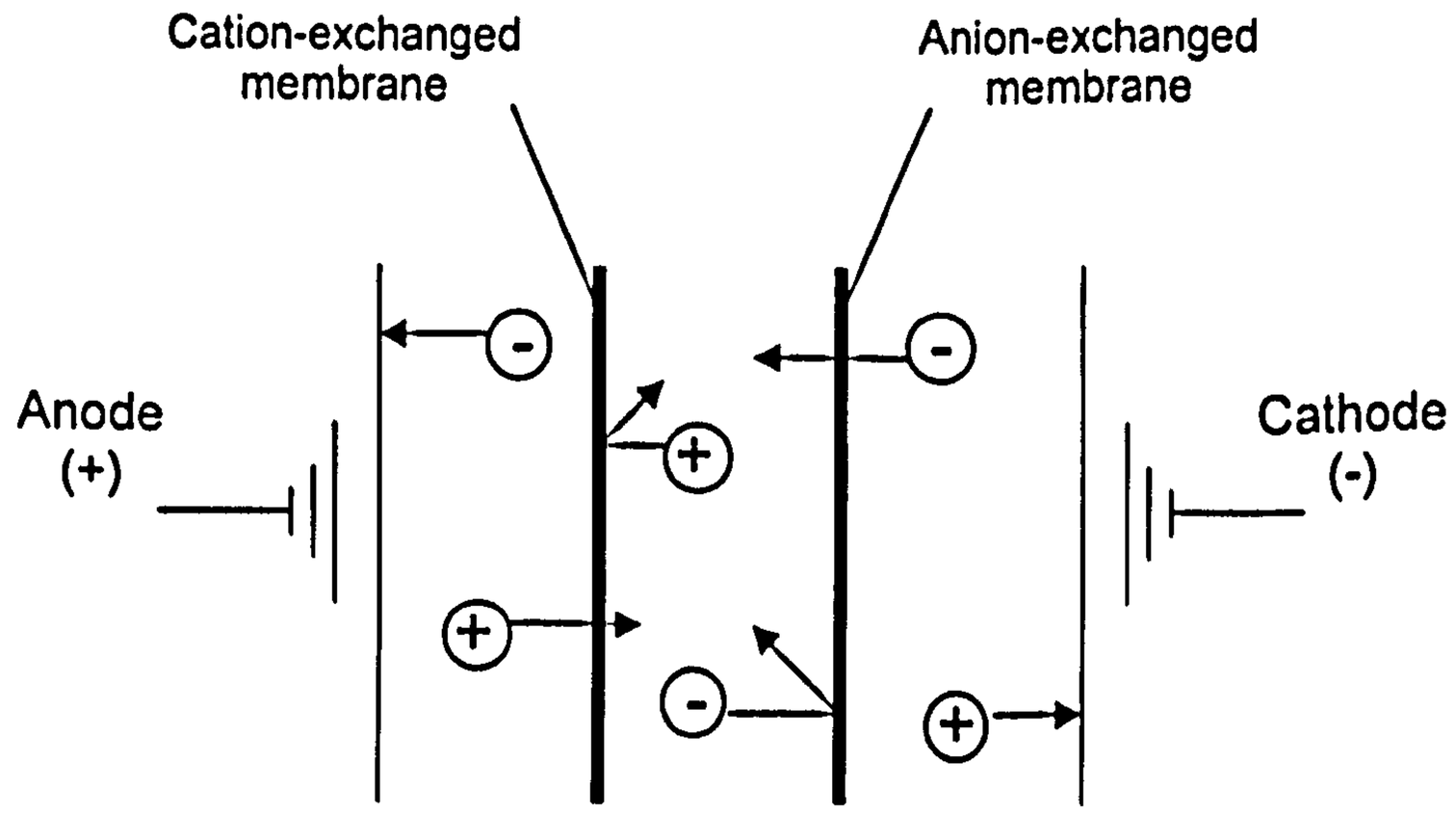

Figure 1.13: Simplified illustration of electrodialysis.

Most ion exchanged membranes are produced as an isotropic film 50-200 μm thick. Ion-exchange membranes are highly crosslinked because ion groups tend to absorb water and charge repulsion of the ionic groups can cause the membrane to swell excessively, so a crosslinked membrane is use to limit the swelling. However, this causes the membrane to become brittle, so the membrane is usually stored and handled wet to allow absorbed water to plasticize the membrane. Electrodialysis is an alternative method to reverse osmosis for desalination.

The use of electodialysis membrane in Franz cell investigations, whether to mimic skin or quality control would be unsuitable. This is because of the present of high membrane charged-surface will encourage the solute-membrane interactions. The solutes could be either from the drug formulation or the receptor solution which dissociated in aqueous solution.

1.3.2.3 Gas separation

Gas mixtures are effectively separated by synthetic membranes. For example, O_2 and N_2 gas separation produced either O_2-enriched air for medical or metallurgic application or N_2-enriched air for blanketing of fuels and stored food to provide nontoxic protection for fire and pests that require O_2. The separation occurs due to the different selectivity and diffusivity of the gas molecules in the membrane matrix. The membranes used for gas separation have no pores; rather, the separation takes place in a dense isotropic polymer layer of only microscopic thickness. One problem faced by early gas separation membranes was that the membrane was very senstitive to minor defects, such as pin-holes in the membrane layer, which can dramatically reduce the selectivity of gas separation. The Monsanto group made anistotropic porous membranes (polysulfone) then coated the membrane with a thin layer of highly permeable silicone rubber [Henis and Tripodi, 1980]. This coating sealed the defects but does not affect the gas molecule flux through the

polysulfone membrane. Development of such silicone-coated anisotropic membrane is a critical step in successful gas separation membrane for H_2/O_2 separation. Another type of gas separation membrane is the multilayer anisotropic composite membrane where a finely microporous support membrane is overcoated with a thin layer of the selective rubbery polymer (silicone). Recently, ceramic- and zeolite-based composite membranes have begun to be used for their extraordinary high selectivities performance in gas separation. These membranes consist of a thin selective ceramic or zeolite layer coated onto a microporous ceramic support. However the high cost has been a drawback for employing these membranes in gas separation.

1.3.2.4 Pervaporation

Pervaporation is a newly emerging separation process. It involves the separation of liquid mixtures in which the permeate is removed in vapour form from the other side of the membrane. The evaporation produces a separation because of the different volatilities of the components of the liquid mixture. The transport through the membrane is induced by the vapour pressure difference between the two side of the membrane and this vapour pressure difference is usually maintained via vacuum pump drawing a vacuum on the permeate side of the membrane. Figure 1.14 below shows a simplified pervaporation process.

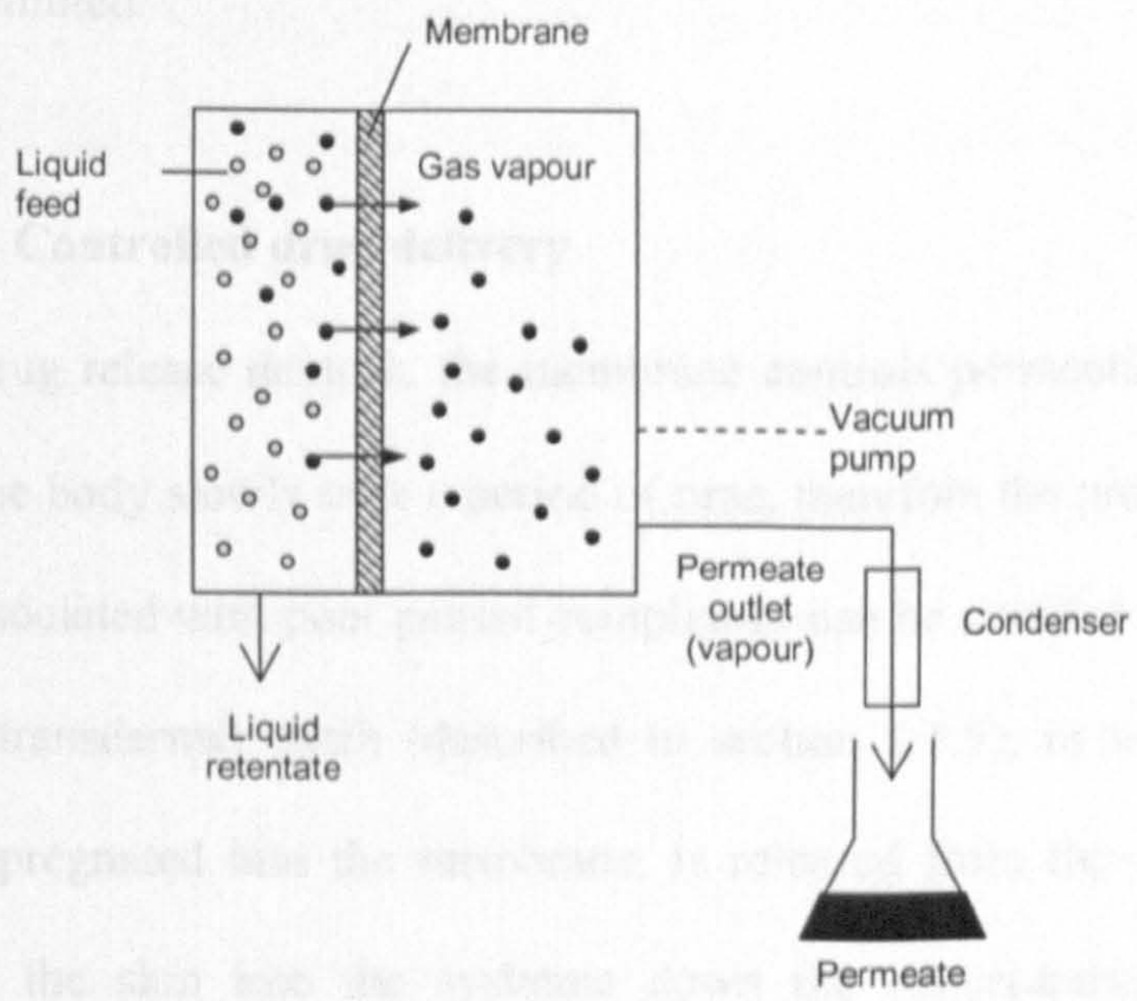

Figure 1.14: A simplified schematic of pervaporation process.

Like the gas separation process, the selectivility and diffusivity of the molecules in the membrane is the determining factor for good separation. Most pervaporation membranes are anisotropic composites formed by solution-coating the selective layer onto a microporous support. And depending of the applications, the membrane composition varies. For example, the removal of water from concentrated alcohol solutions uses microporous polyacrylonitrile coated with 5-20 μm layer of cross-linked polyvinylalcohol (PVA) because it was reported that the PVA is hydrophilic hence favours permeation to water [Hollein *et al.*, 1993]. In contrast, rubber silicone coated onto microporous support is widely used for separation of volatile organic component (e.g. acetone) from water because silicone rubber is a hydrophobic material [Hollein *et al.*, 1993]. Other rubbers such as ethylene-propylene polymers and polyamide-polyether block copolymers are also used.

Synthetic membranes for gas separation and pervaporation are designed for separation of small molecules which have high diffusivities in polymers. Such separation requires non-porous membranes or a porous membrane coated with non-porous polymer layer in which the membrane materials are highly selective to the diffusivity of a specific gas. Because such membranes are made for such high specificity, the drug types to be tested with Franz cells would be limited.

1.3.2.5 Controlled drug delivery

In controlled drug release devices, the membrane controls permeation of the drug from a reservoir into the body slowly over a period of time, therefore the problem of overdosing or underdosing associated with poor patient compliance can be avoided. One example of these devices is the transdermal patch (described in section 1.1.5), in which the drug from a reservoir or impregnated into the membrane, is released from the membrane and slowly diffuses across the skin into the systemic down the concentration gradient. Another example is the intrauterine device (IUD), Progestasert® which also uses ethylene vinyl

acetate (EVA) to control the drug release of progesterone (Figure 1.15). IUD itself interferes with the implantation; while the progesterone is to prevent the ovulation and thicken the cervical mucus, which prevents sperm from entering the uterus. This then further decreases the chances of pregnancy. This is a long lasting contraceptive device which is effective for up to a year when place in the uterus.

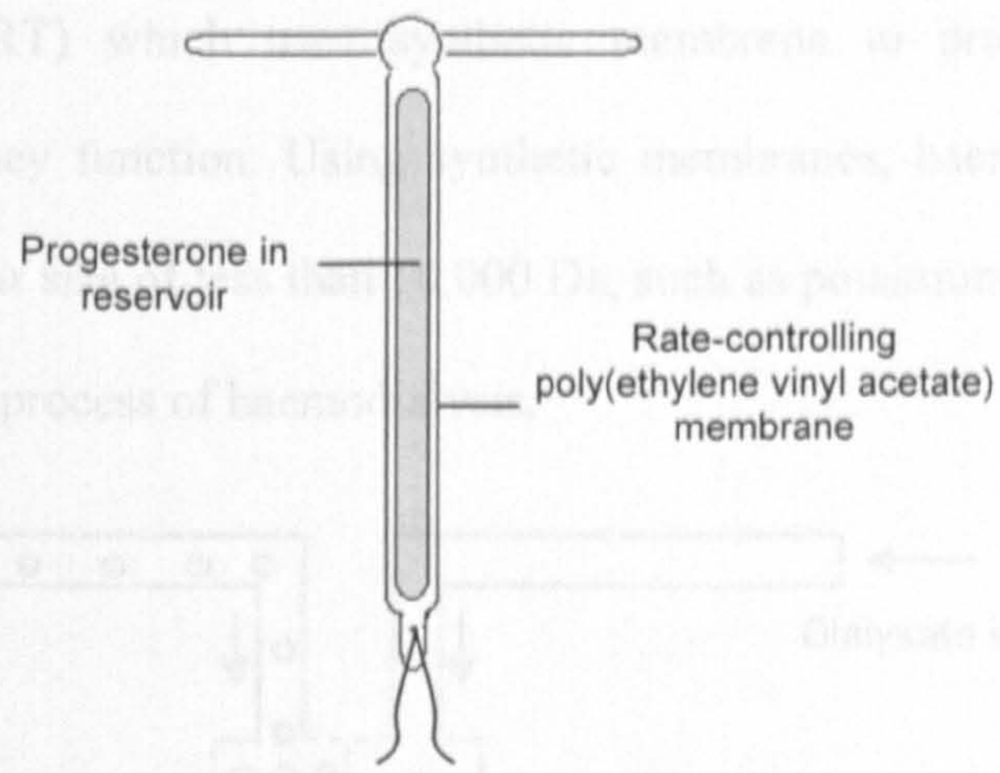

Figure 1.15: Intrauterine devices which uses synthetic membrane as the control the rate of drug release.

1.3.2.6 Microfiltration and ultrafiltration

Microfiltration refers to the removal of particles ranging from diameters 0.05 μm to less than 2.0 μm by membranes. Typical polymer materials for microfiltration membrane are polysulfone, polyethersulfone, polycarbonates, polypropylene, polyvinylidene fluoride, and polytetrafluroethylene. The membranes are usually chemically resistant to various types of solvents, thermally stable, and physically flexible. The microfiltration membranes are classified as 'depth filters', where the particle is retained in the matrix of the filter, and 'membrane filters' where the particles are retained on the surface of the membrane. The major application of microfiltration is sterilisation. Removal of bacteria from buffers and detection of foreign matter in pharmaceutical products are examples of laboratory microfiltration.

Ultrafiltration is not very different fundamentally from microfiltration. The ultrafiltration membranes separate particles size of 0.1 to 100 nm and are manufactured to retain macromolecules (e.g. proteins) and colloids of 100 to 100,000 Da. Ultrafiltration is a membrane process in which hydrostatic pressure forces a liquid against a semipermeable membrane. In medicine, ultrafiltration is the basic principle of haemodialysis, i.e. a renal replacement therapy (RRT) which uses synthetic membrane to provide an artificial replacement for lost kidney function. Using synthetic membranes, haemodialysis process separates solutes molecular size of less than 10,000 Da, such as potassium, urea from blood.

Figure 1.16 illustrates the process of haemodialysis.

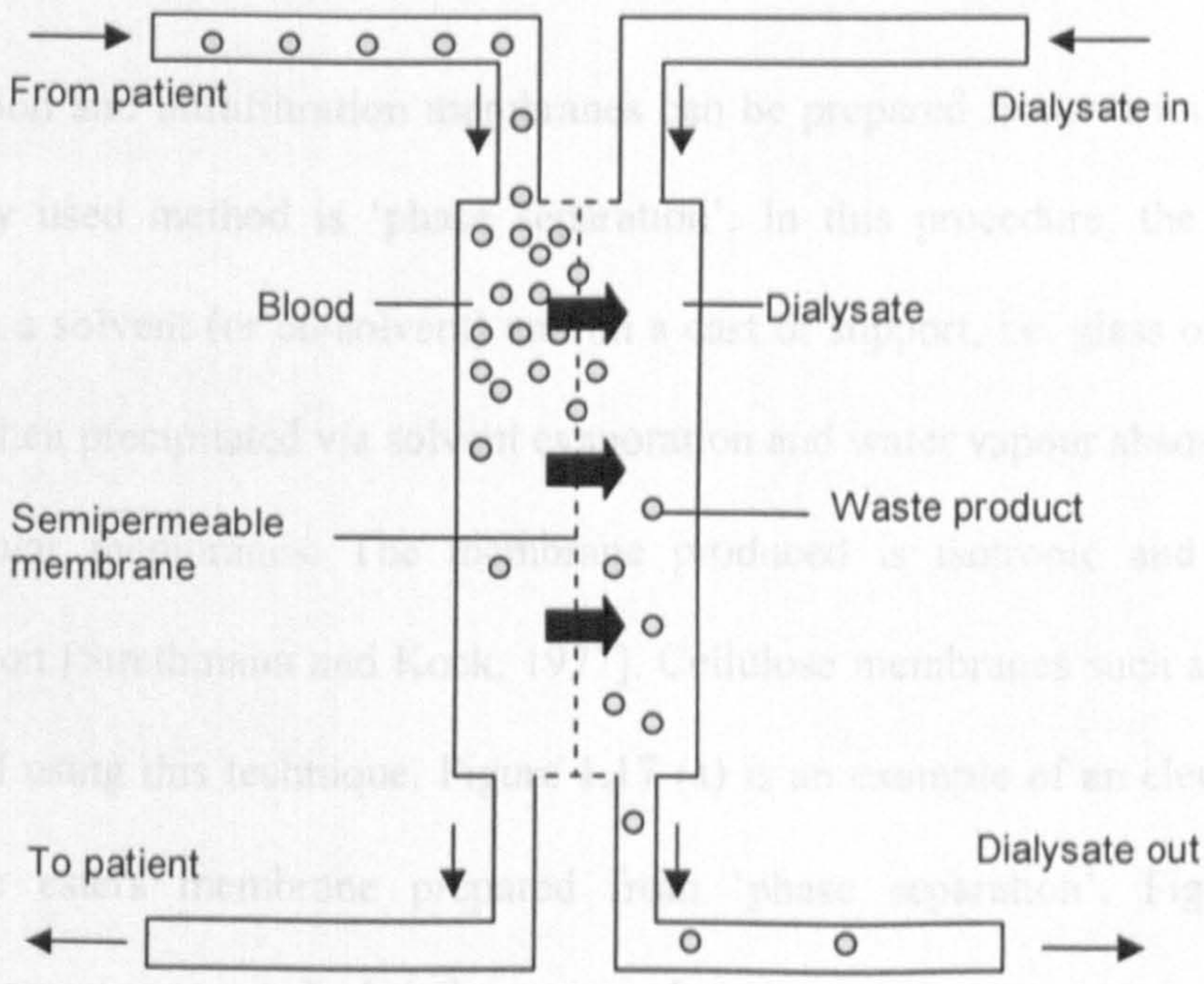

Figure 1.16: Schematic illustration of haemodialysis [adapted from Matsuura, 1994].

In Figure 1.16, the blood flows from the body into the dialyser where the waste products (potassium and urea) and free water are permeate across the semi-permeable membrane into the dialysate. The waste products are carried away by the dialysate while the cleansed blood is returned to the patient.

The synthetic membranes employed during haemodialysis can be divided into two categories: cellulose-based and polymeric-based membranes [Bellomo and Ronco, 2001].

The cellulose-based membranes (e.g. Cuprophan, Hemophan, Cellulose Acetate) are generally considered as 'low flux' membranes, i.e. membranes with a permeability coefficient to water (Km) <10 ml/h.mmHg/m^2 [Bellomo and Ronco, 2001]. Cellulose based membranes are very thin (5 to 15 μm of wall thickness) and have a symmetrical structure with uniform porosity, and they strongly hydrophilic. The polymeric-based membranes (e.g. polysulfone, polyamide, polyacrylonitrile, polymethylmethacrylate) are high flux membranes with a Km >30 ml/h.mmHg/m^2. Polymeric-based membranes retain larger molecules (10–30 000 Daltons) and are generally hydrophobic in nature [Bellomo and Ronco, 2001].

Microfiltration and ultrafiltration membranes can be prepared from various processes. The most widely used method is 'phase separation'. In this procedure, the polymer is first dissolved in a solvent (or co-solvent) and on a cast or support, i.e. glass or metal plate, the polymer is then precipitated via solvent evaporation and water vapour absorption thus obtain flat or tubular membranes. The membrane produced is isotropic and widely used in microfiltration [Strathmann and Kock, 1977]. Cellulose membranes such as cellulose esters are prepared using this technique. Figure 1.17 (a) is an example of an electron micrographs of cellulose esters membrane prepared from 'phase separation'. Figure 1.17 (b) is anisotropic membrane made by the same phase separation procedure except that the polymer precipitation step is done via immersion in water bath. This process is well known as the Loeb-Sourirajan technique and is a common procedure for almost all ultrafiltration as well as reverse osmosis membranes [Loeb and Sourirajan, 1963]. Polycarbonate Nuclepore® shown in Figure 1.17 (c) is a 'Track-etched' membrane and the preparation of this membrane is a two-step process. During the first step, the polymer film is irradiated with charged particles from a nuclear reactor, leaving tracks where the chemical bonds in polymer backbone are broken. In second step, the irradiated film is placed in an etching bath where the damaged tracks are etched forming cylindrical pores [Fleischner *et al.*, 1972]. Figure 1.17 (d) shows the expanded-film membrane. This membrane is prepared via

stretching propylene film in a direction in which pores are visible as elongated or 'stretched' under electron microscope. This membrane consists of alternating fibres and lamella which are formed by a process whereby a highly crystalline polymer are melt-extruded and subsequently recrystallized under high stress. This technique is developed at Celanese and propylene membrane produced by this procedure under the trade name Celgard [Bierenbaum *et al.*, 1974].

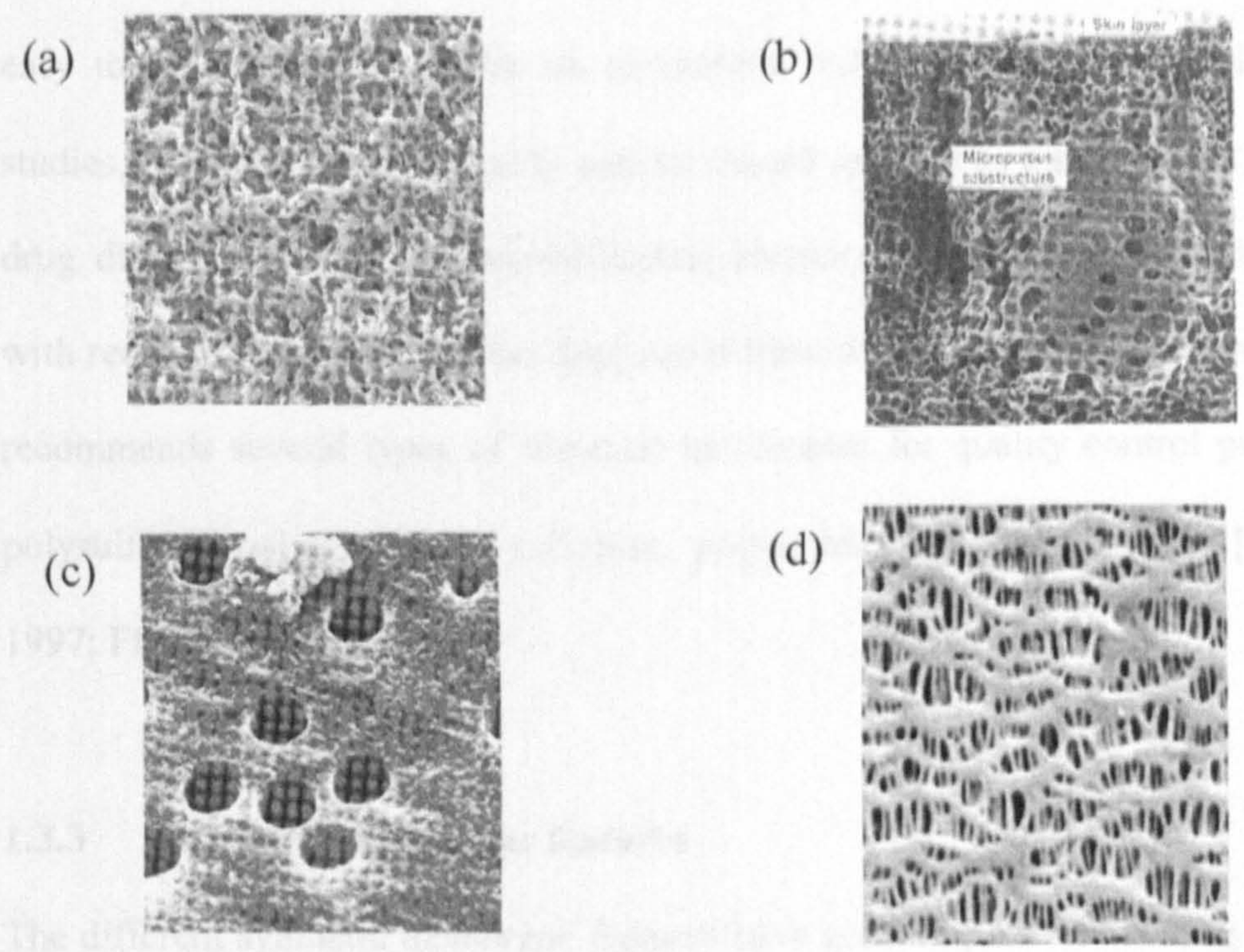

Figure 1.17: Scanning electron micrographs at approximately the same magnification of four microporous membranes (a) Cellulose esters (Millipore, Corp.) by phase separation; (b) Anisotropic polysulfone membrane made by Loeb-Sourirajan phase separation process; (c) Nuclepore® polycarbonate 'track-etched' film; and (d) Celgard® (polypropylene) expanded film membrane. [Adapted from Baker, 2004a - exact magnification not given]

It is emphasised that the shape of the pores and the pore tortuosity of synthetic membranes are very much influenced by the method of preparation. Phase separation and Loeb-Sourirajan technique produces porous membranes with high tortuosity (~1.5), while Track-etched membrane pores lack tortuosity because they possess cylindrical pores which have

the tortuosity value of close to 1. In terms of the shape most porous membranes possessed spherical pores, but from the micrographs above expanded film membranes has 'elongated' pores due to its manufacturing process.

In the literature, the synthetic membranes used with Franz cells for topical product assessment are mainly obtained from ultrafiltration and microfiltration applications. This is because these membranes have fulfilled the membrane criteria for quality control, i.e. inert, easy to obtain and may offer no diffusional resistance to drug diffusion. In Franz cell studies, the membrane for quality control should only act as a support but not as a barrier to drug diffusion. Ultra- and microfiltration membranes possess interconnected pores filled with receptor fluid in which the drug can diffuse directly into the receptor media. The FDA recommends several types of filtration membranes for quality control purposes, including polysulfone, polypropylene, cellulose, polyamide, and polyacrylate. [FDA-SUPAC-SS, 1997; Flynn *et al.*, 1999].

1.3.3 Synthetic membrane features

The different synthetic membrane features have great impact on the drug diffusion in Franz cell experiments. In Fick's Law, the stratum corneum is treated as a homogenous layer. So, the synthetic substitute for skin mimicry in Franz cell studies is often a homogenous membrane rather than heterogenous. But for quality control, as long as the synthetic membrane does not resist drug diffusion, the membrane can be either homogenous or heterogenous. Generally, the synthetic membrane can be 'isotropic' or 'anisotropic', which many Franz cell investigators may not appreciate.

The principle types of membranes are shown schematically in Figure 1.18 below. Isotropic membranes have a uniform composition and structure throughout and can be porous or dense as showed in Figure 1.18 (a) to (c). Microporous membranes have pores which are uniformly distributed, while dense membranes are non-porous and relatively thicker.

Electrically charged membranes can be dense or microporous, with pore walls carrying fixed charged ions. On the other hand, anisotropic (asymmetric) has heterogenous structure, and may contain pores or layered structures. Both Figure 1.18 (d) and (e) are typical anisotropic synthetic membranes. Figure 1.18 (d) describes an anisotropic microporous membrane which consists of an extremely thin layer supported on a much thicker porous sublayer. Whilst Figure 1.18 (e) is a composite membrane where a dense polymer layers are coated onto the surface of a microporous support.

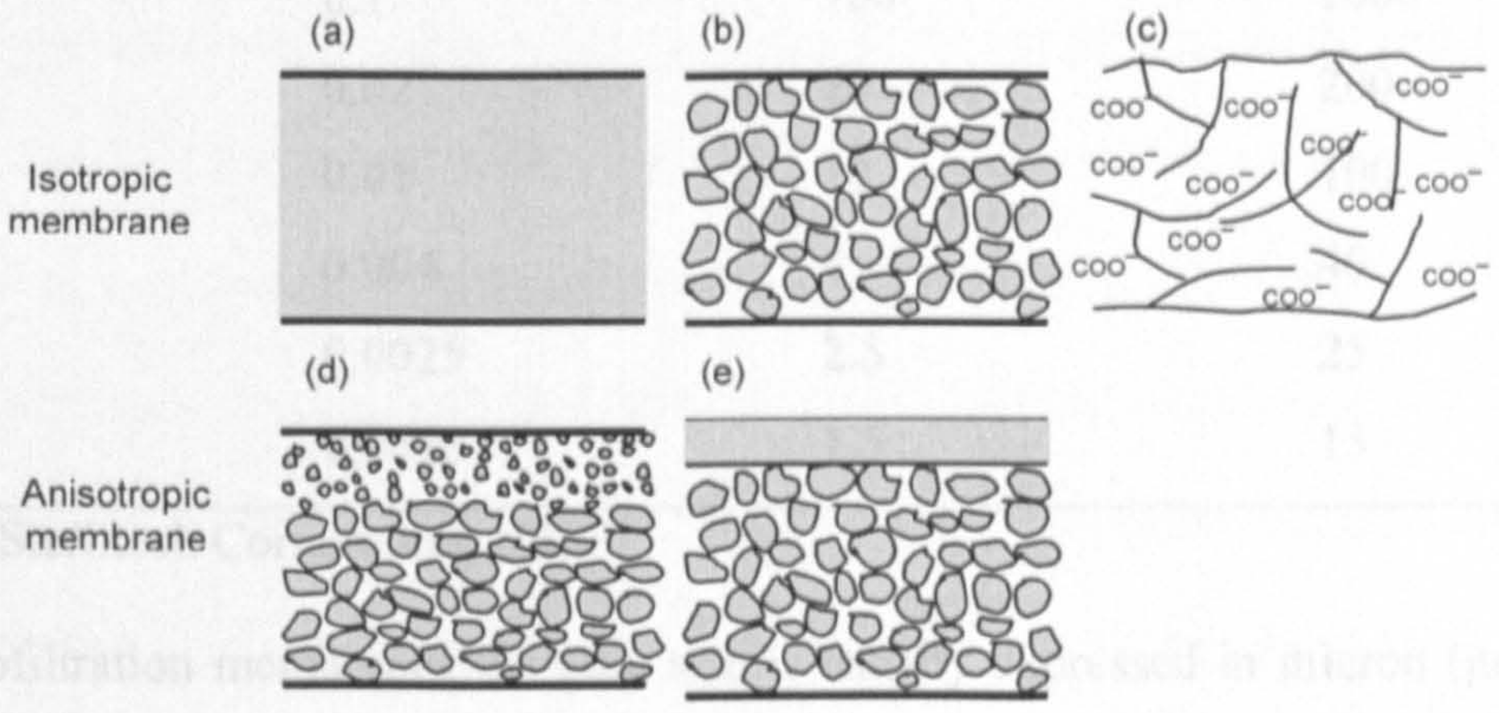

Figure 1.18: Isotropic (a) Isotropic microporous membrane; (b) Non-porous dense membrane; (c) Electrically charged membrane. Anisotropic (d) Loeb-Sourirajan anisotropic membrane; (e) Thin-film composite anisotropic membrane. [adapted from Baker, 2004b]

Another feature in which Franz cell investigators may overlook when using synthetic membranes is the description of the membrane 'pores'. In the context of porous membranes, it is useful to understand the definition of 'pore size' and 'molecular weight cut-off'. In porous membranes, the pores usually do not have the same size but exists as a normal distribution of sizes. The term pore size of a membrane represents the nominal or average of the pore diameter measured. (Pore size should not be confused with the term porosity (section 1.3.4) which is the fraction of pore volumes in a membrane). The molecular weight cut-off (MWCO) is defined as that molecular weight is 90% rejected by the membrane. For example, a membrane has a MWCO of 10,000 Da implying that all solutes with a molecular

weight greater than 10,000 are more than 90% rejected. Dalton (Da) is the non-SI unit for molecular weight but it is often used to express in MWCO. KiloDalton (kDa) is equal to 1,000 Molecular Weight Cut-Off (MWCO). A solution having a molecular weight of 1,000,000 would be equivalent to 1,000 KD. The table listed below gives a general relationship between kiloDalton to Microns (micrometers), Nanometers, and Angstroms:

Table 1.5: The relationship between Daltons, microns, nanometers and angstroms.

kiloDalton (kDa)	Microns (μm)	Nanometers (nm)	Angstroms ( )
1,000	0.1	100	1000
500	0.02	20	200
200	0.01	10	100
50	0.004	4	40
10	0.0025	2.5	25
5	0.0015	1.5	15

Source: Sterlitech Corporation, USA

In microfiltration membranes the pore size is usually expressed in micron (μm) while for ultrafiltration membranes, the term 'molecular weight cut-off' (MWCO) is preferred.

1.3.4 Mass transport theory via synthetic membrane

The synthetic membranes in Franz cells are used for skin simulation and formulation quality assessment. The former (e.g. silicone membranes) often employs non-porous membrane while the latter uses porous membrane (e.g. polysulfone, cellulose esters). The route of a drug molecule transport across a porous and non-porous membrane is shown in Figure 1.19.

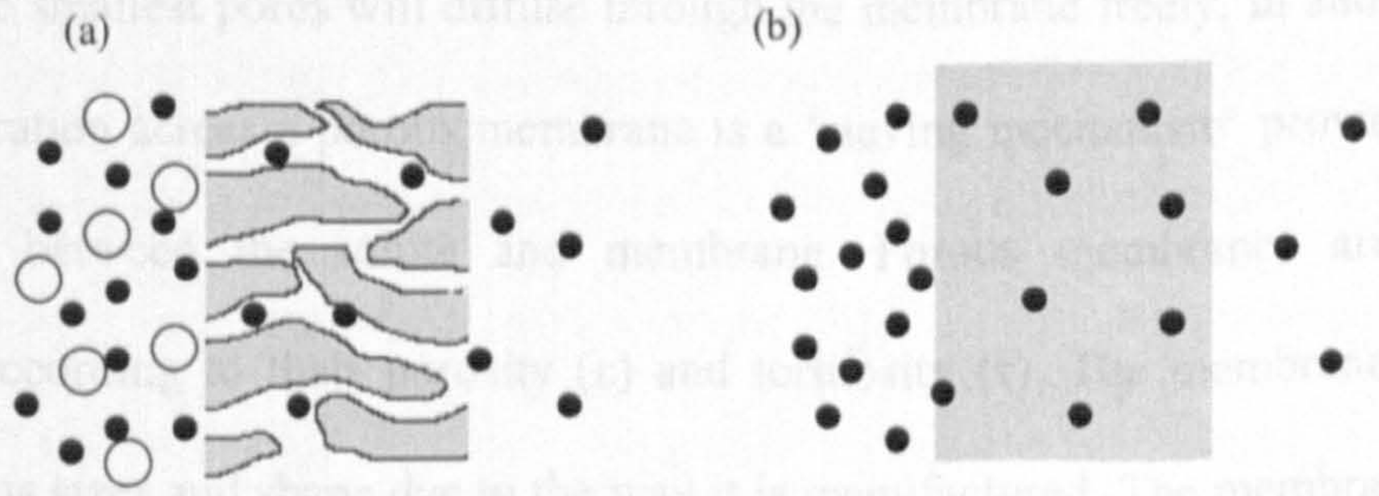

Figure 1.19: Illustration of solute transport across a porous (a) and non porous (b) membrane.

The transport across non-porous membrane is dependent on the chemical nature and structure of the polymeric membrane and the interaction between the polymer and the drugs. The non-porous membranes usually exhibit crystalline or semi-crystalline structure. The permeants traverse the membrane through the tiny spaces in between the polymer chains caused by thermal motion of the polymer molecules. The solutes are transported across a non-porous membrane via diffusion process and the selectivity of the solute is depended upon the partition coefficient between the solute in the vehicle and the membrane, as well as the diffusivity of the solute within the membrane. Examples of such solute transport are observed in gas separation and pervaporation. The permeation of solute through a non-porous membrane can be described using solution-diffusion model. The solution-diffusion model requires the permeant to dissolve in the membrane material, and then diffuse through the membrane down a concentration gradient. This model suggests that a steady-state permeation rate (J) is based on Fick's Law of diffusion. Hence Equation 1.3 again applies, i.e. J =D.K.Cv/h.

Porous membranes are structurally rigid and contained randomly distributed, interconnected void volume (pores). Separation of solutes (e.g. in microfiltration and ultrafiltration) is mainly governed by the function of molecular size and pore size distribution. Particles larger than the largest pores are completely rejected by the membrane; particles smaller than the largest pores but larger than the smallest pores are partially rejected and particles much smaller than the smallest pores will diffuse through the membrane freely. In another words, the solute separation across a porous membrane is a 'sieving mechanism' provided there is no interaction between the solute and membrane. Porous membranes are normally characterized according to their porosity (ε) and tortuosity (τ). The membrane pores can appear in various sizes and shape due to the way it is manufactured. The membrane porosity is defined as the fraction of the total membrane volume that is porous, or

$$\text{Porosity (\%)} = \frac{\text{total pore volume}}{\text{total membrane volume}} \times 100\ \%$$

Figure 1.20 illustrates three porous membranes with equal porosity but different pore diameter.

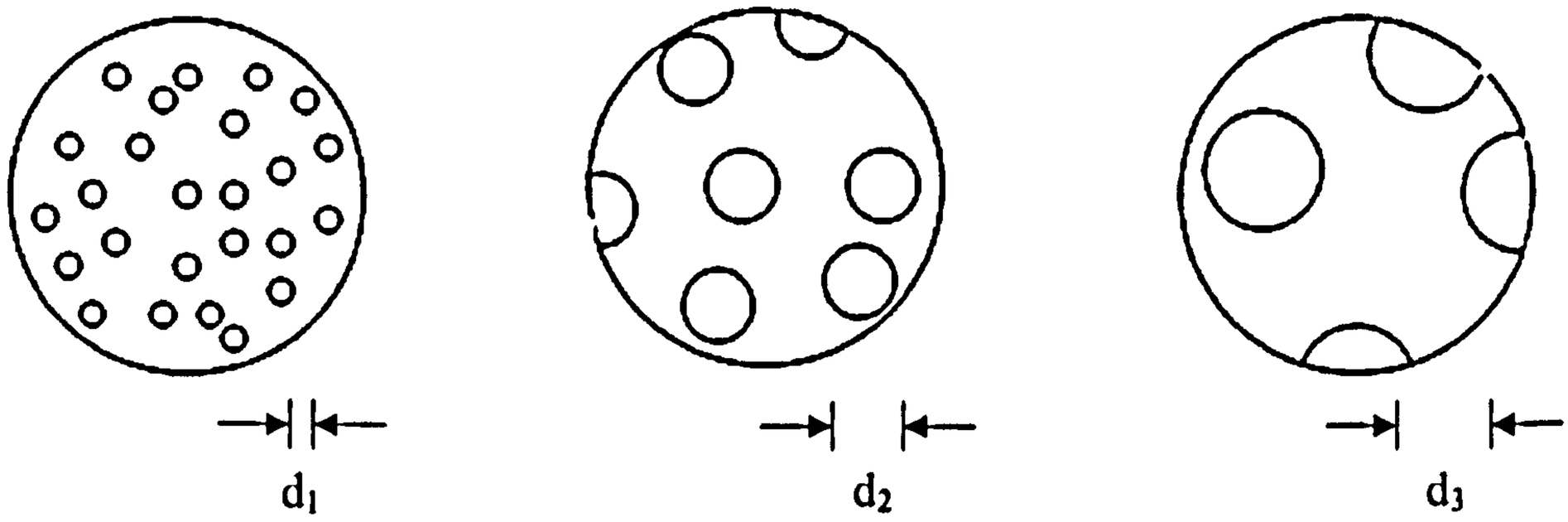

Figure 1.20: Surface view of porous membranes of equal porosity (ε) but differing in pore size (pore diameter $d_3 > d_2 > d_1$).

Typical microporous membranes have average porosity of 30-70%. This can be obtained by weighing the membrane before and after filling the pores with an inert liquid. However, this should be treated with caution if the membrane is asymmetric, where the porosity varies from place to place. For example, Loeb-Sourirajan membranes may have an average porosity of 70-80 % (including membrane support), but the actual porosity of the layer that performs the separation maybe as low as 50%. The term porosity is not the same as 'pore size' (pore diameter), although the literature often uses the terms interchangeably.

Membrane tortuosity is simply the average pathlength over the membrane thickness. It reflects the length of the average pore compared to the membrane thickness. For cylindrical perpendicular pores, the tortuosity is equal to unity (Figure 1.21). Solutes usually take the meandering path and the typical tortuosity of a porous membrane is within 1.5 – 2.5.

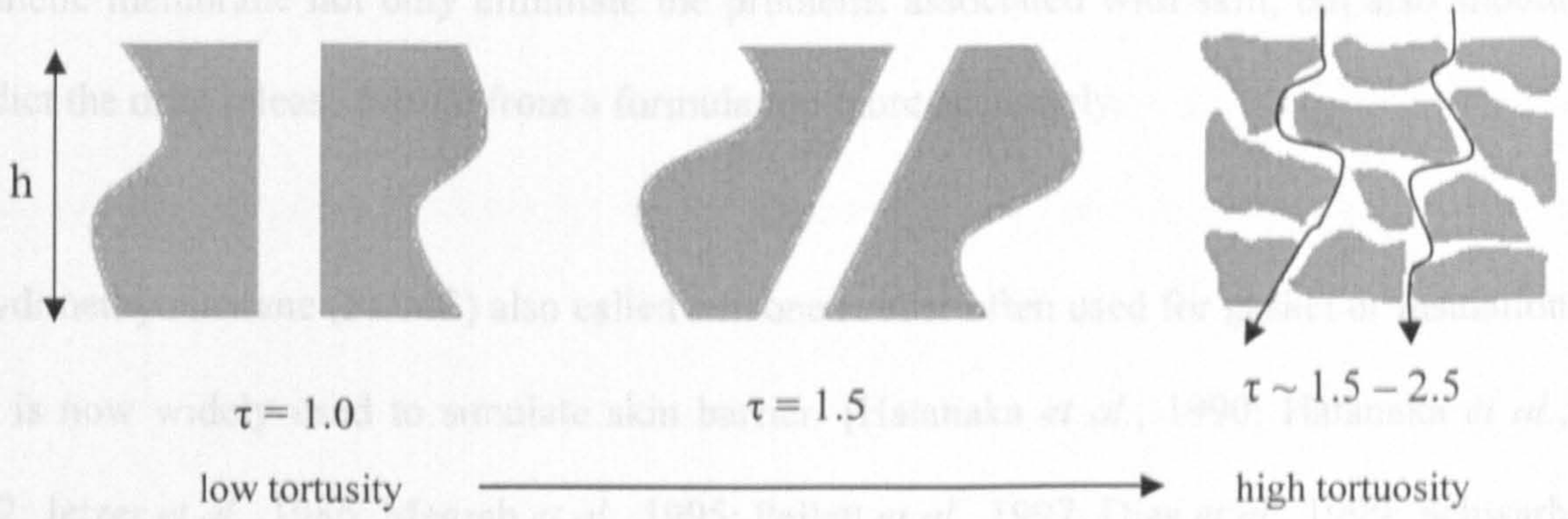

Figure 1.21: Cross-sections of porous membranes of different tortuosity (τ).

Equations 1.1 to 1.3 have been extensively studied in the past, mostly in *in vitro* studies where excised skin is used with diffusion cells. These equations are also applied for porous synthetic membranes but several parameters such as membrane porosity and pore tortuosity have been considered. For example Hatanaka and co-workers attempted to modify Fick's Law to allow for the fact that the drug transport is via the pores, thus the tortuosity and porosity factor of a membrane were included in a modified equation [Hatanaka *et al.*, 1990]:

$$J = \frac{D_v.K'.\varepsilon .C_v}{\tau.h} \qquad \text{Eq. 1.7}$$

where K' is the partition coefficient of the drug between the solvent in the membrane pore and the drug vehicle, ε is membrane porosity, τ is tortuosity and D_v is the diffusion coefficient of the drug into the vehicle that fills in the membrane pore (denote by subscript 'v').

1.3.5 Synthetic membranes for skin mimicry

Natural skin is not always readily available, especially human skin. The handling and storage procedure is tedious [Diembeck *et al.*, 1999]. In addition, skin itself exhibits biological variations such as skin age, and regional body variability [Wester and Maibach, 1992]. The use of a model synthetic membrane to simulate skin is desirable because

synthetic membrane not only eliminate the problems associated with skin, but also should predict the drug release profile from a formulation more accurately.

Polydimethylsiloxane (PDMS) also called silicone rubber often used for gasket or insulation mat is now widely used to simulate skin barrier. [Hatanaka *et al.*, 1990; Hatanaka *et al.*, 1992; Jetzer *et al.*, 1986; Megrab *et al.*, 1995; Pellett *et al.*, 1997; Dias *et al.*, 1999; Schwarb *et al.*, 1999; Smith and Irwin, 2000]. It is hydrophobic in nature and possesses similar rate-limiting permeation properties as skin thus making it a suitable choice for prediction of drug permeation. Drug transport across PDMS membrane can be represented using Fick's Law of diffusion. The rate-limiting property of PDMS membrane is not suitable for routine quality control evaluation of semisolid products since performance of the formulation can not be detected. Furthermore, the release through the PDMS can be slow making increasing testing time beyond what would be reasonable for quality control testing.

Although the *in vitro* methods are widely employed to examine the performance of a drug formulation, there is still some discrimination from the realistic situation. For example, metabolic activity within the epidermis which may with the interfere transport of a topically applied drug not so dominant with excised skin [Guzek *et al.*, 1989]; and drug testing for diseased skin conditions such as psoriasis is less applicable using *in vitro* model. Thus, *in vitro* data can not be directly translated into clinical situation, but only use as a qualitative prediction. It is also emphasized by many regulatory bodies that such a test is not a surrogate test for *in vivo* bioavailability or bioequivalence [Shah, 2005; Shah *et al.*, 1998b]. This is particularly important for a development of promising dosage form and prediction of systemic risk from dermal exposure to chemicals [EC, 2004].

1.3.6 Synthetic membranes for quality control

In the very early literature, drug release from a topical semisolid preparation is assessed by placing the dosage form in direct contact with a receiver medium in an apparatus equipped

with an agitator [Dempski *et al.*, 1969; Young *et al.*, 1968]. The amount of drug released was determined by collecting the solution medium periodically. One direct implication was the unwanted dispersion or dissolution of the semisolid in the medium. Physical disturbance of the semisolid surface caused by stirring also occurred. So the requirement for a membrane to separate the formulation from the receptor became crucial. Since the main objective of a release test is to examine the properties of the drug and formulation, the membrane should be inert and act simply to separate the drugs and dissolution media, otherwise the release slope will not reflect the conditions within the formulation.

A numbers of studies concluded that by using artificial membrane, Franz cells can serve as a promising tool for quality control procedure and assuring product batch-to-batch uniformity [Kundu *et al.*, 1993; Shah and Elkins, 1995; Shah *et al.*, 1998a; Shah *et al.*, 1999; Zatz, 1995]. Much attention has been given to the investigation of drug release from semisolid dosage forms such as creams, ointments, gels and pastes [Corbo, 1995; FDA-SUPAC-SS, 1997; Liebenberg *et al.*, 2004; Shah *et al.*, 1999; Shah *et al.*, 1998b; Skelly *et al.*, 1987] because these formulations are very widely used in dermatological products. The usual physical and chemical tests such as solubility, particle size, crystalline form of the active ingredient, viscosity and homogeneity of the product have been carried out to provide reasonable evidence of consistent performance of the finished products. The *in vitro* release rate can show the combined effect of chemical and physical changes such as solubility and rheological properties of the dosage form. Changes in the characteristics of a drug product would be expected to show a difference in the rate of drug release [Shah *et al.*, 1998a]. Therefore, the Franz cell is a useful tool to assess the product changes. In May 1997, the FDA released a guidance entitled 'Scale-up and Post-approval Changes: Chemistry, Manufacturing and Controls, *In vitro* Release Testing and *In vivo* Bioequivalence Documentation for Non-sterile Semisolid Dosage Forms (SUPAC-SS). The guidance recommends that *in vitro* release testing is used as a standard procedure to detect changes that could have a significant impact on formulation quality and performance of the product.

This includes change in the amount of an excipient, batch size or manufacturing equipment, process or site of manufacture [FDA-SUPAC-SS, 1997].

In 1989, Shah and co-workers from the FDA were the first to demonstrate that a Franz diffusion cell system and a synthetic membrane could provide a simple and reproducible method that can be easily adopted for the quality control of a semisolid product [Shah *et al.*, 1989]. The kinetics of drug release from a formulation can be analysed using Franz cell with a suitable synthetic membrane. As opposed to skin simulation, the synthetic membrane in quality control should not be rate-limiting, but only serve to separate the formulation and the receiver media. In 1997, a scientific workshop entitled Assessment of Value and Application of *In vitro* Testing of Topical Dermatological Drug Products outlined a general methodology and technique for the evaluation of topical product performance. The workshop stated that the membrane must have the least possible diffusional resistance, and possess minimal drug binding. The membranes should also have little interaction with the receptor medium and commercially available [Flynn *et al.*, 1999].

Table 1.6 below shows the compilation of topical drug diffusion studies using synthetic membranes employed by various authors. Information includes the drug, vehicle, receptor medium, diffusion cell type, synthetic membranes and analysis methods. From Table 1.6 above, it was noticed that synthetic membranes of various materials, pore size and thickness were used for the assessment of different types of drugs and formulation preparations. Notice that the most commonly used membranes are silicone membrane, cellulose and polysulphone membranes.

Table 1.6: Topical drug delivery diffusion studies using synthetic membranes.

Drug	Vehicle	Receptor Solution	Cell Type	Synthetic membrane pore size or (thickness)	n	Analytical method	Reference
Acyclovir	Creams	0.9% Sodium chloride	Flow-through	Cellulose acetate, 0.45 µm Polyvinylidene difluoride, 0.45 µm Polytetrafluoroethylene, 0.45 µm Cellulose mixed esters, 0.45 µm Dialysis membrane, MWCO 12-14kDa	3	HPLC	Chattaraj and Kanfer, 1995, Chattaraj and Kanfer, 1996
Acyclovir	Gels	Phosphate buffer pH 7.0	Static	Dialysis membrane MWCO 12-14 kDa	3	UV	Bonferoni *et al.*, 1999
Amino diether	Oil-in-water emulsion with various polymers	0.1M Hydrochloric acid and PBS	Static	Silicone (0.125mm)	13	UV	Welin-Berger *et al.*, 2001
Betamethasone 17-valerate	0.1% in isopropyl myristate solution	Isopropryl myristate	Side-by-side	Silicone (0.127 mm) Visking Nuclepore	≥ 3	HPLC	Smith and Haigh, 1992
betamethasone dipropionate	Cream	Hydro-alcoholic v/v mixture	Static	Polysulfone ,Tuffryn, 0.45 µm Polyethersulfone, Supor, 0.45 µm	6	HPLC	Shah *et al.*, 1999

Table 1.6: Topical drug delivery diffusion studies using synthetic membranes (cont.)

Drug	Vehicle	Receptor Solution	Cell Type	Synthetic membrane pore size or (thickness)	n	Analytical method	Reference
Caffeine	Concentrated oil-in-water emulsion	Phosphate buffer pH7.4	Static	Polysulfone Cellulose Silicone	6	HPLC	Clement *et al.*, 2000
Fentanyl	Patch in Pluronic gel	Phosphate buffer pH7.4	Static	Cellulose, 3500 Da	6	HPLC	Liaw and Lin, 2000
Fluocinonide	Co-solvent (Ethanol, PG, Glycerol, water)	Ethanol: PEG (1:1)	Static	Silicone membrane, Sil-Tec™ (0.01cm)	5	HPLC	Schwarb *et al.*, 1999
Hydrocortisone	Creams, ointment, lotion	Phosphate buffer pH7.4, pH 5.0, and 0.9% sodium chloride	Static	Cellulose acetate, 0.45 µm (150 µm) Polyvinylidene difluoride, 0.45 µm	6	HPLC	Shah *et al.*, 1991
Hydrocortisone	Cream	Phosphate buffer pH 5.0 and pH 7.4, 0.9% sodium chloride	Static	Cellulose acetate, 0.45 µm (150 µm) Polysulfone 0.45 µm (165 µm) Glassfiber 0.45 µm, (450 µm) Silastic (250 µm)	6	HPLC	Shah *et al.*, 1989

Table 1.6: Topical drug delivery diffusion studies using synthetic membranes (cont.)

Drug	Vehicle	Receptor Solution	Cell Type	Synthetic membrane pore size or (thickness)	n	Analytical method	Reference
Hydrocortisone, Betamethasone valerate, Triamcinolone acetonide	Cream	Phosphate buffer pH 7.4, 60% ethanol-water	Static	Cellulose ester, 0.45 µm, (150 µm)	6	HPLC	Shah *et al.*, 1993
Ketoprofen	Gel, carbomer and poloxamer	Phosphate buffer pH7.4	Static	Polysulfone, Tuffryn, 0.45 µm	3	UV	Proniuk *et al.*, 2001
Ketoprofen	Gel (Carbosil)	Phosphate buffer pH7.4, PEG 400	Static	Silicone (0.13 mm) Nylon, 0.2 µm (57 µm) Celgard, 0.05 µm (26.6 µm)	6	HPLC	Gallagher *et al.*, 2003a
Levonorgestrel	Suspension in co-solvent (ethyl acetate: ethanol)	0.9% Sodium chloride	Flow-through	Polymethylpentene (76 µm) Ethylene vinyl acetate (64 µm) Polyester elastomer (25 µm) Polyethylene, high-density	3	HPLC	Friend *et al.*, 1989
Naproxen	Gel	Phosphate buffer pH 7.4	Static	Cellulose acetate, 0.45 µm	3	UV	Morell *et al.*, 1996

Table 1.6: Topical drug delivery diffusion studies using synthetic membranes (cont.)

Drug	Vehicle	Receptor Solution	Cell Type	Synthetic membrane pore size or (thickness)	n	Analytical method	Reference
Nitroglycerin	Ointments	Phosphate buffer pH7.4	Static	Polysulfone, 0.45 µm Acrylic polymer, 0.45 µm Glass fiber (3.5µm) Mixed cellulose ester, 0.45, 0.8 µm Polypropylene, (10 µm) Polytetrafluoroethylene, (5 µm)	2	HPLC	Wu *et al.*, 1990
Paraben esters	Saturated solutions	De-ionised water	Flow-through and Static	Silicone (0.127 mm)	3	HPLC	Addicks *et al.*, 1987
Piroxicam	Co-solvent (PG/water, 40:60 v/v)	Phosphate buffer pH7.4	Static	Silicone membrane	3	HPLC	Pellett *et al.*, 1997
Piroxicam	Gel, carbomer	Phosphate buffer pH7.4	Static	Cellulose nitrate, 0.2 µm	3	UV	Santoyo *et al.*, 1996
Retinoic acid	Cream	35% Ethanolic-phosphate buffer ph 5.5	Static	Polysulfone Polyethersulfone Nylon Cellulose acetate	6	HPLC	Thakker and Chern, 2003
Salicylic acid, Benzoic acid	Various alcohols	Phosphate buffer pH7.4	Static	Silicone membrane (0.04cm)	3	UV	Dias *et al.*, 2001

Today, the porous synthetic membranes in the literature used for quality control (e.g. cellulose acetate, polysulfone) are often 'borrowed' from the separation and filtration application, mainly from microfiltration and ultrafiltration membranes. Table 1.7 shows the synthetic membranes employed in Franz diffusion cells studies in this thesis. The membrane thickness, molecular-weight cut off (MWCO) range, nominal pore size, porosity and individual manufacturers are also shown. Note that all of the membranes listed are porous because our studies only on membranes for quality control purposes; PDMS (non-porous) was listed for comparison purposes.

Table 1.7: Summary of the synthetic membranes properties. All values are nominal provided by manufacturers (□ - membrane porosity, τ – membrane tortuosity).

Membrane	Polymer[a]	MWCO (kDa)	Pore size (μm)	Thickness (μm)	□ (%)	τ	Source
Cellulose-based							
Visking	RC	12-14	-	20[b]	-	-	Medicell
Cuprophan	RC	10	-	10[b]	-	-	Medicell
Benzoylated tubing	RC	1.2-2	-	35[b]	-	-	Sigma
cellulose ester	CE	0.5	-	80[b]	-	-	Spectrumlab
Cellulose nitrate	CN	-	0.45	125	66-84	-	Whatman
Polymeric-based							
AN 69	PAN	40	-	25[b]	-	-	Hospal
Biodyne	PA	na	0.45	152	50-75	-	Pall
Supor	PES	na	0.45	145	80	~1-1.5	Pall
Tuffryn	PS	na	0.45	145	60	~1-1.5	Pall
Nuclepore	PC	na	0.1	10	8	~1	Whatman
Cyclopore	PC	na	0.1	10	4	~1	Whatman
Celgard 3500	PP	na	0.05	20	35-48	-	Hoechst
Silicone	PDMS	na	-	400	-	-	SAMCO

[a] RC - Regenerated cellulose, CE - Cellulose esters, CN - Cellulose nitrate, PAN - Polyacrylonitrile, PA – Polyamide (nylon), PES - Polyethersulphone, PS - Polysulphone, PC - Polycarbonate, PP - Polypropylene, PDMS – Polydimethylsiloxane.
[b] thickness measured using a digital micrometer (Mitutoyo, UK).

The synthetic membranes listed in the table were membranes employed in this thesis. They were derived from various applications and each of them is briefly described here.

The synthetic membranes employed in Franz cell studies in the literature as well as in this thesis can be broadly categorised as cellulose- and polymeric-based membrane. The cellulose-based membranes include the membranes made of regenerated cellulose and its derivatives. The regenerated cellulose is prepared from pure cellulose, i.e. without modification of the chemical groups on the sugar units. Ultrafiltration dialysis (Visking, Cuprophan and benzoylated dialysis tubing) membranes are made of the regenerated celluloses because they have high molecular clearance and compatible with blood. Cuprophan is a high permeability membrane produced via 'cuproammonium' process. It is fabricated very thinly (~10 μm) chiefly for the enhancement of the filtration efficiency in the dialysis. Cellulose ester is derived from esterification of the purified celluloses with acetic acid or nitric acid, forming cellulose acetate and cellulose nitrates respectively. The cellulose derivatives are chemically modified for the improvement blood compatibility, but in terms of stability the cellulose derivatives are known to be less chemically resistant compared to the pure celluloses (regenerated cellulose). Membranes made from celluloses exhibit excellent molecular clearances but they do exhibit blood incompatibility in some patients. This had lead to the emergence of polyacrylonitrile (e.g. AN69) membrane, another class of ultrafiltration membrane which is commonly used today. The polyacrylonitriles are not only be cast into very thin membrane (down to 5 μm) for high filtration efficiency, but are highly compatible with blood components compared to the celluloses [Chenoweth *et al.*, 1983]. However, the cellulose dialysis membranes are still widely used because they are cheap and readily available. Cellulose membranes are usually dry and brittle when manufactured. Membrane additives such as plasticizers (glycerin) and preservatives are often incorporated to maintain membrane flexibility for ease of packaging and handing. Nevertheless, the complete removal of plasticizer is crucial prior to use in Franz cells in order for the membrane full performance.

Polymeric-based membranes are literally membranes which are prepared from non-cellulosic polymers. Polyacrylonitrile, described above is a polymeric-based membrane. The

polyamides are another class of polymer which are widely utilised to make synthetic membranes. The aliphatic polyamides such as nylon 6,6 and nylon 6 show good chemical stability and may be used in microfiltration and ultrafiltration applications. Nylon membranes are generally hydrophobic because the polymer is a non-polar (polyamide) with terminal amino and carboxyl group. Pall (USA) exploited the unique chemical structure and designed the class of membrane called the 'Biodyne' membrane for the detection of charged macromolecules, such as amino acid and nucleic acid. The Biodyne membrane surface is either positively charged (quaternary ammonium group), negatively charged (carboxylic group) or amphiphatic. This is to facilitate the bonding of charged macromolecules on the membrane surface via electrostatic interactions. Biodyne has also been reported to be used as a support membrane for a novel skin model by fixing liposomes composed of stratum corneum lipids onto the membrane for the skin permeability studies [Matsuzaki *et al.*, 1993]. Synthetic membranes, made from polysulfone and polyethersulfone are also widely used as basic materials for ultrafiltration and as support materials for composite membranes. Tuffryn® and Supor® are examples of polysulfones membranes and they are designed by Pall (USA) for the optimisation of biological, pharmaceutical and sterilising filtration with the features of low protein binding and chemically inert. The track-etched membranes (Nuclepore® and Cyclopore®) are also manufactured for high filtration efficiency due to the lack of tortuosity of the pores. Celgard is a microporous polypropylene membrane made for a variety of barrier applications. This membrane is known as an expanded-film membrane and often contains additional coating which to provide a protective layer for the membrane.

The chemical structures of the membrane polymers are shown in Figure 1.22 below:

Cellulose-based

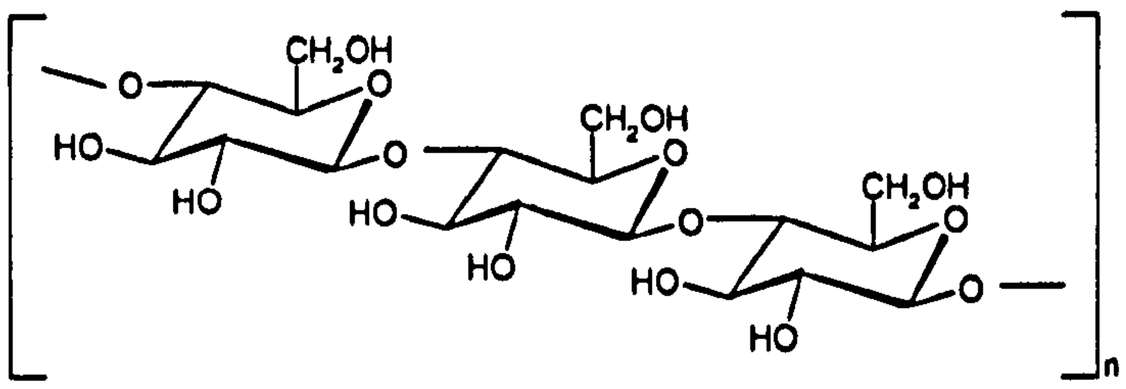

Regenerated cellulose

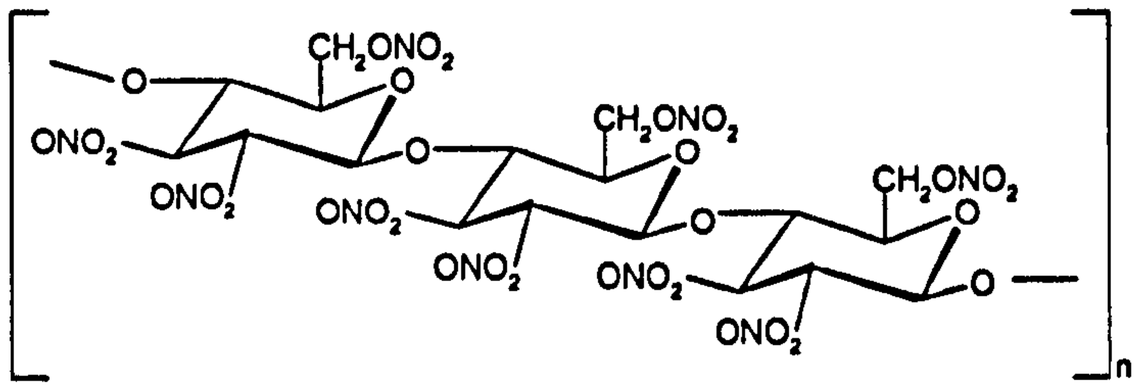

Cellulose Nitrate

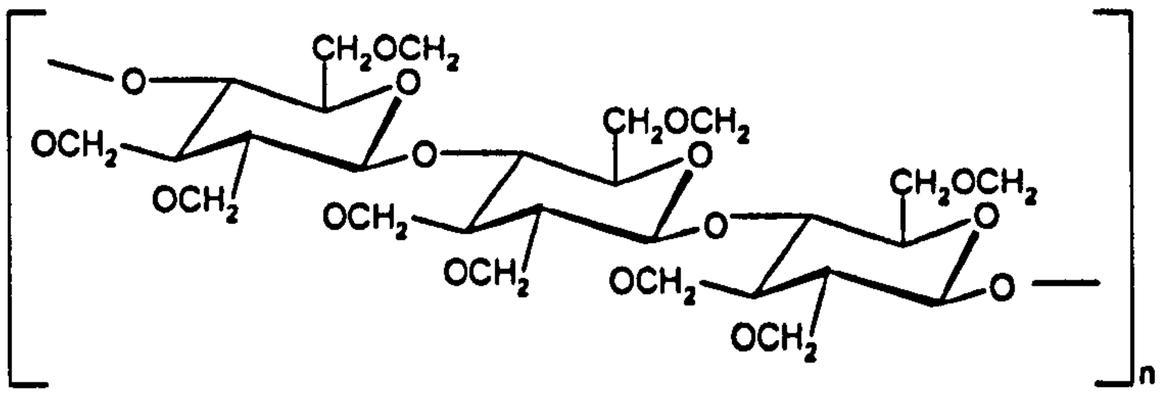

Cellulose Acetate

Polymeric-based

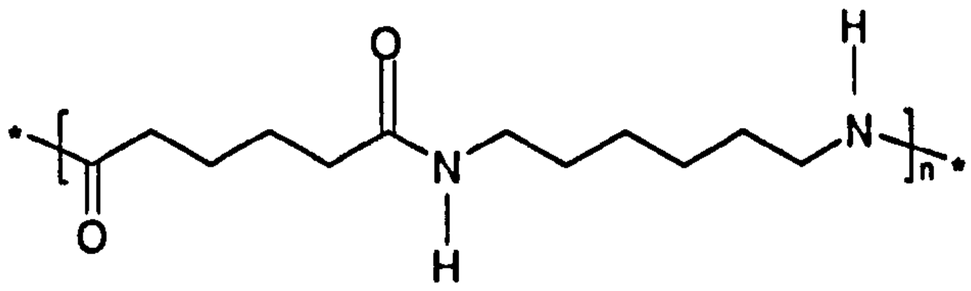

Polyamide (Nylon 6,6)

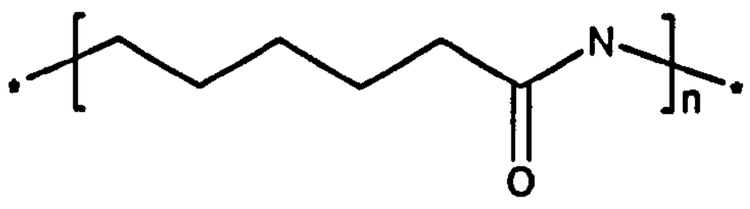

Polyamide (Nylon 6)

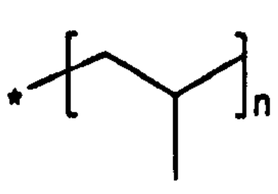

Polypropylene

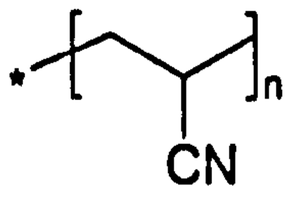

Polyacrylonitrile

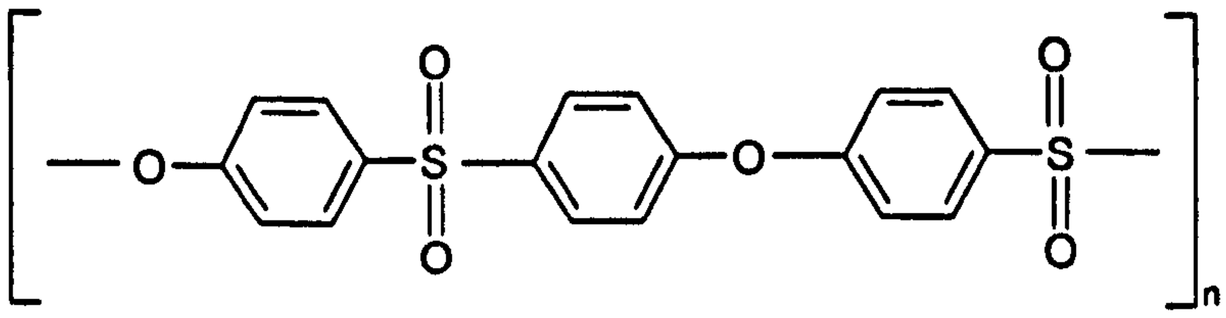

Polyethersulfone

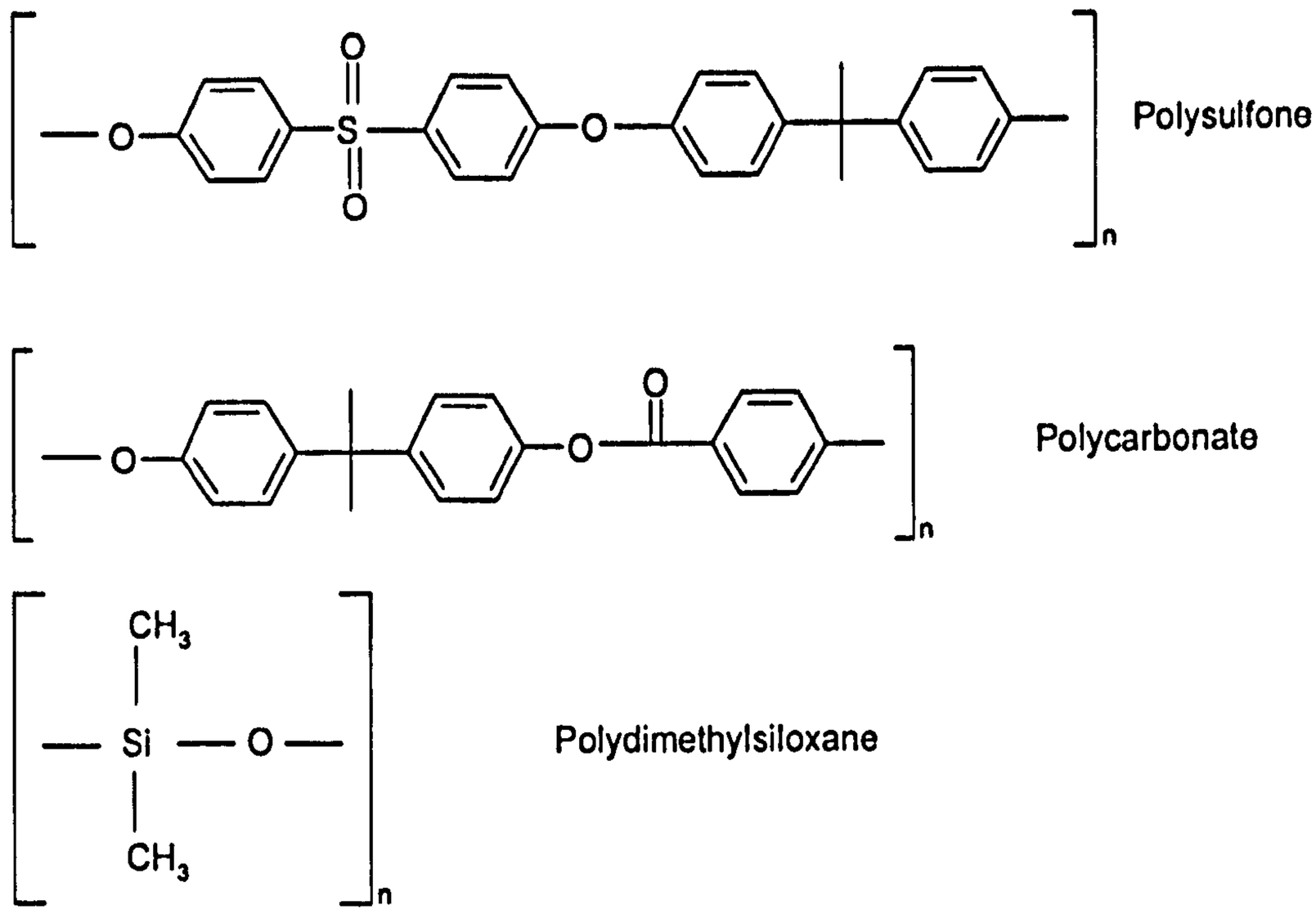

Figure 1.22: Chemical structures of common synthetic membranes.

All of these membranes (except PDMS) possess common features, i.e. they contained pores, are relatively chemically inert, have high compatibility with solvents, and are commercially available. Most investigators take advantage of these membrane features and employ them as their model membrane in Franz diffusion cell experiments for topical product quality control purposes. But these membranes are also intrinsically different, such that they all possess diverse thickness, porosity, tortuosity, and polymer materials, which many researchers have overlooked. In the literature, there is still a lack of information to justify the choice of synthetic membrane for the assessment of topical products taking into account of the different membrane parameters above. Hence an investigation on the influence of different types of the synthetic membranes on the Franz cell diffusion experiment using a model drug and a standard formulation is required.

1.4 Diffusion cell experimental design

In vitro testing is by far the simplest and most cost effective method for characterizing a drug's skin absorption and penetration profiles. The *in vitro* permeation experiments provide

the determination of parameters such as diffusion coefficient, permeation coefficient, lag time and the amount of drug permeating through the skin over time at steady state [Scheuplein and Blank, 1971]. When planning *in vitro* percutaneous absorption studies, there are many considerations that must be addressed to obtain useful results. Depending on the purpose of the investigation, experimental protocol must be designed to solve specific questions. There are several guidelines available which outline the methods for assessment of percutaneous absorption [Howes *et al.*, 1996; Skelly *et al.*, 1987] as well as for cosmeceutical risk assessment [Diembeck *et al.*, 1999; EC, 2004]. But the specific experimental designs remain loose, and investigators are flexible to develop their own methodology. Apart from the membrane (excised skin or synthetic membrane), the basic elements involved in measuring *in vitro* release from topical formulation are:

a) The diffusion cells and heating device

b) The conditions (stirring, temperature, receptor fluid, membrane, sink)

c) The assay

d) Analysis of the data

Reliable drug release data is generated from a well-designed experimental methodology. For *in vivo* simulation, the experimental design is crucial to allow the experimental conditions to be as close to *in vivo* condition as possible. Inappropriate experimental designs will lead to the false interpretation of the data. The following sections discuss the points to consider when setting up an *in vitro* release experiment, and these are general points applied to both skin and synthetic membranes.

1.4.1 Experimental conditions

The diffusion cells can be side-by-side or vertical diffusion cells (Figure 1.9 and 1.10). Excised skin or synthetic substitute is used mainly for *in vivo* correlation while a synthetic membrane support is employed for quality control purposes. The diffusion cells are positioned in a multiple-cell unit console which drives the magnetic stirrer to agitate the

receptor medium at a certain speed. Aliquots are removed from receptor cells and replaced with equal volume of fresh media in order to main sink condition.

By convention, the stirring of the receptor cell is performed by means of magnetic stirrer bar which placed at the bottom of the receptor. The seeking of optimum stirring speed and with the most suitable type of stirring bar is crucial for efficient stirring of the receptor compartment [Morell *et al.*, 1996; Smith and Haigh, 1992]. Determination of stirring efficiency is carried out in several ways. A coloured dye can be used to observe the stirring pattern or for measuring the time taken for the dye to distribute throughout the receptor cell [Gummer *et al.*, 1987]. Another method for checking the stirring efficiency is by sampling drug from top, middle and bottom portion of the receptor cell and check if there are statistical differences [Shah *et al.*, 1993]. The use of magnetic bars, however present a common problem: slow or incomplete stirring, may not disperse the drug into the sampling arms. Many investigators have attempted to modify the cell design, such as using flow-through cells or replacing the stirrer bar with spring coil to improve homogeneity [Shah *et al.*, 1999].

Sample taking with replacement of the receptor medium is carried out at regular intervals. Appropriate sampling time intervals vary with the drug solubility in the receptor medium and membrane permeability and the rate of sampling must be determined experimentally. The typical interval is every 30 to 60 min. Longer time intervals might be required if the drug permeation is slow, especially through the skin or synthetic membrane barrier. In contrast, when flux is high (e.g. quick release of drug from a formulation through a membrane support), shorter time intervals are required for the maintenance of sink conditions.

The choice of receptor fluid is also very important for the maintenance of sink conditions. The selection of receptor fluids is largely dependent on the nature of the drug; aqueous solutions such as phosphate buffer saline (PBS) and 0.9% sodium chloride are common receptor fluids for hydrophilic and moderately lipophilic drugs (up to log P = 2), while for very lipophilic drugs (aqueous solubility < 0.1 μg/mL), alcoholic media, co-solvent systems or the addition of a solubiliting agent into the aqueous solution is employed [Williams, 2003a]. 'The receptor fluid must not influence the membrane properties.

Most *in vitro* experiments are performed at skin temperature (32 ± 1°C) in order to mimic the *in vivo* situation [Skelly *et al.*, 1987]. This is commonly achieved by maintaining the receptor solution at 37°C so that the skin placed at the receptor orifice is slightly cooler than the receptor, i.e. at about 32°C. The can be done by means of water jackets or placing the receptor into temperature regulated heated steel chamber block. Membrane temperature muat be regulated because many studies demonstrate that temperature in diffusion cells has a direct affect on drug flux [Akomeah *et al.*, 2004; Clarys *et al.*, 1998; Ogiso *et al.*, 1998]. Akomeah and co-workers [Akomeah *et al.*, 2004] found that release rates for methylparaben, butylparaben and caffeine doubled with every 7-8°C rise in receptor temperature using silicone membrane and excised human skin. A multilaboratory studies found out that large result variability (up to 35%) exists in the methylparaben drug release through a synthetic membrane and the authors claimed that temperature may also be one of the sources of result variability [Chilcott *et al.*, 2005]. Hence, the maintenance of temperature of Franz cells is critical to achieve standardized drug release.

1.4.2 Finite versus infinite dose

The drug dosage applied onto the skin or synthetic membrane in an *in vitro* model can be a 'finite' or an 'infinite' dose. A 'finite dose' is when the drug dose applied is limiting and depletes with time; while an 'infinite' dose indicates that the drug concentration remains the

same throughout the whole experiment. Infinite dosing is usually achieved via applying saturated formulations and Figure 1.23 represents flux versus time for finite and infinite dose respectively.

The drug flux plot is generally composed of three phases [Franz, 1983]. Phase I represents the lag time, where the drug takes time partitioning into the skin and diffusing across the skin, i.e. no drug in the systemic circulation (receiver compartment) is detected. Shortly after the drug breaches the stratum corneum, the drug enters the capillaries (receiver compartment) causing a rise in drug concentration (Phase II of the curve). The last phase, phase III, is known as linear or falling phase, depending on the amount of drug applied onto the skin. If the drug supply is fixed (finite dose) it may eventually diminish. So shortly after achieving the highest concentration, the flux begins to fall [Franz, 1978]. On the other hand, if the drug is in excess amount (infinite dose) a linear steady state flux will sustain at its highest flux. The relationship between J, Cv, K and D is most easily understand if steady state (infinite dose) is assumed. However, in clinical practice steady state is seldom achieved because a finite dosage is often applied.

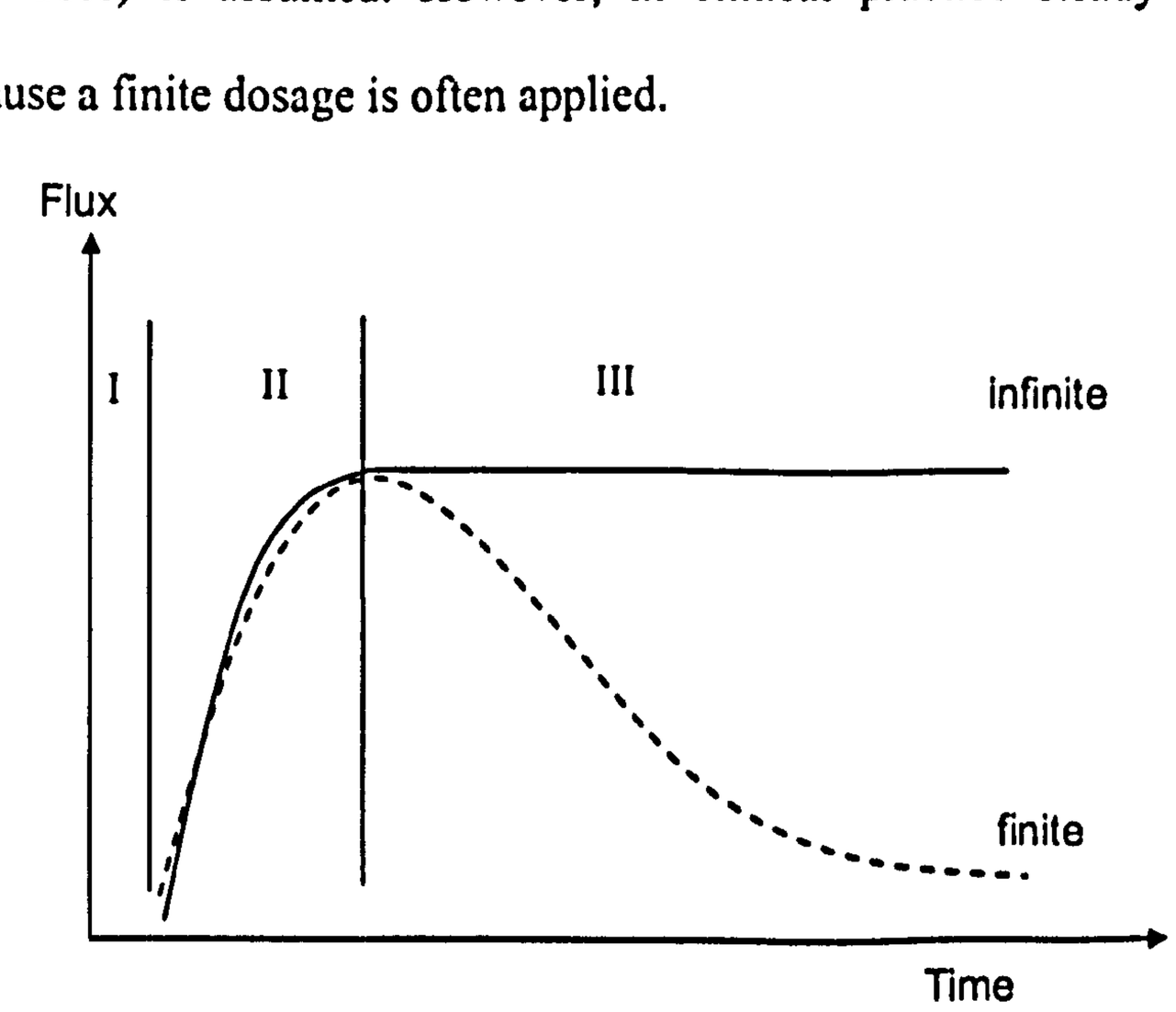

Figure 1.23: Drug flux plotted against time for finite and infinite dose. Phase I - Lag phase, Phase II - Rising phase, Phase III - plateau (infinite) or falling phase (finite).

1.4.3 Drug assay and data analysis

Experiments measuring the rate of drug release from topical preparations using *in vitro* methods may provide useful information. The rate of drug release is determined by measuring the appearance of drug amount in the receptor compartment over time. A reliable, reproducible, validated drug assay is essential in generating the data on which all conclusions will be based. The total drug permeated across the membrane and the drug retained in the membrane can be measured using analytical techniques and equipment. High performance liquid chromatography (HPLC) is by far the most common method. HPLC is versatile assay which can be adapted to separate drug by selecting the appropriate mobile phase, column and detectors. Ultraviolet-visible (UV) spectrophotometric analysis is also widely used. If the drug concentration is high, dilution of the sample is required so that it falls into the detectable concentration range. When drug permeation levels are very low, a chromatographic method may not be sensitive enough to detect the drug. Under such circumstances, radiolabelling drugs (Tritium H^3 and C-14) are employed in the donor formulation; the detection of labels is by liquid scintillation counting in which can measure drugs at very low concentrations.

The cumulative drug release can be expressed in mass per unit area, number of moles or total percentage. Drug flux is derived from the slope, and if a lag time is present, the extrapolation of the graph to the x-axis is made to obtain the intersection. The derivation of Kp and D is described in section 1.2.1.

1.4.4 Reproducibility issues in diffusion cell studies

In order to provide accurate results, the average flux values from a six cell replicates is often used. However, large results variability associating with diffusion cell studies still exist. When excised skin is employed, the main source of results variability was thought to be attributed to the biological variation of the skin [Southwell *et al.*, 1984]. Khan and

colleagues reported CVs (coefficient of variation) of testosterone and caffeine through porcine skin were 127.9% and 63.4% respectively; but when a PDMS synthetic membrane was used the CVs of testosterone and caffeine were reduced to 64.9% and 32.3% respectively [Khan *et al.*, 2005]. Thus skin biological variability could account for approximately 30-60% variation in the results depending on the drug. Van de Sandt conducted a multicentred (10 laboratories) drug diffusion study of three model drug, namely benzoic acid, caffeine and testostersone, through excised human skin [van de Sandt *et al.*, 2004]. All participating laboratories performed their studies according to a detailed protocol. The experimental conditions: dose, drug vehicle, exposure time, receptor fluid, membrane preparations, and analysis method were standardised. The CVs varied for the three drugs: benzoic acid 6.3 - 52.5%, caffeine 12.0 - 91.4% and testosterone 6.3% - 111.0%. The author proposed that the results variation observed may be attributed to human variability and the skin source; skin thickness was thought to be a critical variable in this study. Another multilaboratory study involved 18 laboratories was carried out by Chilcott using a synthetic membrane (PDMS) [Chilcott *et al.*, 2005]. This study was conducted mainly to assess the intra- and interlaboratory variation of methylparaben absorption under a quasi-standardised condition. As with Van de Sandt's study, a detailed protocol including information such as dose, drug vehicle, receptor fluid, temperature, membrane treatment, and analysis method was provided. In this study, the CVs between the laboratories were ~35% while the intralaboratory variation averaged 10%. They also reported that receptor volume, sampling volume, surface area, diffusion cell types (static of flow through) had no significant effect on flux. This is an interesting piece of information because PDMS is a synthetic membrane and such result variability should not occur with a synthetic membrane. Large results variability in *in vitro* diffusion cell experiments may also be attributed to human error or unvalidated equipment.

1.5 Conclusion and Aims of study

Synthetic membranes introduced for *in vitro* release studies are intended to reduce biological variability associated with human and animal skin such as age of skin, anatomical sites and gender. Depending on the purpose of investigation, the type of synthetic membrane used varies. The basic criteria required for a synthetic membrane depend on whether it is to correlate with *in vivo* or for quality control. The criteria are summarised in Table 1.8 according to investigation purpose.

Table 1.8: Summary of the criteria of synthetic membrane for various topical *in vitro* investigation purposes.

Investigation Purpose	Synthetic membrane basic criteria
Correlate *in vivo*	• Inert. • Hydrophobic. • Rate-limiting like skin. • Adhere to Fick's Law of diffusion.
Quality Control	• As a support to separate topical drug product from receptor medium. • Should not react with the drug product or the receptor medium in any way. • Should be permeable to drug substance and should not be rate limiting in drug release process. • Should not adsorb drugs • Commercially available

In the literature a diversity of synthetic membranes are used, varying in pore size, porosity, thickness, and chemical nature being used. Often these membrane factors are not reported. Although there are no strict standards for *in vitro* research using synthetic membranes, the criteria for selection of an 'appropriate' membrane was defined recently [Flynn *et al.*, 1999]. These include (1) it does not bind to the drug, (2) little interaction with the vehicle, (3) little diffusional resistance between the donor and the receptor, and (4) easy to obtain and

commercially available. The criteria are lenient and this makes comparison between experiments difficult. Some membranes may be unsatisfactory because of the physical properties of the drug. There are various types of membranes being investigated, but the literature is often confused about the appropriate choice of membrane. This is because commercial membranes have intrinsic variations such as membrane polymer, pore size, porosity which mask the true formulation effects that can be vital in interpretation of the reported release data. In addition, certain membrane information for example the membrane filler content, plasticizer and excipient composition are not provided by the manufacturers for the protection of trade secrets.

The overall objective of this PhD study is the investigations into the use of various synthetic membranes upon drug diffusion in Franz diffusion cell experiments. The aims are to encompass:

1) The validation of Franz cell equipment and methodology in our laboratory for the minimisation of results variability.
2) The evaluation of the influence of a range of different types of commercial synthetic membranes on the rate of drug release using ibuprofen as a model drug, and to evaluate whether the diffusion is influenced by the membrane properties.
3) The correlation and classification of the synthetic membranes according to their physical properties and their influence on ibuprofen and riboflavin drug release.
4) An investigation of the influence of drug hydrophobicity using a parabens series on different types of synthetic membranes in Franz cell studies.
5) An investigation and characterisation of lyophilised alginate gels and wafers saturated with ibuprofen drugs using rheology, microscopically and thermal analysis. This involves a comparison of the ibuprofen drug release from ibuprofen saturated alginate gels and alginate lyophilised wafers using Franz cells.

CHAPTER II

MATERIALS AND METHODS

This chapter details the various materials and equipment used in the course of this research. It also contains comprehensive descriptions of all the methods employed in the study and the subsequent analyses. The materials and instruments are listed below with their respective manufacturers or suppliers.

2.1 Materials

2.1.1 Synthetic membranes

Benzoylated cellulose tubing (Batch no. 074K7012), MWCO ≤1,200 and >2,000 was from Sigma-Aldrich Company Ltd. (Dorset, UK.). Cellulose tubing, Visking (Batch no. DTV12000.05.000), MWCO 12,000 - 14,000 was supplied by VWR international Ltd. (Lutterworth, UK). Cellulose ester tubing (Batch no. 131060), SpectraPor®, MWCO 500 purchased from Spetrum Laboratories, Inc., Rancho Dominguez. (California, USA). Cellulose flat sheet, Cuprophan (Batch no. N/A), MWCO 10,000 was obtained from Medicell (London, UK). Nylon 6,6, Biodyne® B (Batch no. 50046) and Biodyne® C (Batch no. 189051), Polyethersulphone, Supor® (Batch no. 55083), Polysulphone, Tuffryn® (Batch no. 60669), pore size 0.45µm, were all from Pall. (Portsmouth, UK). Polycarbonate, Cyclopore® (Batch no. 060.0131/6E8/L-3-L) and Nuclepore® (Batch no. 6018023) pore size 0.1 µm were bought from Whatman, Inc. (New Jersey, USA). Polyacrylonitrile AN69 membrane (Batch no. N/A, membrane was removed from AN69 S-dialyser) from Hospal-Gambro (Huntingdon, UK). Polypropylene, Celgard® 3500 (Batch no. 293485) was purchased from Hoechst Celanese Corporation (New Jersey, USA). Polydimethylsiloxane rubber sheet (Batch no. 19T0.3-1000-60M1) was supplied by Chilcott from SAMCO Silicone Product. (Nuneaton, UK).

2.1.2 Chemicals

Acetic acid, >99%, Basic Fuchsin (Pararosaniline), D-Mannitol, Ethylparaben, >99%, Glycerol <99%, Guar Gum, Methyl green, 89%, Periodic acid, 98%, Phosphate buffered saline, pH 7.4 tablets and sachets and Propylparaben, >99% were bought from Sigma-Aldrich Company Ltd. (Dorset, UK). Butylparaben, >99% and Methylparaben, ≥99% were obtained from Fluka (Buchs, Switzerland). Capmul MCM 8 was from Abitec Corp. (Columbus, USA). Ibuprofen Ph Eur, 99.8% supplied by Medex (Northants, UK). Miglyol 812N was from Sasol (Werkwitten, Germany). Phorpain gel containing 5% Ibuprofen purchased from Goldshield Pharmaceuticals (Croydon, UK). Potassium Permanganate, 99% was obtained from Fisher Scientific (Loughborough, UK). Sodium alginate (low viscosity, glucuronate rich) was supplied by Hopkins & Williams (Essex, UK) and sodium hydroxide pearls, 97.5%, Sodium metabisulphite purity, >90% were bought from BDH laboratory supplies (Poole, UK). Sucrose was purchased from USB Corp, Cleveland (Ohio, USA).

2.1.3 Solvents and Gases

Buffer reference standards (for pH meter), hydrochloric acid 37%, Methanol, analar grade were purchase from Sigma-Aldrich Company Ltd. (Dorset, UK). Methanol, HPLC grade was bought from Fisher Scientific (Loughborough, UK). Acetonitrile, HPLC grade was from Merck Pharmaceuticals (West Drayton, UK). Decon® 90 was from Decon Laboratory Ltd. (Sussex, UK) Helium and Nitrogen (oxygen free) were provided by BOC Gases Ltd., Guildford (Surrey, UK).

2.2 General analytical techniques

2.2.1 Polarised light microscopy

Light waves vibrate in all possible directions. Certain materials have the ability to screen out all vibration except those at one plane, and so produced plane polarised light.

Figure 2.1 illustrates the polarisation of light.

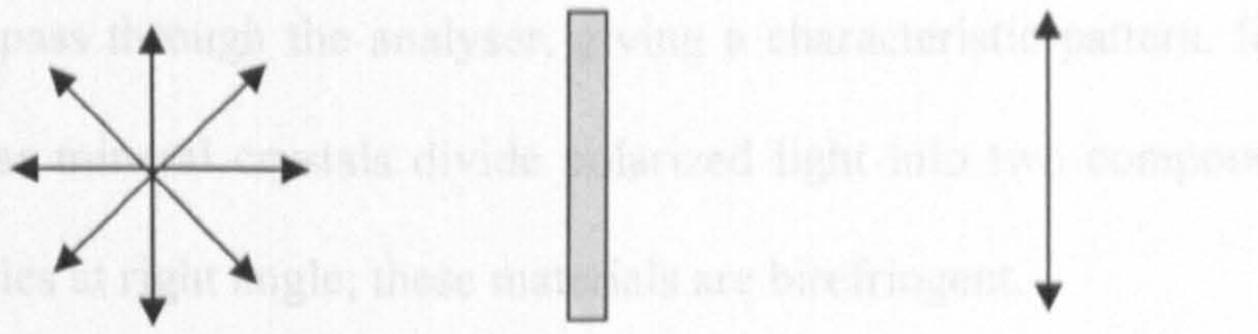

Figure 2.1: Unpolarised light passing through a polarizer. The arrows show the directions of wave vibration.

In Figure 2.1, the polarizer only allows vibrations of the electromagnetic waves that are parallel to the axis to pass through. Any vibrations that are perpendicular to the axis are excluded, thus producing plane polarized light. If a second polarizer is included and both the polarisers are aligned, the light that passes through the first polarizer also passes through the second. However, if the second polarizer is rotated right angles with respect to the first, no light passes through. This is the fundamental principle of the polarized light microscopy.

The polarizing microscope is equipped with a polarizer and an analyzer (a second polarizer) placed in the light path. When the analyzer is set to polarise light in a direction perpendicular to the polarizer; the polars are said to be crossed. The specimen viewed is placed (on the stage) in between the two polarizers.

The speed of light in any material is responsible for the refraction of the light rays when entering or leaving the material and this is signified by its refractive index, or its 'refringence'. Materials in which the refractive index is constant in all direction are known as *isotropic* materials. On the other hand, if the material has different refractive indices in different direction, it is defined as *anisotropic*. The polarized light microscope can be used to differentiate between isotropic and anisotropic materials. Isotropic materials such as water allow polarized light to pass through the ordered plane but will not pass through crossed polars. When an anisotropic material is positioned in plane polarized light, it rotates the

plane polarised light and even when analyzer is at the right angle to the plane of polarization, some light can pass through the analyser, giving a characteristic pattern. Some anisotropic materials such as mineral crystals divide polarized light into two components vibrating at different velocities at right angle; these materials are birefringent.

Microscopic analysis was accomplished using Reichert-Jung Polyvar (Ansberg, Germany) microscope (Figure 2.2). The specimens were prepared on 0.8-1.0 mm thick plain glass slides and 0.17 mm glass cover slips were gently laid over them. The beam splitter was adjusted to divert the light from the specimen to the camera, which was loaded with 35 mm film (ISO 200). At low magnification, the specimen was examined in bright field. The focus was refined using course and fine focus control. Once in focus, the polariser was manipulated to polarise the light transmitted. Hence the same area of the specimen was seen in both polarised and unpolarised light.

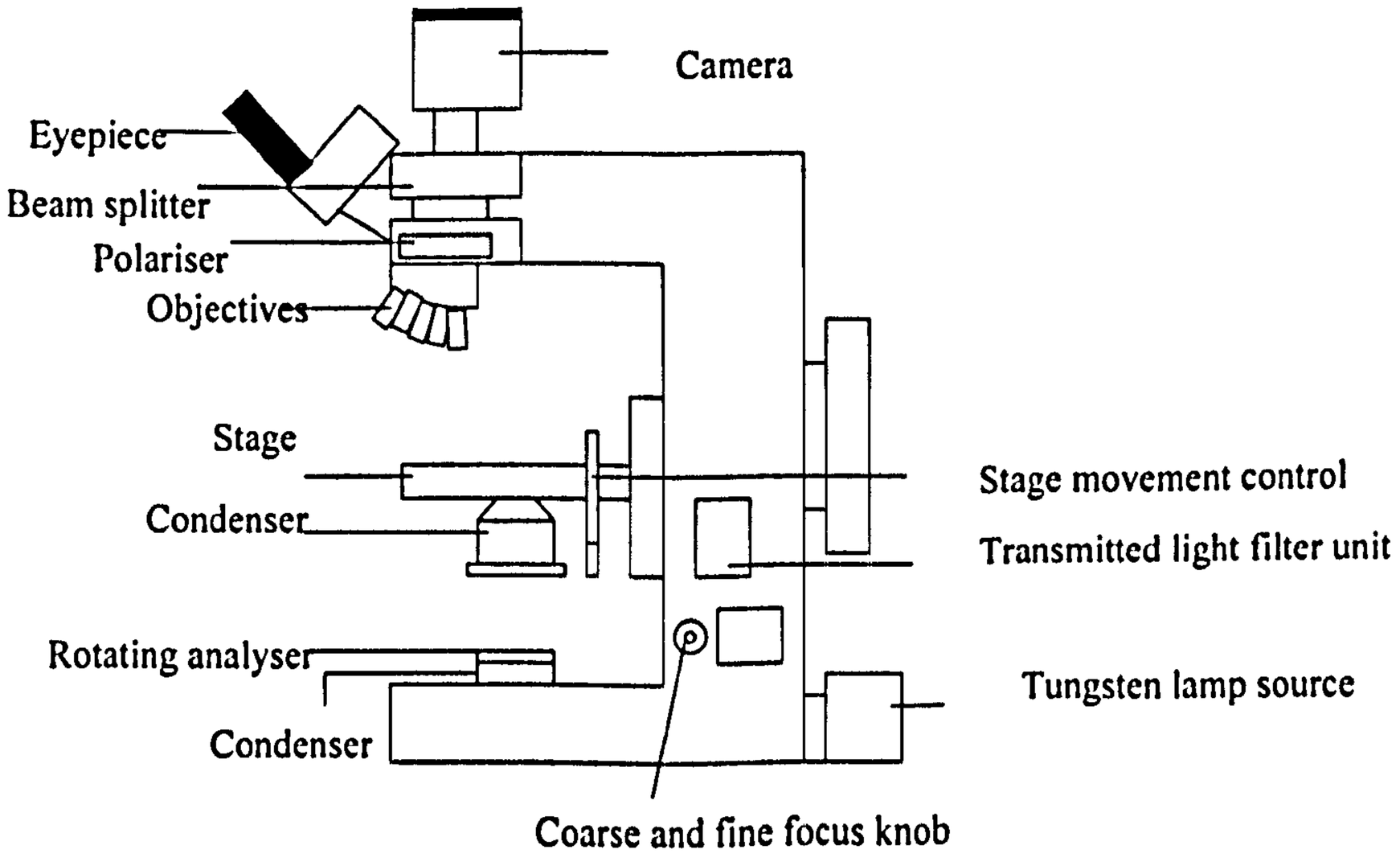

Figure 2.2: Schematic of Reichert-Jung POLYVAR microscope.

The objectives varied from ×10, ×25 and ×40. In order to place a scale onto a micrograph, a photograph of a graticule of 1 mm length was viewed under the desired magnification. The graticule picture taken was superimposed onto the photo micrograph viewed under the same magnification.

Our studies employed the polarized light microscope to examine the structure of lyophilized wafers (Chapter 7).

2.2.2 Thermal Analysis

The thermal techniques used measure specific physical properties of a material as a function of temperature. These include the measurement of weight changes with temperature and energy absorbed (endothermic) or evolved (exothermic) during a phase transition or a chemical reaction. Thermal analysis is of interest pharmaceutically because important information such as melting point, polymorphic transition temperature, glass transition temperature, purity, thermal stability and heats of transition can be derived. Two thermal techniques i.e. thermogravimetric analysis (TGA/SDTA 851^e) and heat-flux differential scanning calorimetry (DSC 822^e) are used in this study and will be described in detail below (Mettler-Toledo Ltd, Leicester, UK). In our laboratory, both these instrument are connected to TS0801RO sample robots and linked to the same control unit via a computer (Star^e software v 8.10).

2.2.2.1 Thermogravimetric analysis; TGA

TGA is performed to determine weight change in a sample as a function of temperature. This information can reflect a material's thermal stability and the weight loss on dryness as the specimen is heated. The simplified schematic of Mettler Toledo TGA/SDTA 851^e (Leicester, UK) used in our laboratory is showed in Figure 2.3.

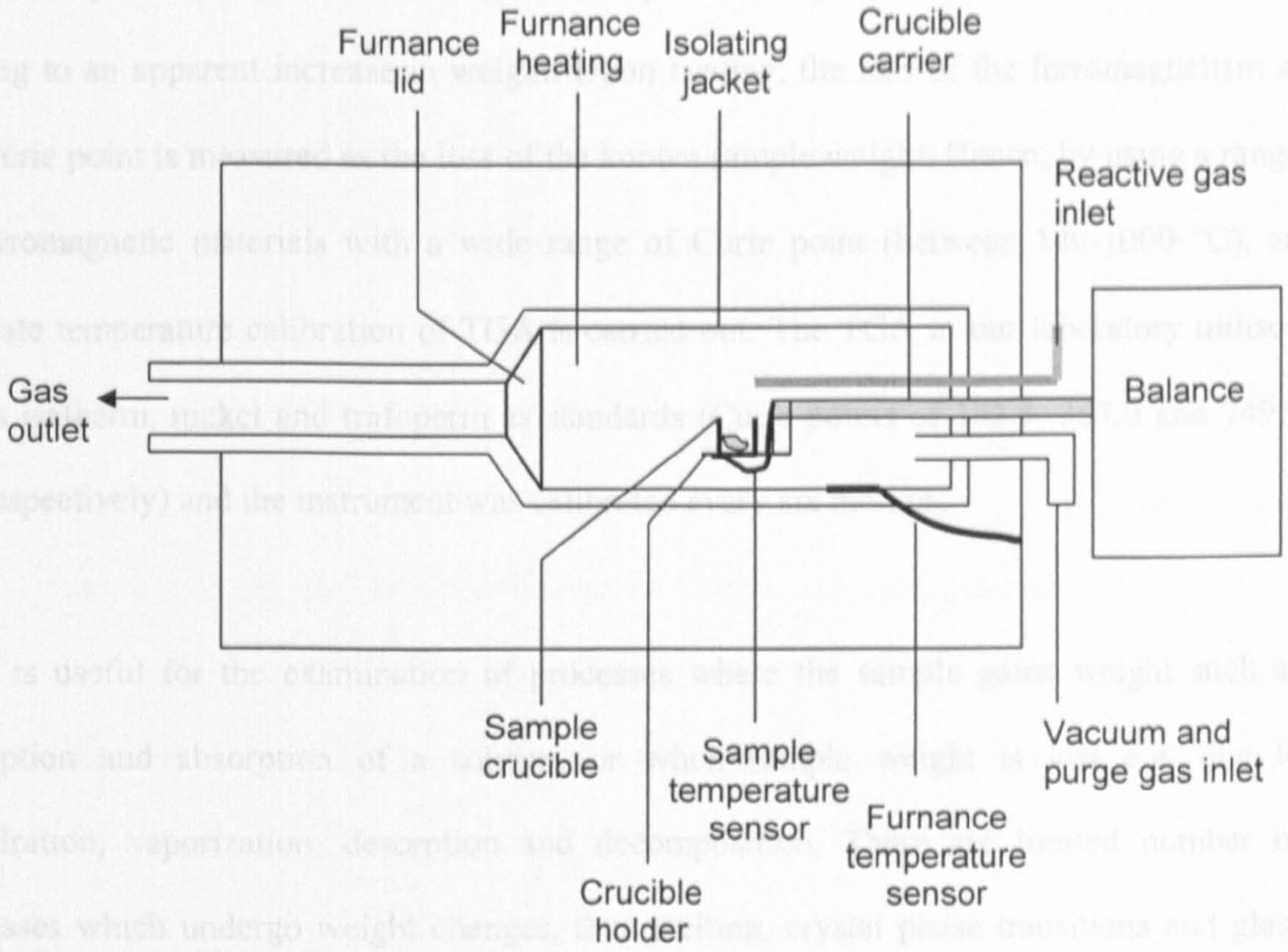

Figure 2.3: Simplified schematic of a Mettler Toledo Thermogravometric Analyzer [redrawn from Mettler Toledo TGA/SDTA 851^e userguide].

The main components of a TGA instrument are an electronic microbalance, a furnace, a temperature sensor (thermocouple) as well as a computer for recording the weight change and a temperature ramp. The aluminium crucible is suspended on a highly sensitive balance (resolution of 1 μg) over a precisely controlled furnace. Nitrogen gas is used to purge air in the chamber as well as to remove any gaseous byproduct produced from the heating of the sample. TGA measurement of a sample is carried out in an inert atmosphere and the sample weight is recorded as a function of increasing or decreasing temperature.

The temperature calibration of TGA uses the Curie point method. The Curie point is the temperature where ferromagnetic metals such as iron lose their magnetism. In brief, when a ferromagnetic standard is placed in the sample crucible of the balance, and a large permanent

magnet is placed below the crucible, the sample will experience a downward attraction leading to an apparent increase in weight. Upon heating, the loss of the ferromagnetism at the Curie point is measured as the loss of the known sample weight. Hence, by using a range of ferromagnetic materials with a wide range of Curie point (between 140-1000 °C), an accurate temperature calibration of TGA is carried out. The TGA in our laboratory utilised alloys isatherm, nickel and trafoperm as standards (Curie points of 142.5, 357.0 and 749.0 °C, respectively) and the instrument was calibrated every six months.

TGA is useful for the examination of processes where the sample gains weight such as adsorption and absorption of a solvent, or when sample weight is lost e.g. due to dehydration, vaporization, desorption and decomposition. There are limited number of processes which undergo weight changes, thus melting, crystal phase transitions and glass transitions cannot be studied using TGA. In such instances, differential scanning calorimetry (DSC) is used.

2.2.2.2 Differential scanning calorimetry; DSC

DSC measures the heat changes of a sample as a function of temperature. It involves heating the sample in an aluminium pan and a similar reference pan simultaneously in a dry nitrogen atmosphere. When heat change (endotherm or exotherm) occurs due to a physicochemical change in the sample, the furnace will need to be varied in order to maintain the temperature of the two pans so that it stays the same. The instrument measures the amount of energy required to keep the sample pan at the same temperature as the reference pan whilst the furnace temperature increases or decreases at a set rate. Thus by monitoring the difference in heat supplied to the pans, the enthalpy changes in the sample can be determined. The heat flow (enthalpy) is expressed in joules per unit mole of a compound (SI unit).

When a sample is subjected to a heating or cooling cycle, phase changes may occur. The phase transition of the sample causes heat input or output, so in DSC excess or less heat will need to flow to the sample in order to maintain both sample and reference pan at the same temperature. For instance, when as solid sample melts to liquid, it absorbs heat from the environment (endothermic), so more heat flows into to the sample to increase its temperature at the same rate as the reference. In the DSC plot, an endotherm peak is observed. Likewise, crystallization involves the formation of solid crystal from a liquid and releases heat (exothermic). DSC may also be used to observe more subtle phase changes, such as glass transition, a temperature where a material is transformed from crystalline phase (glassy state) to liquid-like rubbery state. Figure 2.4 illustrates the various phase changes that can be detected in a sample using DSC.

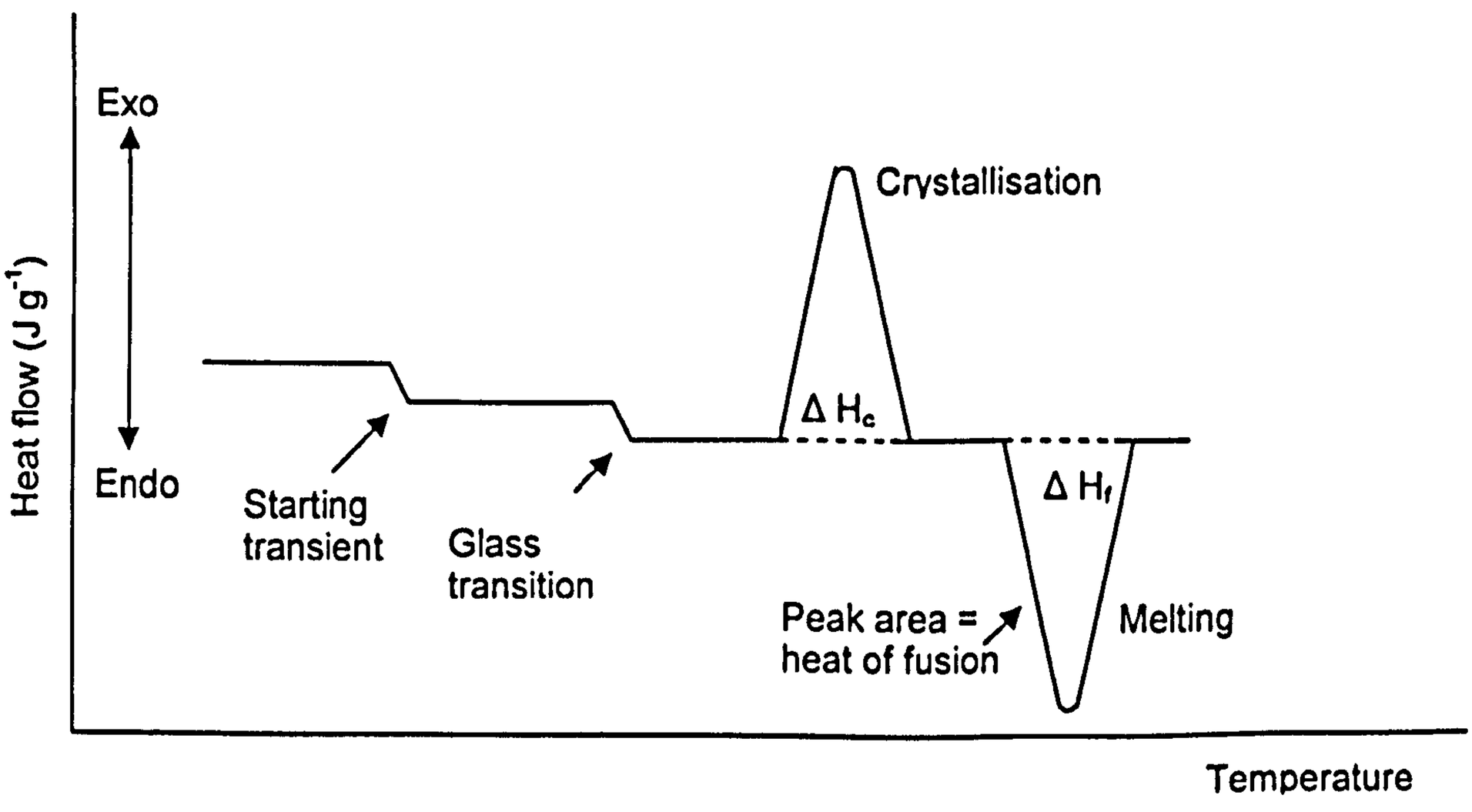

Figure 2.4: The various phase changes in DSC scan [adapted from Wells and Aulton, 2000].

Glass transitions cause a baseline shift. Crystallization is a typical exothermic process and melting a typical endothermic process, the heat of fusion is calculated from the area under the peaks.

In general, there are two main types of DSC: power compensated and heat flux DSC. In power compensated DSC, the two pans are heated separately by separate electrical heaters. Both the sample and reference pans are heated at exactly the same rate while monitoring the electrical power used by the heaters. When the sample undergoes changes, the power (energy) applied to or removed from the heater to compensate for the sample energy is measured. This is a classic DSC design pioneered by the Perkin-Elmer company.

The DSC used in this study was a heat flux DSC (Mettler Toledo, Leichester, UK). In heat-flux (heat exchanging) DSC, the sample and reference pans are heated by a single furnace. The pans are placed on separate platforms which sit on a heated metal disc. Thermocouples are used to monitor heat flow from the disc to the sample and reference. The furnace needs to be varied in order to maintain the heating rate the same as the reference. The differential heat flow between the sample and reference pans will then reflect the different thermal behaviour of the sample and reference. Figure 2.5 shows a cross section of Mettler Toledo DSC 822^e cell used in this study.

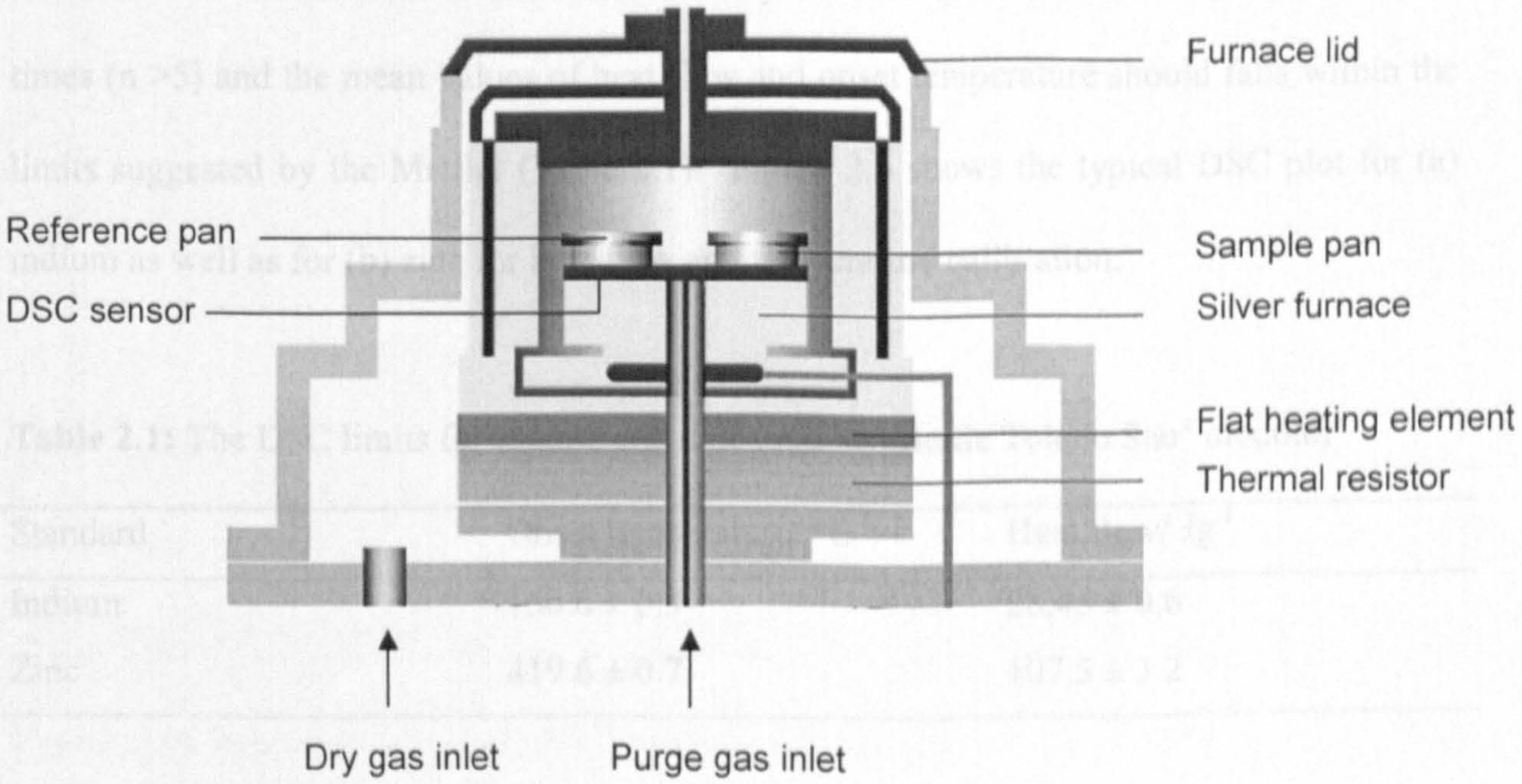

Figure 2.5: Cross-section of heat flux DSC822^e used in this study [reproduced from Mettler Toledo DSC822^e module].

For the DSC822^e the following three calibrations were performed: tau-lag, heat-flow and temperature calibration [Mettler Toledo Star^e system manual]. Tau-lag calibration accounts for the time takes to reach temperature equilibration between the sample and temperature sensor. In the furnace, the temperature sensor does not measure the temperature directly in the sample, but only in the vicinity of the sample. The difference between the sample temperature and sensor temperature could change when different heating rates are applied. The tau-lag calibration was based on the onset temperature (the starting point of a peak) of a standard indium determined with several different heating rates.

Heat flow calibration checks the required amount of energy to melt a standard of known weight and enthalpy. This is important because it reflects the sensitivity of the DSC sensor. Temperature calibration checks sensor which records the melting of known material within the acceptable range. The heat flow and temperature checks of the DSC were carried out using standards indium and zinc with known heat-flow and onset temperature. In practice, the standards were accurately weighed and subjected to a heating rate. The onset temperature and heat flow were derived from the endotherm plots. The calibration was carried out several times (n >5) and the mean values of heat flow and onset temperature should falls within the limits suggested by the Mettler (Table 2.1). Figure 2.6 shows the typical DSC plot for (a) indium as well as for (b) zinc for heat flow and temperature calibration.

Table 2.1: The DSC limits for indium and zinc (source: Mettle Toledo Star^e module)

Standard	Onset temperature/ °C	Heat flow/ Jg^{-1}
Indium	156.6 ± 0.3	28.45 ± 0.6
Zinc	419.6 ± 0.7	107.5 ± 3.2

In this study, DSC was used to examine the thermal changes of sodium alginate solution prepared in various solutions (Chapter 7).

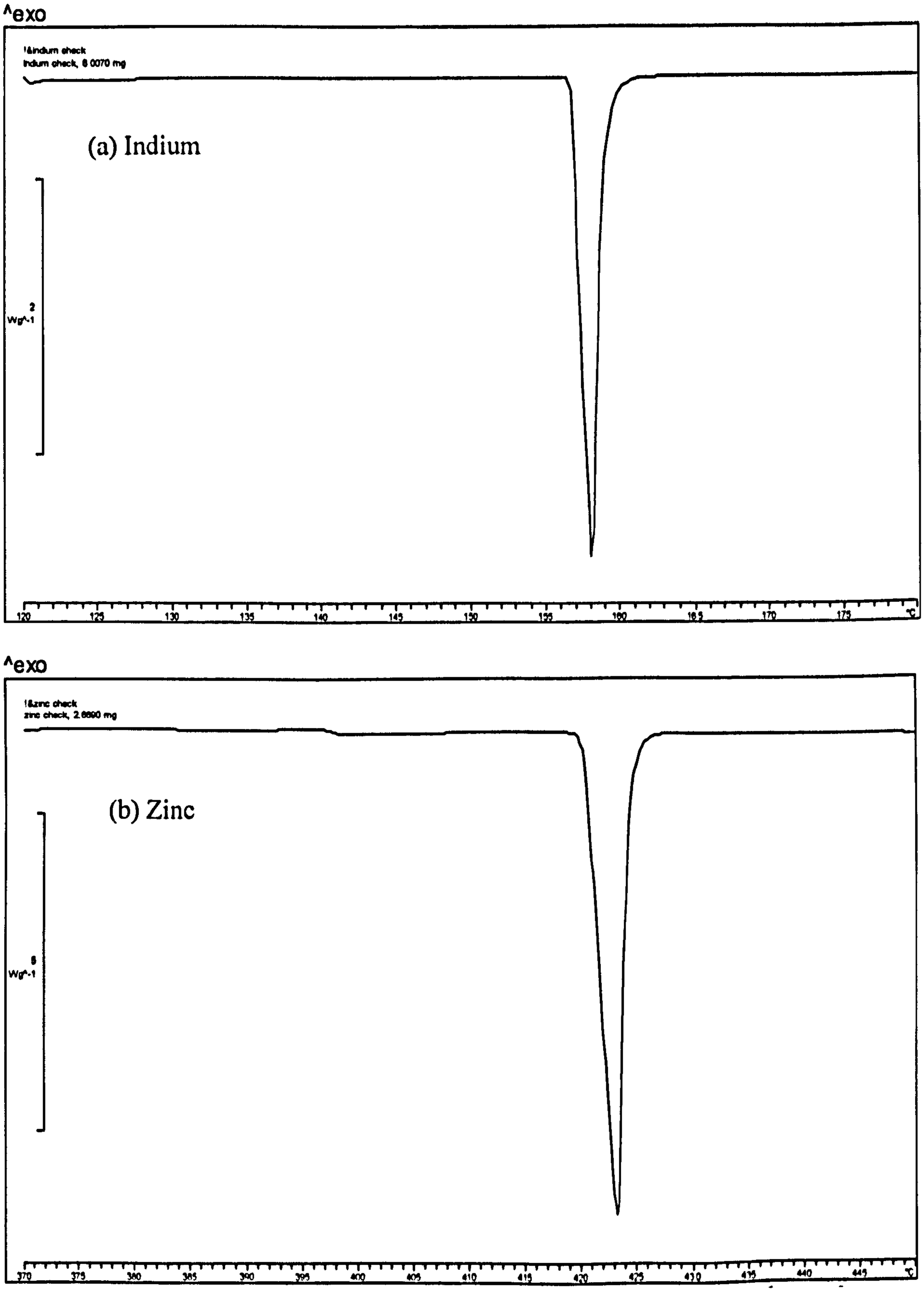

Figure 2.6: Typical temperature and heat flow DSC calibration plots using (a) indium and (b) zinc.

2.2.3 Rheological measurement

Rheology is as the study of the flow and deformation of materials. The need for a proper understanding of the rheological properties of pharmaceutical semisolids such as gel and creams is essential to the preparation, developmental and evaluation of dosage form.

Viscosity is a property of fluids that indicates resistance to flow when a stress is applied. Elastic materials strain instantaneously when stretched and just as quickly return to their original state once the stress is removed. Viscoelastic materials have elements of both of these properties and, as such, exhibit time dependent strain. The phenomenon of viscosity can be illustrated hypothetically by a cube of fluid made up by an infinite number of parallel plates which slide over one another like a pack of playing cards. This is also known as the Newtonian model illustrates the laminar flow of fluids (Figure 2.7).

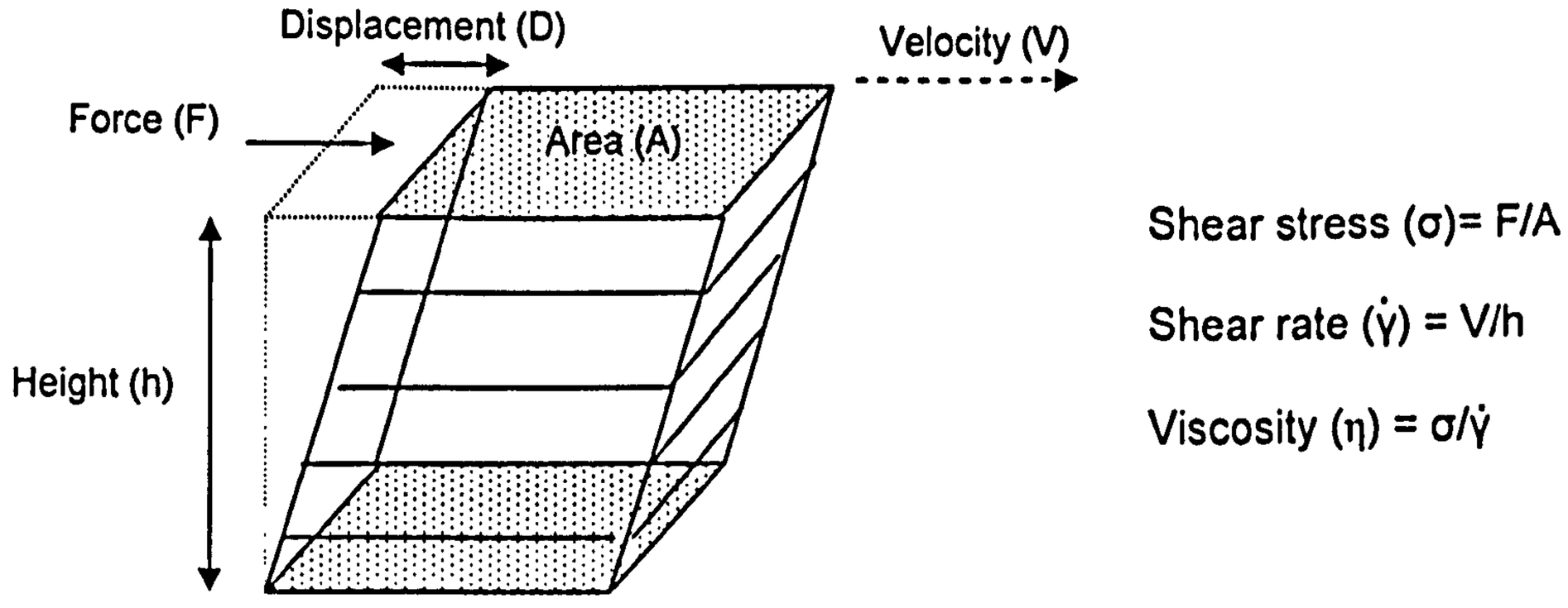

Figure 2.7: Illustration of displacement of a viscous material caused by shear stress [adapted from Marriott, 2000].

When a force (F) is applied to the top plate (area A) with separation height from the bottom plate (H) at a velocity of V, then a displacement (D) occurs. *Shear stress* is the force per unit area (F/A) acting on a plane within the liquid. *Shear rate* is the velocity gradient or the

change in velocity with distance in the system when the force is applied (V/H). Newton's law states that shear stress (σ), is proportional to the shear rate ($\dot{\gamma}$). The proportionality constant is known as the viscosity (η). Simple fluids which follow the relationship are referred to as Newtonian fluids, and fluids which deviate are known as non-Newtonian fluids. Figure 2.8 shows the shear rate vs. shear stress plots, which are also known as *rheograms*.

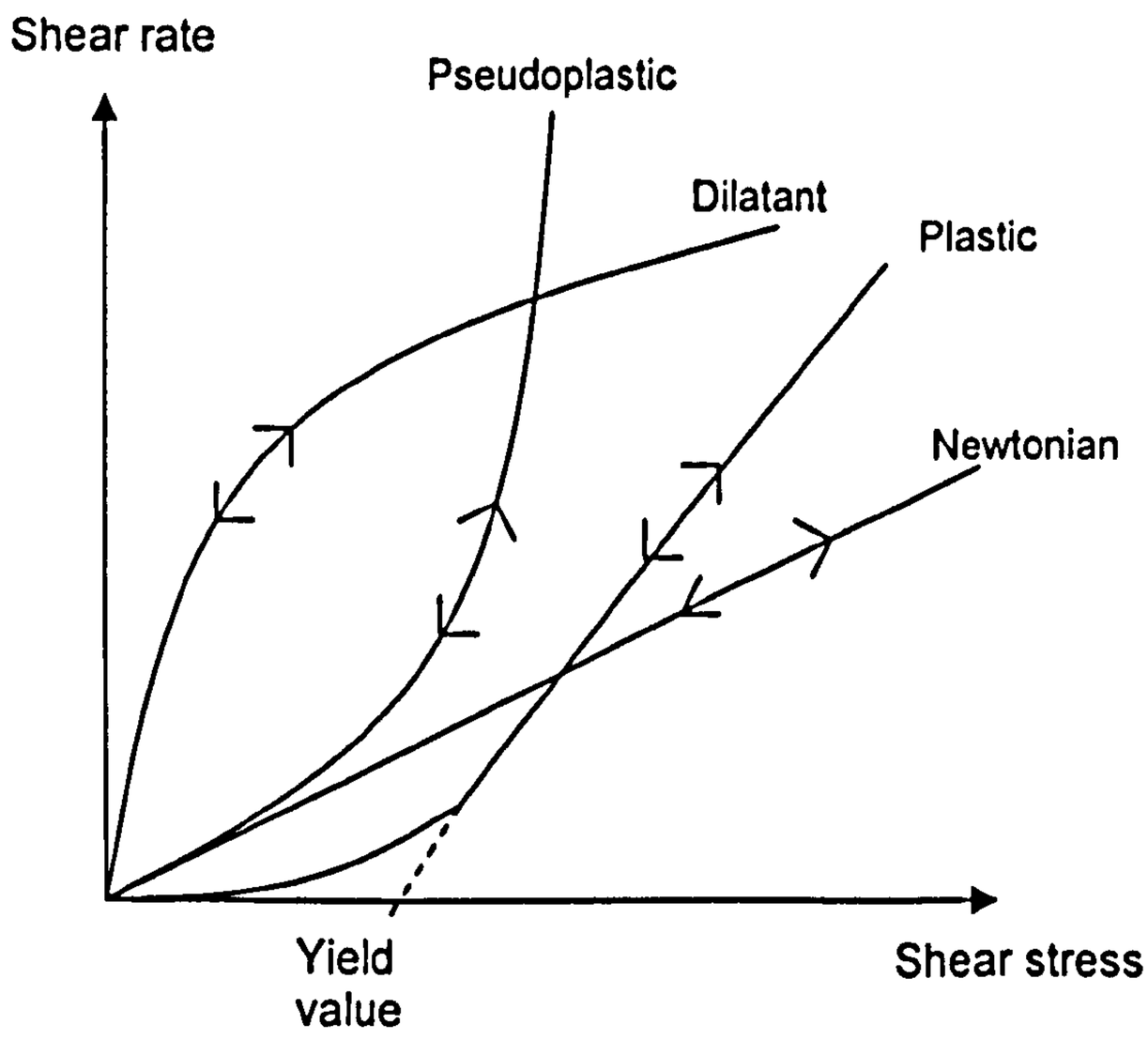

Figure 2.8: Flow curves or rheograms representing Newtonian and non-Newtonian flow properties [redrawn from Hoang, 2005].

The Newtonian fluid is a straight line which passes through the origin. Examples of Newtonian fluids are simple liquids e.g. water, propylene glycol and very dilute colloidal system. Non-Newtonian liquids have complex structure containing suspended particles, droplets or dissolved molecules. Plastic flow, pseudoplastic and shear thickening are examples of non-Newtonian fluid flow. *Plastic flow* material will flow when the applied stress exceeds the 'yield value'. Below this stress, the material behaves essentially as an elastic solid. In *pseudoplastic flow*, the material decresese in viscosity with increasing shear

rate (shear-thinning). Pharmaceutical materials which exhibit pseudoplastic flow are natural and synthetic gels, in which the long and high molecular weight molecules are tangled with immobilization of solvents. Under shear stress the molecules become disentangle and align with the flow, causing the release of entrapped water which results in lower viscosity of the solution. In contrast of pseudoplastic flow, the *dilatant* material exhibits increase viscosity with increasing shear rate (shear thickening). Dilatant flow is less common than plastic and pseudoplastic flow but is found in certain suspensions with high concentration (>50%) of finely divided, deflocculated particles. These particles are closely packed at rest with minimal interparticle voids; but when shear stress is increased, the particles displaced and formed clumps which in turn create larger voids. The liquid now is insufficient to fill the voids and drains away, so the resistance to flow increases and viscosity rises, resulting in shear thickening effect.

Most dermatological products are semisolids (e.g. creams and gels) and they exhibit both viscous and elastic properties (viscoelastic). The flow techniques above only measure the viscous property a semisolid and overlook the elastic element. Creep and oscillation tests measure the viscoelastic characteristics of semisolids. Unlike the viscosity tests, the creep and oscillation are non-destructive procedure, i.e. the sample material does not lost its viscous properties however many times it is repeated.

A deformed elastic material is able return into its original state when a constant stress is applied. But unlike elastic material, viscoelastic has viscous component in which some energy will be dissipates in viscous flow while the rest is used for recovery when the stress is removed. The viscous and elastic elements can be represented using simple mechanical models: dash-pot (piston fitted into a cylinder containing an ideal Newtonian fluid) and spring respectively shown in Figure 2.9 (a) and (b) below. The molecular movement in a viscoelastic polymer can be described using combination of these two models.

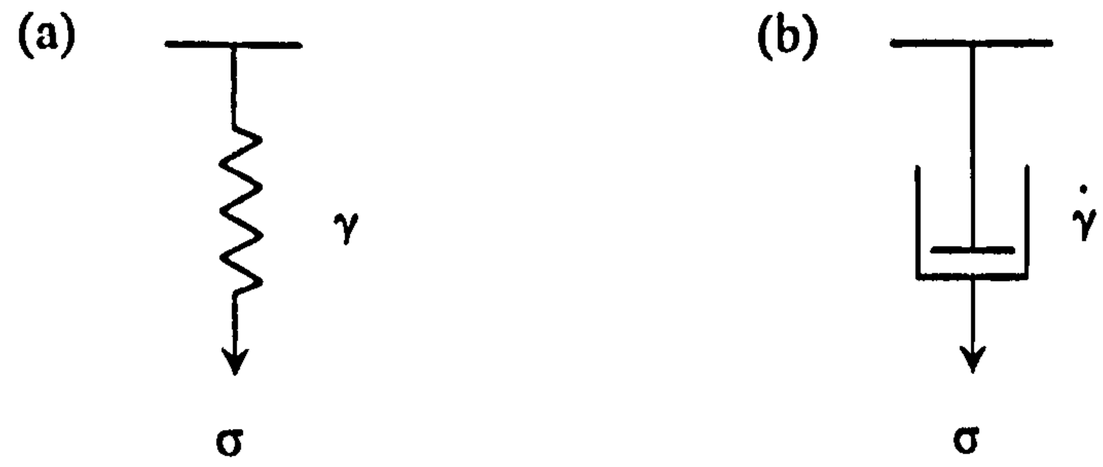

$\sigma = G\gamma$
G is elastic modulus

$\sigma = \eta\dot{\gamma}$
η is viscosity

Figure 2.9: (a) Hookean spring represents elastic component. (b) Dash-pot represents viscous model.

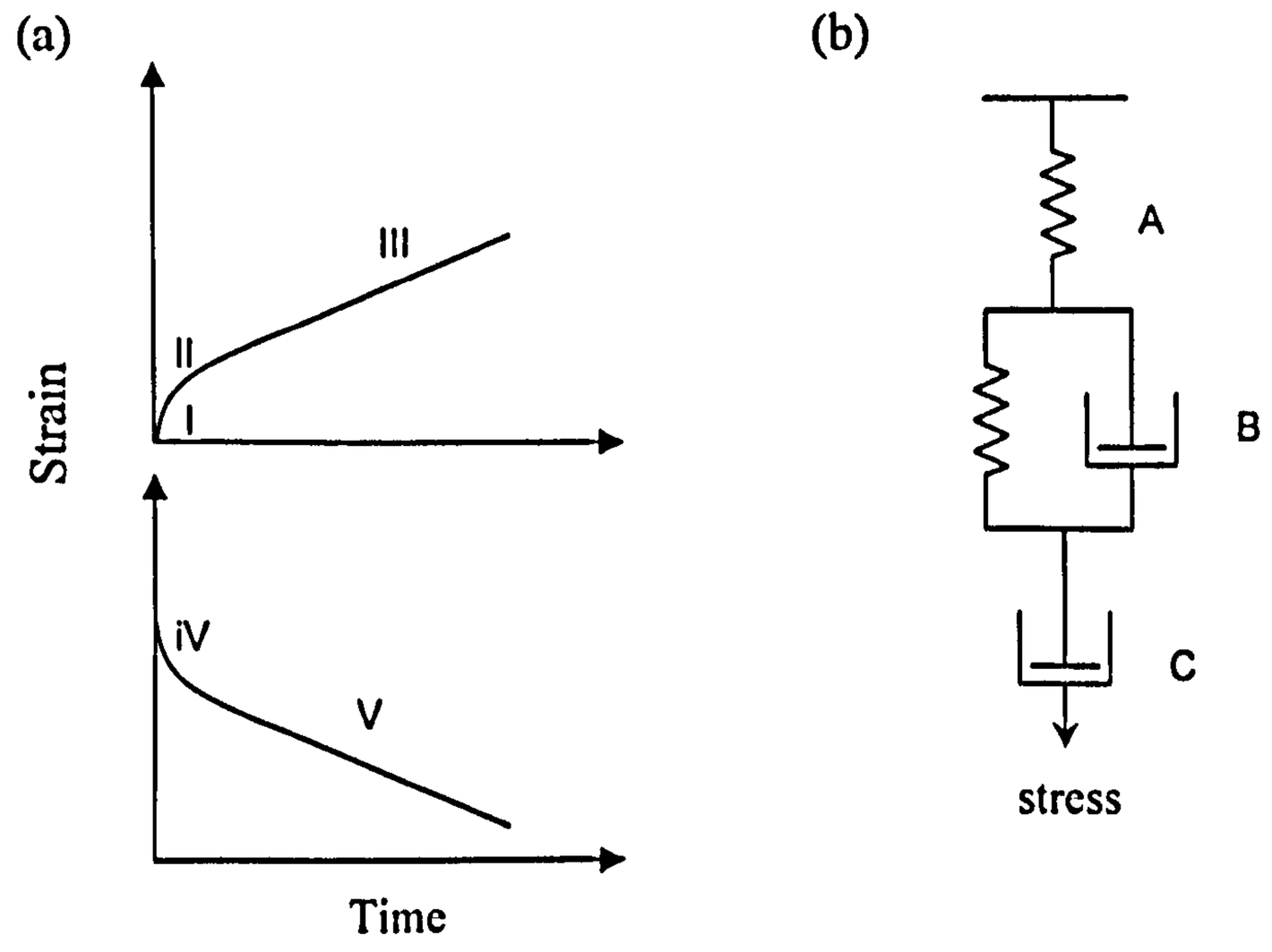

Figure 2.10: (a) Creep test response curves. (b) Mechanical model representation of creep compliance curve [adapted from Marriot, 2000].

When a constant stress is exerted upon a viscoelastic material, the type of strain response can be seen in Figure 2.10 (a). This is also known as the 'creep' test. Initially, there is an elastic response (region I), followed by delayed elastic response with a retardation time (region II) where the material is attempting to flow as viscous fluid but is being retarded by its elastic characteristics. After a long period of time, the viscous flow will eventually predominates

and the curve becomes linear (region III); while the reciprocal of the slope is the viscosity η. Strain response region I to III can be interpreted using mechanical model (figure 2.10 (b)). Region I is the movement of the spring (A), while the retarded movement produced when the dashpot resisting the spring extension (B) just like region II. And region III is viscosity only thus described as C where only the dashpot is strained. But when the applied stress is withdrawn, on the stored energy will be recovered and this is shown by an initial elastic recoil (region IV) which also equivalent to region I and the retarded response of region V is equivalent to region III. The material will not recover fully because some energy is loss during viscous flow.

Oscillatory testing obtained data on the deformation behaviour of viscoelastic material at very low strains. Sinusoidal stress (or strain) is applied onto the material, and the resulting sinusoidal strain (or stress) is measured. Figure 2.11 is typical sine waves showing the stress and strain wave during oscillatory testing. However, because the viscoelastic nature of the material, energy will be lost so that the amplitude of the stress wave will be less than that of the strain wave: it will be also lag behind the strain wave. The difference is known as the phase lag (δ). If the phase lag and the stress/strain ratio are known, then the elasticity or storage modulus, G' can be determined by the equation $G' = (\sigma/\gamma) \cos \delta$, while the loss modulus G" is $(\sigma/\gamma) \sin \delta$. The ratio between the G" and G' is known as tan δ. Hence, G' and G" are both important parameters obtained from the oscillatory test because they reflect the elastic and viscous component of the material respectively.

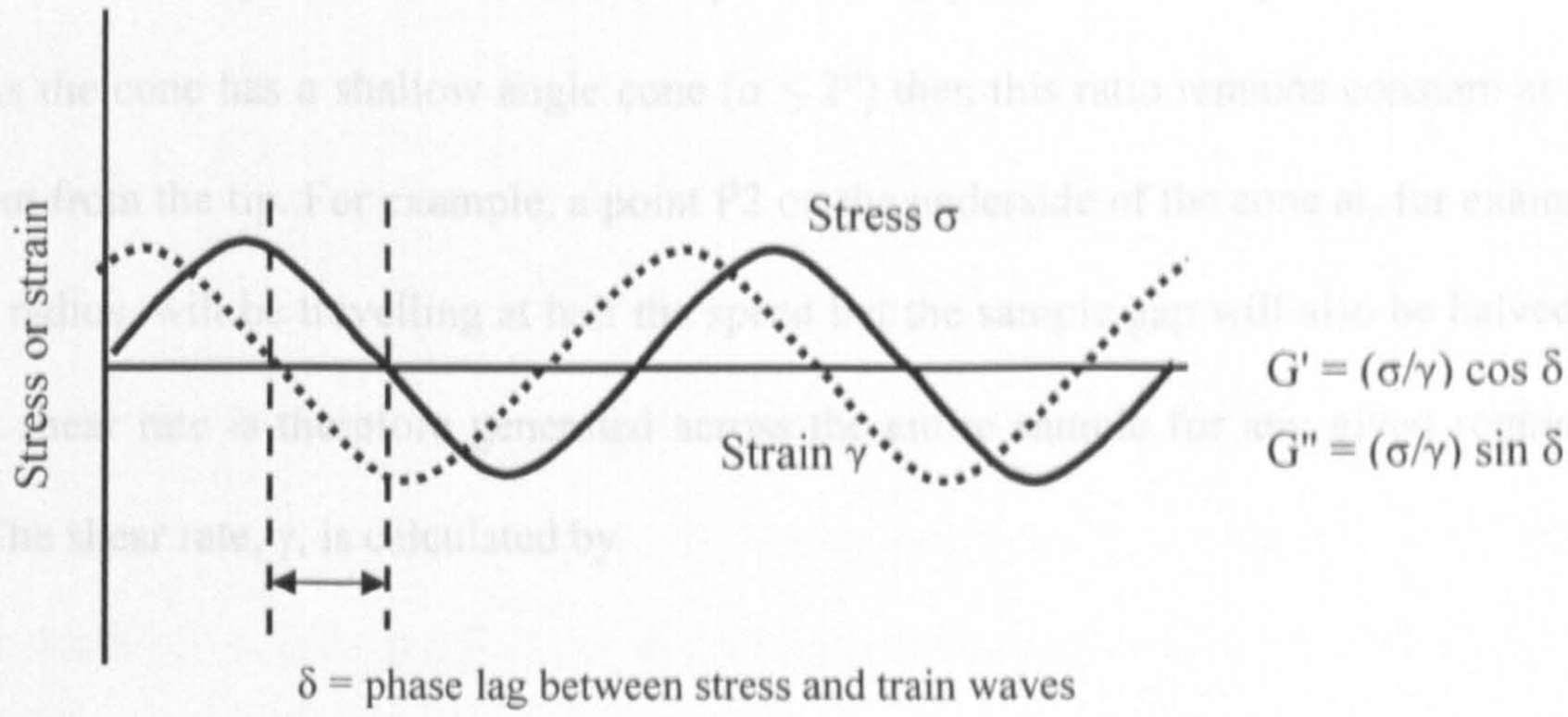

Figure 2.11: Typical sine waves showing the stress and strain wave during oscillatory testing. G' is the elastic modulus and G" is the loss modulus.

Rheological properties of the gels in this study were examined using a Carri-Med cone and plate rheometer (Crawley, UK) in continuous shear. Cone and plate geometry consists of an inverted cone in near contact with a lower plate. The test fluid is constrained in the narrow gap between the two surfaces. Figure 2.12 shows a simple cone and plate geometry.

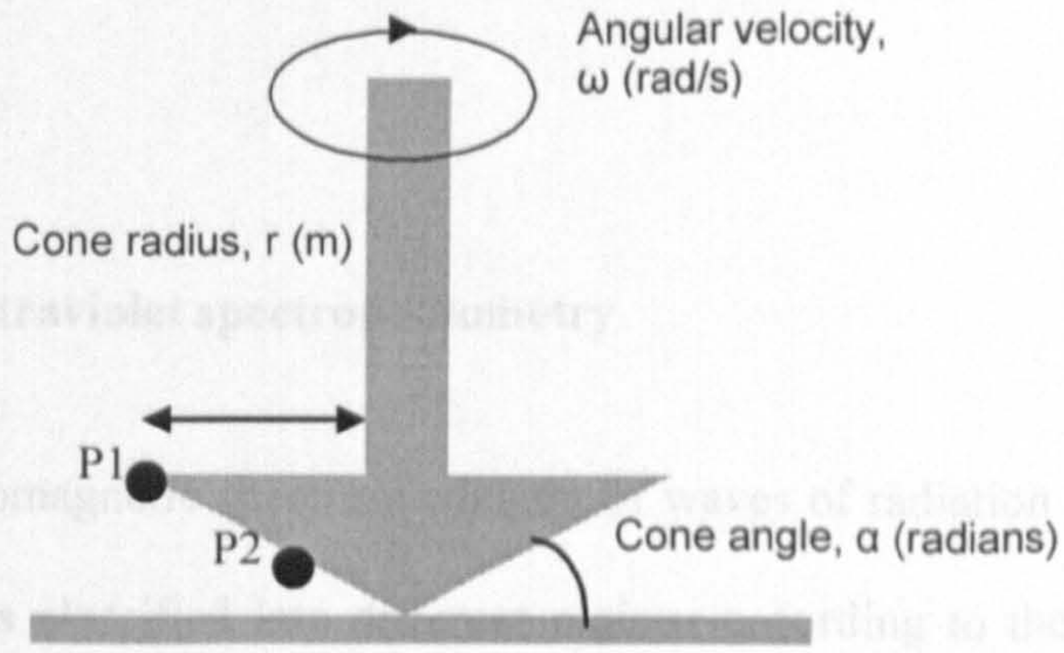

Figure 2.12: Cone-and-plate geometry [adapted from Barnes *et al.*, 1989].

For a fluid undergoing laminar flow, the shear rate is the ratio of the velocity difference across the fluid to the distance over which the shearing rate occurs. The shear rate is uniform in the gap. If we take a point, P1, at the rim of a cone, the shear rate experienced by the

sample beneath that point is the ratio of the speed of that point to the sample thickness at that point. As the cone has a shallow angle cone ($\alpha \leq 2°$) then this ratio remains constant at any radius out from the tip. For example, a point P2 on the underside of the cone at, for example, half the radius, will be travelling at half the speed but the sample gap will also be halved. A uniform shear rate is therefore generated across the entire sample for any given rotational speed. The shear rate, $\dot{\gamma}$, is calculated by

$$\dot{\gamma} = \omega / \alpha \qquad \text{Eq. 2.1}$$

where ω is the velocity and α is the cone angle. While the shear stress, σ, is calculated from the spindle torque, M, and cone radius, r, by the equation

$$\sigma = 3M / 2\pi r^3 \qquad \text{Eq. 2.2}$$

The flow curves of gels in this study were obtained by increasing the shear rate to a pre-determined value, and then decreased accordingly back to shear zero. The shear rate vs. shear stress plot yielded a flow curve. Due to time constraint, viscoelastic properties of gels were not carried out.

2.2.4 Ultraviolet spectrophotometry

The electromagnetic spectrum consists of waves of radiation that passes through space. The spectrum is classified into different regions according to the wavelengths of the radiation. The classification covers very short wavelengths (λ) radiations such as x- and gamma-rays ($\lambda < 10^{-1}$ nm) to wavelength as long as several kilometers like the radio waves. Ultraviolet (UV) and visible light consist a small part of the electromagnetic spectrum but they are very useful for analysis. Ultraviolet (UV) rays λ extends from 10 to 380 nm; while visible light has λ slightly above the UV with λ 400 to 800 nm. When a chemical compound absorbs light in

the UV region, the electrons in the molecules undergo electronic excitation from ground state of the π orbitals to the excited state (π*). The energy absorbed by the electron jump usually requires high energy which falls in UV wavelength region hence it can be measured using a UV spectrophotometry. The energy absorbing group in a molecule is called the *chromophore*, examples are benzene, amine, ethylene, ketone, aldehyde and azo groups. They usually possess unpaired electrons or conjugated π systems (multiple double/triple bonds separated by single bonds) so that the delocalized electrons are readily excited.

The dual beam UV spectrophotometer used in this study is Spectronic™ Helios gamma (Thermo-Spectronic, Cambridge, UK). The UV spectrophotometer schematic diagram is described in Figure 2.13.

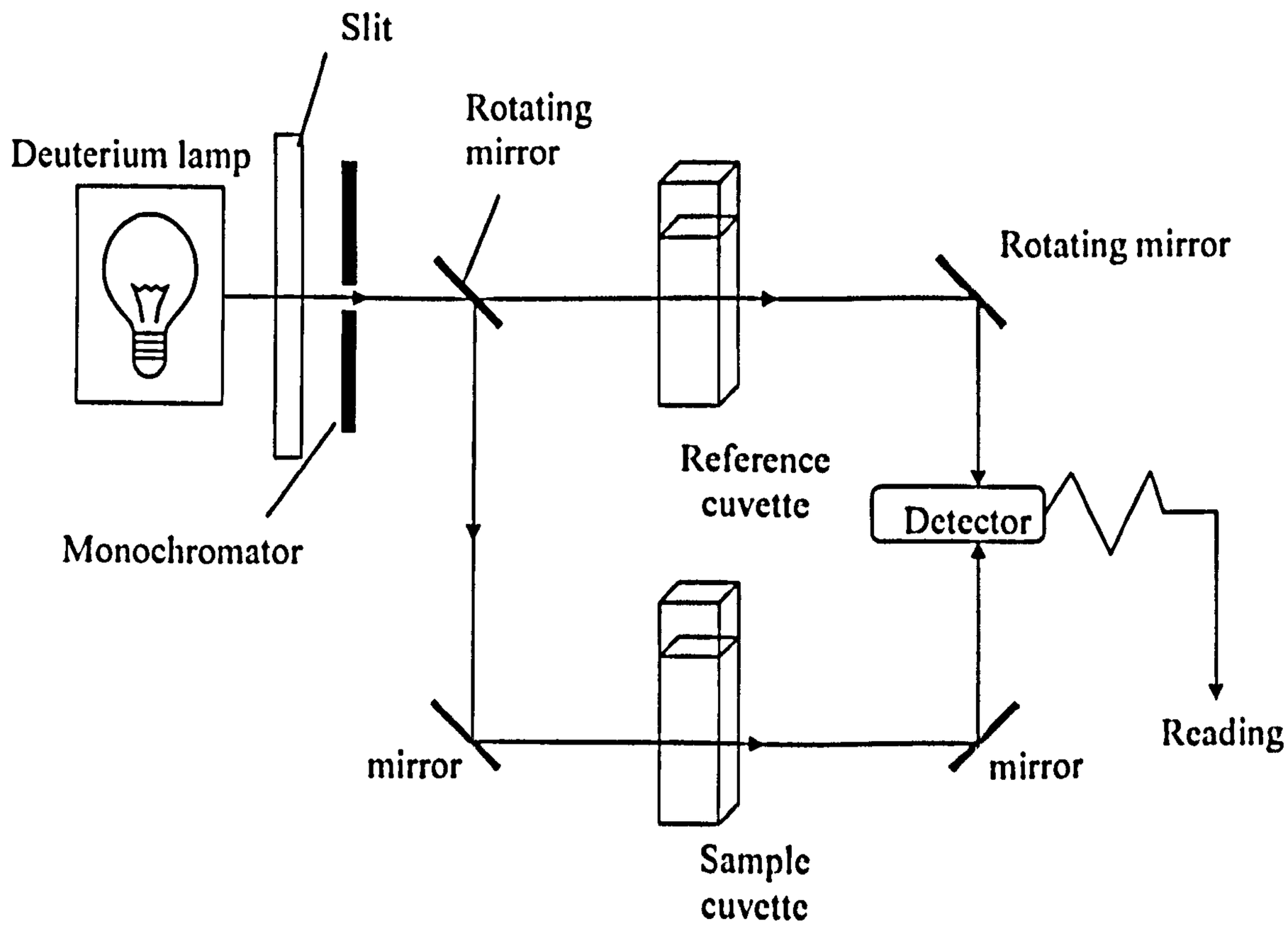

Figure 2.13: Schematic Diagram of a dual beam UV spectrophotometer [adapted from Bashford, 1987].

The light source is a deuterium lamp to cover the UV range (200-370 nm) or a tungsten filament lamp to cover the visible range (370-800 nm). A monochromator (diffracting grating) is used to select a narrow band of radiation at a particular wavelength. A slit further narrows the selected band of radiation to ca. 0.5 nm. A photomultiplier tube or silicone photodiode is used as the detector, which amplifies the signal to give a measurable reading. The dual beam UV spectrophotometer split the light path from the source so that half of the light passes through a reference cell filled with solvent; this cancels out background absorbance and any reflectance of UV radiation by the cell. With single beam instrument the cell with blank solvent has to be used to zero the background prior to taking readings.

The fraction of radiation absorbed by a solution of an absorbing analyte can be quantitatively related to its concentration using Beer-Lambert Law. According to the Beer-Lambert Law, the absorbance is directly proportional to pathlength (b) and concentration (c):

$$\text{Absorbance} = a.b.c \qquad \text{Eq. 2.3}$$

while a is the absorptivity (constant). When c is expressed as g/100 mL or % (w/v), a is known as the specific absorbance. The specific absorbance becomes A (1%, 1cm) when absorbance is measured at concentration of 1 % (w/v) in a 1 cm cuvette cell. In practical, dilute solutions are often used, typically between 0.001 to 0.01 % (w/v), to give absorbance values ideally in the absorbance range of 0.5-1.5. The Beer-Lambert law only applies when there is a linear correlation between absorbance and concentration. Linear regression analysis is usually undertaken to confirm the linearity. In practice, it is crucial to ensure that absorbance measurements are carried out within the linear range.

In the Franz cell studies, the spectrophotometer was used to quantify the amount of drug release into the receiver compartment at time intervals. A calibration graph of absorbance vs. concentration for a series of standard solutions of the drug is first constructed. The sample

drug concentration can then be read from the calibrated curve constructed. A typical standard UV calibration curve for ibuprofen drug is shown in Figure 2.14. The standard calibration curve was carried out each time prior to a Franz cell drug release experiment.

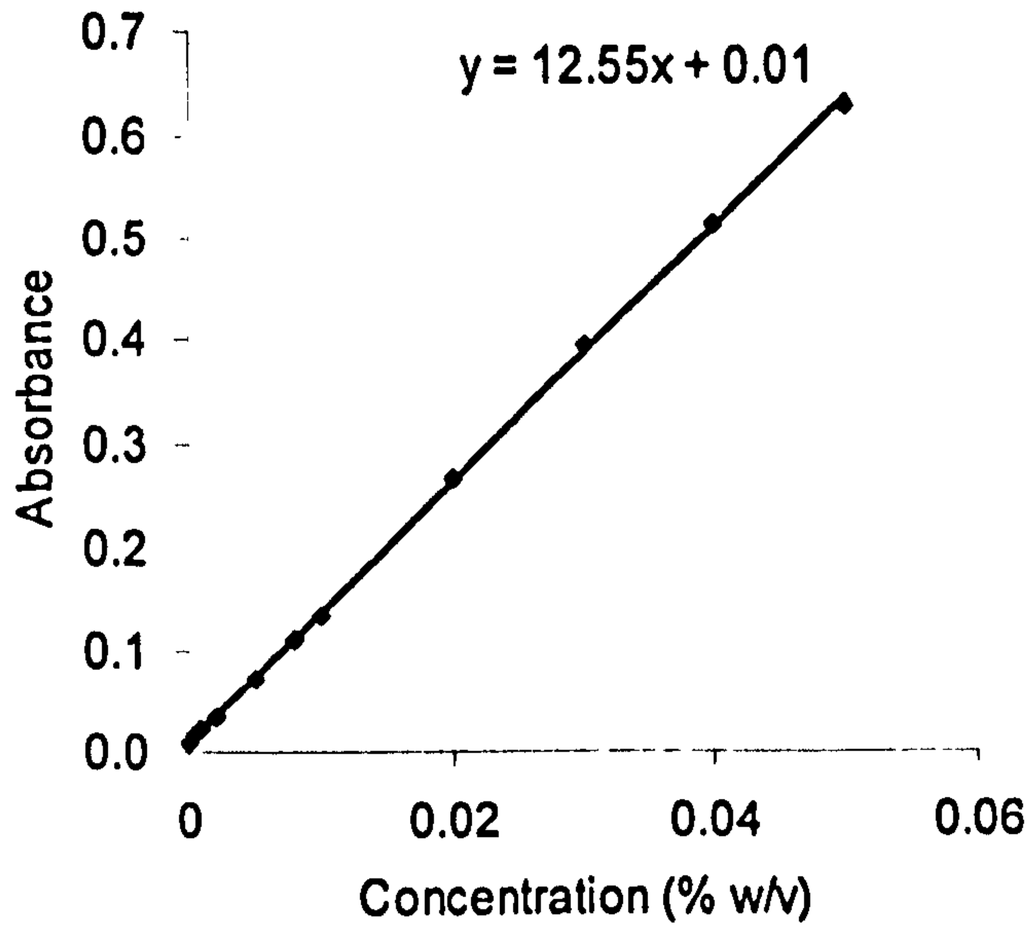

Figure 2.14: Typical calibration curve of ibuprofen for UV analysis

2.2.5 High Performance Liquid Chromatography (HPLC)

HPLC is the method used extensively in pharmaceutical quantitative analysis. It also uses UV spectrophotometry to detect the sample. The liquid mobile phase is pumped through a column packed with beads of stationary phase under high pressure (up to 6000 p.s.i.) at a specific flow rate. The analyte is loaded into the column and the separation of solutes in a mixture is based on the solute relative solubility between the stationary phase and the mobile phase. Depending on the degree of interaction between the compound and the stationary phase, the time of which each compound spent in the column vary. This time is known as the 'retention time'. There are two different modes of HPLC, namely the 'normal phase' HPLC and 'reverse phase' HPLC. The former consists of a polar silica-packed column, and a non-polar mobile phase (e.g. hexane and chloroform). Polar solutes interacts with the column will

be retained whereas non-polar solutes will be eluted out. However, the retention time of non-polar solutes can be increased via increasing the polarity of the mobile phase (e.g. by adding polar solvent such as isopropyl alcohol or methanol). The reverse phase HPLC is the opposite to that of the normal phase HPLC, where the column is non-polar and the mobile phase is polar solvent. Alkyl silanes, such as octadecylsilane (C_{18}) and octylsilane (C_8) are the common stationary phases, while the mobile phase usually contains a mixture of water or aqueous buffer with polar solvents such as methanol, acetonitrile or tetrahydrofuran. The reverse phase HPLC mechanism of separation is due to partitioning of the lipophilic portion of a molecule into the stationary phase, while less lipophilic molecules will be eluted out quickly.

A simplified schematic diagram of HPLC used in this study is shown in Figure 2.15 and this was a reverse-phase HPLC.

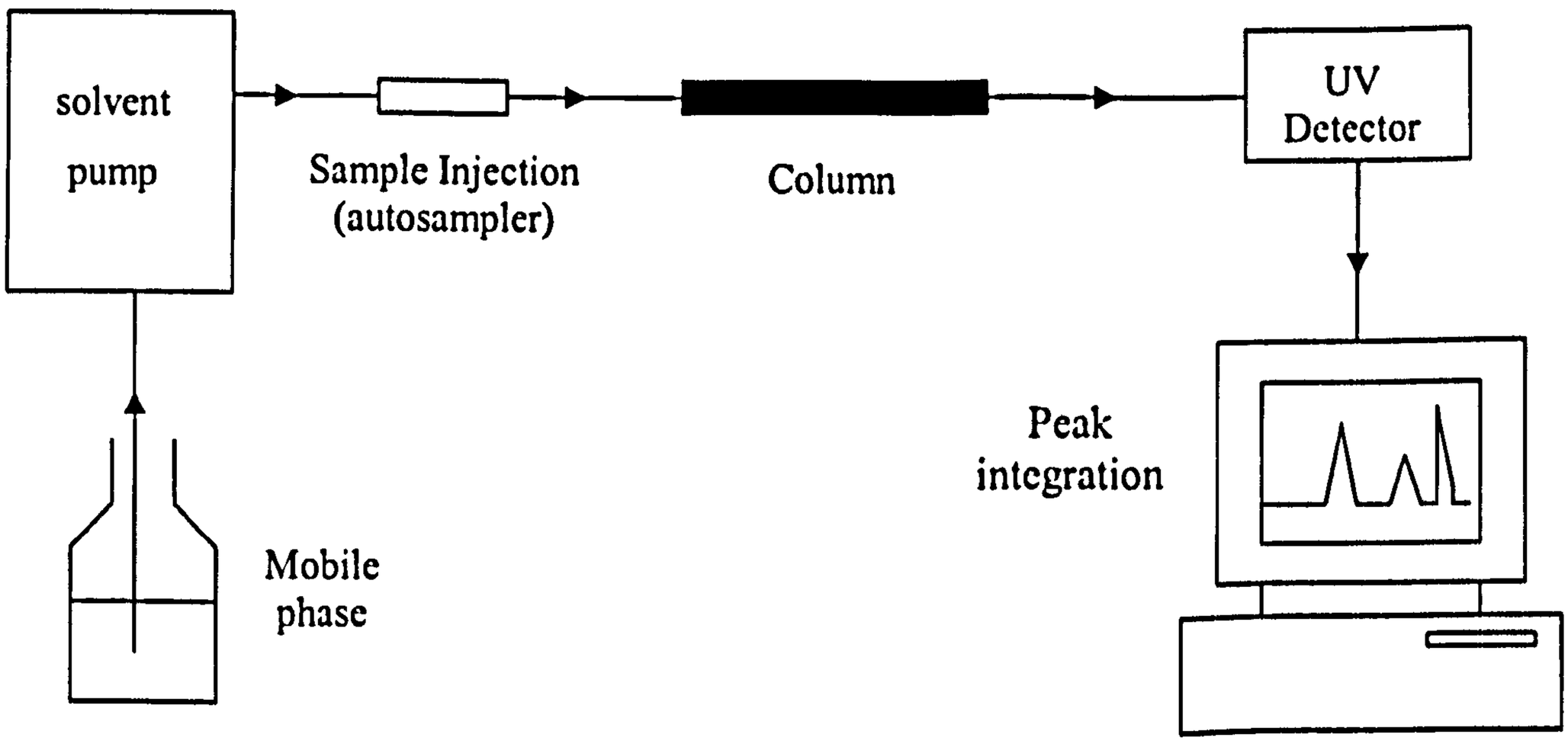

Figure 2.15: Schematic diagram of HPLC setup [adapted from Watson, 2005].

The HPLC measurements in this work were carried out using a Perkin-Elmer series 200 (Boston, USA), LC pump with an autosampler, connected to a UV absorbance detector 759A

(Applied Biosytems, USA). The stationary phase was Symmetry® ODS C_{18} column (Water Corp, Massachusetts, USA), 4.6 x 150 mm, 3.5 μm, with mobile phase comprising of acetonitrile/water (45:55 v/v). This was a chromatographic method developed for parabens detection (Chapter 6). The mobile phase solvent containing parabens is pumped through at high pressure carrying the injected sample (5 μL) into the column at the flow rate of 1 mL/min. The molecule eluted with time was detected by UV and the amount of paraben present was integrated as peaks.

The HPLC system suitability and reproducibility was regularly checked with two standard solutions using a proportionality constant method. The proportionality constant, k, is defined as

$$k = A/C \qquad \text{Eq. 2.4}$$

where A is peak area and C is the concentration. The system suitability was accepted when percentage nominal concentration, i.e. the percentage difference between both calculated and actual concentrations, are within 100±1%.

An example of percentage nomimal concentration calculation for one of the parabens (methylparaben) spreadsheet is presented in Table 2.2 below. In this instance, two standards (standard 1 and 2); both containing about 0.2 mg/mL of methylparabens weighed accurately in acetonitrile/water (50:50 v/v) were prepared. Standard 1 was run in triplicate and the mean peak area was obtained. The proportionality constant, k was obtained by peak area divided by the actual concentration of standard 1. Then the standard 2 was run and the mean peak area was also obtained. Using k, the concentration of methylparaben in standard 2 was calculated. Then the percentage of nominal concentration is obtained by dividing the calculated concentration over actual concentration of the standard 2.

Table 2.2: The determination of % nominal concentration of two standards of methylparaben (MP).

Standard	Actual MP Concentration (% w/v)	Peak Area[a]	Proportionality constant, k[b]	Calculated MP concentration (% w/v)	% nominal concentration[c]
1	0.2082	4963412	4.19512E-08	-	
2	0.2099	5020971	-	0.2106	100.3

[a]The peak area was the average of the triplicates.
[b]The value k is the peak area divided by actual concentration (arbitrary unit).
[c]This was the percentage of the calculated to the actual concentration of standard 2.

The HPLC was utilised for analysing the methyl-, ethyl-. propyl- and butylparaben in Franz cell release (Chapter 6).

2.2.6 Freeze-drying

Freeze drying, or lyophilisation, is a process of removing water from a material by first freezing into ice then sublimate into water vapour under reduced pressure. The freeze drying process does not damage the integrity of the crystalline structure of a material because the water is removed in the form of vapour. The principle of freeze drying can be described using a water phase diagram (Figure 2.16).

The freeze drying process involves three phases; freezing, primary drying and secondary drying. Freezing of the solution to well below the triple point temperature for pure water is crucial; so that the drying can take place via sublimation, by-passing the liquid phase. The pressure is effectively maintained at below the triple point using the vacuum pump. The vapour formed is removed continually to avoid pressure increase that would stop sublimation. This is accomplished by cooling of the condenser below the sample temperature, so that the vapour is attracted to the cooler surface and trapped in the form of ice. Primary drying (sublimation) removes frozen bulk of 'free' water via heating the in a

series of thermal ramps to room temperature under reduced pressure. Further raising the temperature at the end of the primary drying process to above room temperature removes the residual moisture which adsorbed onto the sample (secondary drying).

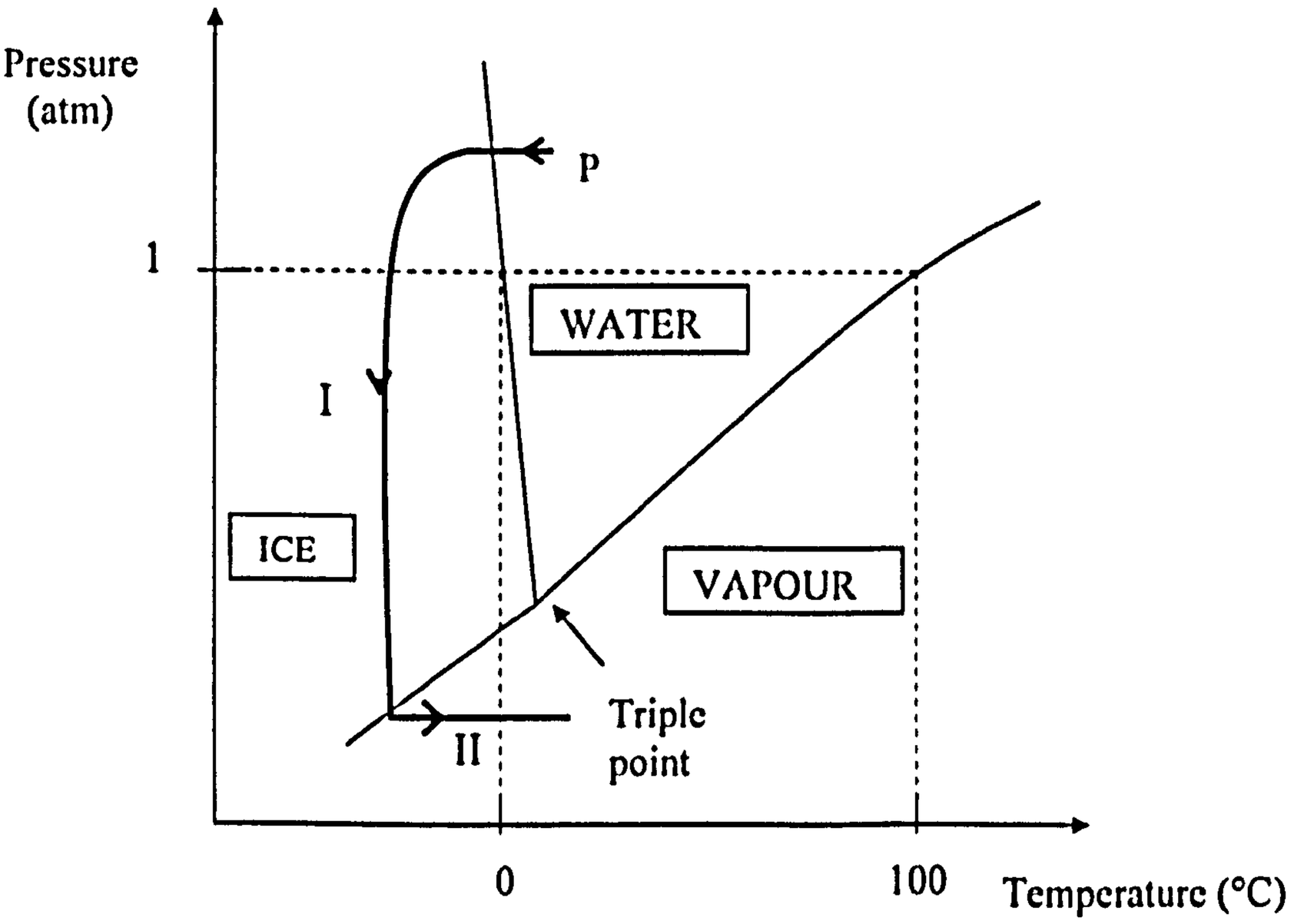

Figure 2.16: The water phase diagram [redrawn from Snowman, 1997]. The bold-line indicates the phase change of water during freeze-drying. The sample (at P) is rapidly cooled to below the freezing point via reducing pressure (I). The water in the sample is frozen into ice. After freezing, the pressure is lowered and enough heat is supplied to the material for ice to sublimate. Then, it is under reduced pressure to accelerate the sublimation (II).

Freeze-drying of gels in our studies was undertaken in a laboratory-scale freeze-drier (Virtis Advantage EL, New York, USA). The schematic of a freeze dryer is shown in Figure 2.17 below. The freeze-dryer consists of a temperature controlled shelves, a condenser to trap water removed from the material, a cooling system to supply refrigerant to the shelves and condenser, and a vacuum system to reduce the pressure in the chamber. The freeze-drying

steps were programmed via computer using freeze-dryer software (Virtis process controller datalogger v 3.0).

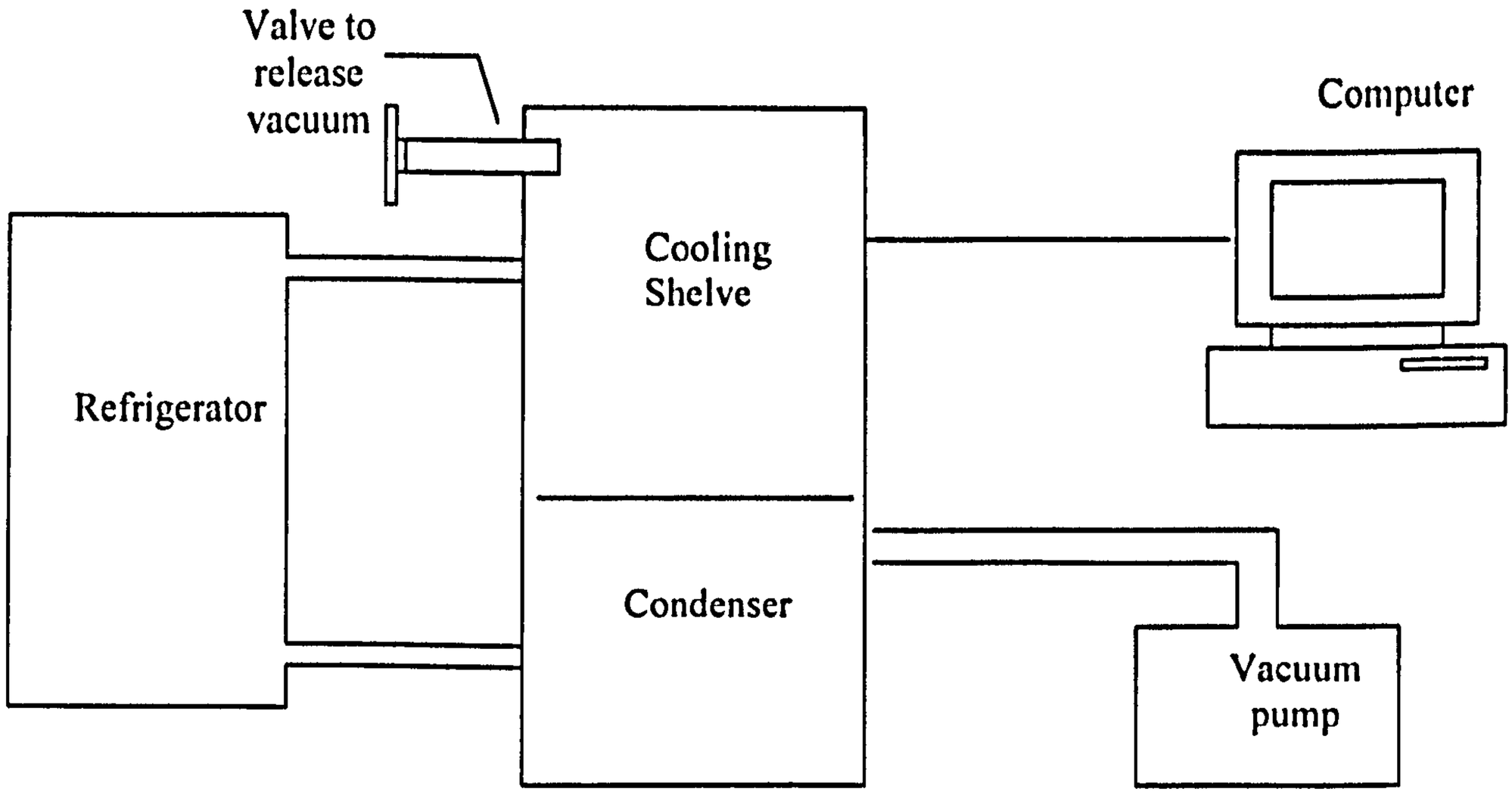

Figure 2.17: Schematic diagram of a freezer dryer [adapted from Virtis advantage manual].

Freeze drying is a very widely used method for in the pharmaceutical and biological products for prolonging shelf life. For example, vaccines and injectables are freeze-dried for the ease of storage and shipping and later reconstituted to original liquid form prior to use. In our studies, the gel was freeze-dried to produce crystalline, porous material known as 'sponges' or 'wafers' (Chapter 7).

2.2.7 Osmometer

When two aqueous solutions of different concentrations are separated from each other by a semipermeable (permeable to water only) membrane, the water will moves from the solution of lower concentration to the solution with higher concentration across the membrane. The movement of water will depend on the concentration gradient and the nature of permeability

of the membrane. This movement of water is called 'osmosis' and the pressure which would need to be exerted to halt its movement is called the *osmotic pressure*. Figure 2.18 illustrates a simple osmosis experiment set up. For example if a 0.1M glucose solution is separated from water by a semipermeable membrane (only permeable to water). The water moves through the membrane and the glucose solution level rises in the tube. The net water flow ceases when the pressure exerted by the column of liquid is equal to the osmotic pressure of the glucose solution.

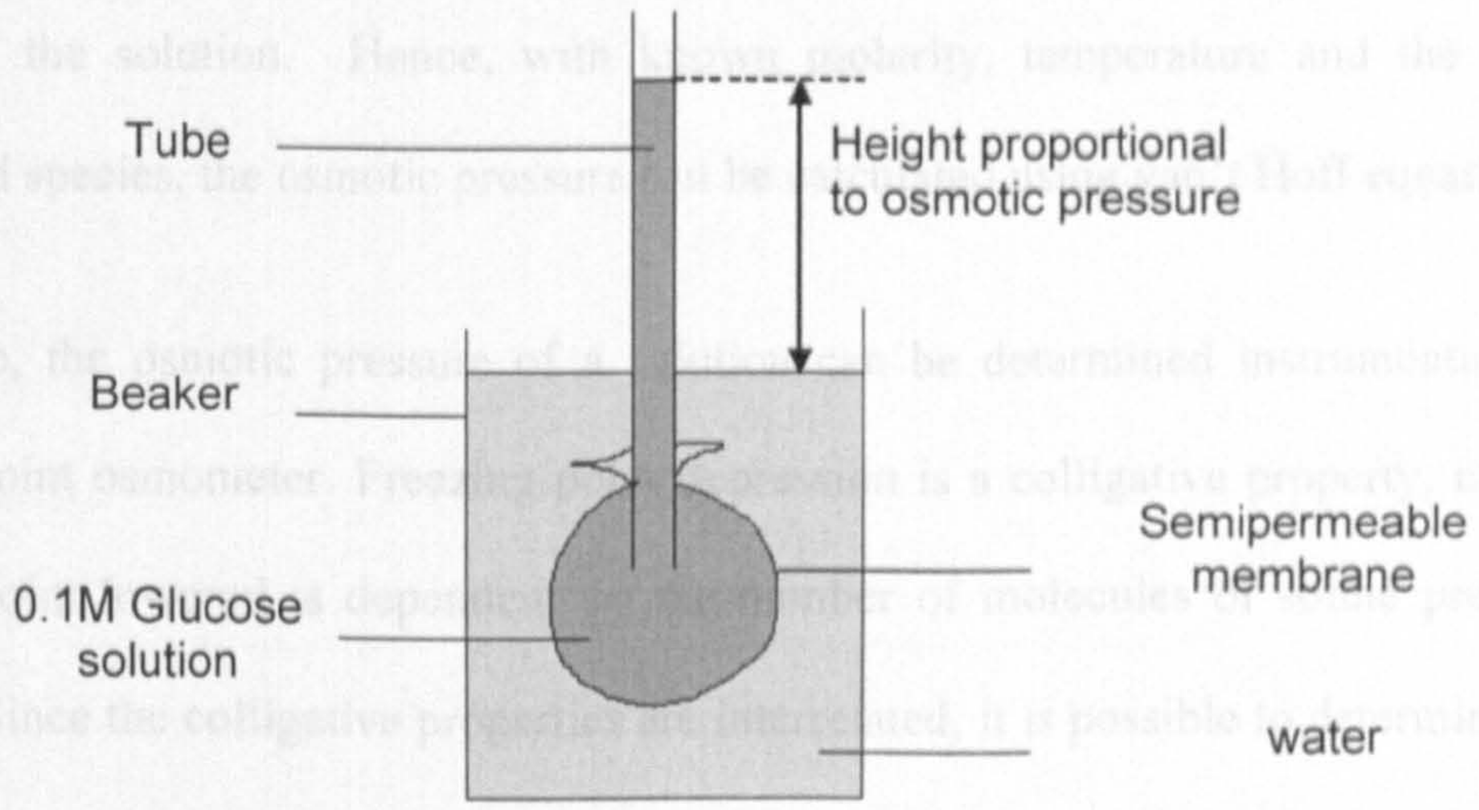

Figure 2.18: Simple osmosis experiment set up. 0.1M glucose solution is separated with water by a semipermeable membrane. Water moves into the glucose column causes the level in the column to increase.

The osmostic pressure is determined by the total number of particles in the solution, regardless of molecular nature (colligative property). The total number of particles will depend on the degree of dissociation of the solute. In the example above, if the glucose solution is replaced by an aqueous solution of potassium chloride of the same molarity, the solution in column would reach a height almost twice as high as the glucose. This is because potassium chloride dissociates into two ions per molecule in water. However in reality, this dissociation is usually incomplete and there might be association between the particles in the solution. The term 'osmotic coefficient' is used to take into such deviation from the 'ideal'

behaviour of the system. The osmotic pressure of a solution is related to the amount of solute using the van't Hoff's equation:

$$\pi = i\,M\,R\,T \qquad \text{Eq. 2.5}$$

where π is osmotic pressure (Pa) , M is molarity (mol L^{-1}), R is the gas constant (J mol^{-1} K^{-1}), T is temperature (K). Since osmotic pressure is a colligative property, *i*, the Van't Hoff's factor, is introduced into the equation to account for the number of dissociated species present in the solution. Hence, with known molarity, temperature and the number of dissociated species, the osmotic pressure can be calculated using van't Hoff equation.

In practice, the osmotic pressure of a solution can be determined instrumentally using a freezing point osmometer. Freezing point depression is a colligative property, in which the freezing point lowered is dependent on the number of molecules of solute present in the solution. Since the colligative properties are interrelated, it is possible to determine the value of one property from knowledge of another. So by measuring the lowering of freezing point, the osmotic pressure of a solution can be determined. The freezing point osmometer expressed osmotic pressure in osmolality, i.e the number of osmoles per kg of water. The relationship of the freezing point depressed (ΔT) is related to osmolality by the equation below:

$$\Delta T = \frac{R.T_f^2.0}{L_f} \qquad \text{Eq. 2.6}$$

where R is gas constant (8.34 $J.K^{-1}mol^{-1}$), T_f is freezing point of water, 0 is osmolality and L_f is the latent heat of water melting (3.33×10^5 $J.Kg^{-1}$). The osmometer measures freezing point lowering (ΔT) and calculates the osmolality automatically.

The osmometer used in this study was a freezing point depression osmometer (Model 3D3 Advance™ Instrument, Massachusetts, USA). The schematic of freezing point depression osmometer is shown in Figure 2.19.

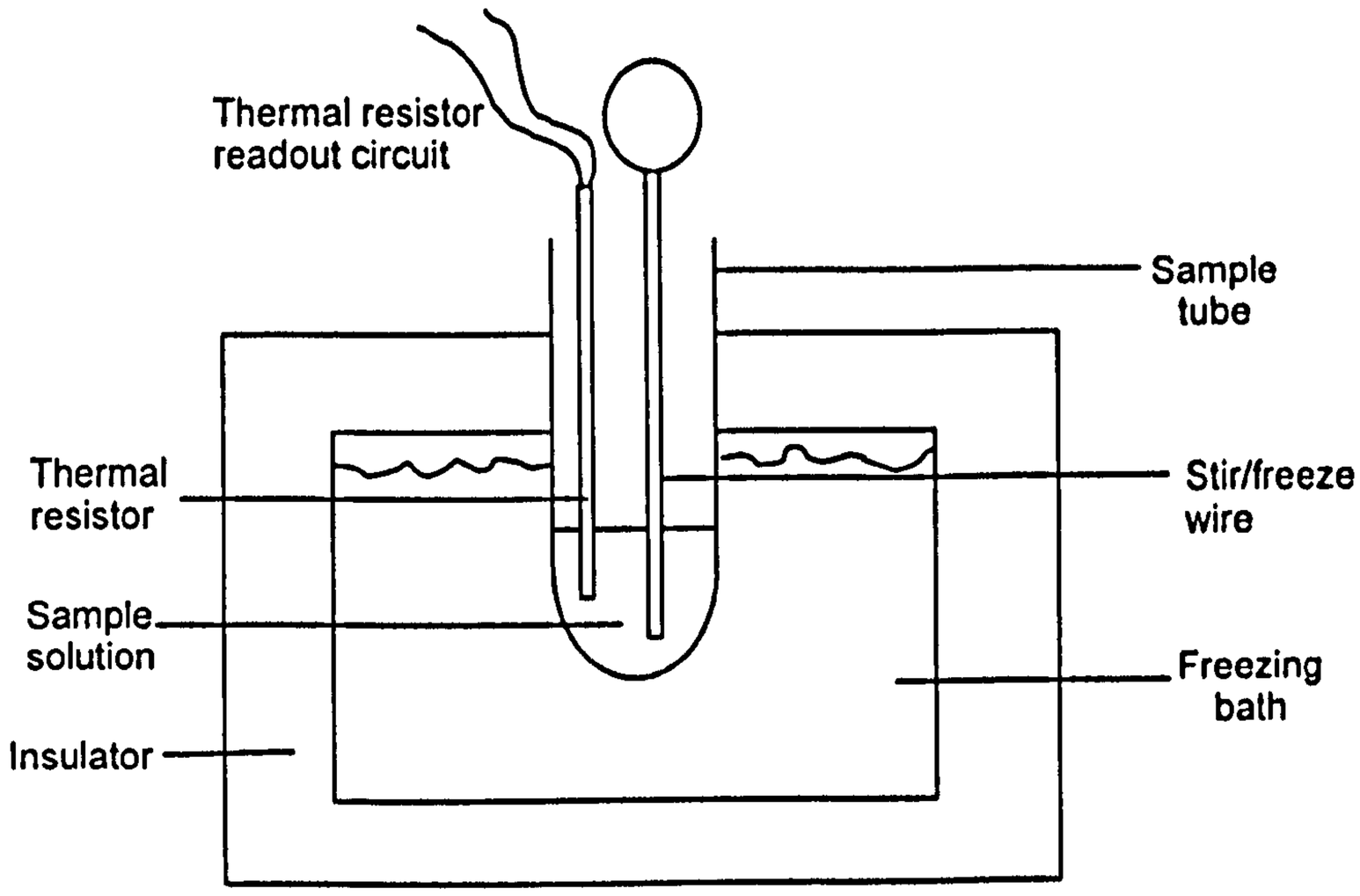

Figure 2.19: Schematic of Freezing point depression osmometer [adapted from Advance™ Instrument Userguide].

The sample solution (0.2 – 0.25 mL) is placed in the sample tube. The sample tube is submerged in the sample well in contact with the freezing bath which contained heat-transfer fluid (coolant). When the osmometer is initiated, the osmometer probe, consists of a stirrer/freeze wire and a thermal resistor, is lowered into the sample tube with the tips immersed in the sample solution. The stirrer/freeze wire vibrates and form ice crystals in the sample solution; while the sensitive thermal resistor monitors the sample temperature as well as measures the freezing point of the sample. The operation of a freezing point osmometer can be illustrated using the temperature-time plot showed in Figure 2.20.

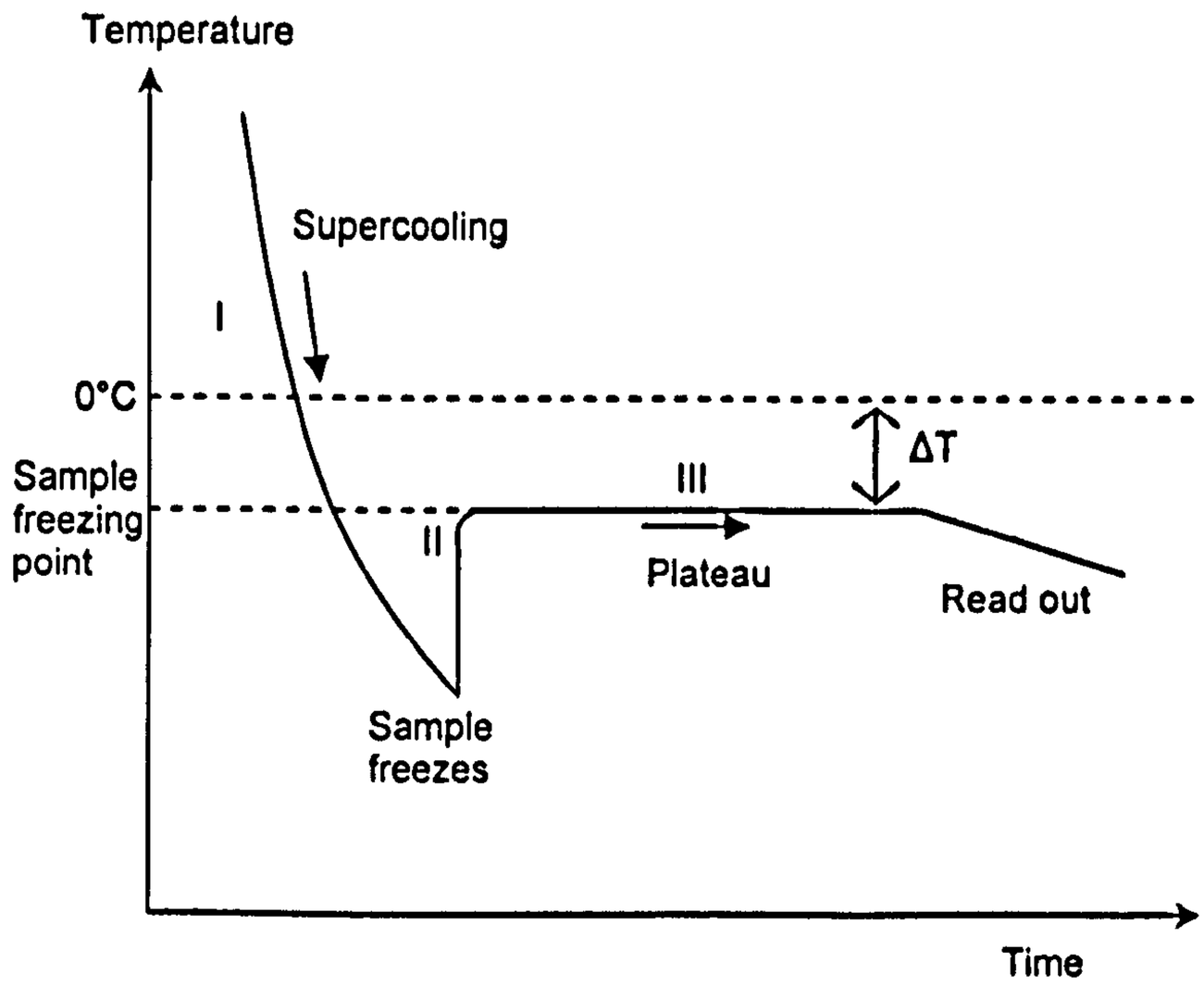

Figure 2.20: Freezing point osmometer temperature-time plot [redrawn from Advance™ osmometer user guide].

The sample solution in the sample tube is supercooled to several degrees below its freezing point and sample crystallisation is initiated (I). As the sample freezes, the heat of fusion is suddenly released; this causes the temperature to rise to the sample freezing point (II). The probe senses the temperature equilibrium temperature and the amount of freezing point depressed (ΔT) is measured. After a time over the sample freezing point is maintained and the osmometer generates a read out (III).

The osmometer in our laboratory was calibrated using an isotonic reference solution (Clinitrol™ 290). The reference solution was run twice before each testing and the osmolality should fall within the expected range stated by the manufacturer (288-293 mOsm/kg). Table 2.3 shows typical calibration readings for reference solutions prior to testing.

Table 2.3: A typical record of reference solution (Clinitrol™ 290) prior to testing.

	Reference Solution osmolality (mOsm/kg)*	
	Reading 1	Reading 2
Batch 1 testing	292	291
Batch 2 testing	290	290

*expected range 288-293 mOsm/kg

The freezing point osmometer is a convenient and rapid method for obtaining results (within a few minutes). It is widely used for clinical applications, such as to determine serum and urine osmolality, as well as in contact lens saline and isotonic drinks. It can also be used to determine the molecular mass of a polymer upon breakdown or formation after a chemical reaction. In our study, the freezing point osmometer was used to measure the osmotic pressure of the receptor solutions in Franz cells (Chapter 4).

2.3 Franz cells studies

All Franz cells employed were static-type diffusion cells. There were three Franz cells arrays used in the whole course of study:

Set 1: University of Strathclyde

Set 2: PermeGear, Inc.

Set 3: GlaxoSmithKline (Harlow)

A basic Franz cell consists of a donor and a receptor compartment held together with a metal clamp. Each Franz cell was placed in a magnetic stirrer block and connected to a heating device. The heating can be by the means of dry (heated block) or wet (water-jacket) approach.

Set 1: University of Strathclyde Franz cells

The glass Franz cells were custom-made (Radleys glass-blower) with measured receptor effective diffusion area of ~ 78 mm^2 and receptor volume of ~12 mL. The donor cells are tall

(5 cm) and the orifice area measurements are 60 mm^2. The Franz cells were immersed in the dry blocks in heated magnetic chambers, as portrayed in Figure 2.21 (a). There were four stirrer chambers and within each chamber there were eight stirrer blocks (Figure 2.21 (b)). Each chamber has a built-in magnetic field circuit and heating device in which the block temperature and magnetic speed can be regulated via its individual controller connected to the chamber. Most of the Franz cell drug release studies during the course of study were undertaken using this array, unless otherwise stated.

Set 2: PermeGear, Inc. Franz cells

PermeGear (Bethlehem, USA) Franz cells and equipment are shown in Figure 2.22 below. The Franz cells possessed smaller receptor diffusion area (~75 mm^2), and receptor volume (~5 mL) and shorter donor height (~1.5 cm) compared to University of Strathclyde Franz cells (Set 1). The receptor chamber was water-jackated, and the sampling arm was longer in length as shown in Figure 2.22 (a). Since this array was a commercial set, the receptor volumes were calibrated and calibrated lines were indicated at the side arms. These Franz cells are placed in a 9-station magnetic stirrer and the water jackets were connected to a thermostatically controlled water-circulator via latex tubes (Figure 2.22 (b)).

Set 3: GlaxoSmithKline (Harlow) Franz cells

This set of Franz cells (Figure 2.23) were water-jacketed receptor Franz cells and the designs were similar with that of PermeGear. The Franz cell possessed receptor diffusional surface areas of ~ 2 cm^2 and receptor volumes of ~ 7.5 mL The donor cells heights were 2 cm. The Franz cells were individually placed in a pyrex container held with a metal clip. The pyrex container was equipped with magnetic stirring device and connected to a speed controller. And the water from the water bath was circulated around the water jacket interconnected using latex tubings.

(a)

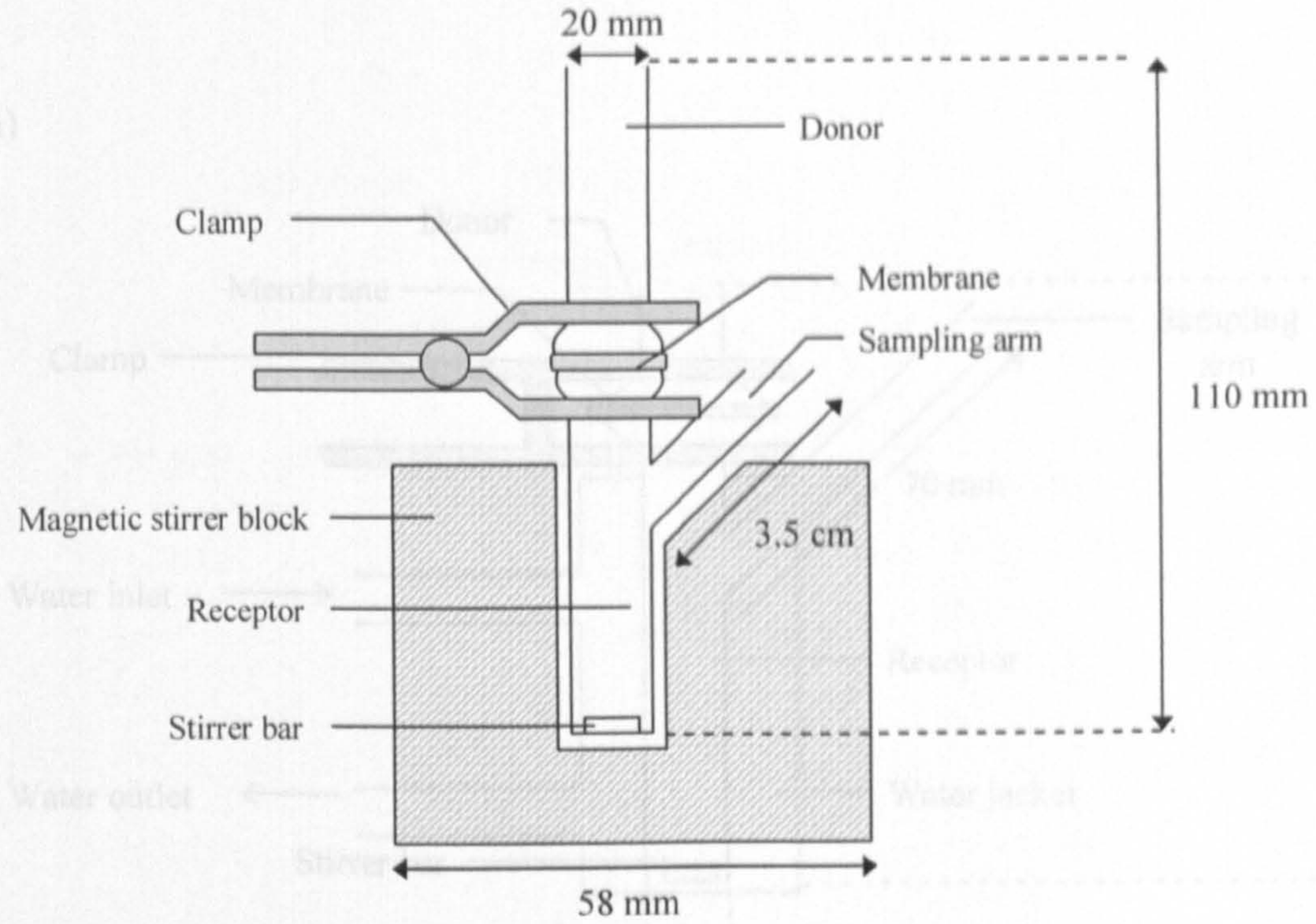

(b)

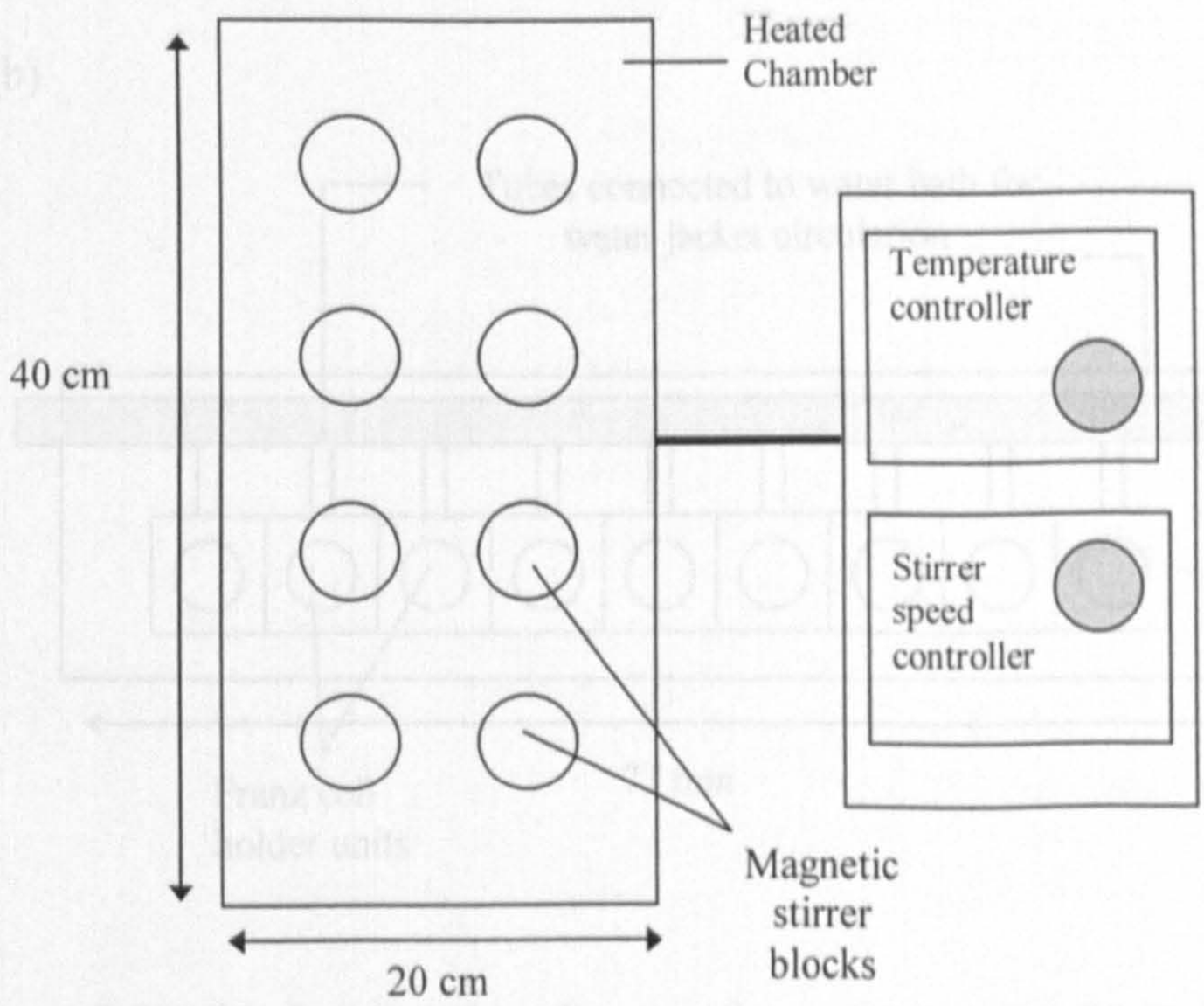

Figure 2.21: Set 1. Franz cell equipment of University of Strathclyde. (a) Franz cell in heated block. (b) Heating chamber connected to stirring and heating controller.

(a)

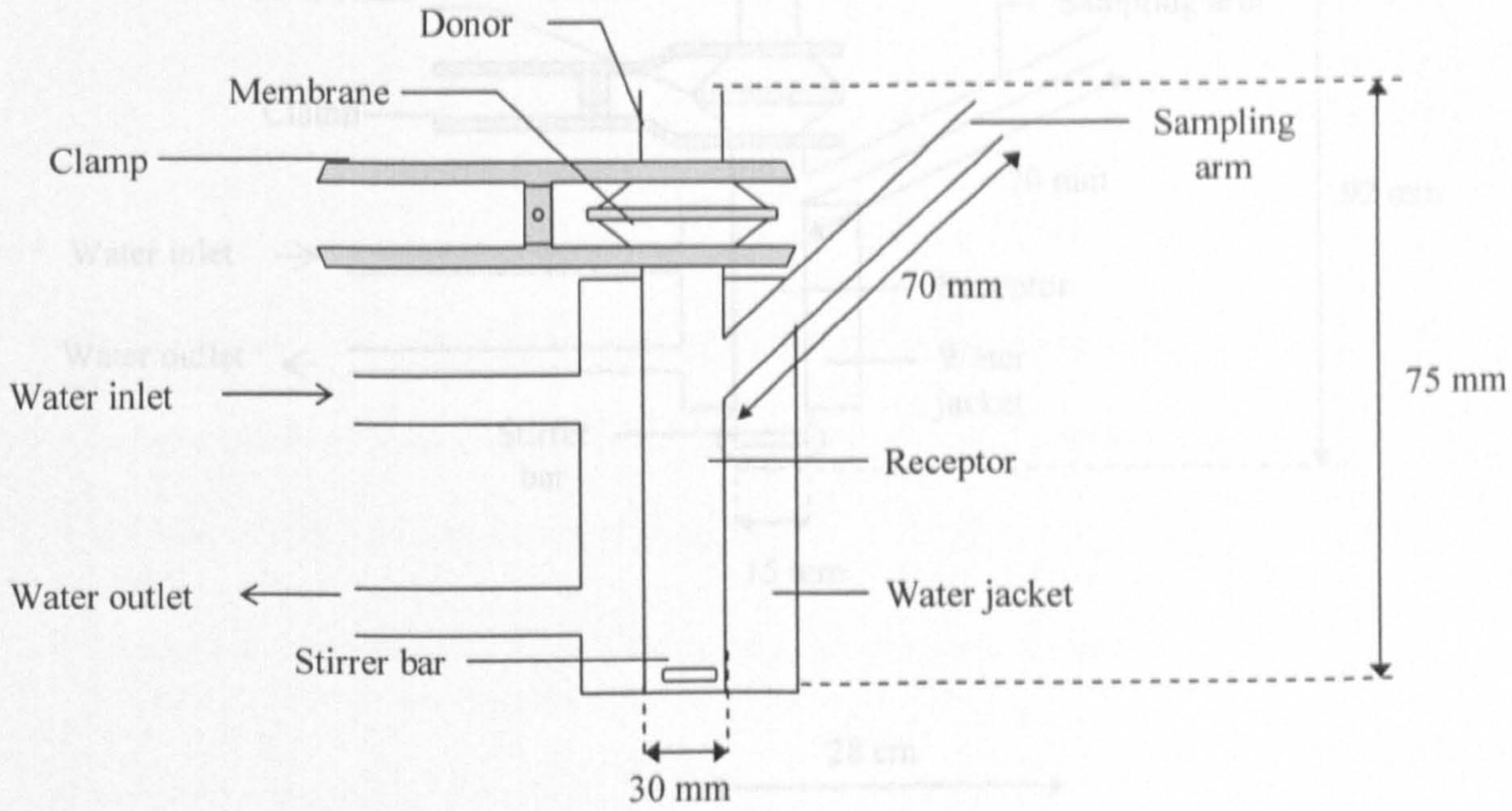

(b)

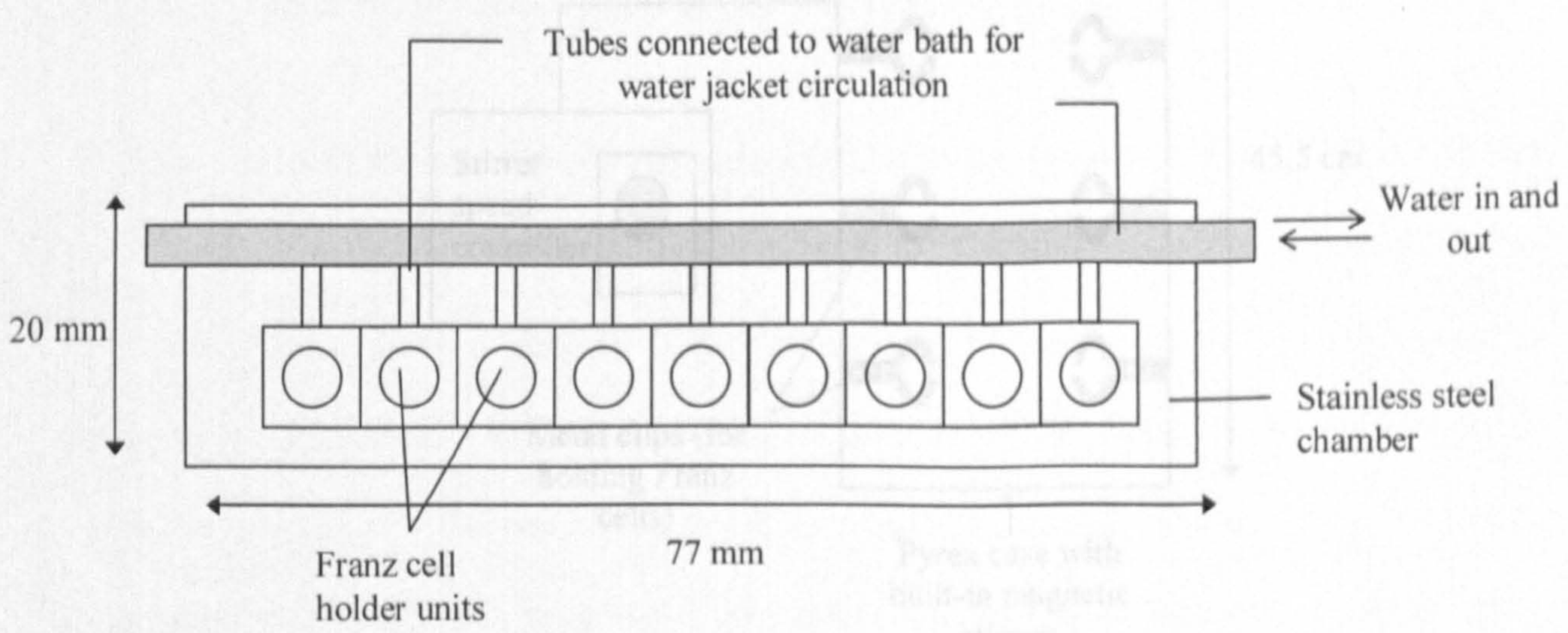

Figure 2.22: Set 2. PermeGear Franz cells equipment. (a) Water-jacketed Franz cell. (b) PermeGear 9-station magnetic stirrer chamber.

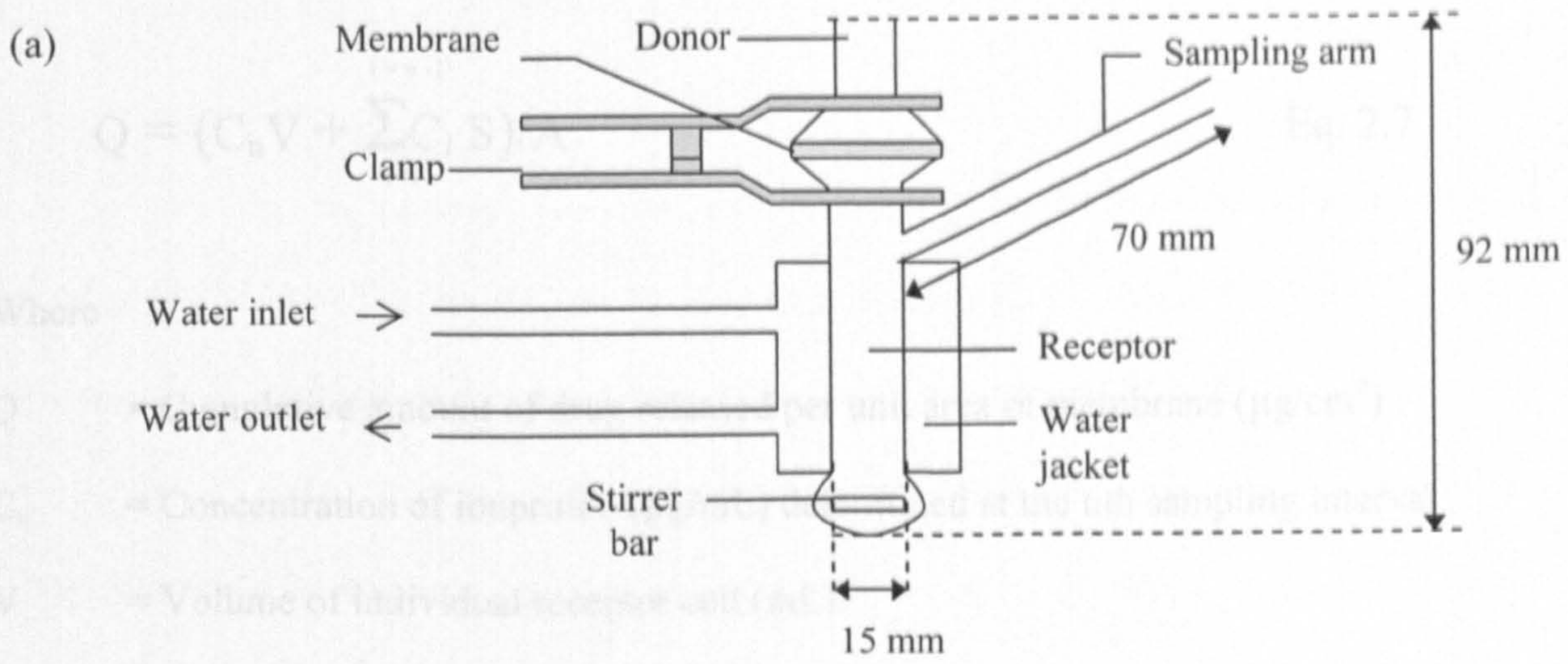

Figure 2.23: Set 3. GlaxoSmithKline (Harlow) Franz cells equipment. (a) Water-jacketed Franz cell. (b) Pyrex container with metal clips connected to stirrer speed controller.

2.3.1 Calculation of drug flux

The drug liberation from dosage form in the donor is measured by collecting the receptor fluid samples at time intervals and subsequently analysing them for drug content. The cumulative amount of drug release per unit area was calculated as follows:

$$Q = (C_n V + \sum_{i=1}^{i=n-1} C_i S)/A \qquad \text{Eq. 2.7}$$

Where

Q = Cumulative amount of drug released per unit area of membrane ($\mu g/cm^2$)

C_n = Concentration of ibuprofen ($\mu g/mL$) determined at the nth sampling interval

V = Volume of individual receptor cell (mL).

$\sum_{i=1}^{i=n-1} C_i$ = Sum of concentrations of ibuprofen ($\mu g/mL$) determined at sampling interval 1 through n-1 (i denotes no. of time interval).

S = Volume of sampling aliquot (mL)

A = Effective diffusion area of receptor cell (cm^2)

All the calculations and plots were accomplished using Microsoft Excel (version 2002) electronic spreadsheet. The steady state flux of the drug (J) was determined from the linear portions of the individual cumulative amount vs. time plot using linear regression analysis ($R^2 \geq 0.99$). The permeability coefficient (Kp) was calculated according to the equation Kp = J/Cv, in which Cv is the concentration of the drug in the donor solution. All results were expressed as mean values ± standard deviations. The statistical difference between mean fluxes was performed using one-way ANOVA, with significance set at $p < 0.05$. The coefficient variation (CV) for all results was calculated as the percentage of ratio of the standard deviation to the mean (equation 2.8).

Coefficient of variation (%) = (standard deviation / mean) x 100% E.q. 2.8

CHAPTER III

VALIDATION OF FRANZ DIFFUSION CELL EXPERIMENT

3.1 Introduction

A large variability in the result obtained with diffusion cells studies persists today [van de Sandt *et al.*, 2004; Khan *et al.*, 2005]. Although biological variations in skin often cause difficulty in predicting skin permeability for a given permeant [Southwell *et al.*, 1984; Kasting *et al.*, 1994], such variability should not occur with synthetic membranes because unlike skin, they do not have complex structure and biological components. On the contrary, they are structurally simple and carefully manufactured.

A recent study involving 18 laboratories using a synthetic membrane under quasi-standardised conditions showed up to 35% variation in drug fluxes between laboratories [Chilcott *et al.*, 2005]. In this study, each laboratory was given a homogenous membrane (silicone rubber), materials, penetrant (methylparaben) and a prescriptive protocol. The fundamental aspects such as temperature, receptor fluid composition, membrane preparation, donor solutions were provided. The laboratories, however, used their individual set of diffusion cells. It was shown that the intra-laboratory variation was averaging 10% while the inter-laboratory variation was up to 35%. These studies illustrate that skin variation was not the only issue. Non-skin related parameters such as apparatus variables, working conditions, operator errors are potential source of variables which many laboratories may have overlooked.

A complete set of Franz cell apparatus comprises of the glass diffusion cells, magnetic stirring equipment and a heating device. Commercial Franz cell apparatus are generally

expensive. Custom-made Franz cells are cheaper alternatives which are commonly employed by many laboratories. Owing to the fact that the latter are tailor-made, design variables between Franz cells, for example the donor and receptor dimensions, the length of the side-arms etc. can exist.

Regulatory guidelines offer only partial-standardisation of *in vitro* skin absorption studies [Skelly *et al.*, 1987; Shah *et al.*, 1991; FDA-SUPAC-SS, 1997; Siewert *et al.*, 2003]. This gives each laboratory a degree of flexibility as to the design of the equipment and experimental protocol this has led to a large deviation in methodology for example membrane treatment, sampling intervals and temperature regulation. Franz cell experiments demand meticulous planning and require a reasonable amount of time for operator training. They are normally performed with a minimum of six replicates to ensure result accuracy and technique reproducibility. Each laboratory has its own individual set of Franz cells with varying design and physical characteristics; however this should not contribute variation in drug flux. A lot of validation work has been carried out on diffusion cells to demonstrate the robustness as well as the reliability of different arrays of diffusion cells such as flow through cells [Cordoba-Diaz *et al.*, 2000], side-by-side cells [Smith and Haigh, 1992] as well as modified Franz cells [Morell *et al.*, 1996; Thakker and Chern, 2003]. However, published work emphasises the method development for a specific drug diffusion test, and does not investigate how validation of Franz cells equipment and stirring equipment influence reproducibility and variability of results.

3.1.1 Aims of study

The aim of this chapter was to investigate tailor-made Franz cell apparatus variables that are potential in affecting drug flux. These include Franz cell dimensions and stirring variables. Other factors investigated were: volume of receptor cell, donor and receptor membrane

contact areas, shape of the base of receptor cell and the angle of the sampling arms. The stirring factors examined include the ideal stirring speed, the types of magnetic stirring bars used and the stirring block efficiency. Experiments with ibuprofen drug release from a gel formulation through a model synthetic membrane (Visking) were performed before and after the validation. After the initial validation, further studies on the temperature, sampling rate and donor volume were also carried out. The Chilcott experiment [Chilcott *et al.*, 2005] was repeated using our validated Franz cells and equipment and the data from this study was compared to that of Chilcott's.

3.2 Method

3.2.1 Franz cell dimensions

Figure 3.1 shows a schematic diagram of a typical Franz cell and the dimensions measured.

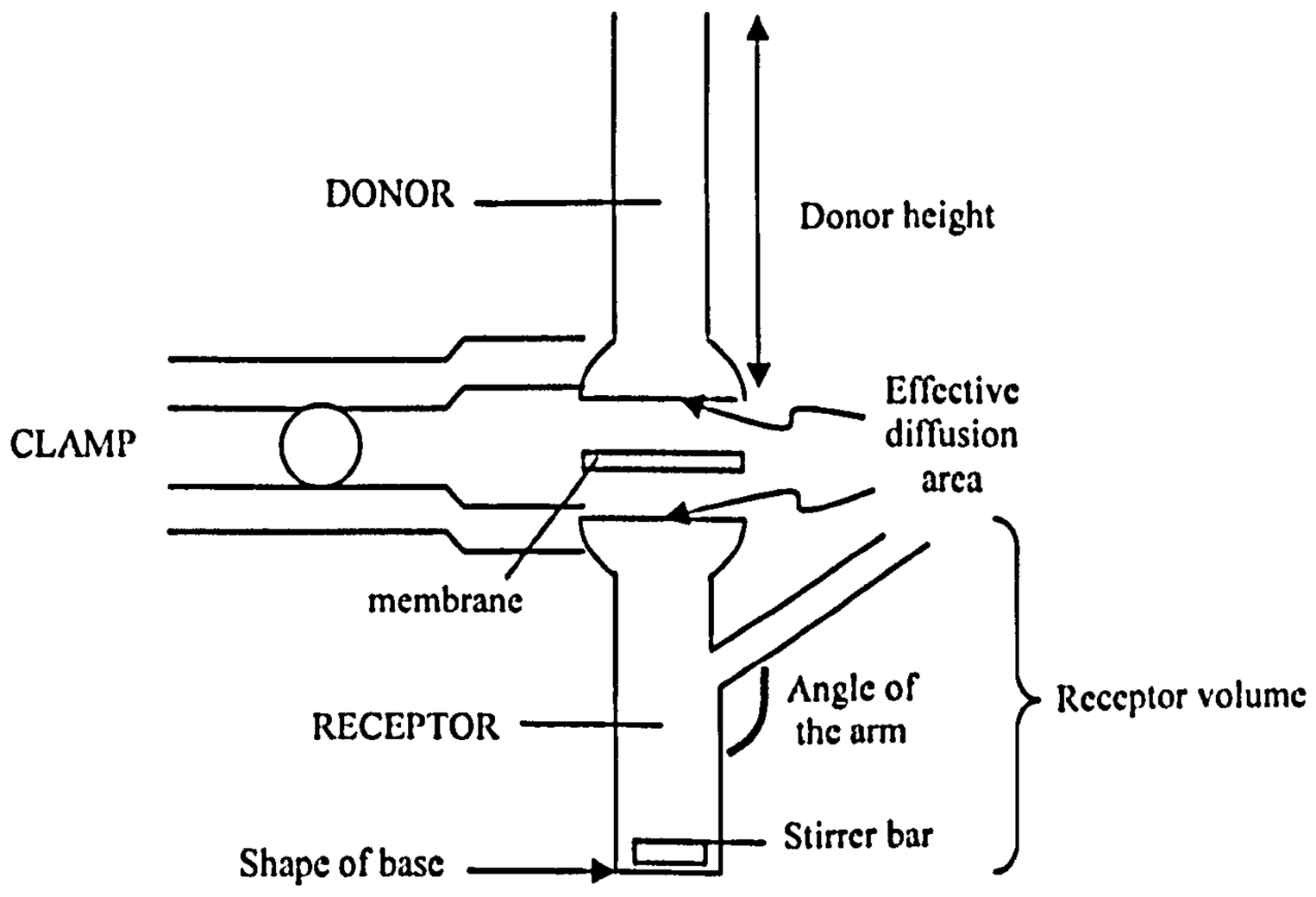

Figure 3.1: Franz cell (tailor-made) and the dimensions investigated.

The height of the donor cells were measured in triplicate using a pair of callipers. The angle of the arm of receptor cells was measured using a protractor. The shape of the base of

receptor cells of was observed visually to identify whether it was flat or convex. A cylindrical magnetic stirring bar (12 x 4.5 mm) was placed into the receptor. Distilled water was carefully filled to the lip of the receptor cell and the exact volume was recorded (n=4). To determine the internal diameter of the donor and receptor, a pair of callipers was placed on the inside, 1-2 mm from the opening; whilst the external diameter the receptor was determined by laying the tips on the outside. The measurement of external diameter of donor was not possible because the lip at the edge of the opening is curved. Effective diffusion area (E.D.A) was calculated for both donor and receptor cells using formula πr^2, where r is the radius. For donor E.D.A, r was the internal radius, but for the receptor the average of both internal and external radius was used. The physical dimensions mentioned above of the custom-made Franz cells (University of Strathclyde) were compared to a set of commercial Franz cells (PermeGear). These Franz cells were described in Chapter 2, section 2.3 (Franz cell set 1 and 2 respectively).

3.2.2 Stirring variables

The receptor stirring was visualised using a dye. Since the model drug for the diffusion studies was ibuprofen (MW 206.3), potassium permanganate ($KMnO_4$, MW 158.03) was employed as the standard dye because it has a similar molecular weight to ibuprofen.

3.2.2.1 Determination of ideal stirring speed

The receptor cells were placed in the stirrer blocks and filled with distilled water. Potassium permanganate powder was gently tapped using a spatula onto the receptor cells. The time taken for the dye to spread to body and arm of receptor cells at increasing arbitrary speed 3, 7, 10, 11, 12, and 14 were recorded. PTFE cylindrical stirring bar of dimension 4.5 x 12 mm was used and experiments were carried out at ambient temperature.

3.2.2.2 Type of Stirring Bar

Three types of stirring bars of different dimensions were used, namely Type I - Teflon cylindrical magnetic stirring bar, 10 x 3 mm; Type II - PTFE cylindrical magnetic stirring bar, 12 x 4.5 mm; and Type III - PTFE pivot ring cylindrical magnetic stirring bar, 12 x 6 mm. Potassium permanganate was also employed as the dye in this experiment. The finely ground dye powder was gently loaded into the receptor cell filled with distilled water at room temperature. For each type of stirring bar, the dye distribution pattern was observed at no stirring, arbitrary low (1.5), medium (5) and high speed (11).

3.2.2.3 Determination of Revolutions per Minute (RPM)

An arbitrary speed of 10 was chosen to determine the revolutions per minute (RPM) of a magnetic stirrer bar spinning in a beaker placed in the to stirrer blocks. After investigation as to which blocks gave good stirring, the dye experiment was repeated on these good blocks.

(i) Calibrating Blocks RPM

A 100 mL beaker containing 50 mL of distilled water was prepared. A marker line was drawn at the base from the edge of beaker towards the centre with a permanent marker (Figure 3.2 (b)). A PTFE magnetic stirring bar, octagonal with pivot ring, of dimension 38 x 10 mm was placed into the beaker. A line was marked at one end of the stirring bar. Together with the stirring bar, the beaker was immersed into the Franz cell blocks at ambient temperature (illustrated in Figure 3.2(a)). At speed 10, RPM, the number of spins per minute was counted visually, where each spin was when the line on the stirring bar passed through the line at the base of the beaker (Figure 3.2 (b)). The behaviour of the stirring bar, whether it was spinning steadily and centrally, was also noted.

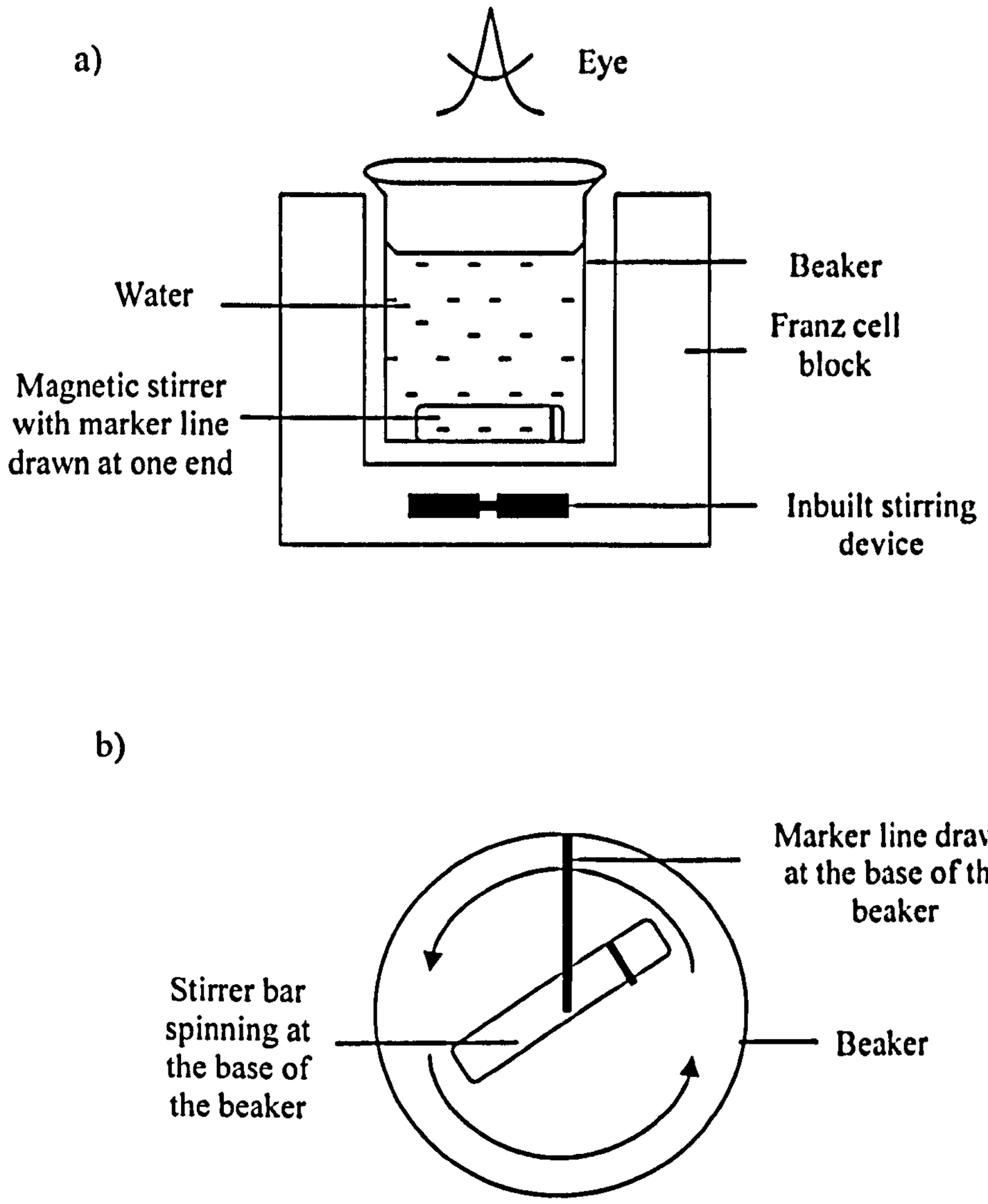

Figure 3.2: Illustration of stirring speed calibration. a) Position of the beaker and stirring bar immersed in a Franz cell block, b) View from above.

(ii) Calibration of stirring blocks

After identifying the blocks that provide good stirring, the receptor cells were filled with distilled water and inserted into these blocks and heated to 37 °C. The dye experiment was repeated using a 12 x 4.5 mm (Type II bar) in the Franz cells and the time for dye distribution throughout Franz cells recorded using a stopwatch.

3.2.3 Investigation of donor volume on sink condition

The donor volume for ibuprofen drug diffusion from saturated solution was 1 mL. However before conducting the drug diffusion test, a simple investigation was conducted to ensure that 1 mL gave sink condition. The saturated solutions of ibuprofen were prepared by adding excess ibuprofen powder (~2 g) to 0.1M sodium hydroxide. The suspension was agitated for 1 hour in a water bath maintained at 60-65°C. Residues of undissolved ibuprofen were removed by filtration at the same temperature and the solution was allowed to cool to 33 °C.

Three Franz cells were then set up. Each receptor compartment was filled with de-gassed 0.1M sodium hydroxide while Visking membrane, pre-saturated in 0.1M sodium hydroxide, was employed as the model membrane. Following a 15 minute temperature equilibration period, each donor compartment was loaded with either 0.1 mL, 1 mL or filled entirely (~3mL depending upon individual donor cell) with saturated ibuprofen solution. After 24 hours, an aliquot from each receptor compartment was withdrawn and appropriately diluted before UV analysis at 272 nm. Each measurement was performed in triplicate. The ibuprofen concentrations in each receptor were calculated.

3.2.4 Ibuprofen drug release studies before and after validation

Ibuprofen drug release from Phorpain gel (contained 5% w/w ibuprofen) through Visking membrane over 7 hours (n=6) before and after validation was conducted using the custom-made University of Strathclyde Franz cells.

3.2.4.1 Before validation

In order to prove the Franz cell apparatus validation was effective, experiments performed before validation are shown here. The donor and receptors were randomly paired and the Franz cells were placed in random blocks and the stirring speed was set at 200 rpm. Type I,

II and III stirrer bars were placed randomly into the receptors. 0.8-1.2 g of gel was placed in the donor while the receptor was filled with de-aerated 0.1M sodium hydroxide. (De-aeration was carried out by bubbling helium gas into the solution for at least 15 minutes.) The donor top, receptor arm and the junction of two chambers were occluded with parafilm in order to prevent evaporation. The Franz cells were left to equilibrate in the heating block for at least 15 minutes before starting the stopwatch. Intervals between sampling were 5 to 30 minutes. During sampling, 1-2 mL of sample was removed from the receptor and fresh receptor fluid of the temperature was replaced into the receptor each time. This maintained a constant receptor volume as well as sink conditions. The air bubbles formed temporarily below the membrane was removed by tilting the Franz cells so that it escaped via the side arm. The ibuprofen content was analysed using UV spectrophotometer at wavelength 272 nm. Plots of average cumulative percentage of ibuprofen against time were derived. The coefficient of variation was calculated for the total ibuprofen content in the receptor chamber at each time point.

3.2.4.2 After validation

After validation of the apparatus, with long operator training and much practice, a standard procedure for Franz cells drug release was developed. The donor and receptor cells were matched according to their effective diffusion area (E.D.A); low E.D.A receptor was paired with a donor that has low E.D.A, and vice versa for receptors which had high E.D.A. The same combinations were used for each experiment to minimise variability. The receptor cell was filled with de-aerated 0.1M sodium hydroxide and was allowed to equilibrate at 37°C in the appropriate heated magnetic block for 15 minutes. The cellulose membrane pre-hydrated for more than 24 hours was mounted between the donor and receptor compartment and 0.8 g-1.2 g of gel was placed on the membrane surface in the donor compartment. All the openings of the Franz cell including the donor - receptor interface were occluded with

parafilm in order to prevent evaporation. The receptor compartment was stirred at 200 rpm at 37 °C. Sample volumes (1-2 mL) were taken for UV analysis at 272 nm and fresh preheated medium replacements of the same volume were reintroduced into the receiver. The same percentage plot was plotted and the coefficient variation was compared to that of the Franz cell data obtained before validation.

3.2.5 Ibuprofen drug release from saturated solution

3.2.5.1 Preparation of ibuprofen saturated solution

Ibuprofen saturated solution was prepared in the standard receptor fluid, 0.1M sodium hydroxide. Approximately 1.5 g of ibuprofen was added to 50 mL of 0.1M sodium hydroxide to give a suspension. The suspension was agitated for at least 1 hour in a shaking water bath maintained at 60-65°C. Any undissolved solid was filtered off at the same temperature and the solution was allowed to cool to 33°C for overnight and ibuprofen crystal growth was visible.

For the preparation of ibuprofen crystals, another batch of ibuprofen saturated solution was prepared according to the procedure described above. The saturated solution was also filtered at 60 °C, but this time it was allowed to cool to room temperature overnight. The saturated solution was passed through a 0.2 μm nylon filter on a Buchner funnel and filtered via vacuum filtration. The ibuprofen crystal collected on the filter paper were scraped off and stored in a tight screw vial for the use in Franz cell experiments. The filtrate was diluted with 0.1M sodium hydroxide appropriately and the ibuprofen saturated solubility was measured with UV at 272 nm.

3.2.5.2 Franz cell drug release procedure

Using the validated Franz cells, the ibuprofen drug release studies were repeated using saturated ibuprofen solutions instead of the commercial gel (n=6). The receptor cell was

filled with de-aerated 0.1M sodium hydroxide and was allowed to equilibrate at 37 °C in the appropriate heated magnetic block for 15 minutes. The pre-hydrated membrane was mounted between the matched donor and receptor compartment and 1 mL of saturated solution was placed on the membrane surface in the donor compartment. All openings including donor top and receptor arm were occluded with parafilm to prevent evaporation. The receptor compartment was stirred at the validated speed (200 rpm). Using a glass syringe, sample volumes (1-2 mL) were extracted for UV assay and fresh preheated replacement medium of same volume was reintroduced into the receptor. Air bubbles formed below the membrane were removed by carefully tilting the Franz cells for the air bubbles to escape via the sampling arm. Intervals between sampling varied from 5 to 30 minutes. Ibuprofen crystals were introduced into the donor solution (~hourly) to maintain its saturated state. The flux obtained from the saturated solution was compared to that obtained from commercial gel.

3.2.6 Temperature control

Temperature monitoring experiments were performed in triplicate. The heater block was pre-heated to 37 °C followed by filling the receptor cells with de-aerated water at room temperature and stirring with a magnetic bar (12 x 4.5 mm). Visking cellulose membranes were employed as model membranes. All openings were sealed with parafilm to prevent evaporation. The temperature monitoring was carried out using a PicoLog TC-08 temperature data logger (Pico Technology Ltd., Cambridgeshire, UK). The Franz cells and temperature data logger were assembled as shown in Figure 3.3. The temperature probes were positioned at three points within Franz cells: ~1 mm above membrane (P), ~1 mm below membrane (Q) and receptor (R). The probes were connected to PicoLog TC08 data logger and temperature values were integrated on a computer.

Firstly, the duration required for the receptor cell temperature to stabilise at 37°C, i.e. the equilibrium time, was investigated. Investigation into this parameter involved positioning thermocouple at site R and the temperature recorded once a minute over 30 minutes (n=9). Then, the temperature change at point P, Q and R was monitored over 7 hours.

It was known that once the Franz cell diffusion process is running, temperature fluctuations can develop in conjunction with sampling. The temperature fluctuations at P and Q induced by sampling were investigated. The sampling involved removing 1 mL of receptor phase and replenishing with fresh distilled water of the same temperature. Sampling was undertaken every 10 minutes for 3 hours and subsequently every 30 minutes for the following 4 hours. After each solution withdrawal but before replenishment, the temperature drop at both points P and Q were recorded (n=4).

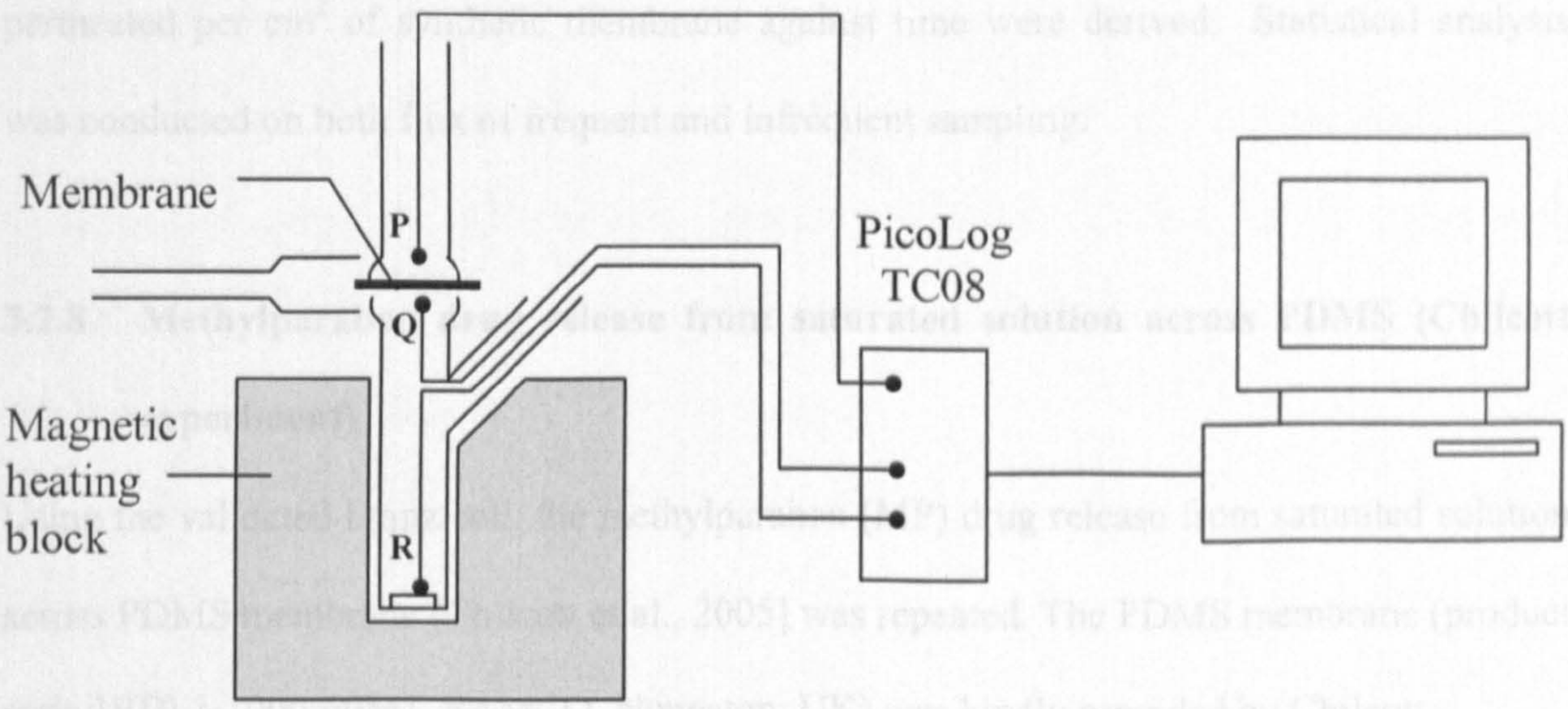

Figure 3.3: Franz cell and temperature thermocouple set up. The three probes were placed at ~1mm above membrane (P), ~1mm membrane below (Q) and the receptor (R) connected to the PicoLog data logger.

3.2.7 Sampling rate

Investigations of the influence of sampling time frequency on drug penetration involved the use of polyacrylamide AN69 membranes. These were soaked for 24 hours with 5 mL of receptor fluid and subsequently rinsed thoroughly to remove glycerin. Six receptor cells were filled with de-aerated (by means of helium) 0.1M sodium hydroxide at 37 °C and the pre-soaked polyacrylamide sections were inserted as model membranes. Six donor cells were then placed in position and each of these was filled with 1 mL of saturated ibuprofen solution. Aliquots of receiver solution were removed over a 7 hour period and assayed for ibuprofen using UV. In three Franz cells, sampling from the receiver solution was undertaken frequently (at 0, 10, 20, 30, 40, 50, 60, 75, 90, 105, 120, 135,150, 165, 180, 210, 240, 270, 300, 330, 360, 390 and 420 minutes) whereas in another three Franz cells sampling was undertaken infrequently (every 30 minutes). Plots of cumulative amount of ibuprofen permeated per cm^2 of synthetic membrane against time were derived. Statistical analysis was conducted on both flux of frequent and infrequent sampling.

3.2.8 Methylparaben drug release from saturated solution across PDMS (Chilcott experiment)

Using the validated Franz cell, the methylparaben (MP) drug release from saturated solution across PDMS membrane [Chilcott et al., 2005] was repeated. The PDMS membrane (product code 19T0.3-1000-60M1, SAMCO, Nuneaton, UK) was kindly provided by Chilcott.

3.2.8.1 Preparation of MP saturated solution and membrane treatment

PBS solution (pH 7.4) was prepared via dissolving sachets of PBS powder into 1 L of distilled water. The MP saturated solution was prepared in PBS solution. 1 g of MP was added into 10 mL PBS solution making up a suspension with concentration of 100 mg/mL. The suspension was then allowed to stir overnight at 25°C on a roller-mixer. The powder on

PDMS was first removed by rinsing with distilled water. Then the PDMS membrane was trimmed into disc (diameter ~1 cm) and pre-soaked in approximately 5 mL of water for 24 hours.

3.2.8.2 Franz cell study

The receptor chamber filled with PBS solution maintained at 37 °C. The MP saturated solution was applied into the donor at the dose of 1 mL per cm^2. The donor chamber was occluded by double-sealing with parafilm. 1 mL of aliquot was withdrawn from the receptor at given time intervals and immediately replaced with fresh PBS of same temperature. Samples was collected at 0, 0.5, 1.0, 1.5, 2.0, 2.5, 3.0, 4.0, 5.0 and 6.0-h intervals and analysed by UV at 254 nm. A minimum of five diffusion cells required. The rate of MP release through PDMS membrane was calculated from the slope of the cumulative drug release profile versus time. The only condition in our study that differed from Chilcott's was the temperature of the receptor was kept at 37°C instead of 35°C. For data analysis, the coefficient of variations (CV) of each laboratory (listed in Chilcott et al., 2005) were calculated. CV produced in our laboratory was compared and contrasted to the CVs calculated from the laboratories.

3.2.9 Statistical analysis

All statistical analysis was carried out using analysis of variance (ANOVA) and the significance level was accepted when $p < 0.05$.

3.3 Results

3.3.1 Franz Cell Dimension

The physical characteristics of University of Strathclyde (custom-made) and PermeGear (commercial) are summarised in Table 3.1 below. It can be seen that the heights of

University of Strathclyde donor cells were greater than those of PermeGear. In terms of effective diffusion areas, the donor cell values were lower for University of Strathclyde while the receptor cell values were similar for both companies. Receiver cell volumes did not vary greatly within manufacturers. However, University of Strathclyde receptors exhibited greater volumes than those of PermeGear but had less steep side arms. Visual observations of University of Strathclyde Franz cells showed that some of the receptor cell bases were convex as a result of manufacturing variations. Interestingly, both types of apparatus exhibited relatively similar dimensional variability, as assessed from coefficient of variation values (see Table 3.1).

Table 3.1: Physical dimensions measurement of University of Strathclyde (custom-made) and PermeGear (commercial) Franz cells.

Parameter	Tailor-made		Commercial	
	mean ± s.d.	CV	mean ± s.d.	CV
Donor				
Height (cm)	5.2 ± 0.3	5.8	1.6 ± 0.1	6.2
E.D.A. (mm^2)	59.6 ± 3.1	5.2	73.8 ± 3.3	4.5
Receptor				
Volume (mL)	11.7 ± 0.1	0.8	5.2 ± 0.1	1.9
Angle of the arm (°)	128 ± 2.7	2.1	135 ± 1.7	1.2
E.D.A. (mm^2)	78.2 ± 3.1	4.0	74.7 ± 3.5	4.7
Shape of base	Flat to convex	-	N/A	-

[a] n = 7 [b] n = 27

3.3.2 Stirring variables

Figure 3.4 portrays three typical phenomena of receptor cell stirring. The potassium permanganate dye distributions pattern in receptor cells are shown in Figure 3.4 (a), (b) and (c). Figure 3.4 (a) shows typical result at no stirring where the dye concentrated at the base of receptor, but the dye would slowly diffuse throughout the whole receptor via concentration gradient. Figure 3.4 (b) portrays poor stirring when the dye was not evenly

distributed in which the no dye was spread to the arm. Figure 3.4 (c) shows the ideal stirring where the dye was fully distributed throughout the receptor.

(a)

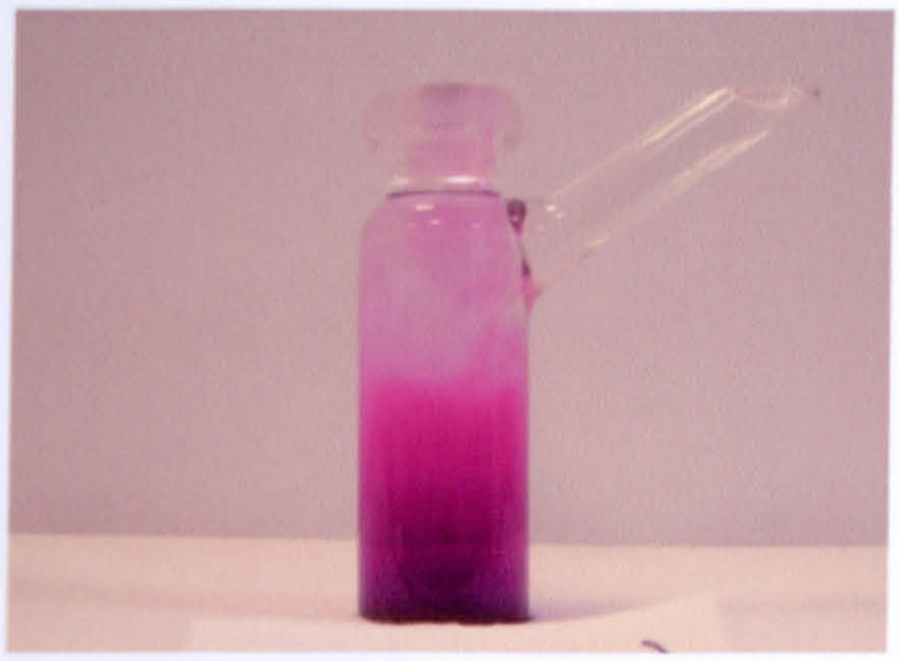

(b)

(c)

Figure 3.4: Dye distribution in receptor cell. a) Control – no stirring b) Dye spread to body only c) Dye spread fully to body and arm.

At low speed, the dye took approximately 8-10 minutes to disperse throughout the receptor cell body, but took more than an hour to climb fully up the arm. At high speeds (9-11 arbitrary units), it also took 10-12 minutes to disperse throughout receptor cell and no vortex was observed. From speed 12 and onwards, although the dye spreaded quickly throughout the receptor, a vortex could be observed at the surface of the receptor.

Type I magnetic stirrer gave inadequate distribution throughout the receptor cell at high speed after 120 seconds, where as Type II stirrer gave a similar result after 60 seconds. Type

III gave the best stirring and achieved full body and arm distribution after 60 seconds at high speed, however, a vortex was observed. A vortex could even be observed at medium speed using Type III stirrer bars.

Satisfactory stirring was observed with Type II stirring bar at speed 10. Speed 10 approximates to 200 rpm (197.5 ± 16.1 rpm) from the previous calibrating of the stirring block. There were blocks which gave consistent RPM measurements, but the stirrer bars did not spin centrally. It was found that only 9 blocks (out of total 24) provided effective central stirring efficiency at 200 rpm and, these blocks were used for all subsequent experiments.

3.3.3 Influence of validation on ibuprofen drug release

Figure 3.5 shows the ibuprofen gel permeation data before (a) and after (b) validation of the variables.

(a)

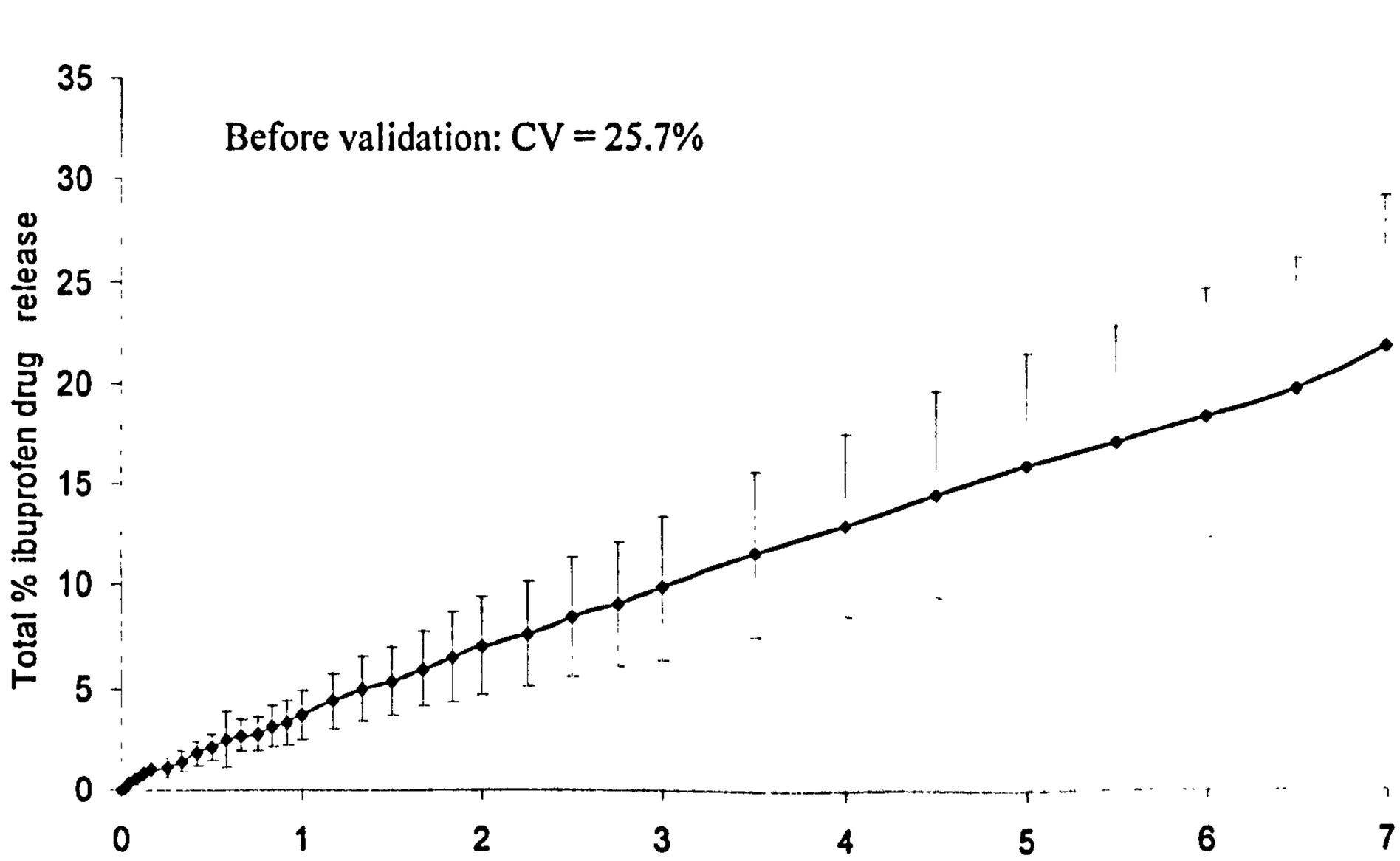

(b)

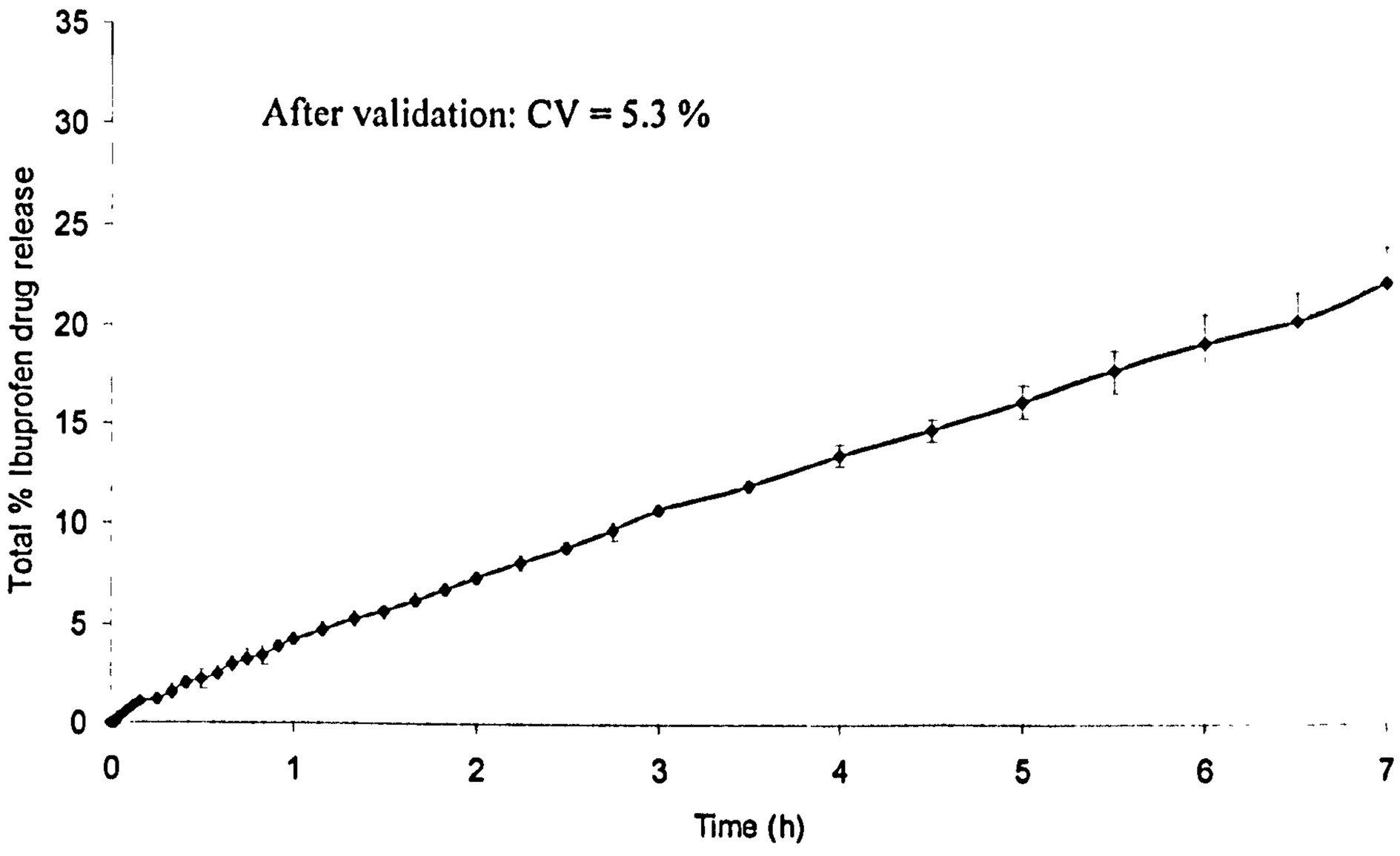

Figure 3.5: Total % ibuprofen drug release from Phorpain gel (a) before and (b) after validation of Franz cells.

The use of the validated equipment and methodology reduced the coefficient of variation from 25.7% to 5.3 % (n=6). When the validated protocol was used to conduct permeation studies involving the same model membrane but using saturated ibuprofen solution (Cs = 2.02 % w/v), the coefficient of variation was 4.1% (Figure 3.6).

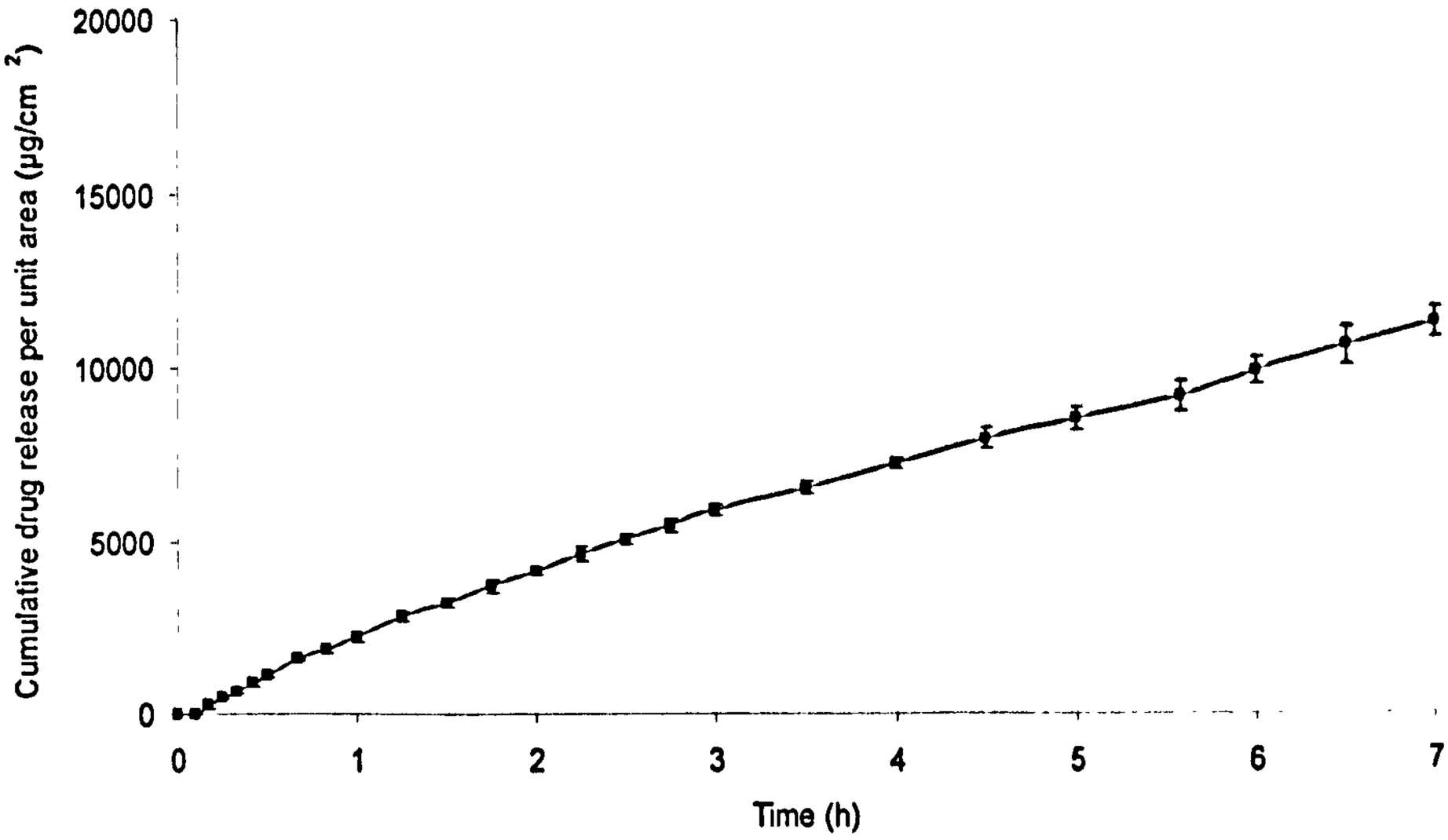

Figure 3.6: Cumulative ibuprofen drug release from saturated solution after validation (CV = 4.1%).

3.3.4 Temperature control

For equilibration temperature experiment, receptor cells in all blocks took approximately 8-10 minutes to equilibrate to 37°C. The temperature observed were rather stable for all three points, with P, 31.48 ± 0.2 °C; Q, 34.12 ± 0.3 °C and R, 36.27 ± 0.1 °C. When sampling was performed, temperature drop was observed at point P and Q and the mean difference recorded were 1.5 ± 0.5 °C and 1.4 ± 0.2 and °C respectively. The temperature change caused by sampling were significantly different from the same time point where no sample was taken ($p<0.05$, $n=10$).

3.3.5 Influence of donor solution volume

The table below shows the receptor concentration after 24 hours of ibuprofen

Table 3.2: Receptor concentration of different donor volume after 24h of ibuprofen

Donor Volume	C (µg/mL)	Sink ?
0.1mL	157.5	Yes
1mL	1252.5	Yes
Full (~3 mL)	2343.2	No

Sink conditions were maintained with donor solution volumes of 0.1 and 1mL, i.e. the ibuprofen concentrations were less than 0.218 % w/v; but sink conditions were not maintained in diffusion cells containing fully filled donor cells (~3mL).

3.3.6 Sampling rate

The rate of sampling from the receiver compartment did not significantly influence ibuprofen flux ($p = 0.21$). As Figure 3.7 shows, the measured drug fluxes for frequent and infrequent sampling experiments were not statistically significant ($p>0.05$). However, infrequent sampling did allow ibuprofen concentrations in the receptor chamber to reach 11.1% (calculated as the ibuprofen receptor concentration at 7 hours divided by ibuprofen saturated concentration) of saturation concentration at 7 hours, which means sink conditions (< 10%) were no longer maintained. In contrast, frequent sampling permitted receiver drug concentrations to attain a maximal value of 9.8%, which was just within sink conditions.

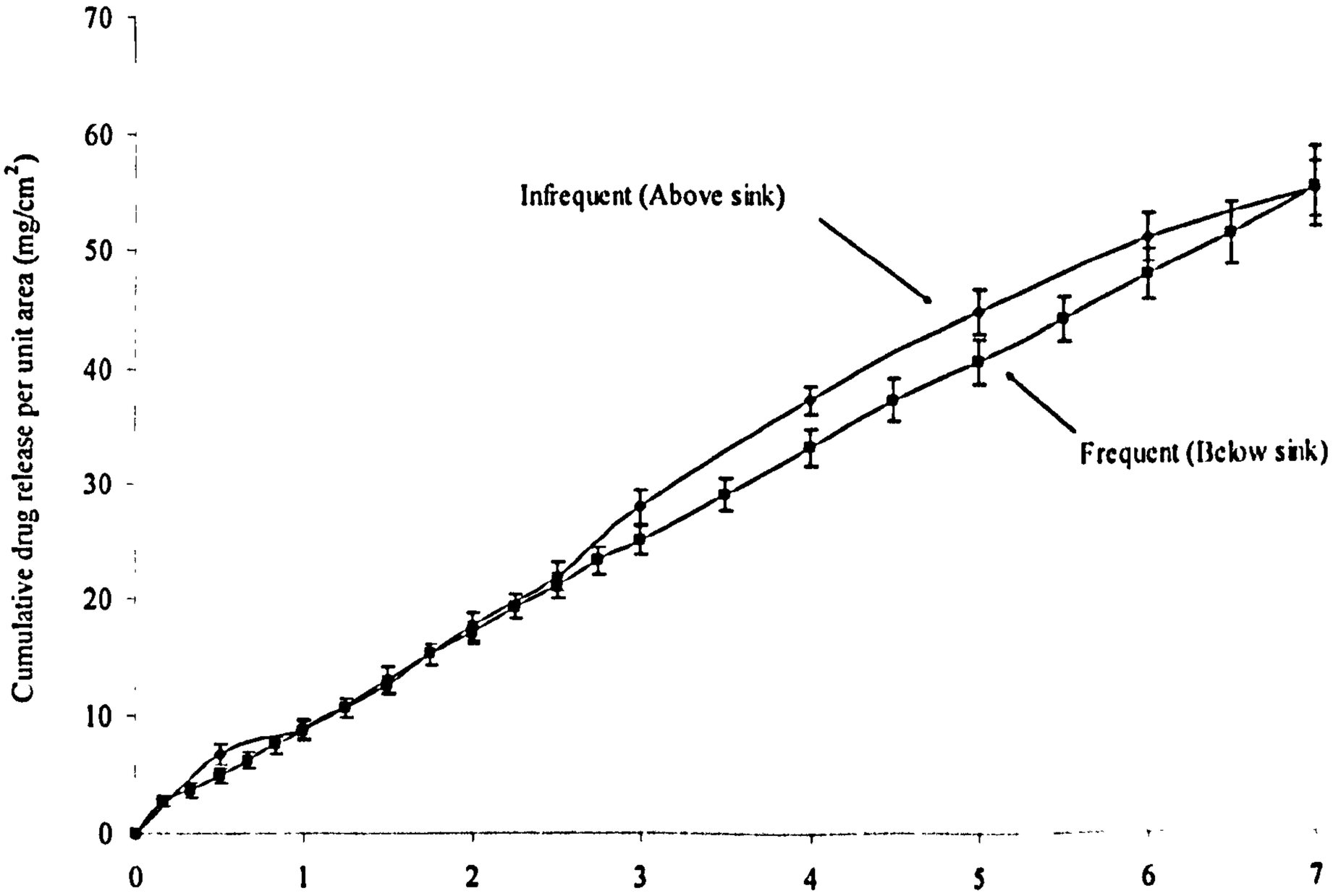

Figure 3.7: Ibuprofen release from saturated solution through AN69 membrane. Frequent sampling (varies from 5 to 30 min); Infrequent sampling (varies between 15 to 30 min).

3.3.7 Methylparaben drug release across PDMS membrane

Figure 3.8 shows the cumulative drug release of MP diffusion from saturated solution across the PDMS membrane supplied by Chilcott. A lag time of approximately 15-20 min was observed. The drug release reaches steady state after 1.5 hour and the drug release profile was linear (r^2 = 0.998). The methylparaben rate of release from saturated solution through PDMS membrane was found to be 36.4 ± 0.6 $\mu g.cm^{-2}.h^{-1}$ (n=5) with the coefficient of variation of 1.7%. This value lies within the 25 laboratories flux range (26.7-101.3 $\mu g.cm^{-2}.h^{-1}$) compiled by Chilcott, where the mean flux from all the laboratories was 60.0 ± 21.2 $\mu g.cm^{-2}.h^{-1}$.

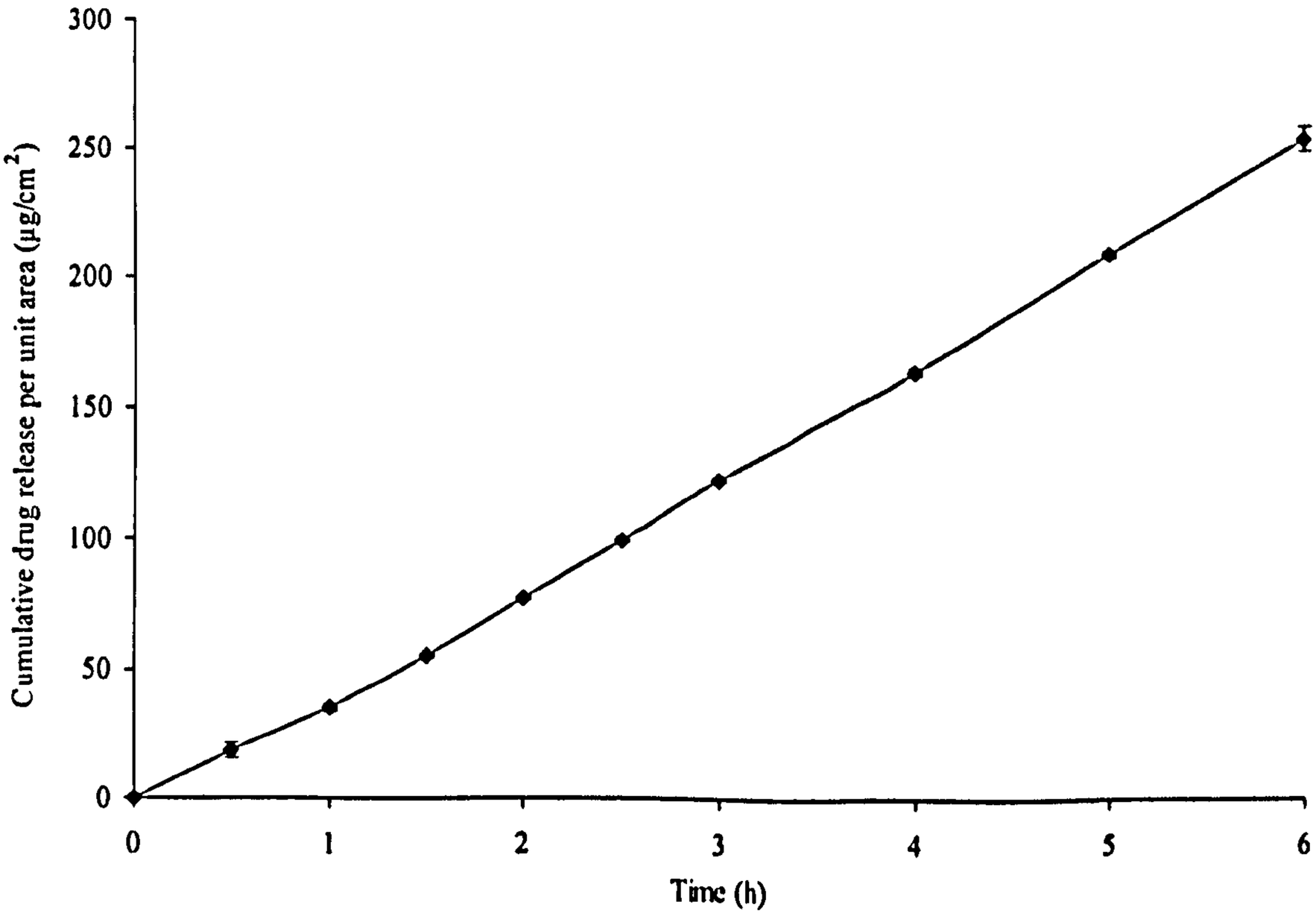

Figure 3.8: Cumulative MP release from saturated solution through PDMS membrane

CVs for each laboratory from Chilcott was re-calculated from average flux and standard deviation and compiled in Table 3.3. They ranged from 2.1% to 35.8%.

Table 3.3: Summary of average MP penetration rate (J) and standard deviation (SD) as reported by individual laboratory (Compiled from Chicott et al., 2005). Coefficient of variation (CV) was calculated as the percentage of SD/J average. n represents the number of replicates

Lab ID	n	J ($\mu g.cm^{-2}.h^{-1}$)	SD ($\mu g.cm^{-2}.h^{-1}$)	CV %
A	6	52.4	1.7	3.2
B	5	46.8	1.0	2.1
C	6	57.5	4.7	8.2
D	6	43.1	7.0	16.2
E	7	57.9	5.5	9.5
F	12	26.7	5.1	19.1
G	10	68.0	4.0	5.9
G	10	78.6	9.1	11.6
H	5	49.4	4.9	9.9
I	8	50.9	2.9	5.7
J	6	72.2	6.0	8.3
K	8	47.5	2.9	6.1
L	7	56.0	3.1	5.5
M	12	50.2	7.2	14.3
N	5	101.3	8.7	8.6
N	5	101.1	11.4	11.3
N	6	86.0	5.8	6.7
N	6	90.3	9.9	11.0
N	6	82.2	29.4	35.8
I	8	40.3	1.6	4.0
O	6	27.7	1.2	4.3
O	6	36.4	1.7	4.7
P	12	57.7	20.0	34.7
Q	8	41.8	10.6	25.4
R	7	77.4	4.6	5.9

Table 3.4: Average flux for laboratories with CV less than 5%, 10% and 20% (recalculation from Table 3.2).

CV	Average flux ± SE ($\mu g.cm^{-2}.h^{-1}$)	no. of Lab
<5%	40.7 ± 4.3	5
<10%	58.0 ± 4.8	16
<20%	60.0 ± 4.6	22

Table 3.4 recalculates flux of the laboratories with CV less than 5%, 10% and 20% from Table 3.2. The experimental flux value reported in our work (36.4 ± 0.6 $\mu g.cm^{-2}.h^{-1}$) falls very closely to the flux value with CV less than 5%.

3.4 Discussion

The popularity of the Franz cell as an *in vitro* model for skin permeation studies has resulted the emergence of several Franz cell manufacturers as well as some FDA standardisation [Skelly *et al.*, 1987]. Commercially manufactured sets theoretically provide the least variability at the greatest cost and are therefore found in industrial laboratories. Custom-made Franz cells constitute a less expensive alternative in which variability depends upon the glass blowers skill of the individual technician. One notable feature in our study was the effective diffusion area difference (E.D.A.) between the donor and receptors of the custom-made Franz cells was approximately 20 mm^2 difference as compared to the commercial array, in which the donor and receptors E.D.A. was only about 1 mm^2 difference. Another variable feature observed with the custom-made Franz cells was the convex base in some cells as a result of manufacturing variation. This prevented the stirring bar from spinning centrally and achieving good mixing. However, the variability of other physical dimensions was surprisingly similar in magnitude for both types of apparatus (CV < 5%). In fact, appreciable variation was observed in all physical characteristics measured.

The custom-made Franz cell array possessed tall donor cells. This was an unusual feature for Franz cells design. Donor cells are often designed to be short (e.g. PermeGear) because drug permeation across skin is slow and only small dose volume (< 0.5 mL) are usually investigated. However, the tall donor cells are useful that in a large dose volume (> 1 mL) or an infinite dose are investigated. This feature is also useful when the drug diffusion is very rapid especially when synthetic membranes are employed. Large doses are required to maintain drug concentration in the donor. The static Franz cell receptor volumes are commonly small, typically range from 3 to 15 mL. The University of Strathclyde set of Franz cells possess larger receptor volumes compared to the PermeGear. Large receptor volumes are useful to create sink conditions especially when the flux is rapid. But when the drug release into the receptor is small, small receiver volumes are suitable to provide a measurable concentration. Variations in side-arm steepness also existed. The inadequate mixing in the side arm hinders receptor phase homogeneity yielding high variability when sampling. This problem was resolved by standardizing the stirrer bar type and speed within the receptor. The diameter of the side-arm orifice is also important because sufficient space is required in the side arm to eliminate air bubbles during sampling. The presence of air bubbles is not desirable as their presence at the membrane underside reduces the E.D.A..

Stirring is another important issue to consider in validation. Stirring of the receptor fluid is critical for maintenance of uniform distribution of drug molecules and temperature equilibrium [Gummer *et al.*, 1987]. The time taken to achieve such uniformity determines the minimum time for the first sampling interval of an experiment and time between subsequent samples. Inefficient stirring can be fast stirring at receptor base with little or no stirring at upper part of the receptor, especially the vicinity of the sampling arm [Gummer *et al.*, 1987]. Such effects cause local deviation from sink conditions as the drug is not distributed evenly throughout the receptor cell. The drug solutes diffuse across a membrane

would first partition out into the stagnant layer below the membrane, then diffuse into the bulk receptor solution through concentration gradient. The stirring rate in the receptor should be fast enough to ensure rapid distribution of the permeant but not so fast as to create a turbulence or vortex below the membrane. This would disrupt the stagnant layer which changes one of the assumptions of Fick's law, namely that the calculation of the diffusion coefficient includes a contribution from the boundary layer. The ideal stirrer speed and stirrer bar combination for any Franz cell system is the one that gives fastest mixing without a vortex. In this work, a simple type II stirrer bar operating at 200 rpm was found to be optimal.

Temperature maintenance in Franz cells is crucial because it has direct effect on drug flux. As a general rule of thumb, percutaneous flux tends to double for every 10°C rise in temperature [Scheuplein, 1978]. More recently, it was shown that the flux of methylparaben, butylparaben and caffeine through synthetic membranes doubled with every 7-8°C rise in receptor cell temperature [Akomeah *et al.*, 2004]. A rise in receptor temperature also enhances flux across skin for dihydrotestosterone, terodiline, prednisolone, and isoniazid flux from various vehicles [Ohara *et al.*, 1995; Clarys *et al.*, 1998; Ogiso *et al.*, 1998]. In our study, the validation of the heating systems revealed good temperature control in the receptor and the membrane. This study also found out that there was a fluctuation of temperature during sampling. Sampling caused an air bubble to form below the membrane which led to a temporary drop in temperature of less than 1 minute. In order to remove the air bubbles, the Franz cell was tilted into an angle so that the bubble could escape from the side arm. Because there was an uncontrollable heat changes on membrane due to air bubble, such maneuver should be as swift as possible to avoid further cooling of the system. It is crucial to ensure that the fresh fluid is always pre-heated to the same temperature. Replacement with cooler fluid can caused momentarily drop in receptor temperature which in turn decrease in drug

solubility and diffusivity, this also changes the drug concentration at which sink conditions are maintained. This simple temperature experiment indicates that withdrawing sample can alter the temperature drop significantly, if necessary, less sampling should be carried out in order to lessen the interruption of drug flux which could lead to results variability. Within this context, de-aeration of receptor fluid prior to experimentation will prevent air bubble-associated cooling as well as the E.D.A. decrease mentioned above.

Often, researchers are given the freedom of determining the time interval for drug sampling in Franz diffusion cell experiment. From our data, the different sampling rate did not affect drug flux, but affects sink in the receptor. Increase sampling frequency could help to attain sink condition especially when the drug flux was high because the replacement of fresh fluids into receptor can help dilute the receptor concentration.

When using a rate-limiting synthetic membrane like PDMS, it would be expected that a tight data would be observed assuming all other factors were controlled. However Chilcott compiled results showing 35% variation between laboratories [Chilcott *et al.*, 2005]. We were able to show that validation of Franz cell apparatus and methodolgy provided a dramatic decrease in permeation data variability. Coefficient of variation (CV) reflects the precision of a data. The low CV in our studies gave confidence that this flux was reproducible under the test conditions. Specifically, validation resulted in the coefficient of variation for ibuprofen permeation being reduced from 25.7% to 5.3 % (n=6). MP drug release through PDMS membrane had been carried out using Chilcott's method and the flux value obtained corresponded to the average flux calculated from laboratories with CV < 5%. And flux values was corresponded to the group of laboratories with calculated CV < 5%. The high CVs (more than 5%) generated by the laboratories indicates that some of the results were not reproducible especially those at the higher end of CV. Using statistically tests,

Chilcott also proved that 'receptor volume, sample volume, surface area, and diffusion cell type' employed by the different laboratories should have no significant effect on methylparaben flux. So variation in flux among the laboratories can only be explained by unvalidated techniques and operator errors. But it is indeed technically demanding to run a static diffusion cell drug release experiment because it requires good manual skills. And often this requires long operator training and practice.

By using synthetic membrane, we have ruled out the biological variation of skin. Our studies show that validation of equipment, methodology and operator training has dramatic influence on result variations. The validation of equipment is crucial to eliminate the all these variables so that the formulation or membrane being investigated is the sole reason for all results. This paradigm may not just apply to typical Franz- diffusion cells, but also other diffusion cells apparatus available for percutaneous absorption such as side-by-side cells and enhancer cells. A further appropriate application of synthetic membrane is in validation experiment prior to the use of skin and in regular checking of operator training and competence.

3.5 Conclusions

The preliminary studies have identified the possible apparatus variables attributed to results inconsistency in Franz cells. The conclusions from these works were:-

1. It is essential to match donor and receptor cells. For the customised Franz cells, the receptor and donors of similar effective diffusion are (E.D.A) should be matched. Low E.D.A receptor was paired with a donor that has low E.D.A, and vice versa for receptors which had high E.D.A. The same combinations must be used for future experiment to minimise variability.

2. The validation of the stirring equipment showed that using Type II stirrer bar at 200 rpm gave satisfactory stirring efficiency. Note only the blocks which calibrated with good stirring efficiency were employed.
3. The repeatability of the ibuprofen drug release from gel has greatly improved after preliminary experiments on parameters such stirring rates, type of magnetic bar employed, matching donor and receptors have been standardised.
4. The validation of the heating systems revealed good temperature control in the receptor and the membrane. But we also found that there was a fluctuation of temperature during sampling.
5. Sampling did not appear to influence drug flux, but appear to affect sink condition in the receptor.
6. The tight data obtained from the repetition of Chilcott's experiment has again proved the reproducibility of our validated equipment.

CHAPTER IV

INVESTIGATION OF FACTORS RELATED TO SYNTHETIC MEMBRANE IN FRANZ CELL EXPERIMENTS

4.1 Introduction

Synthetic membranes for Franz cell studies are usually immersed in the receptor medium prior to the experiment to allow for full hydration. Regenerated celluloses possess dense hydrophilic hydroxyl groups which swell when hydrated and this is known to be important when used for dialysis application [Halary *et al.*, 1980]. It is crucial to examine the mass gained after water absorption as this changes the membrane physical properties such as thickness and membrane integrity. This should ensure that the membrane does not become an experimental variable in the Franz cell studies

Synthetic membranes in industrial separation application are often manufactured on a large scale. Because such membranes are thin and fragile, careful steps are performed to prevent membrane damage especially during packaging and transportation. It is often necessary to keep the membrane moist and supple. Some synthetic membranes are supplied in water-pack to keep the membrane moist; for example, benzoylated dialysis tubing (Sigma-Aldrich) and SpectraPor® cellulose esters (SpectrumLab, Inc.). But when the membrane is supplied dry, additives such as plasticisers and softeners are often incorporated to maintain membrane suppleness. Glycerin is a common plasticiser found in membranes such as Visking, Cuprophan and Polyacrylonitrile (AN 69). The removal of glycerin from such membranes is essential for the membrane full performance. The manufacturer usually recommends that the glycerin is washed off the membrane via running under warm water (Cuprophan and Visking) or by boiling the membrane (Medicell Ltd.). For Franz cell experiments, it is

important to ensure that all of the glycerin is removed because it can block pores, or leach into the receptor medium and interfere with subsequent analysis [Haigh and Smith, 1994].

Periodic acid Schiff assay is a staining method employed in histology to stain glycoprotein and glycogen in tissues and to detect glycerin in bacteria [Baddiley *et al.*, 1956; Gale and Folkes, 1965]. The reaction of periodic acid selectively oxidizes the hydroxyl groups, produces aldehyde groups which in turn react with the Schiff reagent and creates a purple-magenta color solution [Hotchkiss, 1948]. The compound being oxidised must contain the 1,2-diol groups in unsubstituted form in which the hydroxyl groups can be convert to 1,2-aldehydes. Therefore substances such as glycogen and glycerin give strong reactions with Schiff reagent [Hotchkiss, 1948].

Another problem associated with synthetic membranes is the movement of solvent from the receptor to the donor compartment - osmosis. Generally, osmosis describes the net movement of water across a semi-permeable membrane (only permeable to water) driven by a difference in solute concentrations on the two sides of the membrane. The net flow of water is from the solution with the lower solute concentration into the solution with higher solute concentration. The synthetic membranes employed here, are however permeable to both water as well as drugs molecules – it is a permeable rather than semi-permeable membrane. In a Franz cell setting, there is a possibility that when the drug is diffusing from the donor into receptor, the water molecules also moves against the drug concentration gradient between the two chambers. So, the process diffusion and osmosis might occur simultaneously and instantaneously in Franz cells as both are passive processes which do not require energy.

Theoretically, osmosis could be prevented by balancing the osmotic pressure on both sides of the membrane. In a Franz cell, when a saturated solution is placed in the donor, the receptor essentially has zero drug concentration for sink condition; therefore the water travels from the receptor into the donor. The Van't hoff equation (Eq. 2.5, $\pi = i\ M\ R\ T$) takes into account the temperature and concentration difference between the donor and receptor compartments and the amount of tonicity agent required to be added into the receptor compartment to counterbalance the osmotic pressure could be determined.

4.1.1 Aims of study

This chapter explores the factors which might arise when using synthetic membranes in Franz cell studies. A simple experiment was conducted to investigate the membrane mass increase due to fluid uptake over time. The presence of glycerin in a synthetic membrane was examined using a modified procedure of periodic acid Schiff (PAS) assay. Using the PAS assay, the effectiveness of membrane washing procedure for Franz cell experiment was determined. Then, the effect of glycerin on flux variability was investigated using ibuprofen as the model drug and polyacrylonitrile (AN69) as the model membrane. Preliminary experiments were performed to demonstrate the occurrence of osmosis in Franz cells with synthetic membranes. Attempts were carried out to counteract the osmotic pressure difference and its effect on ibuprofen drug flux.

4.2 Methods

4.2.1 Membrane hydration

Four synthetic membranes, Visking, Cuprophan, polyacrylonitrile (AN 69) and nylon (Biodyne) were examined. The membrane hydration was carried out by recording the mass gain due to fluid absorption over time. Firstly, the membranes were trimmed into

approximately 5 mm x 5 mm pieces and the dry masses were recorded. The dry membranes were then soaked in 5 mL of distilled water in a vial and stored at 25°C. To determine the hydrated mass, the membrane was first removed slowly from the vial using a flat-tip tweezers and dabbed gently at the lip of the vial to remove any large droplets of water. The procedure was carried out as swiftly as possible to avoid evaporation. The membrane wet mass was determined at time points 4, 6, 8, 12 and 24 hours. Membrane experiments were carried out in triplicate. The mass ratio for the membranes at each time point was calculated as follows:

$$\text{Water mass gained (\%)} = \frac{\text{wet mass - dry mass}}{\text{dry mass}} \times 100\ \% \qquad \text{Eq. 4.1}$$

The average water mass gained (%) was then plotted against time for all membranes. Then, the relationship between water mass gained at 24 hour and membrane hydrophilicity and membrane pore size was investigated.

4.2.2 Glycerin assay (Periodic acid Schiff Assay)

This section describes the adapted Periodic acid Schiff (PAS) assay methodology [Gale and Folkes, 1965; He *et al.*, 1998] for glycerin assay. For the preparation of Schiff reagent, 20 mL of 1M hydrochloric acid was added to 100 mL of 1% w/v basic Fuchsin (Pararosaniline). Sodium metabisulphite (2 g) was added to this solution, which was then incubated at 37°C for 120 minutes. In order to prepare periodic acid reagent, 10 mL of 50 % w/w periodic acid solution was added to 7 mL of 7 % w/v aqueous acetic acid. To construct a calibration curve, six aqueous solutions of glycerin were prepared exhibiting concentrations ranging between 6.25×10^{-3} to 5×10^{-2} % w/v. A 0.1 mL aliquot of periodic acid reagent was added to each test solution, which was incubated at 37 °C for 120 minutes. The solutions were allowed to cool to room temperature and 0.1 mL of Schiff's reagent was added. Distilled

water was employed as a control. After 30 minutes, the absorbance of each test solution was measured in quadruplicate on a UV spectrophotometer using a detection wavelength of 540 nm.

All four membrane types were assayed for glycerin content both before and after washing. Sections of Visking, Cuprophan, Polyacrylonitrile (AN69) and Benzoylated cellulose membranes, weighing between 5 to 10 mg, were cut out and the precise dry mass of each sample was recorded. Each membrane sample was immersed in a 5 mL volume of distilled water in a vial. The vials were capped and rotated for at least 12 hours at 37 °C. Subsequently, 1 mL aliquot of solution from each vial was assayed by adding Periodic acid Schiff (PAS) reagent. The same membranes were rinsed with distilled water and transferred to clean closed vials containing 1.2 mL of distilled water. Following a further 24 hour storage period, 1 mL aliquots of solution were again assayed with PAS reagent.

4.2.3 Glycerin effect on drug release

The effect of glycerin on ibuprofen Franz cell release from saturated solution was investigated. The model membrane employed was Polyacrylonitrile (AN 69) because it possessed very high glycerin content (40-50%). In order to test the effect of glycerin on drug release, the polyacrylonitrile membrane was used as supplied; and this was compared to the results from the polyacrylonitrile membrane subjected to the standard washing procedure described above. The donor phase was loaded with 1 mL of ibuprofen saturated solution (cf. in Chapter 3, section 3.2.5). The standard receptor fluid 0.1M sodium hydroxide was employed. All openings including donor top and receptor arm were occluded with parafilm to prevent evaporation. The ibuprofen drug release was measured by removing aliquots from receptor compartment at every 15 to 30 minutes for 7 hours. Ibuprofen crystals (Chapter 3, section 3.2.5) were added into the donor phase in hourly interval to maintain ibuprofen

saturated state. The ibuprofen concentration was analysed using UV spectrophotometer. The cumulative ibuprofen release before and after glycerin removal over 7 hours was plotted against time and coefficient of variation of flux was determined.

4.2.4 Osmosis

4.2.4.1 Evidence of osmosis in Franz cells

Franz cells were set up as follows: The donor was loaded with ibuprofen saturated solution while the receptor was filled with de-aerated 0.1M sodium hydroxide. The donor and receptor arm openings were tightly occluded with parafilms. The Franz cells were placed into the magnetic blocks heated to 37°C. The model membranes investigated were Visking, Cuprophan, polyamide (Biodyne), and polycarbonate (Nuclepore). The initial level of donor was marked. The changes in donor level over 7 hours were observed. No sampling or ibuprofen analysis was performed. The correlation of donor level rise with membrane hydrophilicity, pore size, thickness, and membrane swelling was also investigated.

4.2.4.2 Effect of osmosis on ibuprofen drug release

A simple Franz cell experiment using ibuprofen saturated solution (Chapter 3, section 3.2.5.1) as a model formulation was conducted to investigate the effect of osmosis on drug release of ibuprofen and the influence of the addition of tonicity agents. The receptor fluid with tonicity agents (calculations see below) was de-aerated by means of helium and used as the receptor medium. Previous observation revealed that Cuprophan caused the most evident osmosis in Franz cells, so it was employed as the model membrane. The pre-hydrated membrane was mounted between the matched donor and receptor compartment and 1 mL of saturated solution was placed on the membrane surface in the donor compartment. The receptor compartment was stirred at the validated speed (200 rpm). All openings including donor top and receptor arm were occluded with parafilm to prevent evaporation. 2 mL of

sample volumes were withdrawn from receptor at time intervals for UV assay (blank: sodium hydroxide with tonicity agent subtracted) and fresh preheated replacement of medium of same volume was reintroduced into the receptor. Intervals between sampling were 10 to 30 minutes for 7 hours. Ibuprofen microcrystals were added into the donor phase in hourly interval to maintain ibuprofen saturated state. The cumulative drug release per unit area over 7 hours was plotted and the ibuprofen fluxes were compared and contrasted. In this study, two types of tonicity agents, namely mannitol and sucrose were employed. The receptor fluid with tonicity agents was prepared as follows: 4 g of sodium hydroxide was dissolved in 100 mL of distilled water to make up the standard the 0.1M sodium hydroxide receptor fluid. Then the tonicity agents 32.3 g for sucrose (MW 342.2), 17.2 g for mannitol (MW 182.2) was accurately weighed and dissolved into the receptor fluid. The amount of tonicity agent required in the receptor compartment was determined using the van't Hoff equation (Eq 2.5). Below presents the calculation for the amount of tonicity agents required to stop the osmosis in our Franz cell experiment.

The Van't Hoff equation: $\pi = i$ MRT (Eq. 2.5) was used, where P is the osmotic pressure (Pa), T is the temperature (K), R is the gas constant, 8.314 J K^{-1} mol^{-1}, M is the molarity in donor or receptor compartment ($mol.L^{-1}$) and i is the number of species present in the solution, including undissociate as well as dissociated solutes (unitless). Osmosis is inhibited when the osmotic pressure of donor is equivalent to the receptor.

<u>DONOR</u>

Donor compartment contained ibuprofen saturated solution prepared in 0.1M sodium hydroxide.

Species present (i_D) : Na^+, OH^-, IBU, $i = 3$;

Molarity of ibuprofen saturated solution (M_D) = 0.197 M;

Temp (T_D): 306.16 K

RECEPTOR

The receptor fluid contained 0.1M sodium hydroxide and tonicity agent.

Species present (i_R) : Na^+, OH^-, tonicity agent, $i = 3$;

Molarity (M_R): NaOH = 0.1 M, tonicity agent = ? M, Total M = 0.1 + ? M ;

Temp (T_R): 310.16 K.

When the osmotic pressure of the donor was equated to that of the receptor, the total molarity of the receptor (M_R) can be determined. Hence,

$i_D . M_D . R . T_D = i_R . M_R . R . T_R$

$(3)(0.197)(R)(306.16) = (3)(M_R)(R)(310.16)$

M_R, the total molarity in the receptor was 0.1945 M

The theoretical amount of tonicity agent required was the total molarity (M_R) subtracted with receptor fluid containing 0.1M sodium hydroxide. This was equivalent to 0.0945 M. Therefore, an additional of 0.0945M of tonicity agent was added into the receptor to stop osmosis.

The experiment in section 4.2.4.1 was repeated with tonicity agents and the donor rise over 7 hours was again observed.

4.2.4.3 Ibuprofen solubility in receptor fluid containing tonicity agents.

To ensure that the tonicity agents did not alter the ibuprofen solubility in receptor fluid (which in turn the sink condition), the effect of tonicity agents on ibuprofen solubility in 0.1M sodium hydroxide was examined. Approximately 1.5 g of ibuprofen was added to 50 mL of 0.1M sodium hydroxide as well as 0.1M sodium hydroxide containing 0.0945M mannitol or sucrose. The suspensions were agitated for at least 1 hour in a shaking water

bath maintained at 60-65°C. Any undissolved solid was filtered off at the same temperature and the filtrates were allowed to cool to 25°C for overnight and ibuprofen crystal growth was visible. The ibuprofen crystals were filtered using 0.22µm syringe filter and solutions were dilute appropriately, then the ibuprofen solubility was determined using UV spectrophotometer at 272 nm. Each solubility tests were carried out in triplicate. The average ibuprofen solubility prepared in 0.1M sodium hydroxide containing tonicity agents was compared to ibuprofen solubility in 0.1M sodium hydroxide only using statistica analysis.

4.2.4.4 Solution osmolality

The osmolality measurement was carried out using freezing point depression osmometer (Model 3D3, Advanced Instrument Inc.). The osmolality of ibuprofen saturated solution (donor solution), 0.1M sodium hydroxide, 0.1M sodium hydroxide with sucrose, 0.1M sodium hydroxide with mannitol were determined. The solutions were filtered with 0.22 µm polysulphone syringe filter in order to eliminate particles. The solutions for the receptors were filtered at 37 °C while the ibuprofen saturated solution was maintained at filtered 33 °C prior to reading. This was aimed to simulate the receptor and donor temperatures respectively. Each solution was measured in duplicate. The osmometer was calibrated with the reference solution (Clinitrol ™).

4.3 Results

4.3.1 Membrane hydration

Mass ratio measures the total fluid uptake per unit of dry membrane mass. The percentage water mass gained (%) of Visking, Cuprophan, Polyacrylonitrile (AN69) and Biodyne over 24 hours are shown in Figure 4.1.

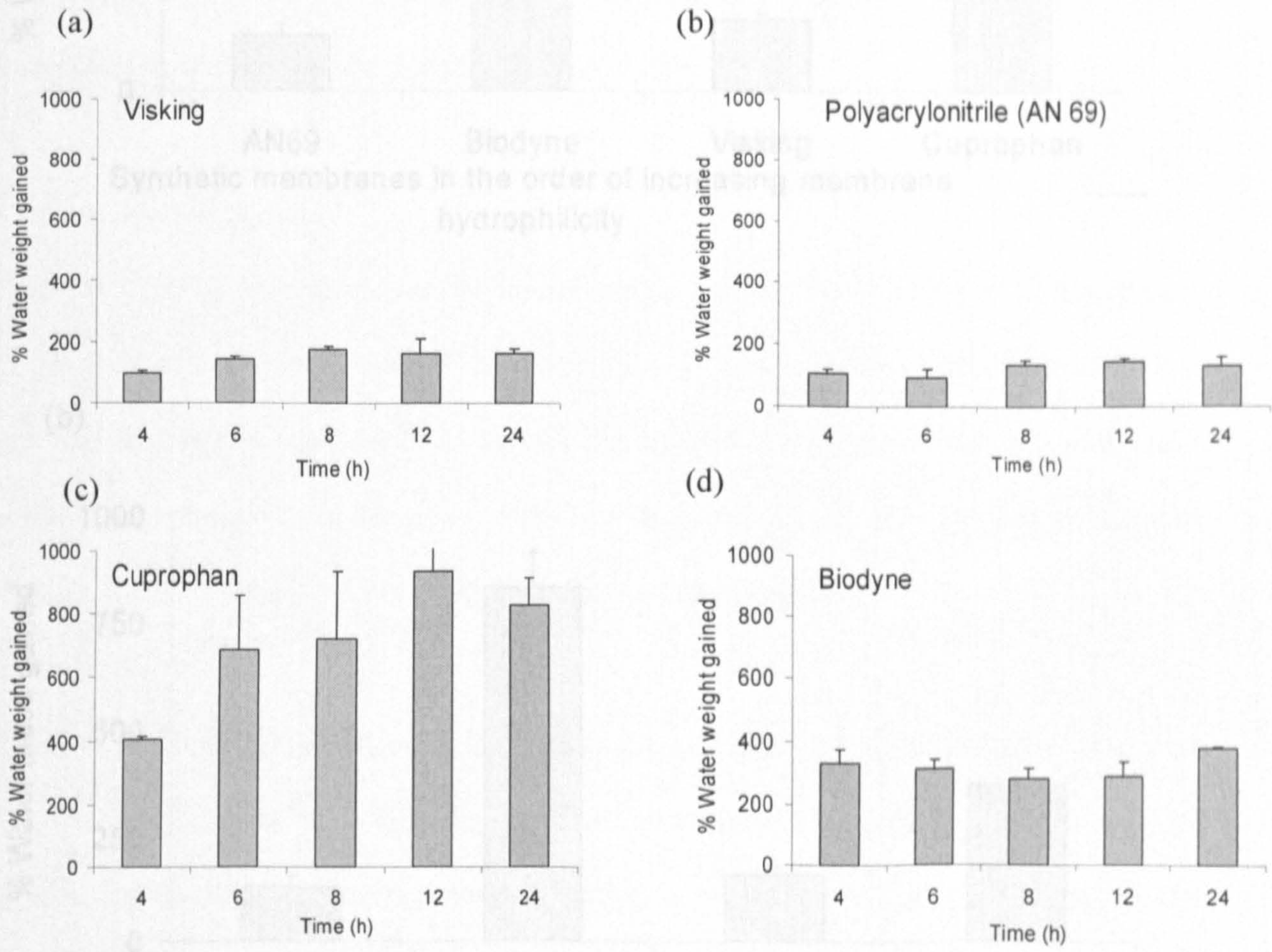

Figure 4.1: Synthetic membrane average hydration mass ratio over 24 h. (a) Visking, (b) Polyacrylonitril (AN69), (c) Cuprophan and (d) Polyamide (nylon) Biodyne.

Figure 4.2 plots the relationship between the % water mass gained at 24 hour and (a) membrane hydrophilicity and (b) membrane pore size.

(a)

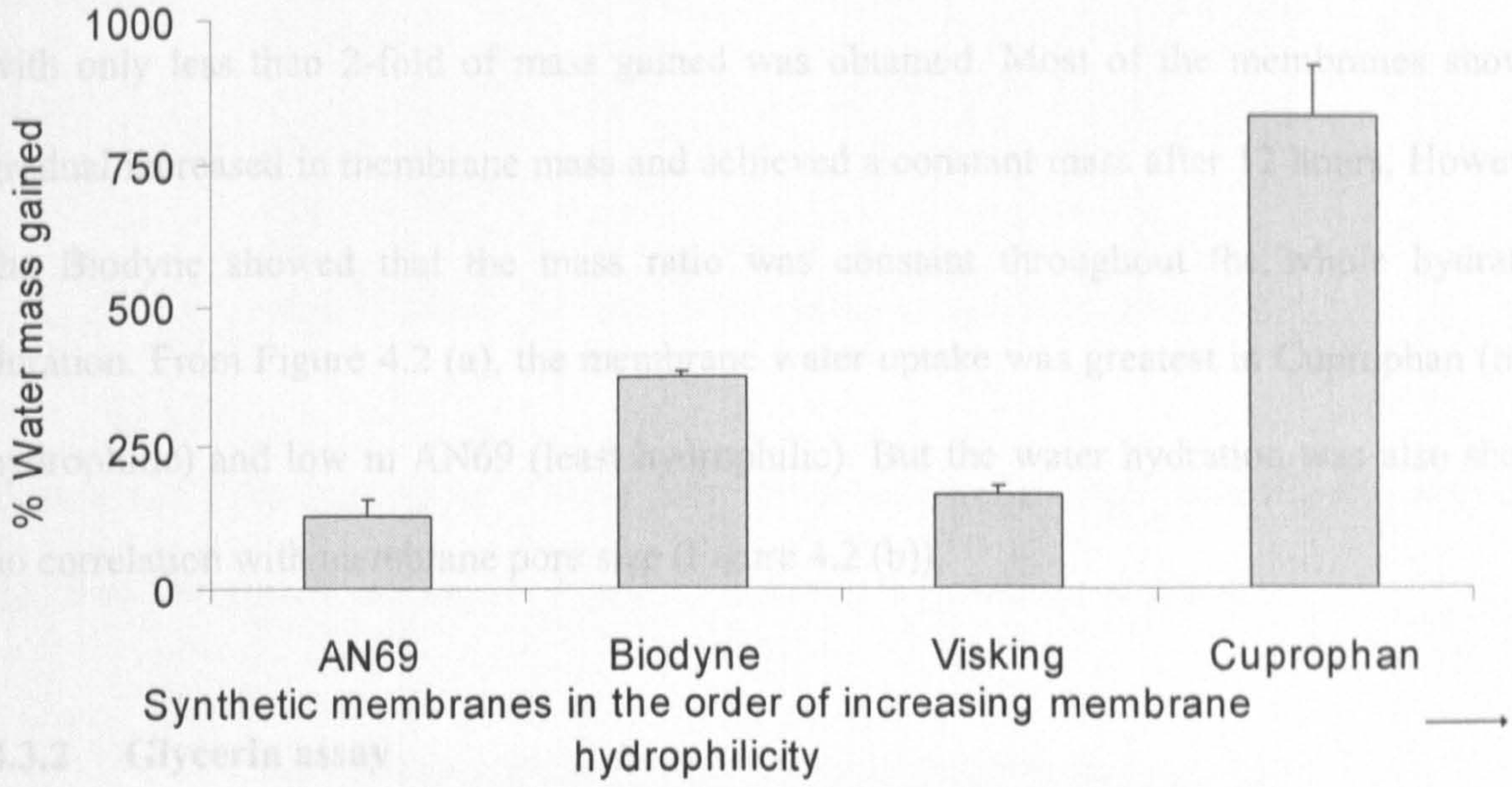

(b)

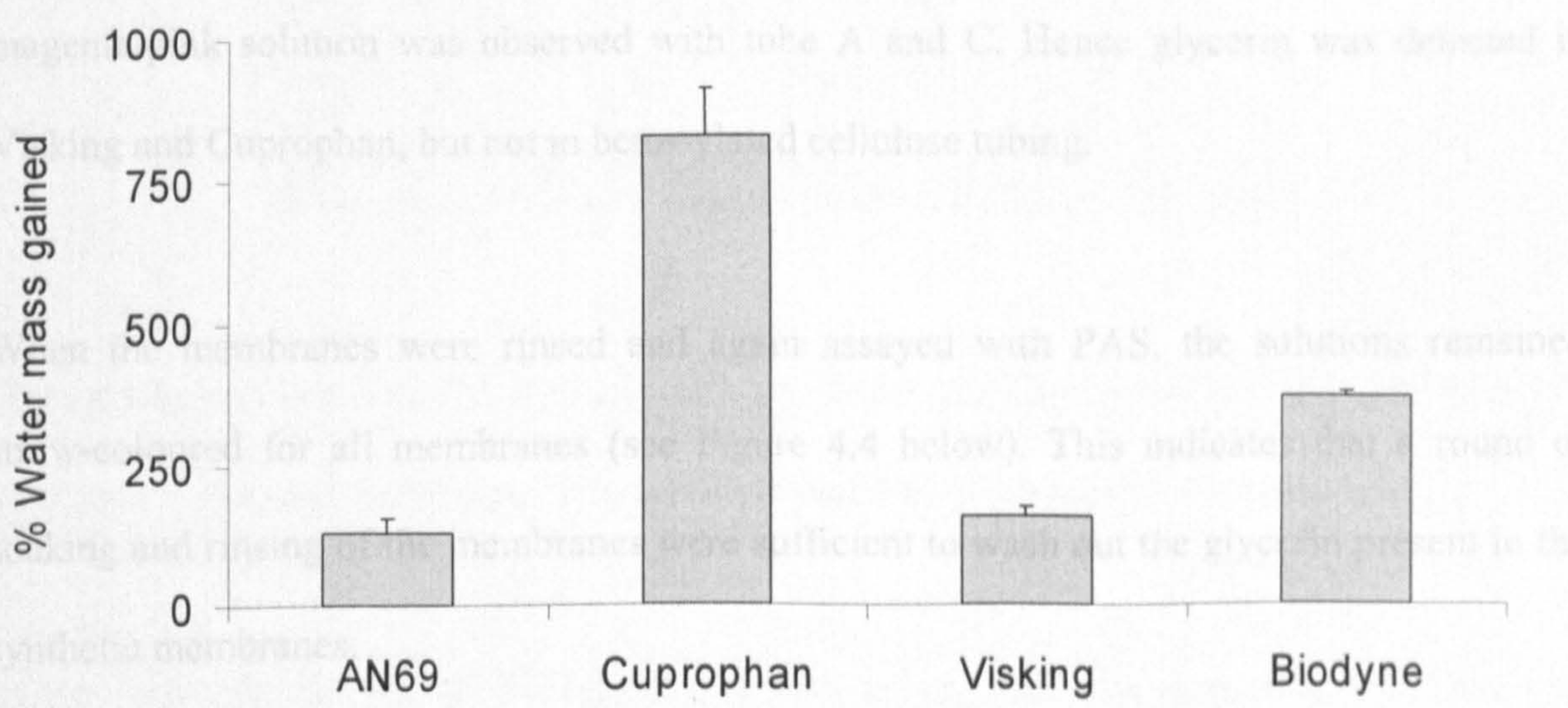

Figure 4.2: The plot of synthetic membrane % water mass gained at 24 h placed in the order of increasing (a) membrane hydrophilicity and (b) pore size.

From Figure 4.1, all mass measured showed mass gained over 24 hours during hydration. Cuprophan membranes showed the highest mass increased, with mass ratio up to 10-fold after 24 hours of hydration. While the polyacrylonitrile AN69 revealed the least mass gained, with only less than 2-fold of mass gained was obtained. Most of the membranes showed gradual increased in membrane mass and achieved a constant mass after 12 hours. However, the Biodyne showed that the mass ratio was constant throughout the whole hydration duration. From Figure 4.2 (a), the membrane water uptake was greatest in Cuprophan (most hydrophilic) and low in AN69 (least hydrophilic). But the water hydration was also shown no correlation with membrane pore size (Figure 4.2 (b)).

4.3.2 Glycerin assay

Figure 4.3 shows four tubes with solutions which were previously soaked with different membranes and analysed using PAS assay. Tube D was a control showed straw colour solution; tube B was straw-coloured as well indicating that no glycerin was detected. Light magenta-pink solution was observed with tube A and C. Hence glycerin was detected in Visking and Cuprophan, but not in benzoylated cellulose tubing.

When the membranes were rinsed and again assayed with PAS, the solutions remained straw-coloured for all membranes (see Figure 4.4 below). This indicates that a round of soaking and rinsing of the membranes were sufficient to wash out the glycerin present in the synthetic membranes.

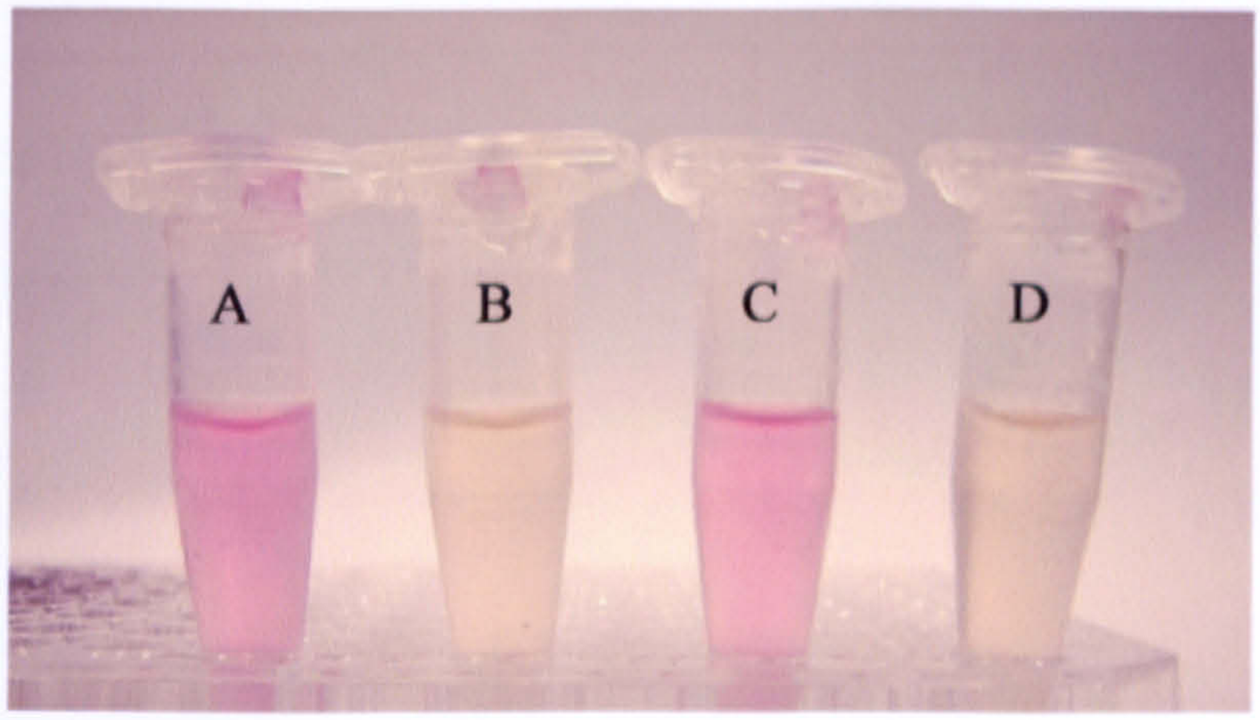

Figure 4.3: PAS reaction of Visking (A), Benzoylated (B), Cuprophan (C) and reference (D). Pink coloured solutions, i.e. A and C, indicated the presence of glycerin.

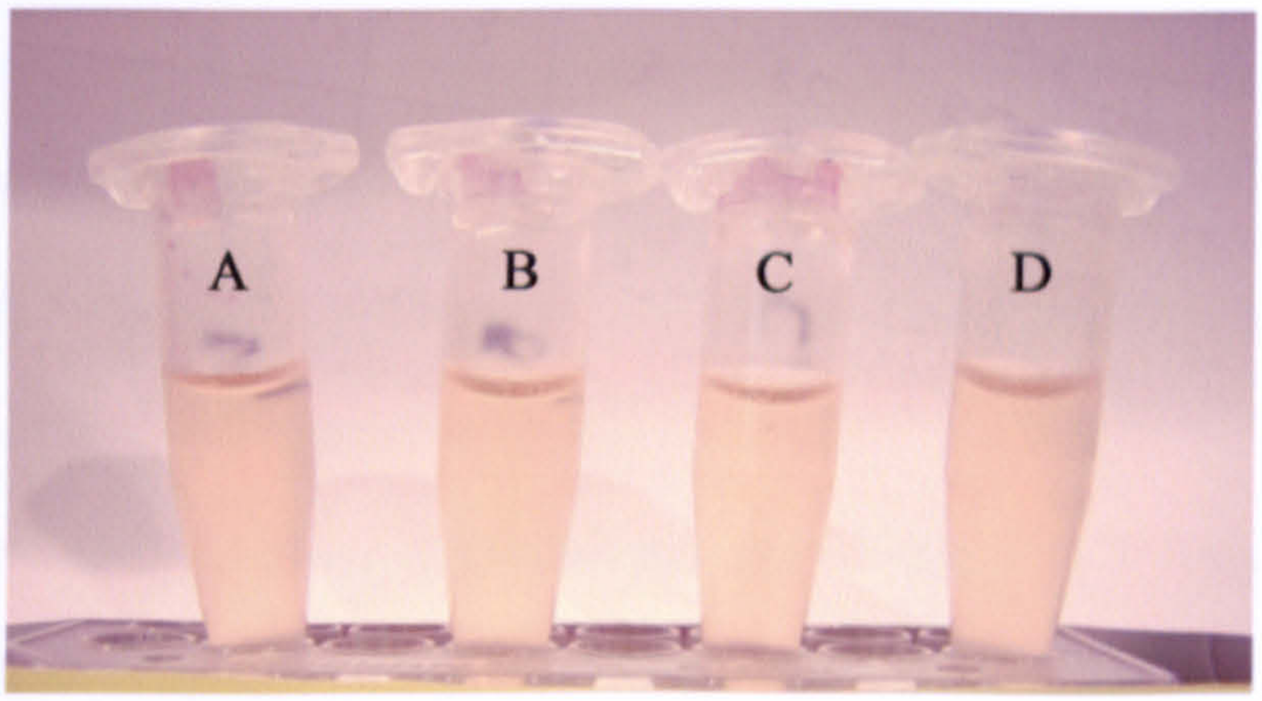

Figure 4.4: PAS reaction of Visking (A), Benzoylated (B), Cuprophan (C) and reference (D) after second soaking and rinsing. No colour change was observed for all membranes.

At detection wavelength of 540 nm, the amount of glycerin was measured. The minimal concentration for detection was 3.12×10^{-4} % w/v. Table 4.1 below showed the percentage glycerin quantified using PAS assay as well as the glycerin values quoted by the manufacturers.

Table 4.1: Percentage of glycerin detected in synthetic membranes (n = 4).

Membrane	% Glycerin from manufacturers	% Glycerin detected using PAS reagent
Benzoylated	0[a]	0.06 ± 0.01
Visking	9-13[b]	11.6 ± 2.6
Cuprophan	13-15[b]	13.5 ± 2.5
Polyacrylonitrile (AN 69)	40-50[c]	56.9 ± 16.3

[a] Sigma; [b] Medicell; [c] Hospal-Gambro

4.3.3 Glycerin effect on drug release

The ibuprofen drug release before and after the glycerin removal were shown in Figure 4.5 (a) and (b) respectively. Both the ibuprofen flux showed linear drug release with time. The ibuprofen fluxes produced were 7.77 ± 1.34 and 8.41 ± 0.38 mg/cm^2/h before and after glycerin removal respectively. The presence of glycerin was found to cause larger results variability (CV = 13.2 %) compared to that of 'washed' membrane (CV = 5.7%). This demonstrated that glycerin on membrane interfered with drug flux reproducibility and that glycerin removal was essential prior to Franz cell experiment.

(a)

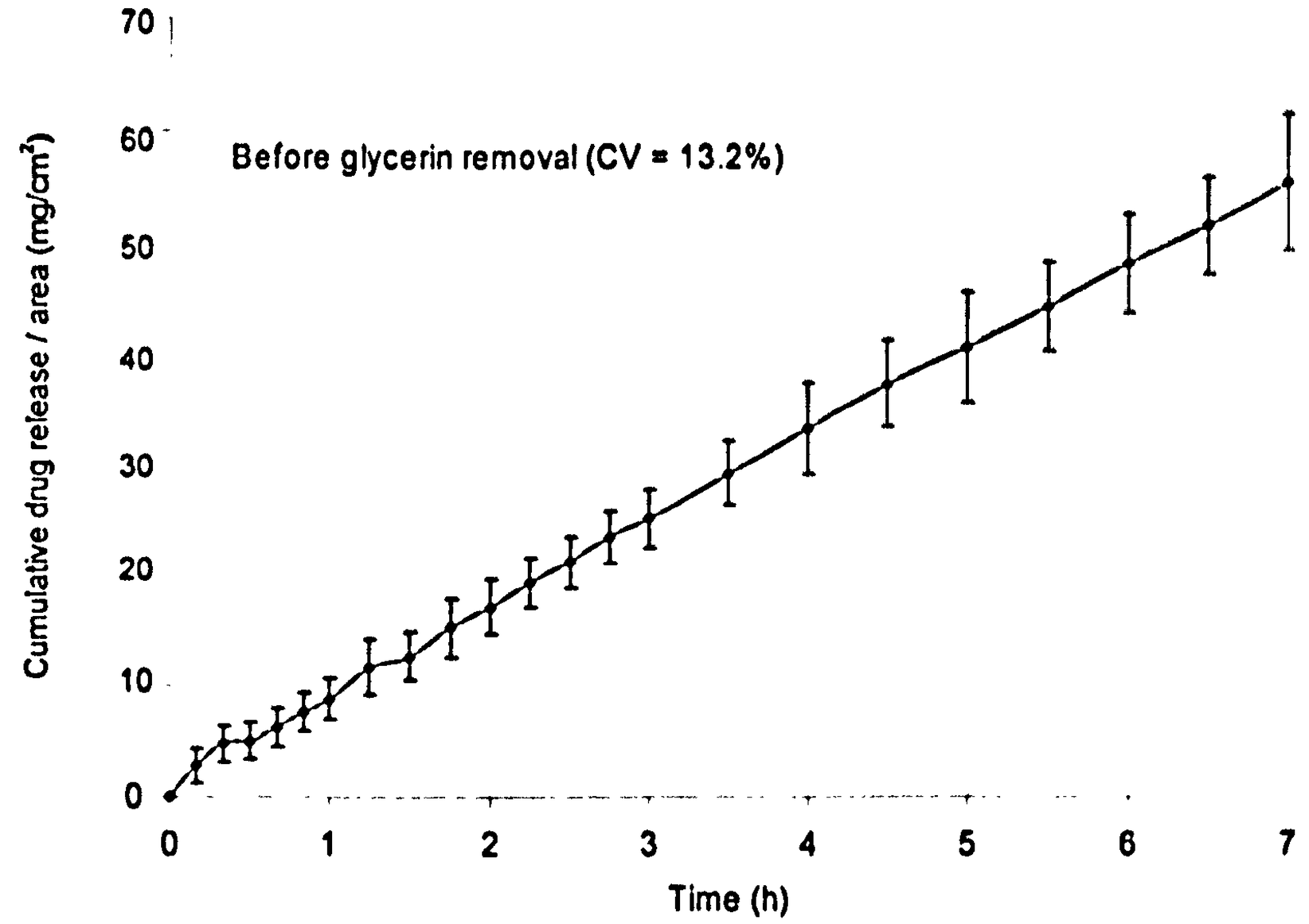

(b)

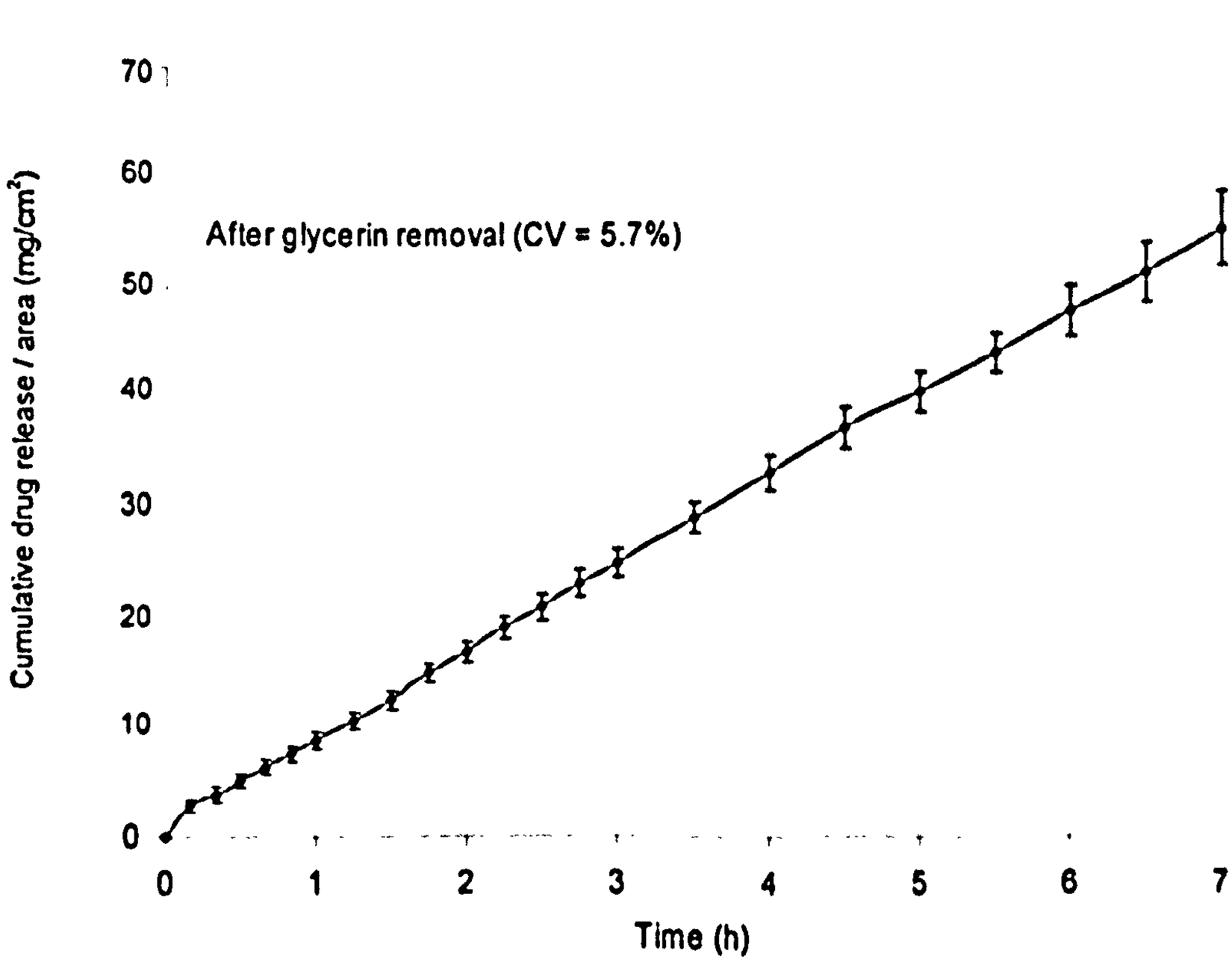

Figure 4.5: Ibuprofen drug release plots across polyacrylonitrile (a) before and (b) after glycerin removal.

4.3.4 Osmosis

4.3.4.1 Evidence of osmosis in Franz cells

Figure 4.6 (a) shows the typical Franz cell with donor lever rise after osmosis. The osmosis occurred in the direction from the receptor into the donor (illustrated by arrow in Figure 4.6 (b)).

(a)

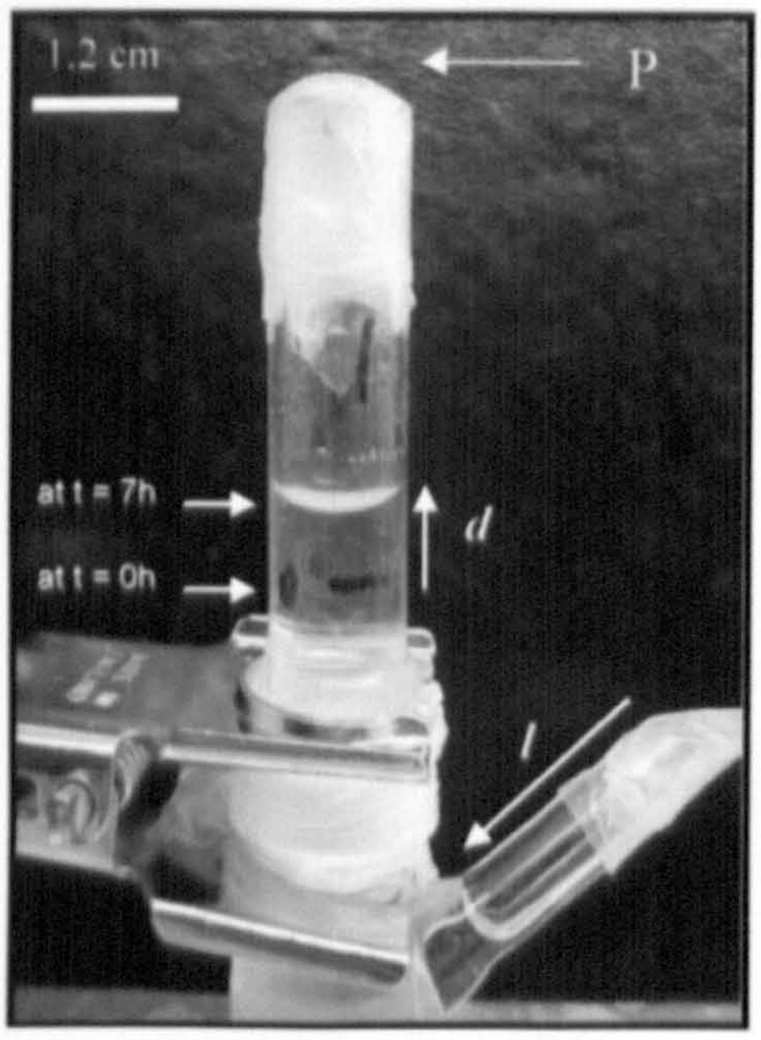

(b)

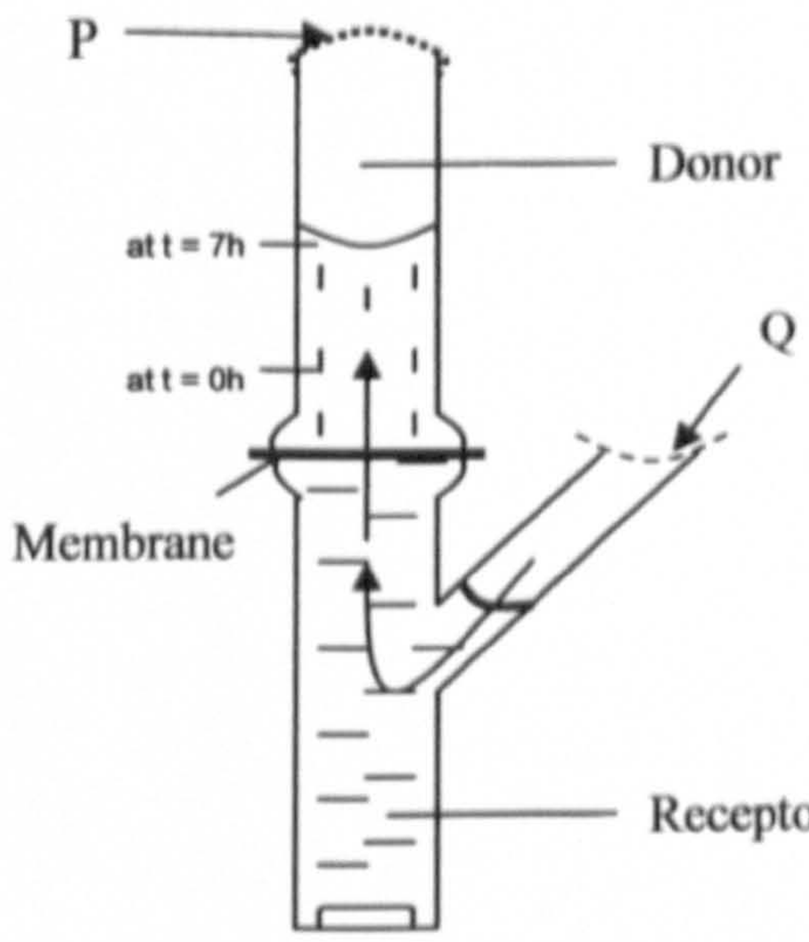

Figure 4.6: (a) Typical observation of osmosis in Franz cells. (b) Schematic diagram of Franz cell back diffusion due to osmosis. The measurement ***d*** at the donor indicates the donor rise after 7 hours with the corresponded drop in arm level ***l***. As the fluid travelled up, the gaseous space above the donor liquid caused the parafilm to bulge outward (point P), and depression of parafilm at the sampling arm (point Q).

The evidences of osmosis occurred in Franz cells were shown in Table 4.2 and Figure 4.7. It was found out that the extent of osmosis was depended on the membrane type.

Table 4.2: Donor level rise in Franz cells using different synthetic membranes.

Membrane	Type	Thickness (μm)	Donor level rise, d (mm)[a]		
			2 h	4 h	7 h
Visking	Cellulose	20	2.0	2.5	3.0
Cuprophan	Cellulose	10	2.0	3.0	5.0
Biodyne	Polyamide (nylon)	152	0.2	0.2	0.2
Nuclepore	Polycarbonate	10	0.2	0.5	0.5

[a] average of 2 cells

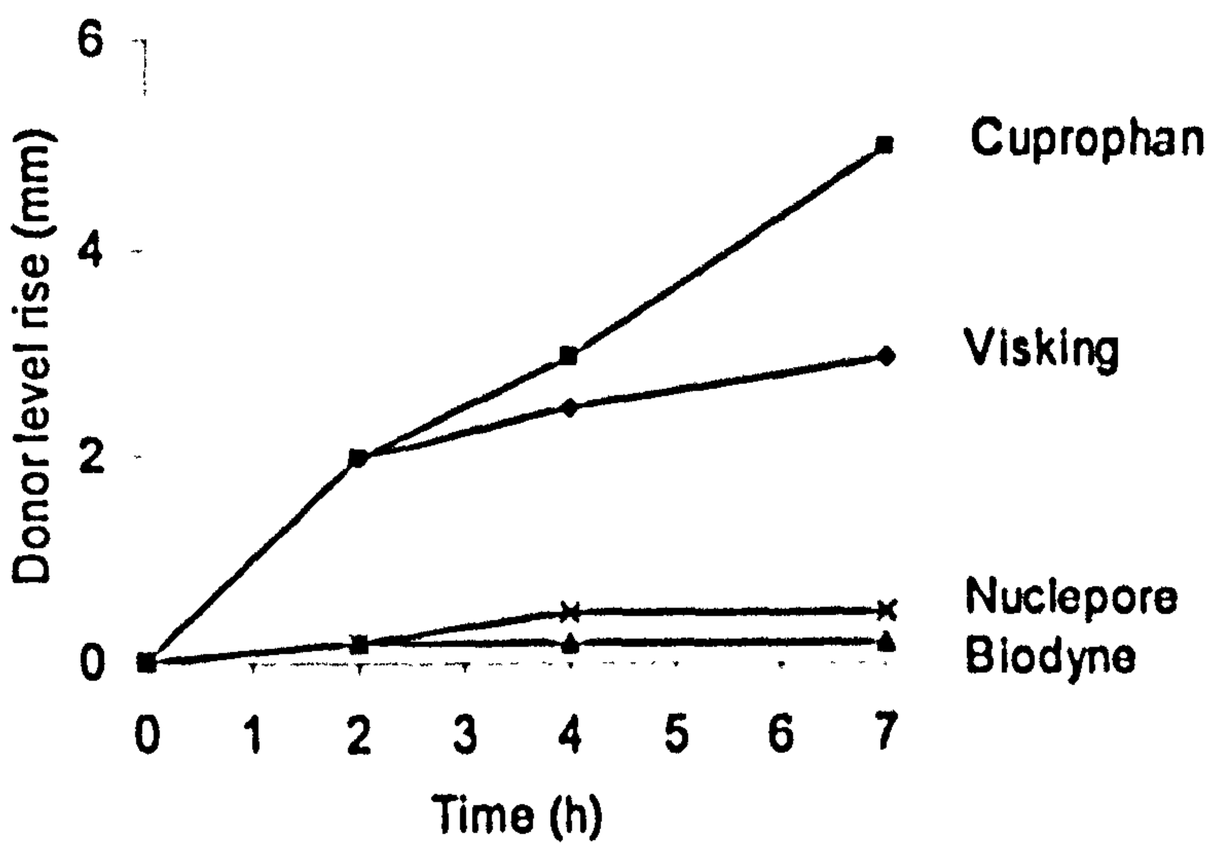

Figure 4.7: The rise in donor saturated solution level over 7 hours when Visking, Cuprophan, Nuclepore and Biodyne membranes were employed.

The rise in donor level was observed with all membranes but at different rates. Both the regenerated cellulose (Visking and Cuprophan) showed rapid donor rise compared to the polymeric nylon Biodyne and Nuclepore.

Figure 4.8 shows plots three membrane factors plotted against donor rise: pore size, thickness, degree of membrane hydrophilicity and water mass gained.

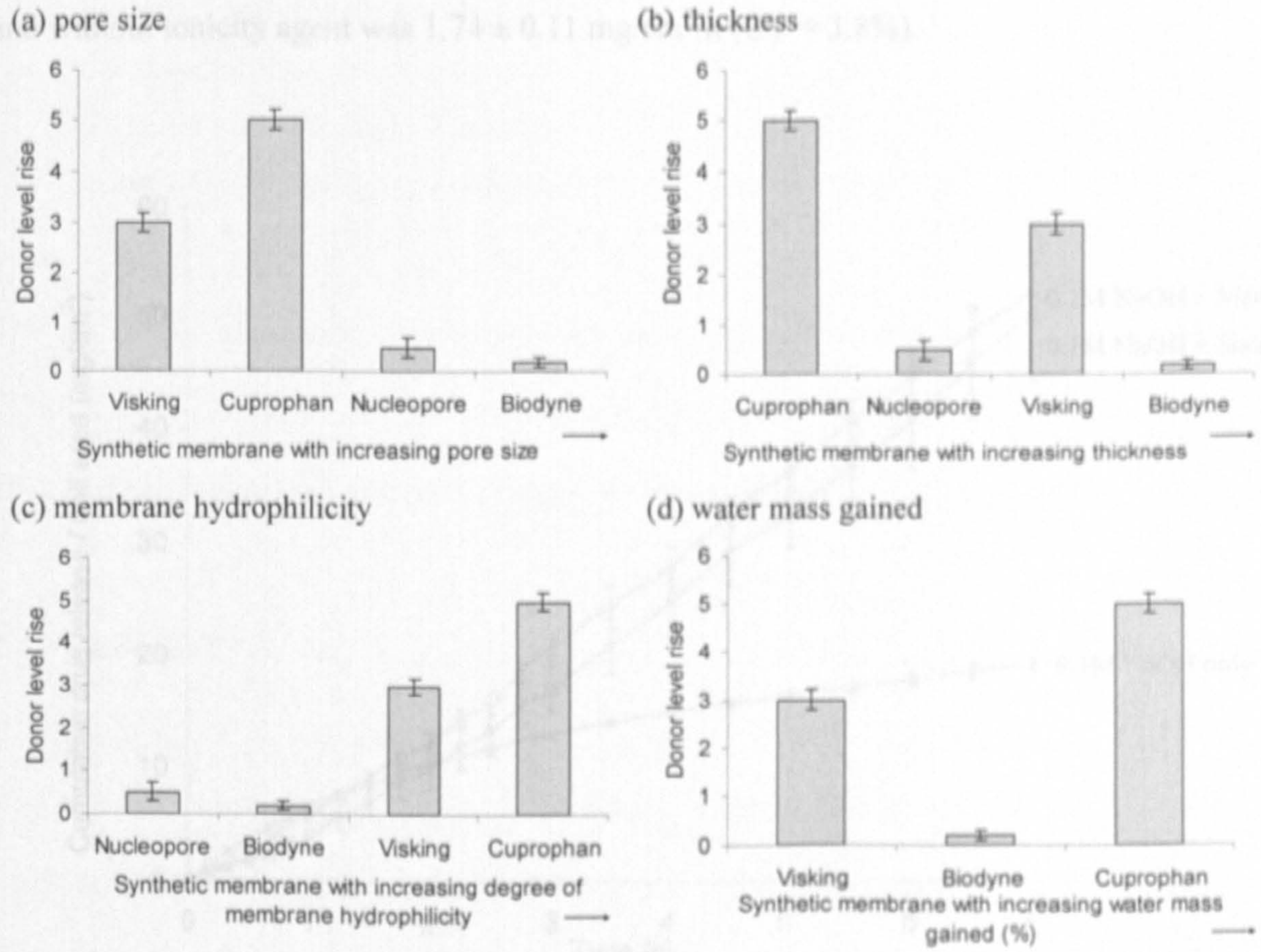

Figure 4.8: The correlation of donor level rise with synthetic membranes (a) pore size, (b) thickness, (c) membrane hydrophilicity and (d) water mass gained.

Here it was observed that the donor level rise increases with increased membrane hydrophilicity but decreased pore size. While the water mass gained and thickness did not show apparent trend towards donor rise.

4.3.4.2 Effect of osmosis on ibuprofen drug release

Figure 4.9 shows the ibuprofen drug release before and after the addition of tonicity agents (mannitol or sucrose). Observation at the donor saturated solution level showed that there was no increase in donor level throughout the experimentation duration. The ibuprofen flux with the two types of tonicity agents was not statistically different ($p > 0.05$). The ibuprofen

flux was approximately 4-fold higher after tonicity adjustment; 7.74 ± 0.84 mg/cm^2/h and 7.94 ± 0.36 mg/cm^2/h for sucrose (CV = 10.4%) and mannitol (CV = 4.5%) respectively; and without tonicity agent was 1.74 ± 0.11 mg/cm^2/h (CV = 3.8%).

Figure 4.9: The ibuprofen drug release through Cuprophan membrane before and after addition of tonicity agents (mannitol or sucrose).

The ibuprofen solubilities in 0.1M sodium hydroxide, 0.1M sodium hydroxide with mannitol and 0.1M sodium hydroxide with sucrose were 2.075 ± 0.03, 2.00 ± 0.08 and 2.12 ± 0.09 % w/v respectively. Statistical analysis shown that the ibuprofen solubility prepared in 0.1M sodium hydroxide containing tonicity agents were not significantly different ($p>0.05$) from the ibuprofen solubility in 0.1M sodium hydroxide. This indicated that the tonicity agents were inert and did not interfere with ibuprofen solubility in the receptor fluid.

The osmolality measurement results were tabulated in Table 4.3.

Table 4.3: Osmolality values of the donor and receptor solutions measured by osmometer.

Solution	Osmolality (mOsm/kg)
Ibuprofen saturated solution	191
0.1M sodium hydroxide only	181
0.1M sodium hydroxide + sucrose	218
0.1M sodium hydroxide + mannitol	252

The additional of tonicity agents (amount predicted using van't Hoff equation) into the receptor fluid had raised the osmotic pressure, but the osmolality values revealed that it was 20-50 mOsm higher than that of the ibuprofen saturated solution (in the donor).

4.4 Discussion

The use of synthetic membrane in Franz cells is widely used for determining the batch-to-batch uniformity of topical semisolids [Wu *et al.*, 1992; FDA-SUPAC-SS, 1997; Shah *et al.*, 1999]. The synthetic membrane is sandwiched in between the donor and receptor but it not meant to serve as a barrier; but only a support to separate the formulation from the receptor media. Since synthetic membranes are artificially made, simpler handling and storage procedure are required compared to skin. Despite the fact that the synthetic membranes are structurally relatively straight forward, several problems have been encountered when using the synthetic membranes with Franz cells.

The impact of membrane hydration is significant when hydrophilic membranes such as cellulose Visking and Cuprophan were employed. This is because these membranes are densely populated with hydroxyl groups which could interact with water molecules and cause the membranes to swell and gel-up when hydrated. The Cuprophan gained greater water mass gained compared to Visking because the Cuprophan has smaller pores so giving rise to a higher surface area for hydroxyl groups and interaction with water molecules.

Among the four membranes, Biodyne has largest pores and the greatest thickness; however it gained higher water content compared to Visking. It was thought that the Biodyne did not 'swell' because of its relative hydrophobic in nature, but rather, it 'entrapped' water within the membrane pores giving a measurable mass gained. In the preparation of Franz diffusion cell experiment, the synthetic membranes are normally pre-saturated in receptor fluid prior to Franz cell experiment. This procedure not only hydrates the membrane but it also displaces any air entrapped within the membrane. Some investigators did not pre-hydrate the synthetic membranes and place them directly on the Franz cells. An untreated membrane has the potential to absorb fluid from both compartments during an experiment and to become saturated with a mixture of both donor and receptor solvents. Consequently, the membrane is likely to change in thickness during the course of study which in turn alters the diffusional pathlength of drug transport. Our results indicated that the investigator should allow ample equilibration time for the membrane to be fully hydrated, possibly more than 12 hours before placing in the Franz cell.

The removal of membrane additives before Franz cell experiment is also another fundamental step that many investigators overlook. Glycerin is a common membrane additive and sometimes it is present at a very high amount in a packaged membrane (e.g. ~50% in AN69). In this study, a glycerin assay using periodic acid Schiff reagent proves to be a quick and robust colorimetric method for glycerin detection present in the synthetic membranes. The washing method adopted in our laboratory, i.e. soaking in receptor fluid for at least 12 hours then rinsing again, has proved to be effective in removing glycerin, as no colour changed from Schiff reagent was observed after second soaking and rinsing. The amount of glycerin present was also able to be determined with UV analysis. It was found that the glycerin content measured for Visking, Cuprophan and AN69 corresponded well with manufacturers' stated glycerin content; while the benzoylated cellulose membrane

contained only trace amounts of glycerin (Benzoylated cellulose membrane was supplied in water pack, so incorporation of plasticizer was not necessary). This show that the Schiff assay not only acts as a colorimetric test for glycerin but also a qualitative tool for determining glycerin content in a synthetic membrane.

Osmosis is a passive process which occurs naturally whenever there are differences in osmotic pressure between two compartments which are separated by a semi-permeable membrane permeable only to water. Franz cell consists of similar setting when a synthetic membrane is employed, but the membrane is often permeable to drugs as well as water molecules. Our study shows that osmotic processes were prominent in Franz diffusion cells. We are not aware of any discussion of this in the literature. This could probably due to the minute (< 500 µL) amount of drug often used so that the osmosis effect was not noticed. This phenomenon should not be confused with 'back-diffusion', in which it described the diffusion of drug in the reverse direction i.e. from the receptor into the donor. Osmosis occurred in Franz cells because there was an apparent difference in osmolarity between the two sides of the membranes where osmotic pressure was generated. Depending on the type of membrane, the solvent travelled from the receptor into the donor at different rates. Osmosis (indicated by donor level rise) appeared faster when cellulose membranes Visking and Cuprophan were used. This might be because that donor level rise was shown to favour hydrophilic, thin and membrane with small pores (Figure 4.8).

Tonicity agents are incorporated into pharmaceutical solutions such as injection, nasal and ophthalmic solutions for tonicity adjustment so that the product has similar osmolarity with physiological fluid to be administered [Richards, 2000]. The use of tonicity agents in our study was not intended to mimic physiological osmolarity but merely to prevent osmosis occurs in Franz cells. Using van't Hoff equation, the amount of tonicity agents required was

calculated. The tonicity agents employed in Franz cells for tonicity adjustment should be 'inert' and should not affect the drug flux or affect the analysis procedure. The fact that both tonicity agents employed in this study (sucrose and mannitol) produced ibuprofen flux values that were not statistically significant showed that the tonicity agents itself did not affect drug flux. This would be expected, as the osmotic pressure is the colligative property, where only the number of molecules (not the nature of the molecule) would pose an effect. However, sucrose produced higher variable results which may be due to the alkaline environment (0.1M sodium hydroxide) where it is susceptible to alkaline hydrolysis.

The ibuprofen flux was shown to be four-fold higher after tonicity adjustment. The possible reason being that when the osmotic pressure was not adjusted, the solvent travelling into the donor causes the dilution of ibuprofen saturated solution. This decreases the concentration gradient between donor and receptor resulting in lower flux. However when the osmotic pressure was balanced, no such dilution effect occurred. The concentration gradient is higher and therefore giving higher drug flux. However, the osmolality values revealed that the van't Hoff equation had slightly over-predicted the amount of tonicity agents required, especially mannitol. Assuming that there was no chemical interaction between the molecule species, addition of excess tonicity agent in this experiment might lead to the fact that osmotic pressure was generated in an opposite direction, i.e. the solvent now flows from the donor into the receptor. This in turn led the ibuprofen to be carried into the receptor fluid via the membrane pores. Further work is required on fine adjustment of the tonicity agents in order to avoid such circumstances.

4.5 Conclusions

The factors relating to the synthetic membranes in Franz cells experiments were investigated. The conclusions from this study were:-

1. Proper membrane treatment is essential to ensure membrane full performance and most importantly that it should not influence the drug diffusion process.
2. Periodic acid Schiff assay was shown to be a robust method in detecting glycerin being removed from synthetic membranes. This PAS test can also be employed to quantify glycerin content in synthetic membranes.
3. The glycerin removal procedure was proved to be effective because no glycerin was detected after the standard membrane washing procedure developed in our laboratory.
4. Osmosis was demonstrated in Franz cells and this was shown to influence ibuprofen flux in Franz cell experiments using synthetic membrane. The Van't hoff equation could be use to predict the amount of tonicity agent for the adjustment of the osmotic pressure in Franz cells.
5. Furtherwork is required for finer tuning of the amount of tonicity agent as well as to investigate the occurrence of osmosis associated with skin.

CHAPTER V

ASSESSMENT OF COMMON SYNTHETIC MEMBRANES USED IN FRANZ DIFFUSION CELL EXPERIMENTS

5.1 Introduction

The different types of synthetic membranes used in *in vitro* percutaneous absorption studies were discussed previously (Chapter 1, section 1.3). Generally synthetic membranes employed in drug diffusion studies have two functions: skin simulation [Twist and Zatz, 1986] and quality control [Corbo *et al.*, 1993]. PDMS is an example of synthetic membrane which often employs for skin mimicry, because it is hydrophobic in nature and possesses rate-limiting properties like skin. On the other hand, synthetic membranes for quality control should have no diffusional resistance to the drug and only act as a support to separate formulation from the receptor medium. This chapter focused mainly on the different types of synthetic membranes used for quality control.

The Food, Drug and Administration (FDA) suggested that porous synthetic membranes are suitable for assessing topical formulation performance as supposedly they can be act as a support but not a rate-limiting barrier [FDA-SUPAC-SS, 1997]. Shah and co-workers from FDA had used different microporous membranes, namely pure cellulose acetate, triton-free cellulose, cellulose with wetting agent, and polysulfone of similar pore sizes and thickness to examine the drug release of hydrocortisone (HC) from two commercial creams (Synacort and Hytone, containing 2.5% HC). They found that the HC flux was consistent for all membranes and statistic tests showed that the flux was not affected by the type of synthetic membranes [Shah *et al.*, 1989]. But there was evidence showing that the various types of

porous membranes had an effect on drug flux. Wu and co-workers from FDA evaluated 10 types of commercially synthetic membranes including polysulphone, cellulose mixed esters, polytetraflouroethylene and polypropylene of different pore size and thickness to evaluate the nitroglycerin drug release from commercial ointments [Wu *et al.*, 1992]. They only did two replicates for each membrane. When the rates of release from the membranes were compared statistically, the authors grouped the membranes into two groups, group 1 and 2. Group 1 showed higher release rates compared to group 2. Group 1 consisted of polysulfone, acrylic polymer, glass fiber, silicone, and mixed cellulose ester; whilst group 2 were PTFE-polyethylene, mixed cellulose ester (of greater thickness), polypropylene, and PTFE. The authors, however, did not explain the results, just reported them. The effect of membrane types upon ketoprofen drug release from a gel was studied by Gallangher and co-workers [Gallagher *et al.*, 2003]. Two filter membranes, namely nylon (0.2 μm pore size, 129.3 μm thickness) and Celgard polypropylene (0.05 μm pore size, 26 μm thickness) and a nonporous silicone membrane (57 μm) were compared. Their results showed that the nylon offerred the least rate-limiting effects for ketoprofen despite being the thicker membrane [Gallagher *et al.*, 2003]. Although the different types of synthetic materials and dosage forms were tested, the choice of synthetic membranes was not explained.

So from the literature, some authors have demonstrated that the type of synthetic membranes have no influence on flux, whereas others found that the opposite occurred. However, all the authors above made the same conclusions that *porous* synthetic membranes must be without significant diffusion barrier effects on the transport of the drug compound from the formulation because pores should not inhibit diffusion.

5.1.1 Aims of study

The aim of this study was to investigate the influence of different types of commercial synthetic membranes (Chapter 1, Table 1.7) upon drug diffusion in the validated Franz cells

using ibuprofen (MW 206.4, log P 3.5) as model drug. An attempt to correlate and classify the membranes according to their physical properties and effect on ibuprofen drug release will be made. A hydrophilic drug, riboflavin (MW 376.4, log P -1.4), was utilised to compare with ibuprofen to investigate the effect of the log P of a drug on the drug diffusion through synthetic membranes. Table below shows the summary of ibuprofen and riboflavin physical and chemical properties.

Table 5.1: Physical and chemical properties of ibuprofen and riboflavin.

Properties	Ibuprofen	Riboflavin
Chemical Structure	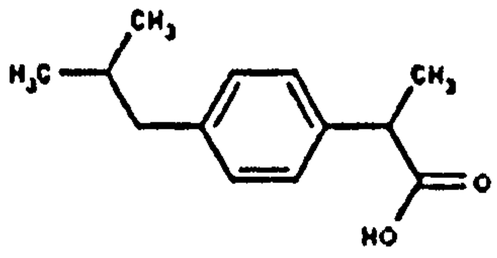	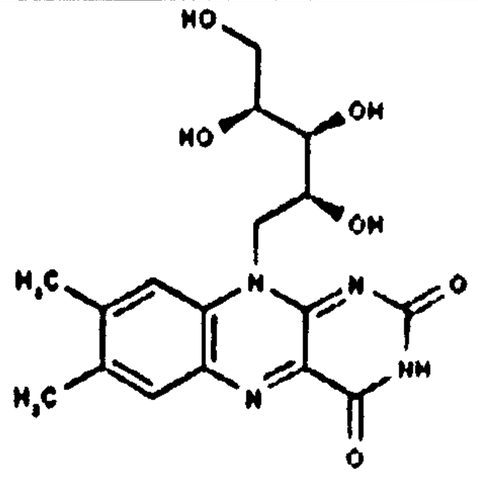
Formula	$C_{13}H_{18}O_2$	$C_{17}H_{20}N_4O_6$
MW	206.38	376.37
Log P (oct/water)	2.5-3.5	-1.4
Melting point (°C)	75-77	290

5.2 Methods

5.2.1 Preparation of ibuprofen and riboflavin saturated solution

Ibuprofen saturated solution was prepared in the standard receptor fluid, 0.1M sodium hydroxide. Approximately 1.5 g of ibuprofen was added to 50 mL of 0.1M sodium hydroxide to give a suspension. The suspension was agitated for at least 1 hour in a shaking water bath maintained at 60-65°C. Any undissolved solid was filtered off at the same temperature and the solution was allowed to cool to 33°C and ibuprofen crystal growth was visible. The pH of the ibuprofen saturated solution was obtained using pH meter.

The ibuprofen saturated solution was prepared fresh for each Franz cell run. Mass balance was carried out in order to ensure the reproducibility of each ibuprofen saturated solution preparation. This was performed by comparing the mass of ibuprofen added and the ibuprofen excess filtered out for every preparation. The coefficient of variation for mass balance was set to be within 5%.

Riboflavin saturated solution was prepared using a different method. This was carried out by dissolving excess (approximately 3g) riboflavin powder in 50 mL of 0.1M sodium hydroxide. The mixture was allowed to stir at room temperature for 6 hours. The stirring was carried out in a sub-due light room and the saturated solution was wrapped with aluminium foil to protect from light (riboflavin degrades with time in 0.1M sodium hydroxide upon exposure to light, see Appendix). After stirring, the saturated solution was transferred to 37 °C prior to Franz cell experiment. The undissolved powder was left suspended in the saturated solution.

5.2.2. Saturated solubility at different temperatures

The saturated solubility of ibuprofen in 0.1M sodium hydroxide at temperature 25, 33, 37 and 60 °C was determined. The ibuprofen saturated solutions were prepared as above. The ibuprofen solubility at 60 °C was determined immediately after the filtration at 60°C. For solubilities at 25, 33 and 37 °C, the filtered saturated solutions were filled into three 7.5 mL vials and closed with screw caps and stored at 25, 33, and 37 °C respectively. After 24 hours, the solutions were passed through 0.2 μm polysulfone filters to remove the excess ibuprofen crystals. The ibuprofen solubility was determined by diluting the solution serially using 0.1M sodium hydroxide and assaying for ibuprofen using UV spectrophotometer at wavelength 272 nm. The solubility at each temperature was determined in triplicate using fresh ibuprofen saturated solution each time.

For riboflavin, the saturated solubilities at 25 and 37 °C were measured. Two batches of riboflavin saturated solution were prepared as above (section 5.2.1). After stirring, the first batch was transferred to the 37 °C room while the other batch was immediately filtered through a 0.2 μm polysulfone filters to remove the excess solids. The filtrate was then diluted serially using 0.1M sodium hydroxide and the concentration was determined with UV spectrophotometer at 445 nm. The first batch was allowed to equilibrate at 37 °C for approximately 24 hours, then the solution was filtered through 0.2 μm polysulfone filters and diluted using 0.1M sodium hydroxide of the same temperature and saturated solubility was determined using UV spectrophotometer.

5.2.3 Preparation of ibuprofen crystals

Ibuprofen saturated solution was prepared at 60 °C as described above in section 5.2.1 and was allowed to cool to 25 °C where crystal growth was visible as needle crystals. The saturated solution was passed through a 0.2 μm nylon filter on a Buchner funnel and filtered via vacuum filtration. The ibuprofen crystals collected on the filter were scraped off and stored in a tight screw vial for the use in Franz cell experiments.

5.2.4 Membrane treatment

All the membranes to be used in the Franz cell experiments were trimmed into circular discs (diameter ~10 mm) sufficient to cover the effective diffusion area of the receptor, and then soaked in receptor fluid for at least 16 hours. For membranes which contained glycerin, further rinsing was carried out before placing them onto the receptor (c.f. Chapter 4). Thin membranes such as Cuprophan and polyacrylonitrile AN69 that might crease or fold when wetted, were hydrated as follows: the delicate membranes were sandwiched in between two microscope glass slides and submerged in the receptor fluid in a Petri dish. A weight (rubber bung) was placed above the glass slides to prevent the floating and separation of the slides

while soaking. Polycarbonate Nuclepore was applied on the Franz cell with the shiny side facing up, as stated by the manufacturer.

5.2.5 Franz cell studies

The ibuprofen and riboflavin drug release from saturated solution across synthetic membranes (listed in Table 1.7) was investigated using the validated Franz cells and equipment. A clean, dried receptor cell was filled with de-aerated 0.1M sodium hydroxide and was allowed to equilibrate at 37 °C in the appropriate heated magnetic block for 15 minutes. The pre-hydrated membrane was mounted between the matched donor and receptor compartment and 1 mL of saturated solution was placed on the membrane surface in the donor compartment. All openings including donor top and receptor arm were occluded with parafilm to prevent evaporation. The receptor compartment was stirred at the validated speed (200 rpm). Using a glass syringe, sample volumes (1-2 mL) were extracted for UV assay and fresh preheated replacement medium of same volume was reintroduced into the receptor. Air bubbles formed below the membrane were removed by carefully tilting the Franz cells for the air bubbles to escape via the sampling arm. Intervals between sampling varied from 5 to 30 minutes. For ibuprofen, crystals were introduced into the donor with solution (~hourly) to maintain its saturated state.

5.2.6 Data Analysis

The flux and cumulative amount of the ibuprofen were plotted as a function of time. The steady state flux of ibuprofen was determined from the linear portions of the individual cumulative amount vs. time plot using linear regression analysis ($R^2 \geq 0.99$). All results were expressed as mean values ± standard deviations. The statistical difference between mean fluxes was performed using one-way ANOVA, with significance set at $p < 0.05$.

5.2.7 Comparison of ibuprofen drug release through membrane of different pore sizes and surface groups

The ibuprofen drug release through cellulose nitrate membranes of two different pore sizes, i.e. 0.1 μm and 0.45 μm were compared. While for surface group charges, the ibuprofen drug release through Biodyne B (positive charged surface groups) and Biodyne C (negatively charged surface groups) were also compared.

5.2.8 Regression analysis of ibuprofen flux with membrane parameters

The co-relationship of flux and membrane pore size, molecular weight cut-off (MWCO), and thickness (from Table 1.7 in Chapter 1) was investigated using linear regression analysis. Due to the fact that not all the membrane parameters were given by the manufacturers, such as pore size and MWCO, so only those values given were correlated with flux values.

5.3 Results

5.3.1 Drug solubility and mass balance

The average ibuprofen solubility at 25, 33, 37 and 60°C was 1.962 ± 0.002, 1.963 ± 0.002, 1.953 ± 0.001 and 2.116 ± 0.08 % w/v respectively. The ibuprofen solubility measured at these four temperatures was not statistically significant (p = 0.574). The riboflavin solubility at 25 and 37 °C was 3.09 ± 0.23 and 3.14 ± 0.09 % w/v respectively and they were also not statistically not significant (p = 0.307). The ibuprofen crystal growth was observed as needle-like structure formed in the solution when saturated solution was cooled from 60 °C to 33 °C. The pH of ibuprofen saturated solution was neutral 7.2. A typical mass balance result of ibuprofen saturated solution preparations are shown in table 5.2 below.

Table 5.2: A typical mass balance result (at 60 °C) for ibuprofen saturated solution.

Preparation #	Amount of ibuprofen added (g)	Amount remained on the filter paper (g)	Amout of ibuprofen dissolved in 50 mL (g)	Concentration, % (w/v)
1	1.657	0.616	1.041	2.082
2	1.621	0.591	1.030	2.060
3	1.637	0.579	1.058	2.116
4	1.620	0.559	1.061	2.122
5	1.767	0.746	1.021	2.042

The average of amount of ibuprofen added into the 50 mL of 0.1M sodium hydroxide for this five preparation was calculated to be 1.04 ± 0.02; while the coefficient of variation of the mass balance of these five preparations was 1.92 %. While the riboflavin mass balance (not shown) produced 2.96 ± 0.19 % w/v with coefficient of variation of 3.3 %. This typical result showed good repeatability preparations of saturated solutions.

5.3.2 Drug release across synthetic membranes

5.3.2.1 Ibuprofen

The cumulative ibuprofen drug release per unit area from saturated solutions across the various synthetic membranes over 6 hours were plotted on two separate scales shown in

Figure 5.3 (a) and (b). The flux values of ibuprofen, total drug release after 6 hours and coefficient of variation are shown in Table 5.2.

(a)

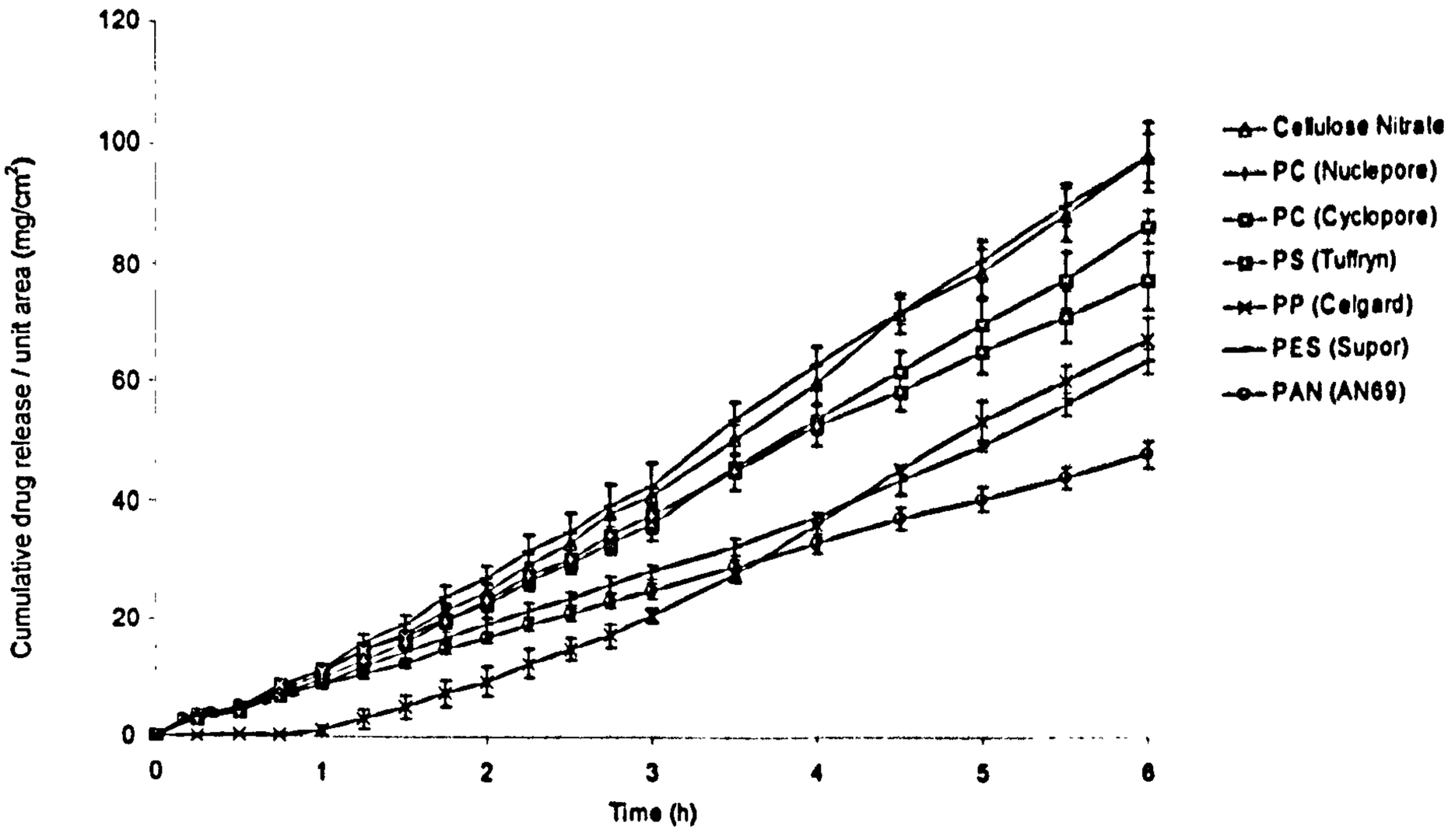

(b)

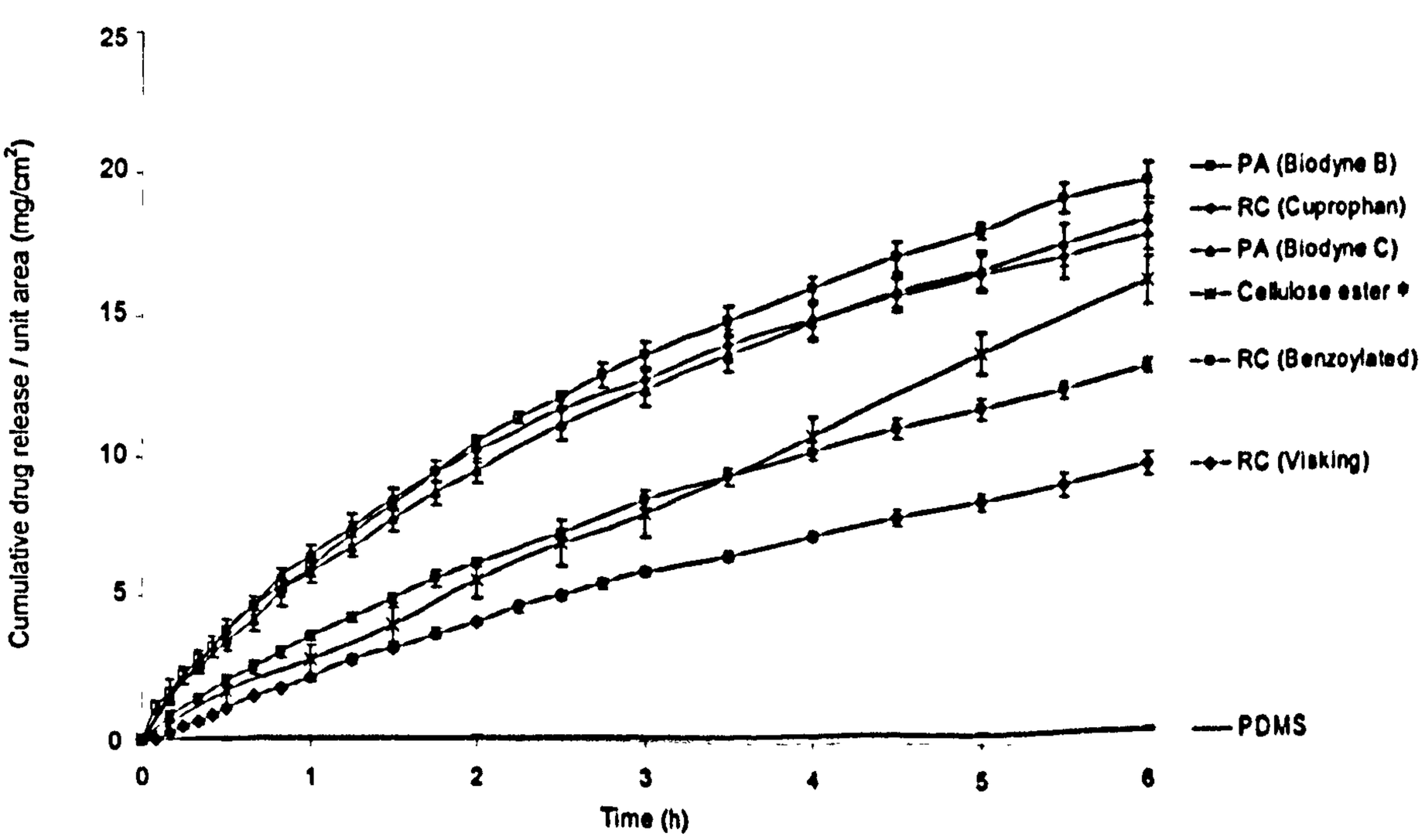

Figure 5.3: Cumulative ibuprofen release per unit area over 6 hours plots (a) high flux membranes (b) low-flux membranes. *membrane maybe unstable in the system.

Table 5.3: Summary of average ibuprofen flux from saturated solution (n = 6), total release after 6 hours and the coefficient of variation (CV) for individual synthetic membranes.

Membrane	Flux (mg/cm^2/h)	Total release after 6 hours (mg/cm^2)	CV (%)
Cellulose nitrate	17.65 ± 2.06	97.89 ± 5.79	11.7
Nuclepore	17.38 ± 0.79	97.75 ± 4.01	4.6
Celgard	15.45 ± 1.02	67.28 ± 3.66	6.6
Cyclopore	14.87 ± 0.50	86.32 ± 2.77	3.4
Tuffryn	13.54 ± 0.49	77.23 ± 4.80	3.6
Supor	10.48 ± 0.31	63.63 ± 2.08	2.9
AN69	8.14 ± 0.38	47.84 ± 2.25	4.7
*Cellulose ester	2.66 ± 0.19	16.30 ± 0.84	7.3
Biodyne B	1.96 ± 0.07	19.32 ± 0.62	3.6
Biodyne C	1.77 ± 0.17	18.44 ± 0.59	4.4
Cuprophan	1.57 ± 0.15	17.94 ± 0.69	4.7
Benzoylated cellulose	1.51 ± 0.04	13.32 ± 0.24	2.9
Visking	1.39 ± 0.09	9.88 ± 0.37	6.2
PDMS	0.09 ± 0.01	0.45 ± 0.002	6.0

* Membrane unstable in receptor fluid.

The membranes listed in Table 5.3 followed a decreased order of the ibuprofen flux. The ibuprofen flux produced ranged from the 0.09 (PDMS) to 17.65 (Cellulose nitrate) mg/cm^2/h. The coefficient of variation (CV) for all membranes ranged between 2.9 – 6.6%. However, cellulose nitrate and cellulose esters had high CVs of 11.7 and 7.2 % respectively. It was observed that the cellulose-type membranes generally produced lower flux while the polymeric-type membranes gave higher ibuprofen drug release.

5.3.2.2 Riboflavin

Similar drug release studies were repeated with riboflavin saturated solution, but only selected membranes were used. Figure 5.4 below shows the riboflavin drug release from

saturated solution through AN 69, Cuprophan, Visking, Benzoylated cellulose and cellulose ester membranes.

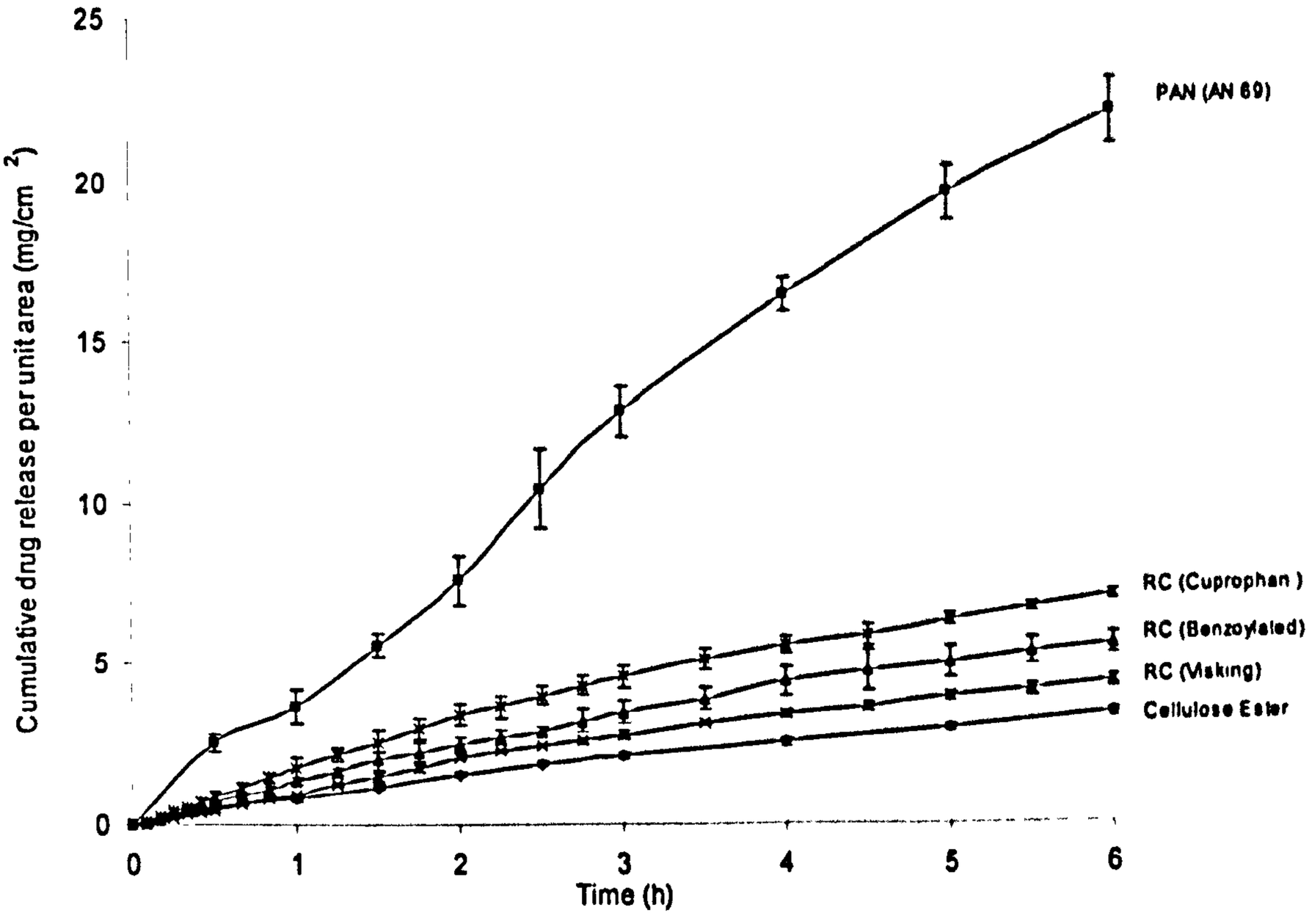

Figure 5.4: Cumulative riboflavin release per unit area over 6 hours plots

Similar trend was noted that the riboflavin fluxes across the cellulose membranes were low ranging from 0.62 to 1.14 mg/cm^2/h; while the riboflavin flux through a polymeric membrane, AN69 was approximately 6 times higher (7.66 ± 0.31 mg/cm^2/h) compared to the cellulose membranes. The average CV value for riboflavin fluxes for the cellulose membranes was 6%, but the CV for AN69 was 8.5%.

The riboflavin fluxes for Visking, Benzoylated cellulose, Cuprophan and cellulose esters were statistically significant different from the ibuprofen; but riboflavin and ibuprofen fluxes through AN69 showed no statically significant differences.

5.3.3 Correlation of flux with membrane parameters

Attempts were made to correlate the ibuprofen flux with membrane pore size, molecular weight cut-off (MWCO), and thickness. However, no direct strong correlations were found ($R^2 < 0.99$), see Figure 5.5. Note that pore sizes were correlated within high-flux membranes and MWCO were investigated within low-flux membranes.

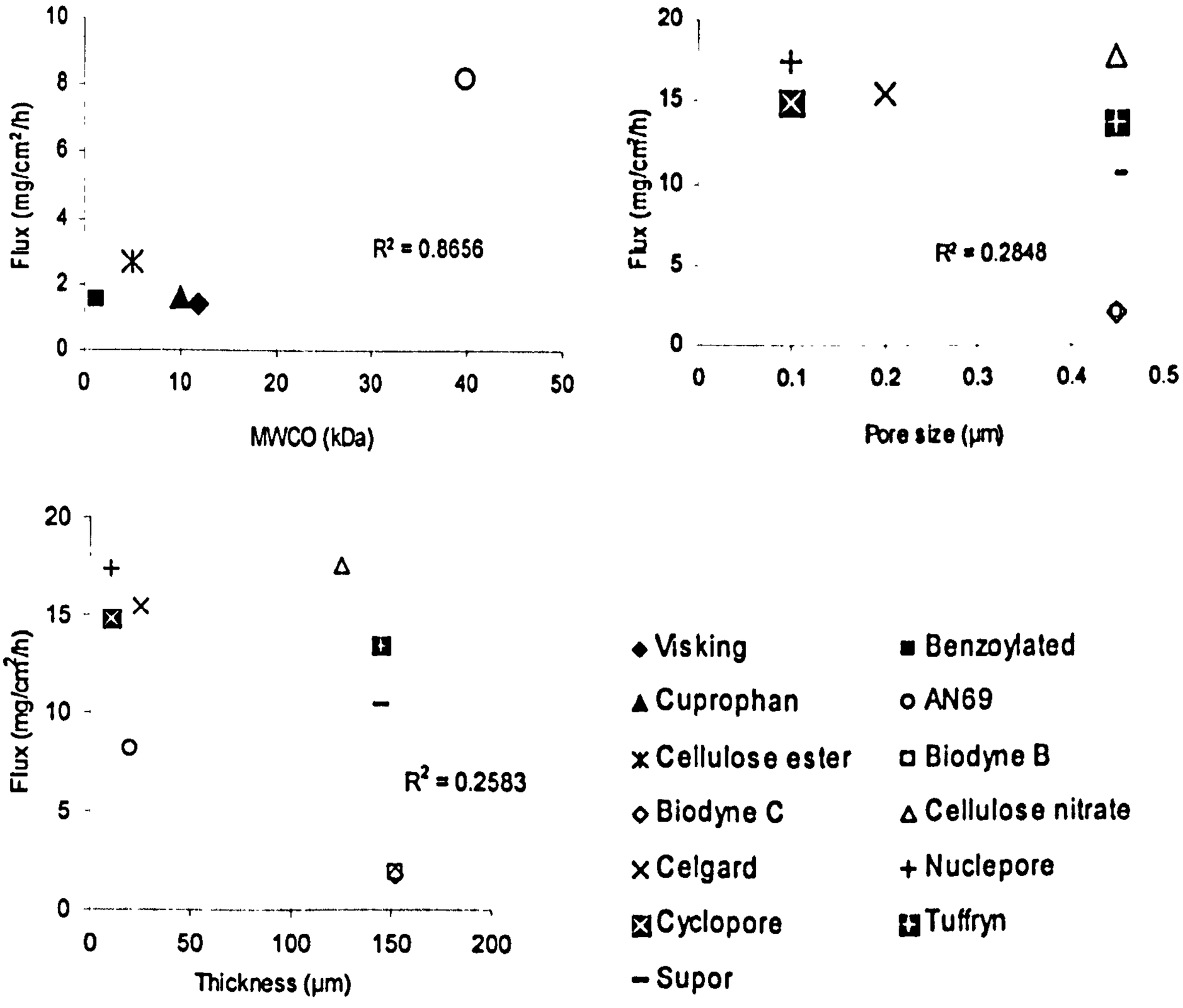

Figure 5.5: Correlation between ibuprofen flux with membrane molecular weight cut-off, MWCO, pore size and membrane thickness.

The cumulative ibuprofen drug release versus time plot through membrane of different pore sizes and surface groups are showed in Figure 5.6 (a) and (b) respectively. It was found that

there were no statistically significant between the ibuprofen fluxes when using membrane of different pore sizes or surface groups.

(a)

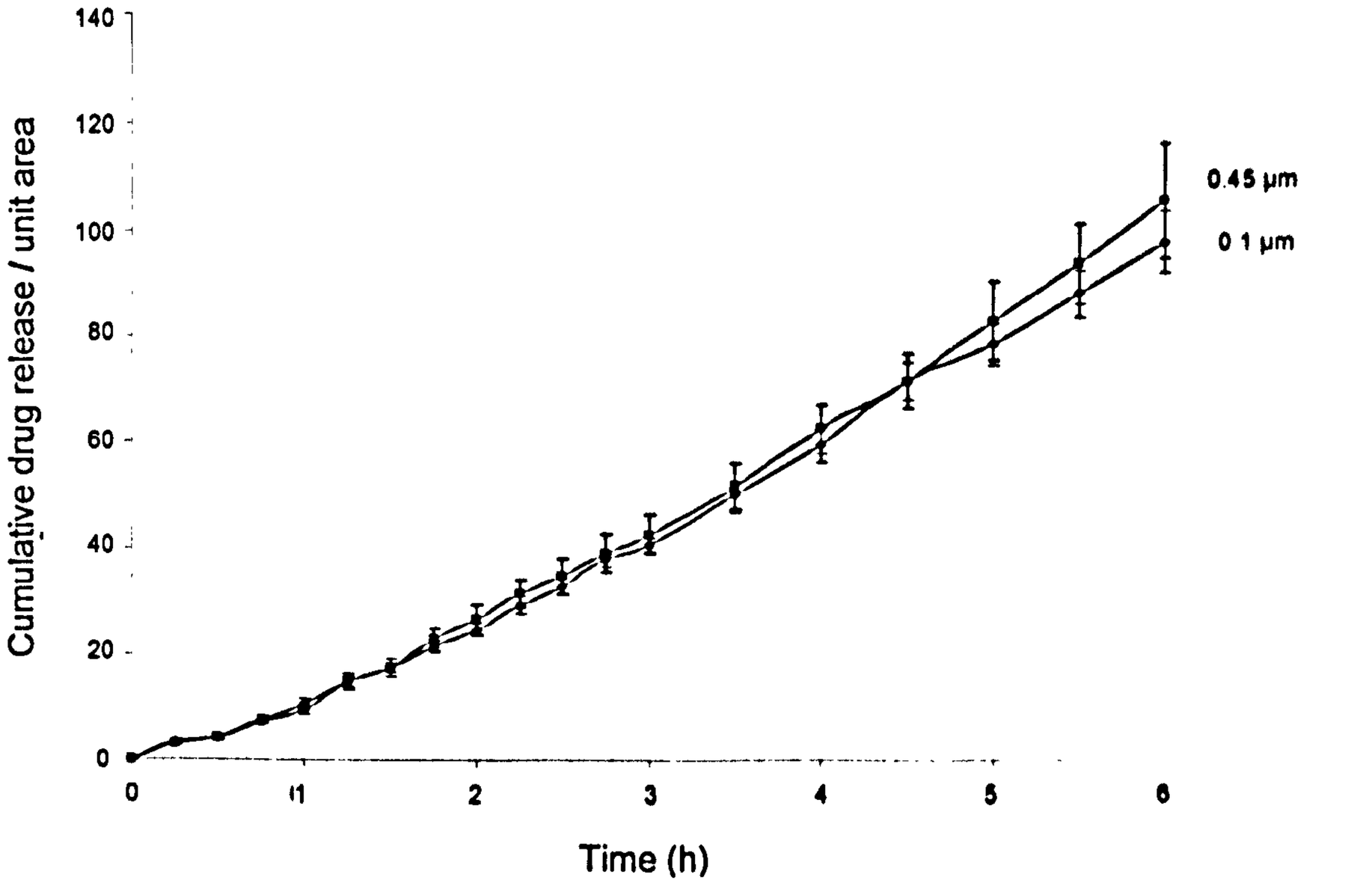

(b)

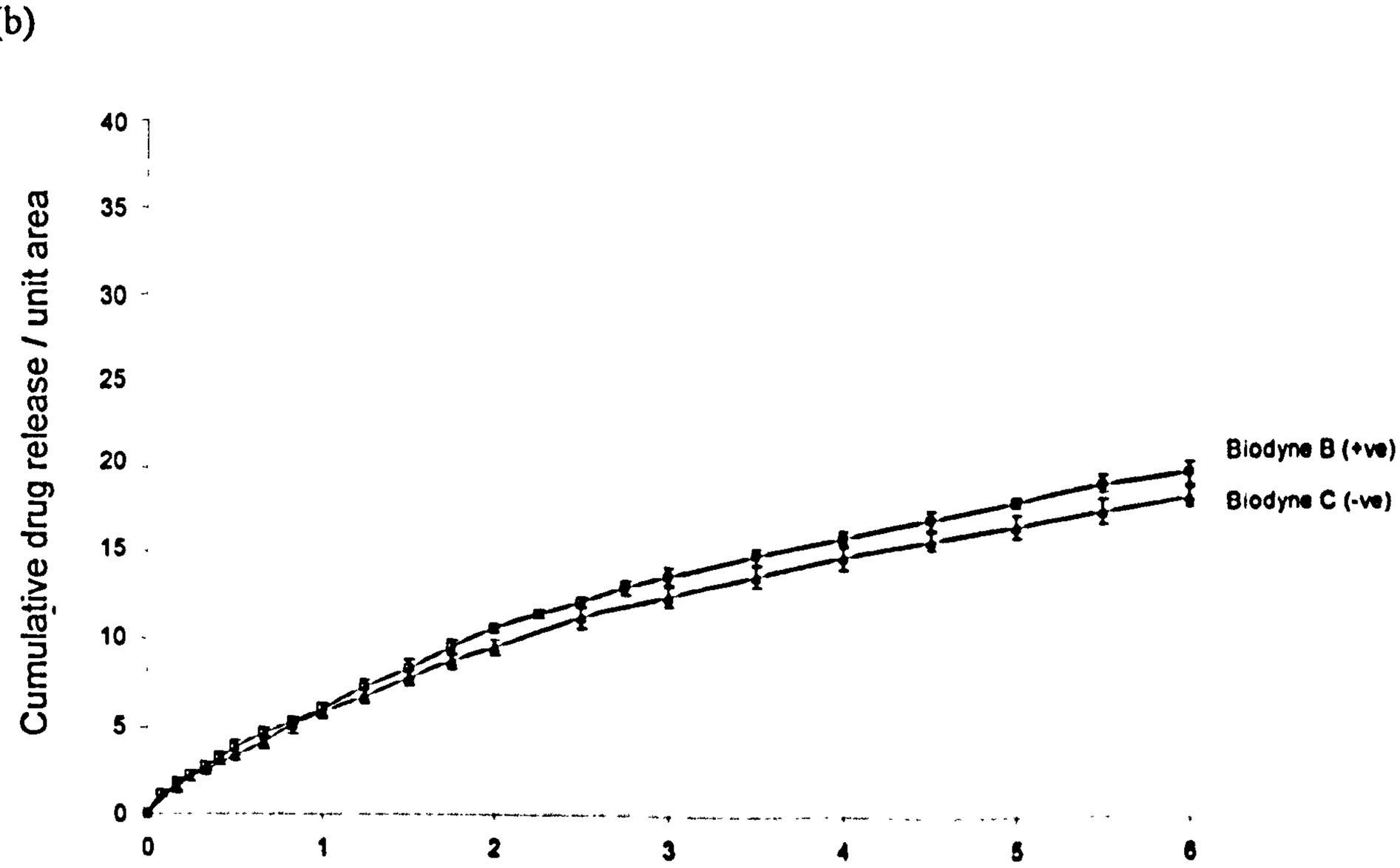

Figure 5.6: (a) Ibuprofen drug release through cellulose nitrate membrane of different pore sizes; (b) ibuprofen drug release through membrane of different membrane surface groups.

5.4 Discussion

Ibuprofen is a weak acid with the pKa of 4.5 [Avdeef *et al.*, 1999]; but when it was prepared as saturated solution in dilute alkaline 0.1M sodium hydroxide, an approximately neutral solution (pH = 7.2) was produced. Ibuprofen is a hydrophobic compound (log P = 3.4) and practically insoluble in water (< 0.1 % w/v). However ibuprofen was about 20 times more soluble in 0.1M sodium hydroxide (~2 % w/v). From the validation procedure the temperature above the membrane were measured as 31.2 ± 0.2 °C while below the membrane was 34.1 ± 0.3 °C. The consistent solubility values indicated that the thermodynamic activity of the drug should not fluctuate greatly within this temperature range.

In this Franz cell experiment, the apparatus and experimental conditions were kept constant throughout so that the synthetic membrane was the sole variable factor which affects the ibuprofen drug release. Validated Franz cell equipment was used (c.f. validation experiments, Chapter 3) and the tight data (CV 2.9 - 6.6 %) obtained in this study suggested that the methodology was robust and reproducible. During the Franz cell run, the saturated state was maintained (addition of ibuprofen crystals) over the experimentation duration to keep the thermodynamic activity constant and sink condition was maintained via frequent sampling rates (every 15 - 30 minutes). Since the experimental conditions were kept constant throughout, the differences in ibuprofen flux values obtained from the different types of membranes were related to the physical properties of the synthetic membranes. Furthermore, the thermodynamic activity was constant; the drug diffusion should be linear. So any deviation from the linearity should therefore due to membrane properties.

The data presented show that the flux varies across the different porous membranes; some of the synthetic membranes showed to be more rate-limiting to ibuprofen than the others. Different flux values produced indicated that these membranes cannot be simply acted as a support. The flux produced conveniently grouped the synthetic membranes into two plots: Figure 5.3 (a) shows a greater ibuprofen flux (8 – 18 mg/cm^2/h); while Figure 5.3 (b) shows lower ibuprofen flux (0.1 – 3 mg/cm^2/h). The former and latter are categorised as high-flux and low-flux membranes respectively in this discussion.

It was noticed that both high and low flux membranes showed a very different ibuprofen drug release profile. For the high-flux membranes, the ibuprofen rates showed linear release with time. This drug release profile adhered to the infinite dose zero-order drug release kinetics in which the flux is independent on drug concentration. For the low-flux membranes, the flux profile showed linear rate of release but also showed a slight reduction on the gradient after 3.5 hours, especially the Biodyne and regenerated celluloses. This may be due to the osmosis effect that caused slower flux from hydrophilic cellulose-based membrane (see Chapter 4).

The high-flux membranes were mainly polymeric filters membranes (used for microfiltration); while the low-flux membranes were consisted of cellulose-derived ultrafiltration membranes (Visking, Cuprophan, benzoylated celluloses) and nylon membranes. The PDMS (non-porous) ibuprofen flux measured was the lowest. In Wu's studies, four types of the membranes (out of 10) are similar to our study, namely the polysulfone, the silicone, cellulose esters and polypropylene [Wu *et al.*, 1992]. Both the studies agreed that polysulfone (pore size 0.45μm) membrane was a high-flux membrane. Apart from polysulfone, the rest of the membranes did not agree with the membrane classification in this study. This may be due to a different molecular weight drug (nitroglycerin), or poor experimental designs since there were only two replicates for each

membrane. It was also possible that different flux produced was due to the membrane properties such as pore size and thickness. But such membrane information was not reported in details in Wus' study, so this made the comparison of the two studies difficult.

An investigation was carried out on a very hydrophilic drug of similar molecular weight, (riboflavin, log P -1.4), and results showed that similar trend was observed where the cellulose membranes were categorised as the low-flux membranes while polymeric membrane (AN69) gave high riboflavin flux, thus it was a high-flux membrane. This shows that the drug log P was not an issue. Ibuprofen and riboflavin in this study did not reveal any effect of drug log P upon flux through the different synthetic membranes; further investigations were required.

To explain our data, efforts were carried out to associate the ibuprofen flux with membrane thickness, pore size and MWCO whenever applied; the pore sizes were correlated within high-flux membranes and MWCO were investigated within low-flux membranes. Nevertheless no direct correlations were established. These factors might be inter-related or combine with other parameters in affecting ibuprofen drug flux. We also reported that the pore sizes (0.1 vs. 0.45 μm) of a same membrane or different surface groups had no effect on the ibuprofen drug flux.

The underlying theory which described the transport of drug across a barrier membrane in Franz diffusion cell is the Fick's Law of passive diffusion. Hatanaka and co-workers attempted to modify Fick's Law to allow for the fact that the drug transport is via the pores, thus the tortuosity and porosity factor of a membrane were included in a modified equation Eq. 1.7 ($J = D_v.K'.\varepsilon.C_v/\tau.h$) [Hatanaka *et al.*, 1990]. If Eq 1.7 applies in this study, K', D_v and C_v were constant; so the ibuprofen flux was depended on only three variables, i.e. ε, τ, and h. The microfiltration membrane was known to have larger pore size (up to 1000 times

larger) compared to ultrafiltration membrane. If a microfiltration and an ultrafiltration membrane possess the same thickness and surface area, the ultrafiltration membrane might have a higher porosity compared to the microfiltration membranes. If porosity is the main determinant of drug flux, the ultrafiltration membranes should have higher drug flux compared to microfiltration membranes. But from this study, most of the ultrafiltration membranes were classified as low-flux membrane while microfiltration membranes as high-flux membranes. From this observation, tortuosity was thought to have a greater influence in determining drug flux. An example from this study to show that tortuosity was more dominant over porosity was Tuffryn and Supor: Tuffryn and Supor are both polysulfone membranes which possess same thickness (h = 145 μm) and similar pore size (0.45 μm). According to the manufacturer, Tuffryn has lower porosity ($\varepsilon \sim 60\%$) compared to Supor ($\varepsilon \sim 80\%$). However, the ibuprofen flux across Tuffryn and Supor were the reverse of the membrane porosity values, with Tuffryn 13.54 ± 0.49 mg/cm^2/h and Supor 10.48 ± 0.31 mg/cm^2/h respectively. So membrane tortuosity (values not provided by the manufacturer) was thought to be the factor which determined the ibuprofen flux. And from this study, it was deduced that the Supor membrane was more tortuous compared to Tuffryn.

However, when both membranes possess similar tortuosity, porosity will play a more important role in determining drug flux. This phenomenon was observed with the polycarbonates Nuclepore and Cyclopore membranes. Both of the polycarbonate membranes are manufactured via Track-etched process where the pores generated are cylindrical in shape transversing across the membrane ($\tau \sim 1$). However, the fact that Cyclopore had lower ibuprofen flux (14.87 ± 0.50 mg/cm^2/h) than Nuclepore (17.38 ± 0.79 and mg/cm^2/h) might be due to the slightly lower membrane porosity of Cyclopore (4%) compared to Nuclepore (8%).

Additional membrane support is incorporated to improve membrane integrity, but this may affect the transport across the membrane. Tuffryn and Biodyne membranes possess the same nominal pore sizes (0.45 μm) and relatively similar thickness (145-152 μm). Despite the similar physical characteristics, the Tuffryn was categorised as the high-flux membranes while Biodyne was the low-flux membranes. Tuffryn is a self-supported membrane, i.e. the membrane does not contain any additional layer or support. Biodyne membrane contains non-woven polyester support (thickness 60-90 μm; finished membrane thickness 152 ± 13 μm). This support may be the additional tortuous path for drug transport.

The presence of membrane coating is served as a protective layer for the membrane. But this coating may be barrier or hindrance of drug diffusion. Celgard possesses a proprietary coating, but specific chemical identity of the coating is protected by the manufacturer for trade secret (Hoechst). In this study, lag time (~1 hour) was observed when Celgard was employed. It was deduced that the lag time produced may be associated with this coating. The lag time showed that Celgard was not suitable for this Franz cell studies because of the present of lag time which had essentially mask the vehicle performance especially during the first hour of experiment time. One should be careful when choosing a porous membrane for Franz cell experiment, preferentially without any 'coating' or additional 'physical layer'.

AN69 is an improved haemodialysis membrane and is well known for its high permeability because it is very thin compared to the conventional cellulosic dialysis membranes [Chenoweth *et al.*, 1983]. AN 69 has been categorised as the high-flux membrane in haemofiltration context [Bellomo and Ronco, 2001]. The same trend was obtained in this Franz cell study in which the AN69 produced higher ibuprofen flux compared to the celluloses membranes. As a result it was grouped as a high-flux membrane in Franz cell drug release investigation.

The regenerated cellulose (Visking, Cuprophan, Benzoylated cellulose) and cellulose acetate were classified as low-flux membranes. Cellulose nitrate was an exceptional cellulose derivative which was high-flux. Unlike the other cellulose-modified membranes, ibuprofen drug flux across the cellulose nitrate was very rapid (17.65 ± 2.06 mg/cm^2/h) and statistically not significantly different from Nuclepore. Assuming all cellulose-type membranes possesses similar tortuosity, the rapid ibuprofen flux across cellulose nitrates was due to its high porosity cellulose nitrate membrane (66-84%).

Among the low-flux cellulose membranes, cellulose acetate produced the highest ibuprofen flux. It was found that the cellulose acetate used in this study was not compatible with the receptor fluid; the membrane is only stable in pH 3-8 while the receptor fluid (0.1M sodium hydroxide) has pH of 12. It was likely that the membrane integrity had been weakened and ibuprofen transport across the membrane became less resistant. This may also explain such a high CV (7.3%) was obtained. Consequently, the investigator should always very caution when choosing a membrane which is compatible with the receptor media especially if the experiment time is very long and the membrane must be able to withstand long exposure to chemical solvent.

Although Visking, Cuprophan and Benzoylated are regenerated celluloses, the ibuprofen fluxes generated were different. Among the three cellulose membrane, Cuprophan gave the highest flux, followed by Benzoylated tubing then Visking. Cuprophan is an ultrathin cellulose membrane produced via cuproammonium process; ibuprofen passed through Cuprophan is therefore the quickest. Ibuprofen diffused through the Benzoylated cellulose at a faster rate compared to Visking. This was because Benzoylated is relatively hydrophobic compared to Visking due to the presence of benzoyl groups on the surface.

An apparent slowing down of ibuprofen flux was observed (Figure 5.3) through cellulose (Visking, Cuprophan and Benzoylated) and Biodynes approximately after 3.5 hours. The flux retardation through theses low-flux membranes maybe due to the fact that osmosis had occurred (c.f. Chapter 4) or perhaps the ibuprofen drug had 'caked' above the membranes (because the flux is low) which may block the pores of the membrane thus slowing down the drug diffusion.

PDMS is an isotropic polymer widely used as an alternative model barrier for prediction of drug permeation across skin [Cronin *et al.*, 1998]. The drug release across PDMS follows Fick's law and possesses hydrophobic properties like skin, so making it a good model for the stratum corneum. Here, the PDMS produced the lowest ibuprofen flux. This was because the PDMS matrix is limiting the drug diffusion process. This indicates that PDMS was not suitable for formulation investigation because it can limit the drug permeation which masks the formulation vehicle effect. In constrast, cellulose nitrates and Nuclepore were found to be the least rate limiting for ibuprofen so they are both suitable for formulation screening which contained ibuprofen.

5.4 Conclusions

The conclusions from this study were:-

1. The synthetic membranes employed in this study are commonly found membranes in the literature. The synthetic membranes were categorised as high and low flux membranes according to the rate of ibuprofen drug release over 6 hours. The membrane groupings were similar for both hydrophobic (ibuprofen) and hydrophilic (riboflavin) drugs tested.
2. The high flux membranes were generally microporous membranes while the low flux membranes were ultrafiltration membranes.

3. The ideal high flux membrane for formulation analysis should have high porosity (>60%), tortuosity of 1, and be relatively thin (~ 10 μm). It was found that membranes for microfiltrations were preferred for Franz cells studies compared to membrane of other applications.
4. Non-porous membranes are not suitable for quality control purposes.
5. Membranes with coatings were not favourable. If the membrane contained filler support, the investigator must be caution that the filler support should not have an effect on drug flux.
6. Other factors to consider are the compatibility of the membrane with the donor and the receptor component as well as the cost effective of the membranes.
7. Although there are various types of commercial 'porous' membrane available in the market, each type may produce different drug release properties.
8. All in all, investigators must show caution when choosing the most appropriate membrane to be used with Franz cells for quality control.

CHAPTER VI

EVALUATION OF PARABEN SERIES DRUG RELEASE ACROSS THREE MODEL SYNTHETIC MEMBRANES

6.1 Introduction

Parabens are esters of *p*-hydroxybenzoic acids. There are several members of the paraben family, each with different alcohols esterified to *p*-hydroxybenzoic acid; methyl, ethyl, propyl, and butyl derivatives are commonly available. These compounds have a wide spectrum of anti-microbial activity and are often incorporated in pharmaceutical and cosmetics products as preservatives [Pharmaceutical Codex, 1994]. The chemical structures of the parabens are shown in Figure 6.1 below.

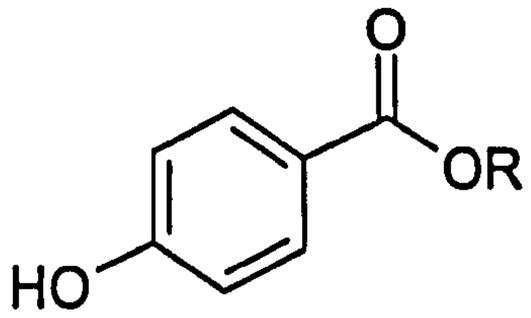

Methylparaben, R = CH_3
Ethylparaben, R = C_2H_5
Propylparaben, R = C_3H_7
Butylparaben, R = C_4H_9

Figure 6.1: Chemical structure of p-hydroxybenzoates.

Paraben esters are relatively lipophilic compounds with Log P values ranges from 2.0-4.0 [Hansch *et al.*, 1995]. As the number of the carbons in the ester increases, the hydrophobicity of the molecule increases. The aqueous solubility of these compounds is generally low and is inversely related to the number of carbons in the ester. Table 6.1 shows the physical characteristics summary of the parabens.

Table 6.1: The physical properties of methylparaben (MP), ethylparaben (EP), propylparaben (PP) and butylparaben (BP).

	MP	EP	PP	BP
Molecular Formula	$C_8H_8O_3$	$C_9H_{10}O_3$	$C_{10}H_{12}O_3$	$C_{11}H_{14}O_3$
Molecular weight	152.15	166.18	180.20	194.23
Melting point (°C)	131	117	97	68.5
Log P (octanol-water) [a]	1.96	2.47	3.04	3.57

[a] Hansch *et al.*, 1995

It has been established that the drug lipophilicity and molecular weight are important factors in predicting skin permeability [Potts and Guy, 1992]. Synthetic membranes are used as a *in vitro* model for skin mimicry and for product regulatory studies. Investigations on the effect on drug lipophilicity on permeation rate across PDMS, a hydrophobic synthetic membrane which often use for skin simulation found that the flux across PDMS increased with increased drug hydrophobicity [Twist and Zatz, 1986]. Ideally, the membrane for quality control should have the least minimal drug binding capacity and only to separate the formulation and receptor medium. However there are studies that show that drug compounds can adsorb onto synthetic membrane. Bin and co-workers have demonstrated that parabens adsorbed onto hydrophobic porous filters via hydrophobic interactions [Bin *et al.*, 1999b]; they also found out that benzalkonium chloride, a quarternary ammounium compound adsorbed the most onto membrane with negative-charged surface [Bin *et al.*, 1999a]. In Chapter 5, we also reported that although riboflavin, a highly hydrophilic drug (log P -1.4) shows similar high- and low-flux membrane characterisation as ibuprofen (log P 3.4), the ibuprofen and riboflavin fluxes within the low-flux membranes were found to be different ($p < 0.05$). This suggests that log P may play a vital role in affecting drug flux. A wide range of porous synthetic membranes are available for quality control use and the membrane can be hydrophilic (e.g. regenerated cellulose, cellulose ester) or

hydrophobic (e.g. polyacrylonitrile, polyamide) in nature. It is crucial that the synthetic membrane property is suitable for the drug being investigated and drug log P was thought to be one of the factors.

Changing the vehicle properties was a common approach in increasing drug solubility as well as skin permeability. Miglyol® 812 and Capmul® MCM C8 are two common pharmaceutical excipients incorporated into formulations to increase the solubility of poorly water soluble drugs. These medium chain glycerides have been used as a solubilising and dispersing agents for poorly water soluble compounds to improve oral absorption and skin penetration from topical creams and lotions products [Kaukonen *et al.*, 2004; Porter *et al.*, 2004; Roy *et al.*, 1995]. The former is a medium-chain triglyceride consists of mixed triglycerides of saturated fatty acids with chain length of 8 and 12 carbons. Capmul® MCM C8 is a mixture of mono- and diglycerides of medium chain fatty acids [ABITEC Corp., ABITEC Corp.ABITEC Corp.,]. The chemical formulae of Miglyol and Capmul are shown in Figure 6.2. The solubility of hydrophobic drugs such as parabens can be increased by formulating them in Miglyol and Capmul.

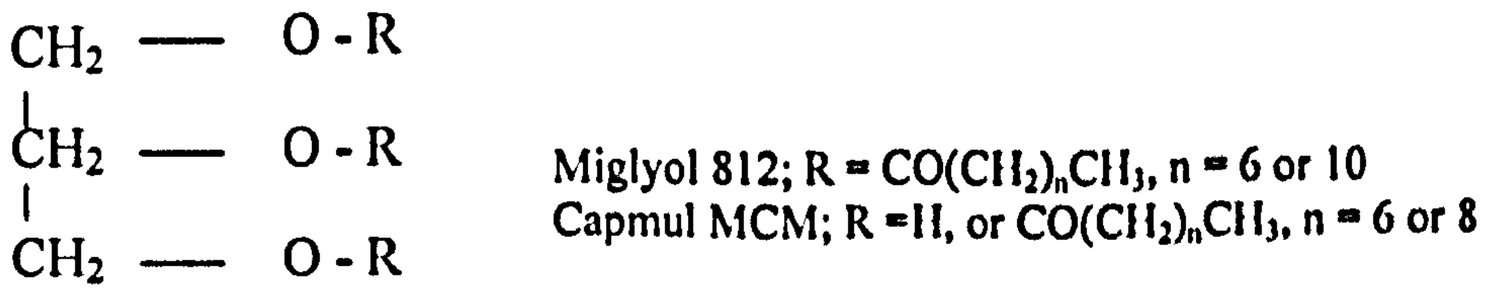

Figure 6.2: The chemical formula of Miglyol 812 and Capmul MCM.

6.1.1 Aims of study

In this study, the increased log P values of the parabens series were utilized to study the effect of drug log P upon flux from simple aqueous PBS saturated solution through three synthetic membranes, namely Visking, Biodyne and PDMS membrane. Both Visking and Biodyne

membranes are porous; the former is hydrophilic while the latter is hydrophobic in nature. PDMS is a non-porous hydrophobic membrane. Table 6.2 summarised the characteristics of the three membranes.

Table 6.2: Summary of characteristics of Visking, PDMS (polydimethylsiloxane) and Biodyne membrane.

Membrane	Type	Thickness[1] (μm)	Nominal pore size[1] (μm)	Nature
PDMS	Non-porous	400	na	Hydrophobic
Visking	Porous	20	na	Hydrophilic
Biodyne	Porous	152	0.45	Hydrophobic

na: not applicable

In addition, this study also aimed to evaluate the effect of increasing paraben solubility in oily vehicle upon drug release through these membranes and to compare the drug release from oily saturated solutions and aqueous PBS saturated solution through dense hydrophobic PDMS membrane and porous hydrophilic Visking membrane. This work was carried out at the GlaxoSmithKline, Pharmaceutical Development site in Harlow (UK). Due to the time constrains, the four parabens were formulated as a mixture in a solution rather than using four individual parabens solutions. Nevertheless, preliminary studies of these 'mixed' parabens were performed to demonstrate that parabens mixure was suitable for this study.

6.2 Methods

6.2.1 Mixed parabens - Preliminary Investigation

The following described the preliminary studies undertaken to validate the mixed paraben prior to Franz cell studies. Firstly, the validation of the HPLC procedure was carried out upon single parabens and paraben mixture. Secondly, the saturated solubility of the paraben mixture as well as of each individual parabens was determined.

6.2.1.1 HPLC

Chromatographic measurements were carried out using a Perkin-Elmer series 200, LC pump with Autosampler connected to a UV absorbance detector 759A (Applied Biosytems, USA). The HPLC procedure for parabens was developed by GSK, Harlow. The chromatographic conditions were as follows: Symmetry® ODS C18 (4.6 x 150 mm, 3.5 μm) column with mobile phase comprising acetonitrile/water (45:55 v/v). The aqueous phase contained 0.1% trifluoroacetic acid. The mobile phase was deaerated using Degasser CSI6150 (Cambridge Scientific Instrument) and the column was heated using Perkin-Elmer 200 peltier column oven to 40°C. The flow rate and injection volume were set at 1 mL/min and 5 μL. The wavelength of detection was set at 256 nm for all parabens. The chromatograms peaks were integrated using computer (Empower) software.

6.2.1.2 HPLC validation of single and mixed paraben

HPLC validation was carried out on single and mixed parabens. The paraben standards of concentration 0.02% w/v were prepared as follows: 2 mg of each paraben was weighed and dissolved in 10 mL of acetonitrile/water (50:50 v/v). For the single parabens standards, each paraben was dissolved in separate 10 mL volumetric flasks; while for mixed paraben, all four parabens (2 mg of each) were dissolved in one 10 mL flask. Hence there were five standards in total, namely the methyl-, ethyl-, propyl-, butyl- and mixed parabens. The standards were subjected to HPLC analysis and the retention times for each parabens were noted.

6.2.1.3 Preparation of mixed parabens calibration standards

A series of standard calibration solutions of mixed parabens, methylparaben, ethylparaben, propylparaben and butylparaben were prepared as follows: 20 mg of each paraben were weighed (total of 80 mg for four parabens) and dissolved in 100 mL of acetonitrile/water (50:50 v/v), making a stock solution of 0.20% (w/v). Five concentrations, i.e. 0.16, 0.12, 0.08, 0.04, and 0.02

% (w/v) were subsequently prepared from the stock solution by appropriate dilution with acetonitrile/water (50:50 v/v). The six calibration solutions were analysed by HPLC. Calibration curves of peak area for each paraben were plotted against concentration and the linearity was checked with linear regression correlation coefficient (r^2).

6.2.1.4 Paraben solubility studies

(i) Preparation of paraben saturated solutions

The saturated solution of mixed parabens in aqueous phosphate buffer solution (PBS) was prepared by weighing approximately 500 mg of each paraben into a bottle containing 50 mL of aqueous PBS solution, making a concentration of approximately 10 mg/mL for each paraben. The saturated oily solution in Miglyol was prepared by adding approximately 4 g of each parabens to 20 mL of Miglyol producing a suspension of concentration 200 mg/mL. Capmul had higher paraben solubility, so a higher concentration (250 mg/mL) was prepared as follows: 5 g of each paraben was added into 20 mL of Capmul. The saturated solutions were stirred overnight on the roller mixer. The powder clumps formed were dispersed by vigorous shaking. The saturated solutions of individual parabens were prepared with similar concentration as the mixed parabens, except that they were prepared separately as four saturated solutions instead of one saturated mixture.

(ii) Determination of paraben solubility

The saturated solubility of individual and mixed parabens solution (aqueous and oily vehicle) was determined. The solubility was determined as follows: 0.4 mL of the paraben suspension was filtered by centrifuging the sample in a Vectaspin microtube with 0.2 µm polysulphone filters at 10,000 rpm for 5 min. The filtrate was diluted 1 in 10 with acetonitrile/water (50:50 v/v) and subjected to HPLC analysis.

6.2.2 Membrane partition coefficient

The partition coefficient of parabens in the three model synthetic membranes, namely PDMS, Visking and Biodyne were determined. The suspension of the mixed parabens in PBS was filtered with 0.2 μm syringe filters. The filtrate (a clear solution) was diluted 1 in 10 in PBS and 2 mL of the resulted mixture was pipette into a clear vial. The membrane was then accurately weighed (about 100 mg for PDMS and 10 mg for Visking and for nylon) and placed into the vial with the 2 mL of solution contained mixed parabens. The samples were allowed to stir on the roller mixer for at least 3 days at 25°C. A vial filled with test solution with no membrane was set as reference. Then, the membranes were removed from the saturated solution. The concentration of the parabens in aqueous PBS was assayed using HPLC. The partition coefficient of paraben for each membrane was determined by the ratio of the amount present in the membrane in % w/w (by subtraction) to the final amount of solute left in the solution after mixing. The determinations were performed in triplicate for each membrane as well as the reference.

6.2.3 Franz diffusion cell experiments

The Franz cell studies were conducted in GlaxoSmithKline (Harlow). The Franz diffusion cell apparatus used in this study were described in Chapter 2, section 2.3 (set 3). All parabens drug release investigated in this study was undertaken on mixed paraben saturated solution. Firstly, the mixed paraben drug release from aqueous PBS saturated solution through the three membranes (Visking, Biodyne and PDMS) was investigated. Then the mixed paraben drug release from saturated solution aqueous PBS and oily phases (Miglyol and Capmul) were compared, with PDMS as model membrane. Finally, the mixed paraben drug release from Capmul saturated solution through PDMS was compared with that through Visking.

1 mL of mixed paraben saturated solution (with suspended solids) was loaded onto the donor while the receptor was filled with appropriate receptor fluid which was previously de-aerated.

Deaeration of receptor fluid was performed by means of warming up the fluid to 37 °C and maintained at the same temperature overnight prior to use. The synthetic membranes were cut into circular discs and placed between the donor and the receptor compartments of the Franz cell. The membranes were previously soaked with PBS for at least 12 hours to hydrate and displace entrapped air in the membrane. The donor top was occluded with parafilm. The temperature of the receptor phase was maintained at 37 °C with water jacket circulation from a heated water bath. A small PTFE stirrer was incorporate into the receptor phase for stirring to ensure event heat and drug distribution. Samples were withdrawn from the centre of receptor using a plastic syringe. Gentle flushing was performed using the syringe while sampling aided the mixing of receptor phase. After sampling, the receptor compartment was immediately re-filled with fresh receptor fluid which was previously heated at 37 °C. Care was taken to remove air bubbles trapped below the membrane. Samples collected at time 0, 0.5, 1.0, 1.5, 2.0, 2.5, 3.0, 4.0, 5.0 and 6.0-h were assayed using HPLC. No crytal was placed into the donor to replenish the saturated state.

6.2.4 Data analysis

The concentrations of each parabens were derived from the HPLC chromatogram. The cumulative amount of each paraben diffused per unit area ($\mu g/cm^2$) were calculated and plotted against time. The linear portion of the plot was taken as being the steady state flux (J). All the obtained permeation rates were determined as an average of six diffusion cells.

6.3 Results

The mixed parabens saturated solution in PBS appeared as white solids suspended in a clear solution. The white suspended solid caked at the bottom of the container immediately on standing but could be resuspended when agitated. The saturated parabens prepared in Miglyol® 812N and Capmul® MCM C8 appeared as opaque oily solution with white suspended solid.

6.3.1 HPLC validation

The HPLC validation showed that the parabens retention times were similar for both mixed and single paraben standards (Table 6.3). The parabens have a retention time of 2.7, 3.5, 5.0 and 7.5 mins for methylparaben, ethylparaben, propylparaben and butylparaben respectively.

Table 6.3: The HPLC retention time for single and mixed paraben preparation.

Paraben	Retention time (min)	
	Single	Mixed
Methyparaben	2.65	2.64
Ethylparaben	3.46	3.45
Propylparaben	4.93	4.93
Butylparaben	7.51	7.55

A typical chromatogram of a standard of saturated mixed parabens is shown in Figure 6.2.

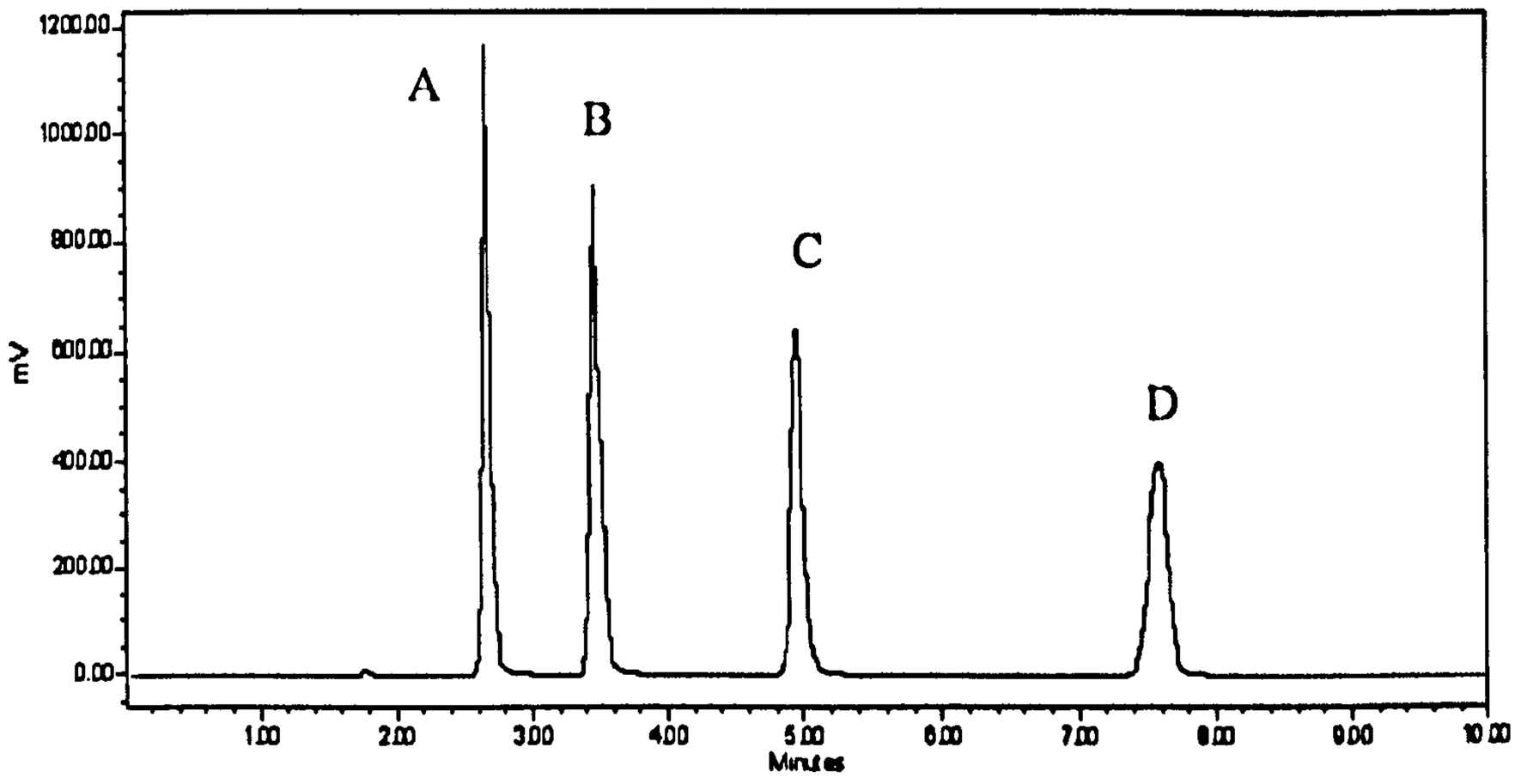

Figure 6.2: A typical HPLC chromatogram displaying peaks of mixed parabens - Methyl- (A), Ethyl- (B), Propyl- (C) and Butylparaben (D).

Although the parabens were prepared as a mixture, the HPLC method developed were able to distinguish the parabens and yield four distinct peaks on the chromatogram.

The standard calibration lines of the HPLC peak area versus concentration for the four parabens prepared as a mixture are shown in Figure 6.3. The calibration standards yield straight lines for all parabens from 0.02 to 0.2 % w/v. The regression correlation coefficient (r^2) showed >0.999 for all parabens.

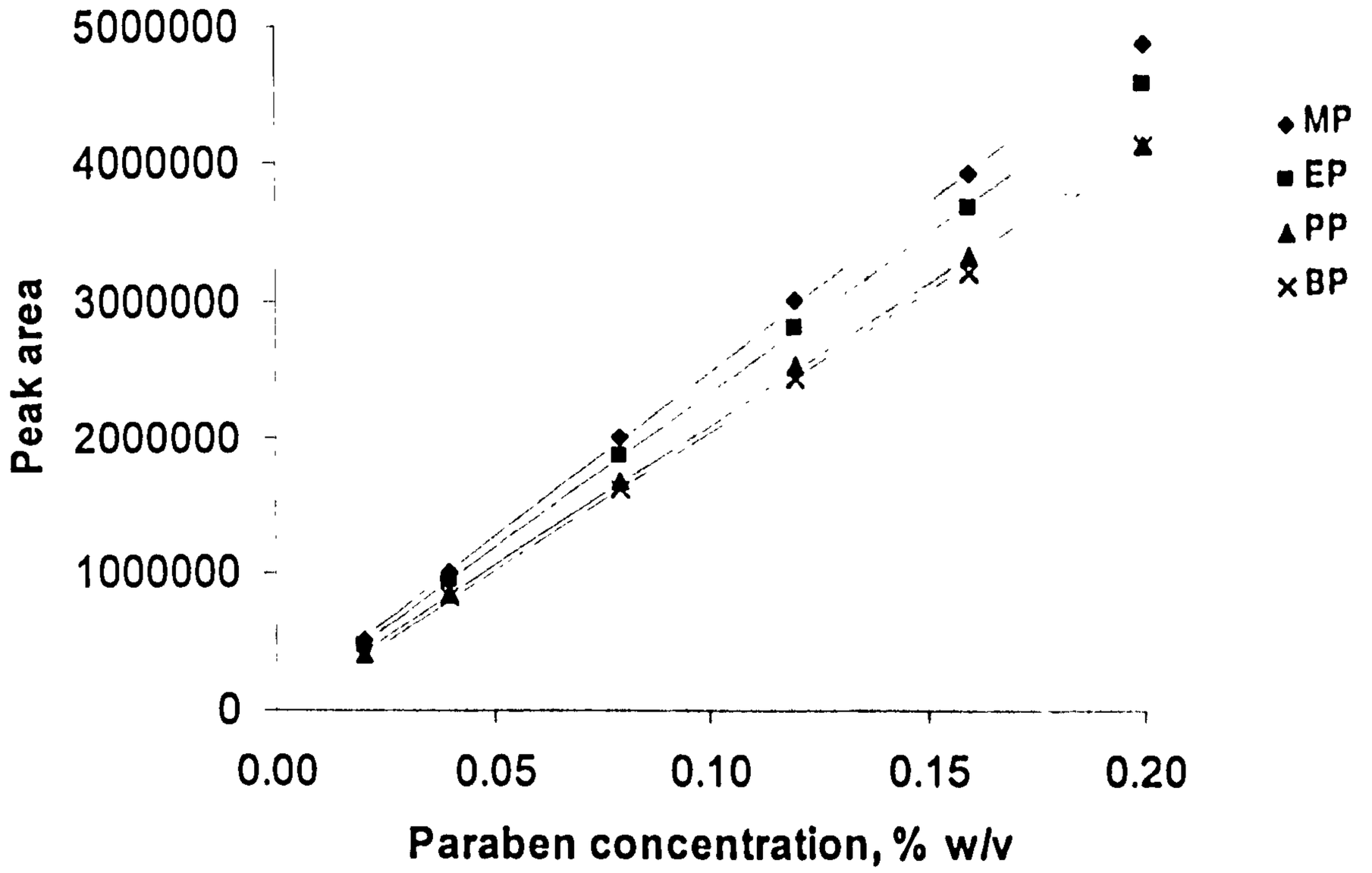

Figure 6.3: The typical calibration line for methylparaben (MP), ethylparaben (EP), propylparaben (PP) and butylparaben (BP) in mixed parabens.

The solubilities of paraben esters in PBS, Miglyol®, Capmul® and water formulated as single component and mixtures are showed in Table 6.4.

Table 6.4: Solubility of parabens as single preparation and as mixture in PBS, Miglyol® and Capmul® ($n \geq 2$, CV<4%). (MP-methylparaben, EP-ethylparaben, PP-propylparaben, BP-butylparaben)

Vehicle	Solubility, mg/mL				Solubility in mixture, mg/mL			
	MP	EP	PP	BP	MP	EP	PP	BP
PBS	2.03	0.83	0.31	0.16	1.97	0.65	0.15	0.12
Miglyol®	33.45	40.39	51.45	117.32	47.02	47.65	42.98	155.47
Capmul®	121.04	124.62	154.09	281.97	99.69	94.52	83.28	158.92
Water[a]	2.45	0.96	0.39	0.20	2.56	0.88	0.20	0.21

[a] Experimental values obtained from Giordano *et al.*, 1999

The solubility of parabens was generally higher in the oily phases (Miglyol and Capmul) as compared to the aqueous phase (PBS). The solubility of the four parabens in PBS was low and comparable with water. When compared the paraben solubility between single and mixture preparations, the propylparaben solubility was constantly lower in mixed parabens preparation for all vehicles; while there was increase or decrease for methylparaben, ethylparaben and butylparaben solubilities.

6.3.2 Membrane partition coefficients

An assumption was made in which the drug distribution between the membrane and solution had reached equilibrium after 3 days of mixing. The paraben partition coefficient in PDMS, Visking and Biodyne are shown in Table 6.5.

Table 6.5: Partition coefficient of PDMS, Visking and Biodyne membrane. (MP-methylparaben, EP-ethylparaben, PP-propylparaben, BP-butylparaben)

Paraben	Partition coefficient		
	PDMS	Visking	Biodyne
MP	0.39 ± 0.01	1.81 ± 1.06	21.66 ± 0.84
EP	1.08 ± 0.02	1.41 ± 0.64	39.33 ± 1.12
PP	3.22 ± 0.27	0.71 ± 0.77	88.63 ± 2.77
BP	11.60 ± 0.21	0.63 ± 0.71	200.44 ± 8.35

The relationship between partition coefficient of the three types of membranes and the alkyl group chain length was plotted in Figure 6.4 below.

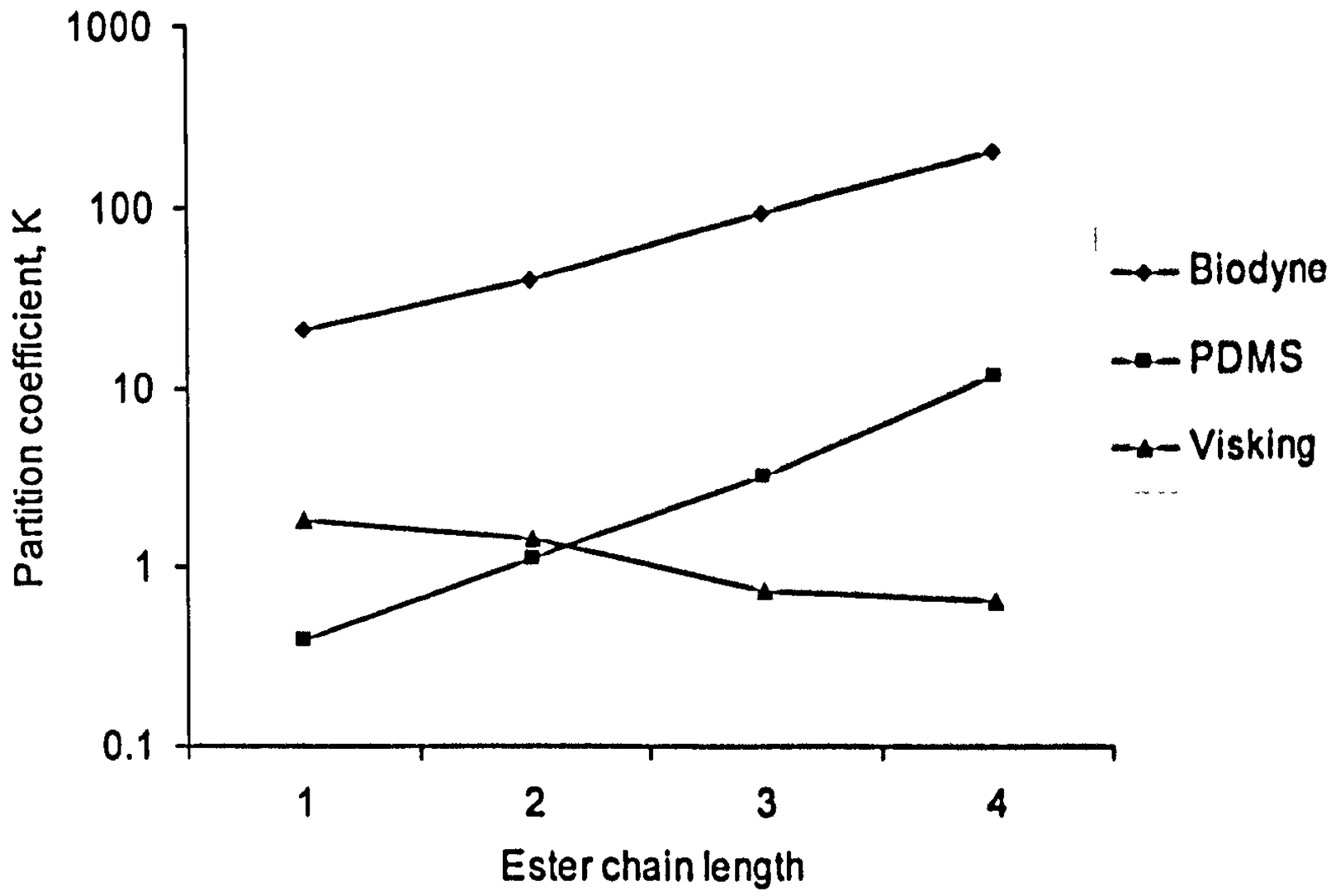

Figure 6.4: The membrane partition coefficient- paraben carbon number length plot.

6.3.3 Parabens flux through various synthetic membranes

6.3.3.1 Permeation profile of parabens from PBS across Visking, Biodyne and PDMS

The cumulative parabens release profile from PBS through PDMS, Visking and Biodyne was plotted in Figure 6.5 (a)-(d) below. The average flux values were tabulated in Table 6.6.

(a)

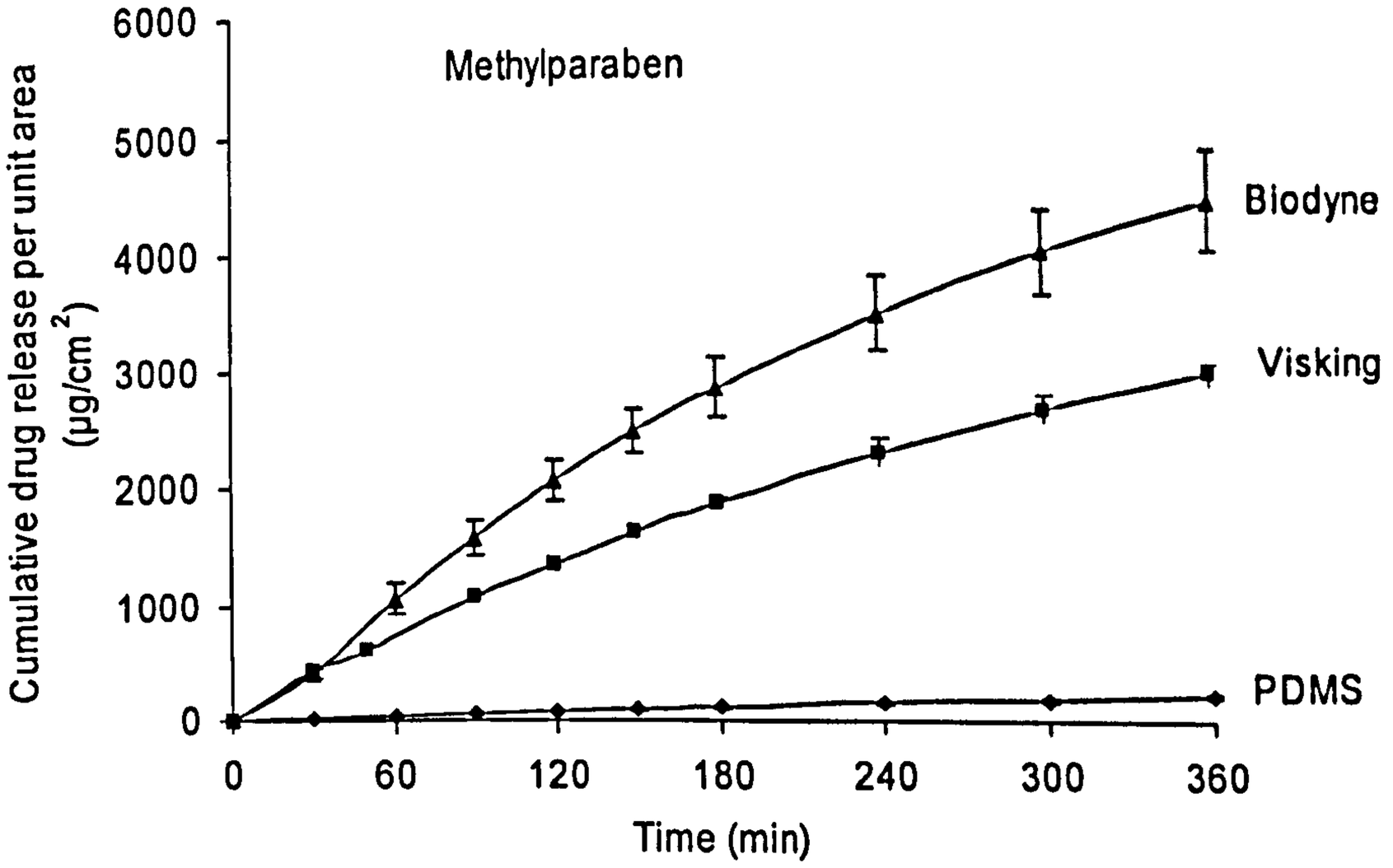

(b)

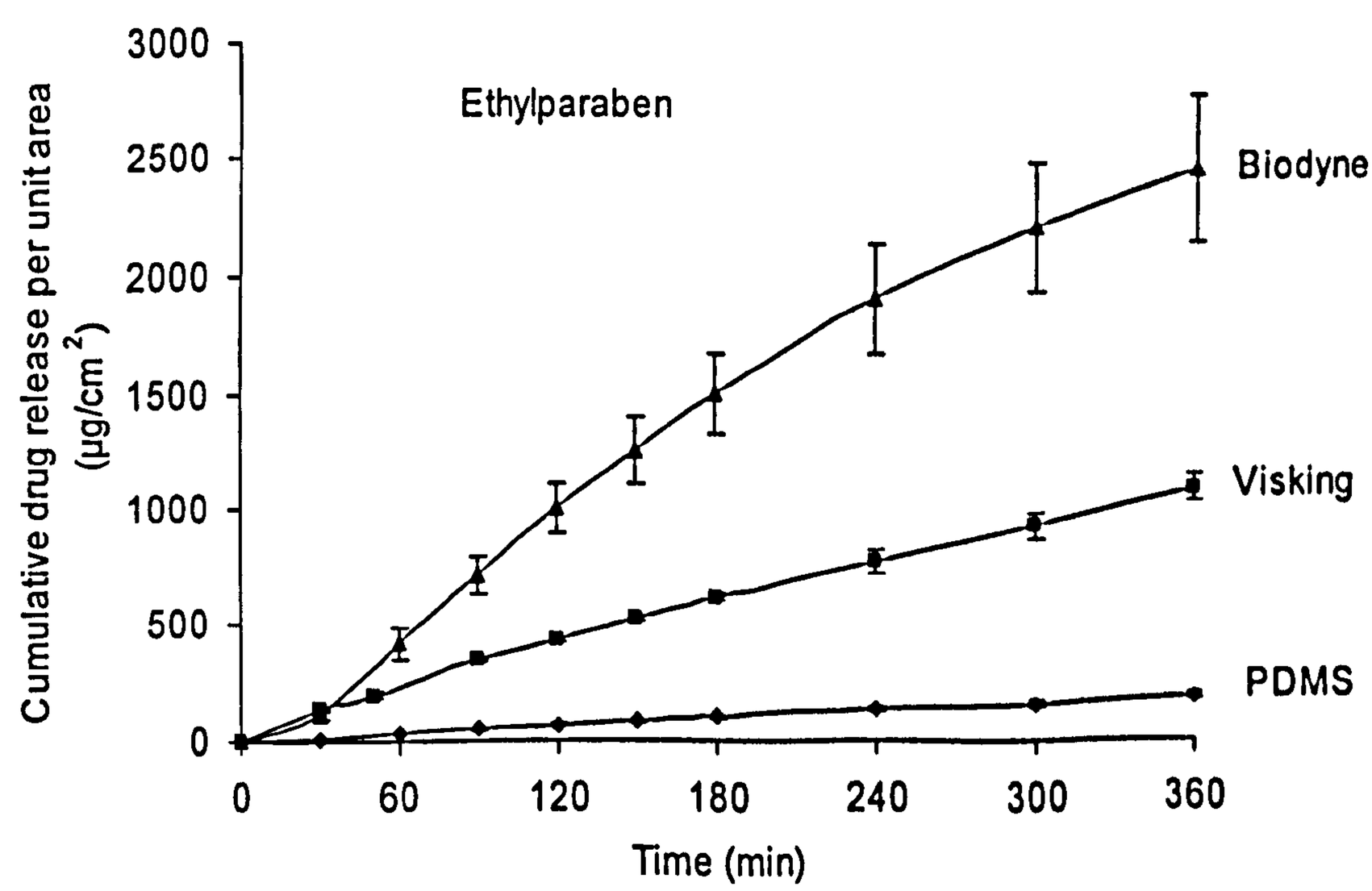

Figure 6.5: Cumulative mass per unit area plots against time of parabens across Biodyne, Visking and PDMS membranes.

(c)

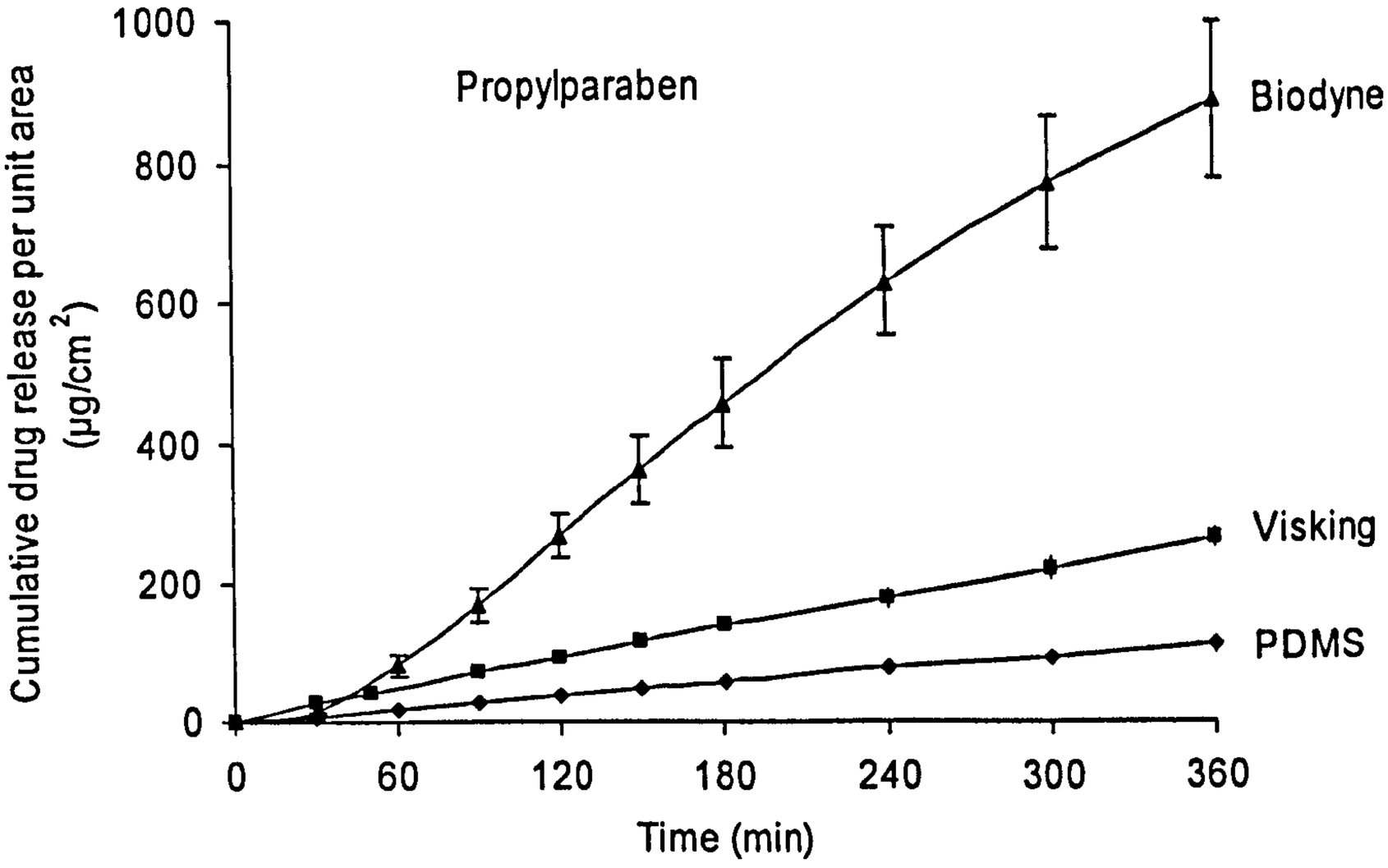

(d)

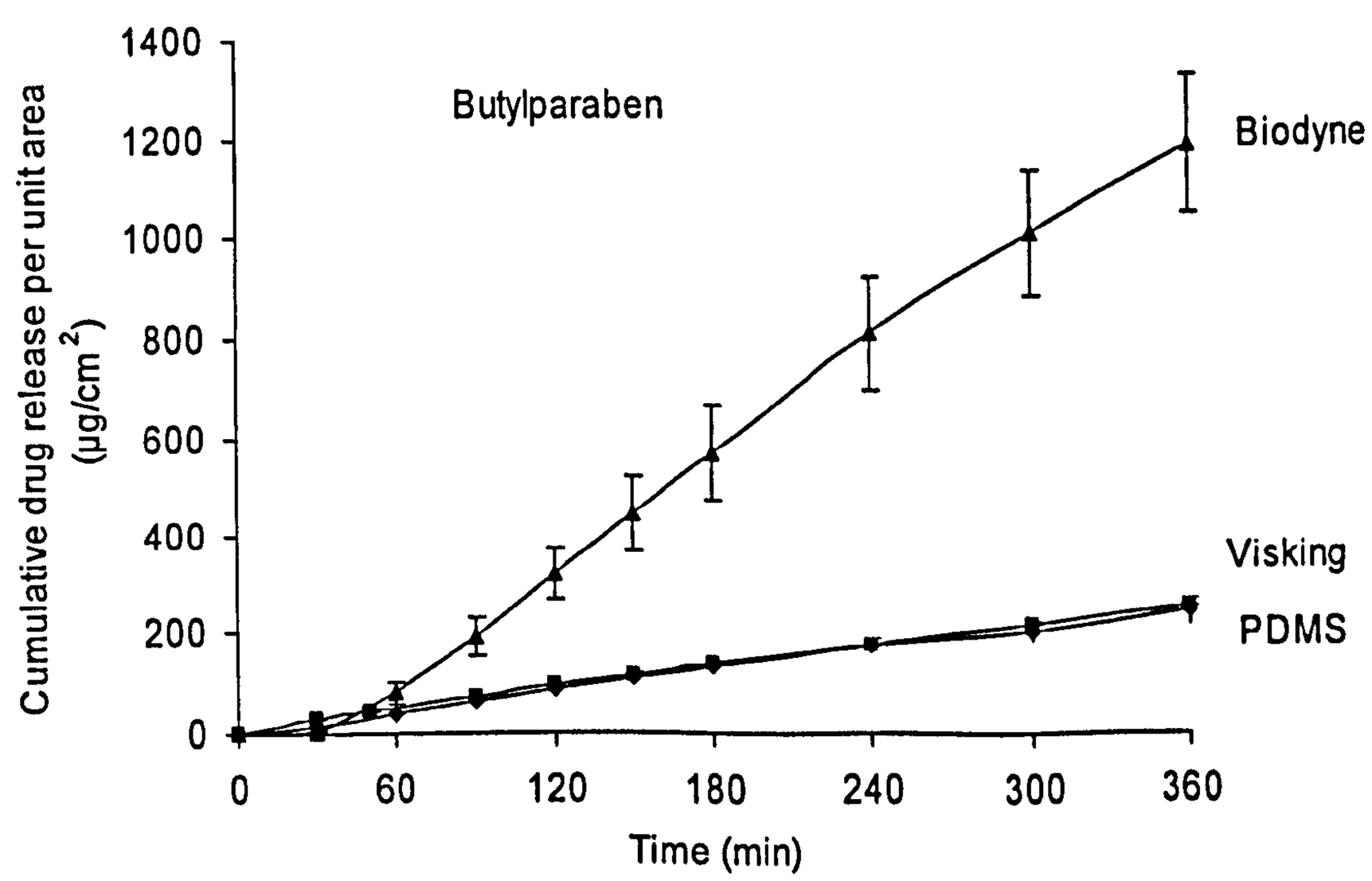

Figure 6.5 (cont.): Cumulative mass per unit area plots against time of parabens across Biodyne, Visking and PDMS membranes.

Table 6.6: Paraben flux from aqueous PBS across PDMS, Visking and Biodyne (mean ± S.D., n=6). (MP-methylparaben, EP-ethylparaben, PP-propylparaben, BP-butylparaben)

Paraben	Flux, $\mu g.cm^{-2}.h^{-1}$		
	Biodyne	Visking	PDMS
MP	981.7 ± 75.7	499.8 ± 5.7	38.0 ± 3.5
EP	570.9 ± 50.0	184.8 ± 4.7	32.1 ± 3.1
PP	186.4 ± 20.1	44.7 ± 1.3	19.1 ± 2.1
BP	232.6 ± 15.9	44.1 ± 1.9	42.3 ± 4.6

For all parabens, the diffusion through Biodyne was fastest, followed by Visking, then PDMS. For methylparaben and ethylparaben, the rates through Biodyne showed sign of slowing down after 4 hours, with the gradual decreasing of gradient; see Figure 6.5 (a) and (b).

The relationship between permeability coefficient and paraben carbon number for the three membranes was plotted in Figure 6.6 below. From the steepness of the line, it was observed that the effect of drug hydrophobicity was greatest on PDMS, followed by Biodyne and the least influence was seen on Visking membrane.

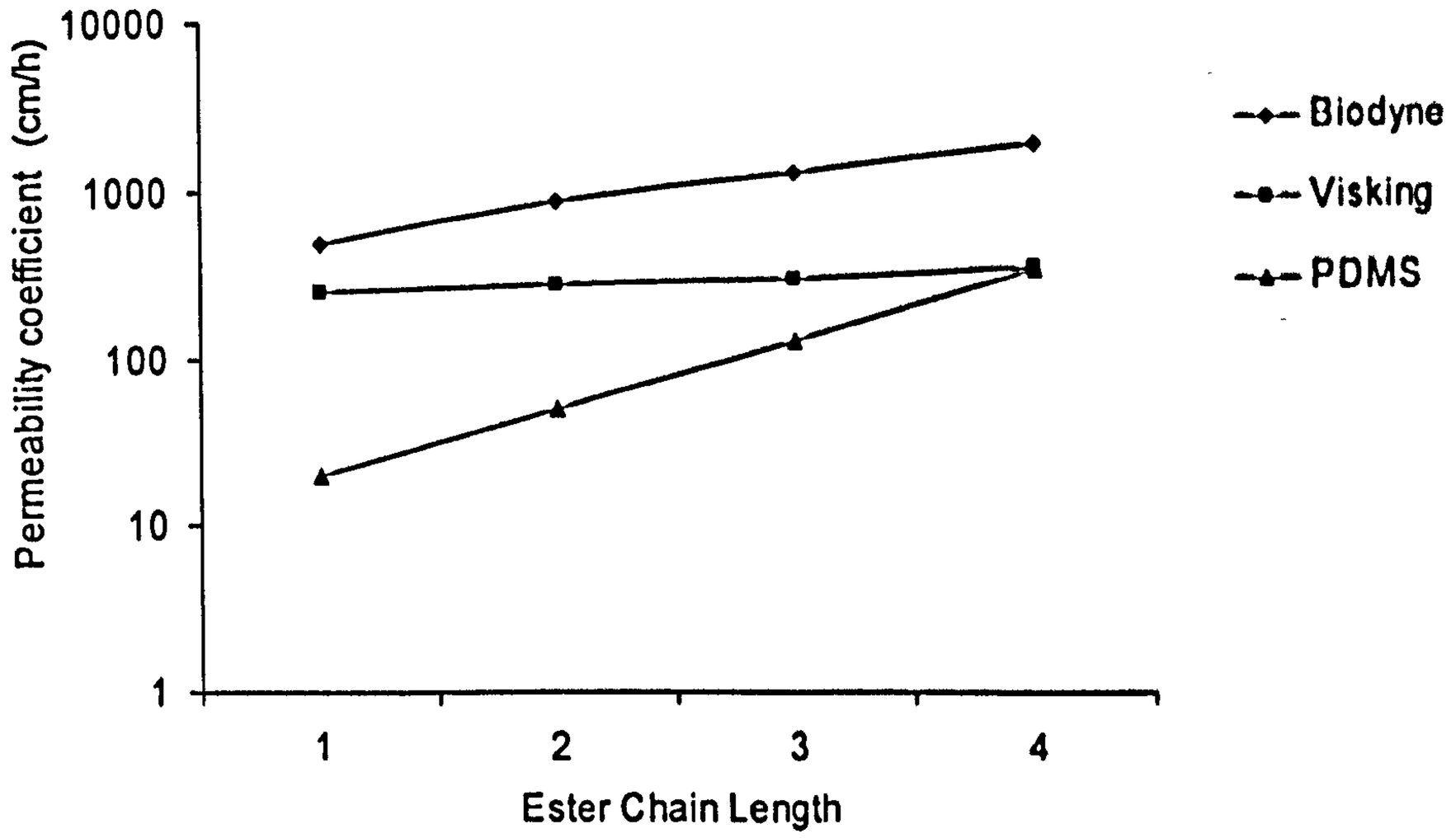

Figure 6.6: The relationship between the membrane permeability coefficient (Kp) and paraben ester chain length.

6.3.3.2 Permeation profile of parabens from aqueous PBS, Miglyol and Capmul through PDMS

The cumulative drug release per unit area of parabens from PBS, Miglyol and Capmul through PDMS membrane is shown in Figure 6.7 (a)-(c).

(a)

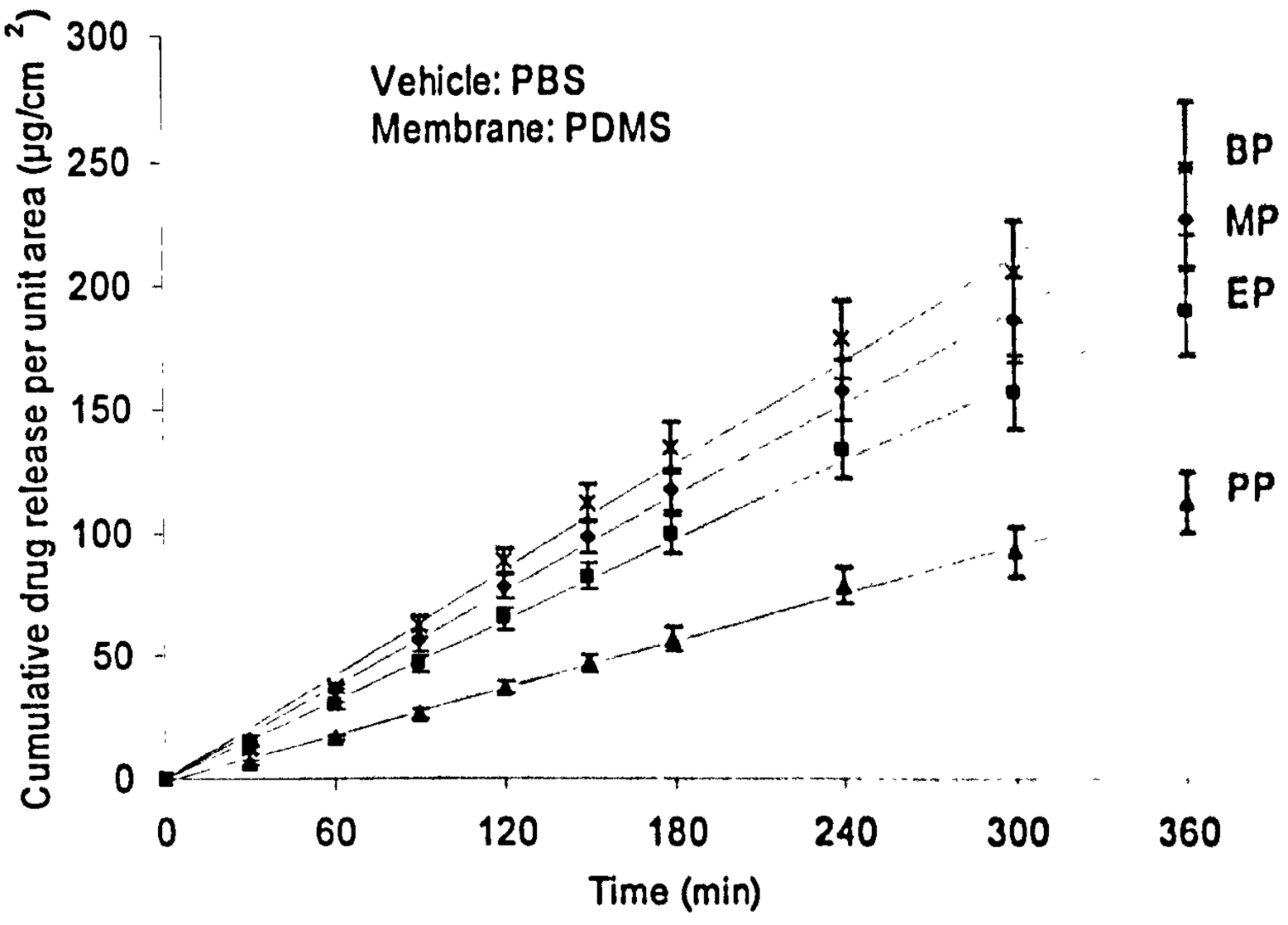
Vehicle: PBS
Membrane: PDMS
Cumulative drug release per unit area (µg/cm 2)
300
250
200
150
100
50
0
0
60
120
180
240
300
360
Time (min)
BP
MP
EP
PP

(b)

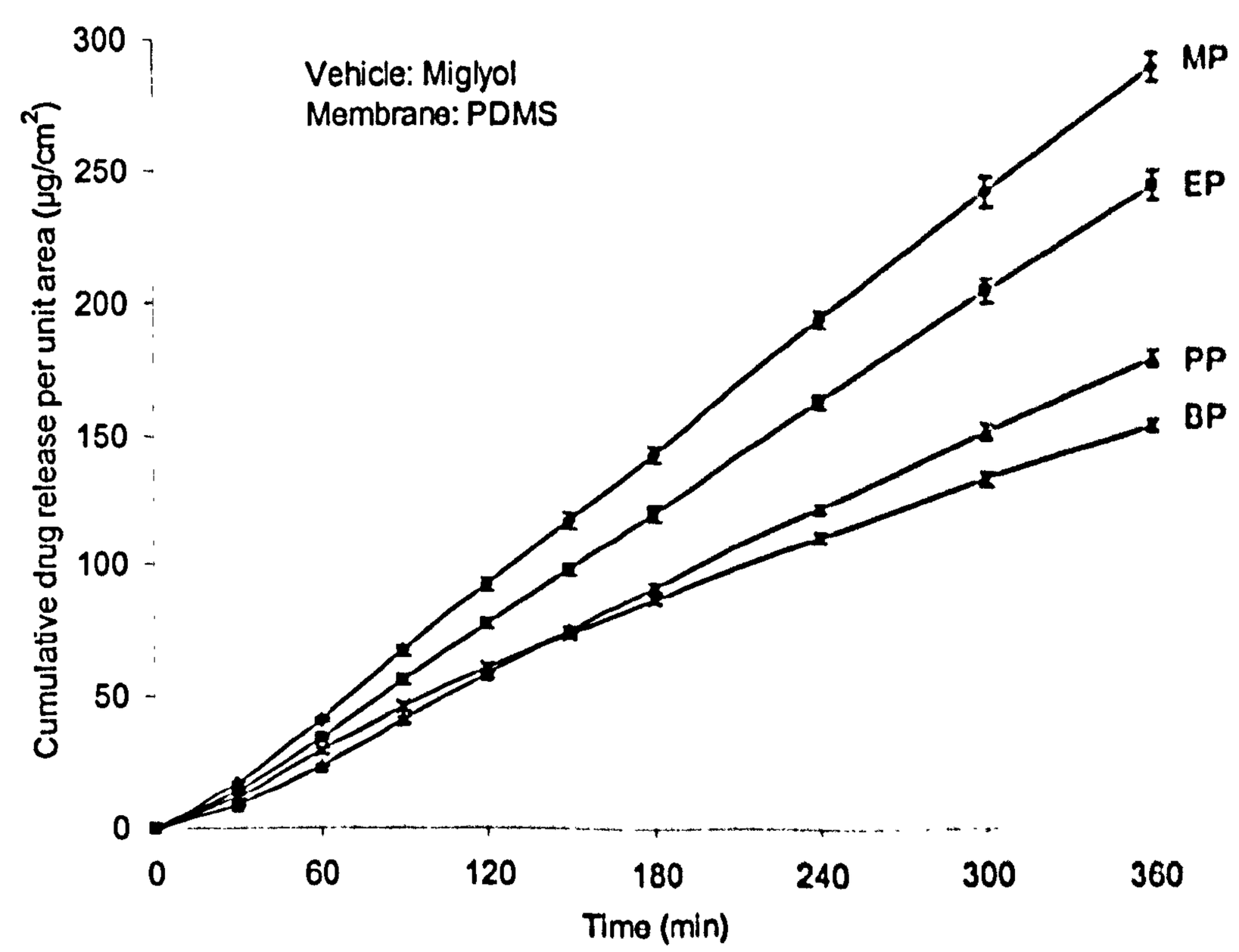
Vehicle: Miglyol
Membrane: PDMS
Cumulative drug release per unit area (µg/cm2)
300
250
200
150
100
50
0
0
60
120
180
240
300
360
Time (min)
MP
EP
PP
BP

(c)

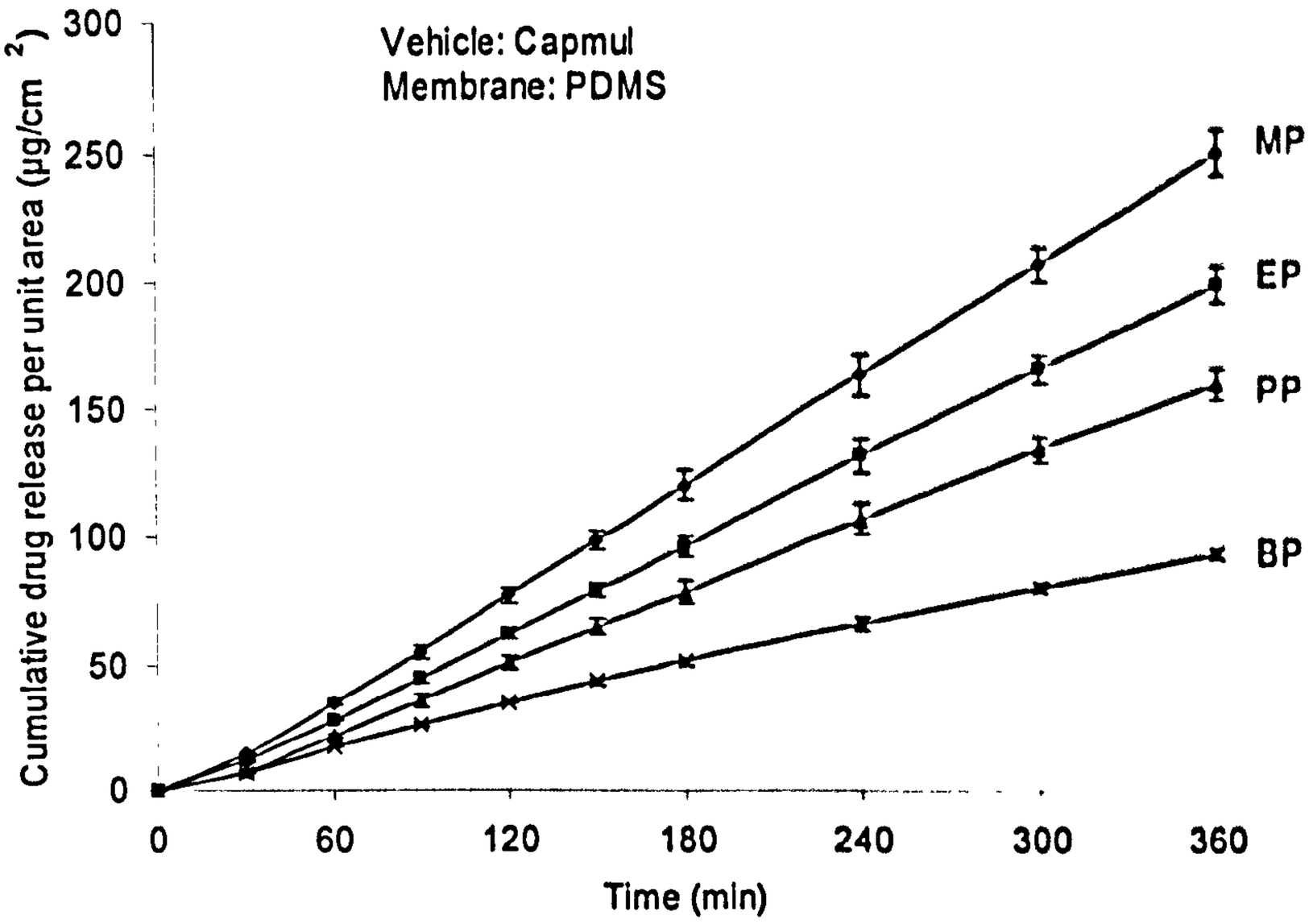

Figure 6.7: Cumulative mass release per unit area of methyl-, ethyl-, propyl-, butylparaben from PBS, Miglyol and Capmul through PDMS over 6 hours.

The rates of release of parabens from all the vehicles follow a linear profile with no apparent lag time. Figure 6.8 below compares the paraben flux value for PBS, Miglyol and Capmul.

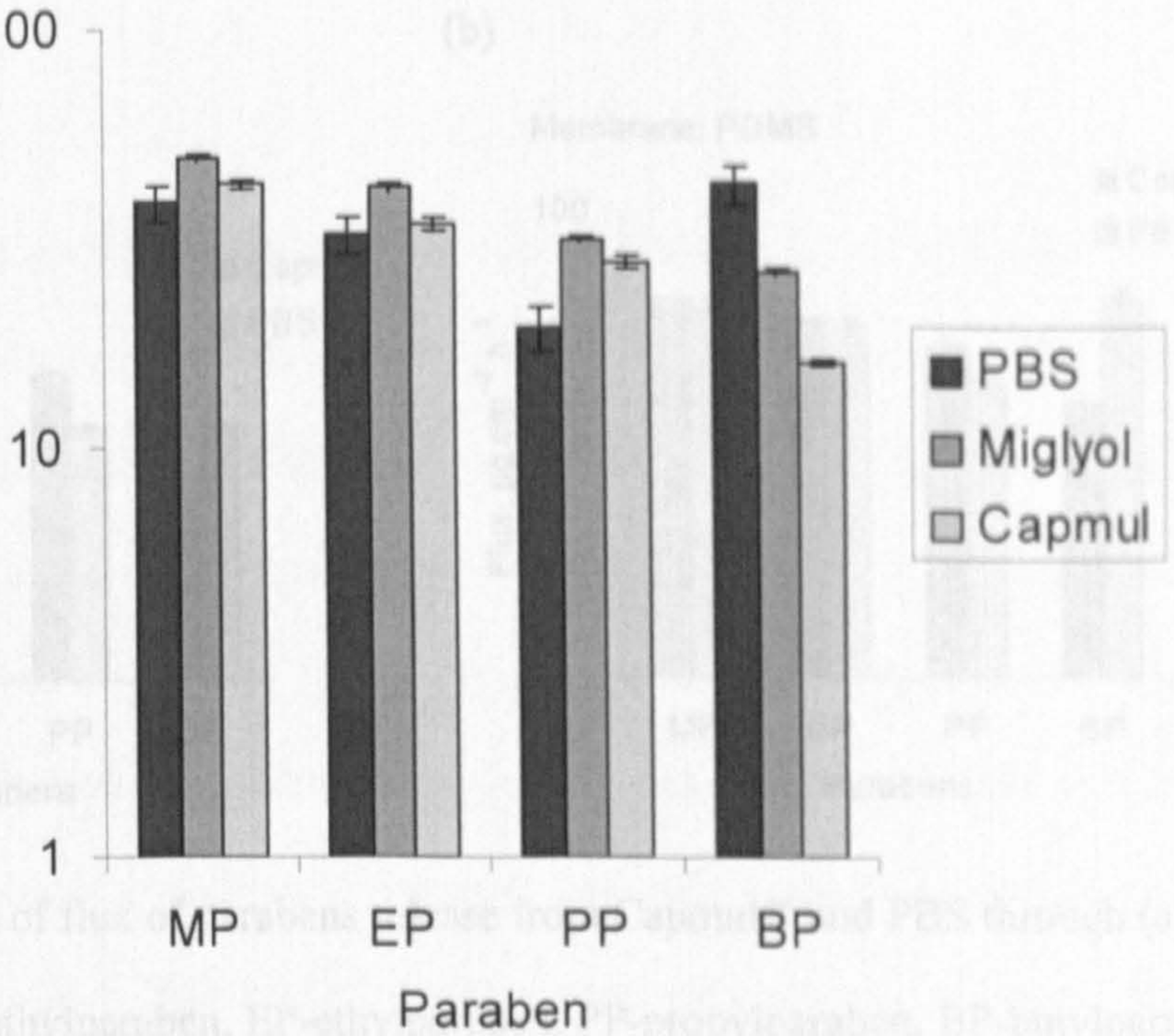

Figure 6.8: Paraben flux from PBS, Miglyol® and Capmul® through PDMS membrane. (MP-methylparaben, EP-ethylparaben, PP-propylparaben, BP-butylparaben)

It can be observed that for both Miglyol and Capmul, the flux across PDMS decreased as the paraben carbon chain length increased. The flux values of the same paraben were significant from each other in different vehicles, but the flux magnitude varies only 2-3 folds, e.g. butylparaben 15.7 $\mu g.cm^{-2}.h^{-1}$ from Capmul® and 42.3 $\mu g.cm^{-2}.h^{-1}$ from PBS. The magnitude of flux showed that parabens diffuse through PDMS were not greatly affected by the vehicles.

Figure 6.9 compared the flux of parabens from Capmul® through PDMS and Visking to that of PBS, while the flux values were tabulated in Table 6.5.

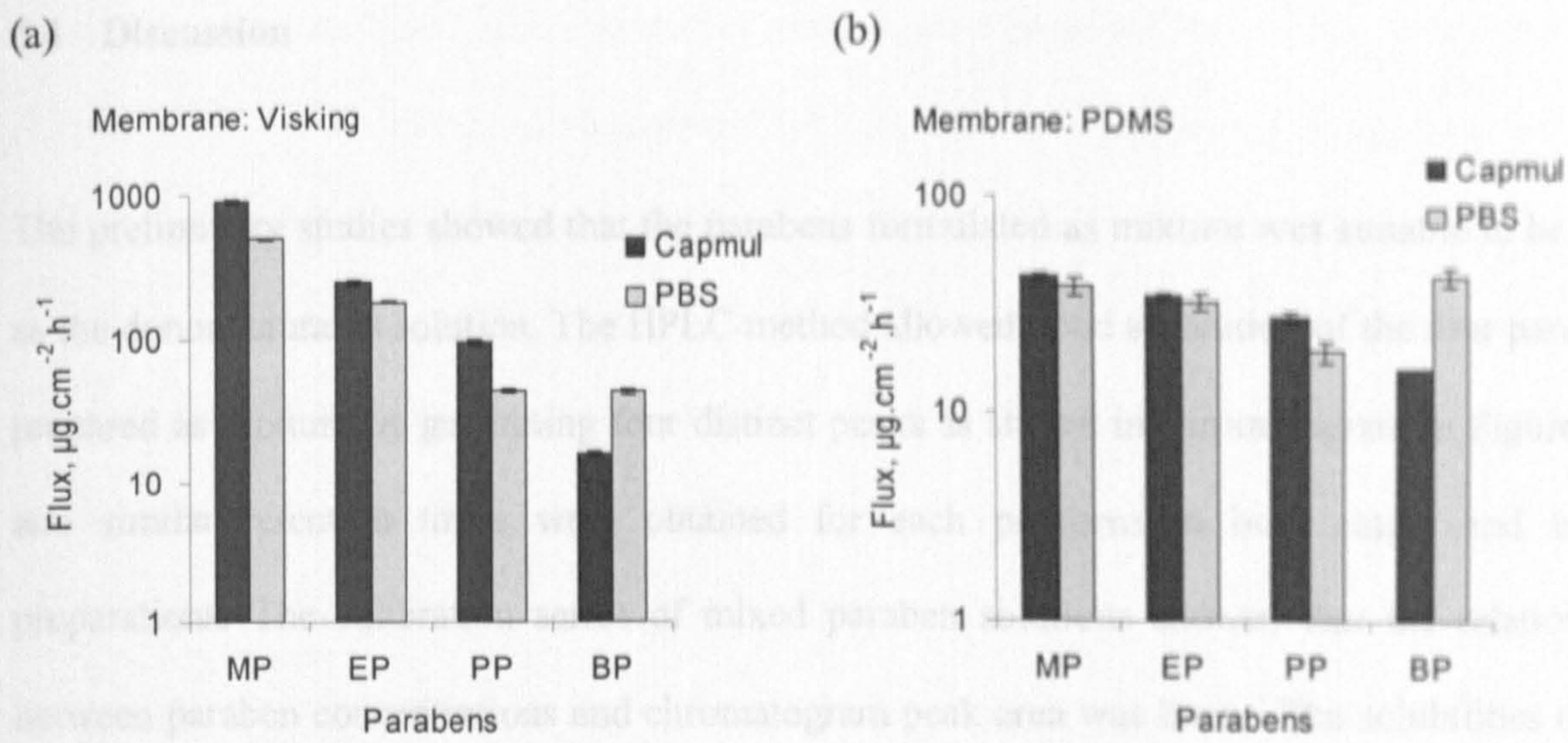

Figure 6.9: Comparison of flux of parabens release from Capmul® and PBS through (a) Visking and (b) PDMS. (MP- methylparaben, EP-ethylparaben, PP-propylparaben, BP-butylparaben)

Table 6.7: Average flux in term of cumulative mass per unit area and of paraben from Capmul across PDMS and Visking. (Ave J ± S.D., n = 6.)

Membrane	Vehicle	Flux, $\mu g.cm^{-2}.h^{-1}$			
		MP	EP	PP	BP
PDMS	Capmul	42.3 ± 1.3	33.8 ± 1.1	27.4 ± 1.0	15.7 ± 0.3
	PBS	38.0 ± 3.5	32.1 ± 3.1	19.1 ± 2.1	42.3 ± 4.6
Visking	Capmul	910.4 ± 34.3	252.8 ± 9.3	98.9 ± 3.4	16.1 ± 0.5
	PBS	499.8 ± 5.7	184.8 ± 4.7	44.7 ± 1.3	44.1 ± 1.9

When the paraben flux across of PDMS was compared to that of the Visking, it was observed the Visking was able to discriminate the effect of vehicles by showing that large difference in flux between vehicles was observed when it was used as the model membrane. However, the butylparaben did not show apparent flux difference when Visking was used.

6.4 Discussion

The preliminary studies showed that the parabens formulated as mixture was suitable to be used as the donor saturated solution. The HPLC method allowed good separation of the four parabens prepared as mixture by generating four distinct peaks as shown in chromatogram in Figure 6.2; and similar retention times were obtained for each parabens in both single and mixed preparations. The calibration series of mixed paraben solutions showed that the relationship between paraben concentrations and chromatogram peak area was linear. The solubilities of the parabens in the mixtures and as a single component were analysed. The parabens solubility in PBS matched closely to water. This was expected as both were aqueous vehicles. Between the two oily vehicles, Capmul solubilised more parabens compared to Miglyol. It was noticed that propylparaben solubility was constantly lower in mixed parabens preparation for all vehicles; while there was increase or decrease for methylparaben, ethylparaben and butylparaben solubilities. The changes in solubility of parabens in mixture were thought to be due to physical changes of the parabens in the vehicle (formation of hydrates or polymorphism) [Giordano *et al.*, 1999]. As long as there was no chemical interaction of between the paraben analogues, the mixed paraben was an acceptable model saturated solution in this study.

The partition coefficient (K) measures the distribution of the drugs between two phases and in this study, the distribution of parabens between the membranes and PBS was examined. From the plots in Figure 6.4, all four parabens possessed the highest partitioning in Biodyne. The solubility increased as the paraben ester chain length increased. The paraben partition coefficient trend for PDMS was similar to Biodyne but at a lower magnitude. While for Visking, the paraben partitioning into Visking decreased with the increasing molecular size. It was apparent that parabens partitioning favoured hydrophobic membranes. Bin and co-workers demonstrated that parabens adsorbed the most onto hydrophobic membrane filters and they proposed the drug

adsorption was attributed to hydrophobic interactions between the parabens and membrane polymer [Bin *et al.*, 1999b]. The hydrophobic interaction was expected to increase with the hydrocarbon numbers on the parabens, hence an increased in partition coefficient values were observed from methyl- to butylparaben. However, the fact that the parabens had very high partition coefficient for Biodyne (almost 50-100 times higher compared to PDMS) might be due to the large pores of Biodyne which were able to entrap aqueous bulk, so less were measured in the solution. The lower partition coefficient of parabens for Visking indicated that the parabens favour less for the hydrophilic membrane; and the values decreased with increased paraben hydrophobicity.

The four parabens drug release from simple aqueous PBS saturated solution across the three membranes were compared. In Chapter 5, a series of commonly used synthetic membranes were screened using the model drug ibuprofen. It was found that the ibuprofen flux across microfilters was generally higher than ultrafiltration membrane types. The former was thus termed as the 'high-flux' membranes while the latter as the 'low-flux' membranes. Although three types of 'low-flux' membranes were used in this study, the different characteristics of the membranes were adequate to carry out the studies. In general, the flux across porous membranes (Biodyne and Visking) was higher than the non-porous membrane (PDMS) for all parabens except butylparaben (Figure 6.5 a-d). This agreed with the findings in Chapter 5 where the drug permeations across the porous membranes were faster compared to non-porous membrane. The same concept applies here for the porous membranes (Biodyne and Visking), which allow the dissolved parabens to be carried through the pores. In contrast, the transport across non-porous membrane (PDMS) involved solubilising in the dense polymer matrix which was rate-limiting, so low fluxes were measured. Between the two porous membranes, the fact that higher flux were obtained with the Biodyne was because the Biodyne membrane possessed a higher porosity compared to Visking.

As stated in Fick's Law of diffusion, the rate of drug release is proportional to the drug solubility (Cv) in the vehicle (see equation 1.3). From the table 6.3, the methylparaben flux values were the highest for all the membranes simply because methylparaben was solubilised the most in aqueous PBS. Likewise for ethyl- and propylparaben, the flux reduced as solubility in PBS reduced. However, butylparaben did not have the similar fashion: despite being the least soluble drug in PBS, the flux showed relatively higher (Biodyne and PDMS) or similar (Visking) flux compared to propylparaben. This does not agree with Fick's Law. The likely explanation for the butylparaben was there were interactions between the drug and membrane. For the non-porous PDMS membrane the high butylparaben flux may be attributed to the high partition coefficient (11.60). So the partition factor here played a major role in accelerating the drug flux across PDMS. For the porous membrane, the increased in butylparaben flux was likely to be due to the hydrophobic interactions between the butylparaben and membrane polymers [Bin *et al.*, 1999b]. The hydrophobic interaction was proposed by Bin and co-workers to explain high adsorption of hydrophobic drug onto hydrophobic filters. The drug flux across porous membranes was governed by the partitioning of the drug between the solvent in the membrane pore and the formulation vehicle (represented as K' in Eq 1.7). The hydrophobic interactions may enhance K' because the hydrophobic drugs have a higher 'affinity' towards the membrane, thus higher amount of drug may be found in the solvent within the pores. This would then in turn enhance drug flux.

The impact of paraben hydrophobicity upon each membrane could be observed from from the permeability coefficient plot in Figure 6.6. It was shown that the drug hydrophobicity had the greatest impact on PDMS (steepest plot), lesser extent on Biodyne membrane and the least effect was observed on Visking.

In our studies, the solubilities of the parabens in oily and aqueous vehicle showed differences up to approximately 150-fold (e.g. butylparaben Cs (Capmul) = 158.92 mg/mL vs. Cs (PBS) = 0.12 mg/mL), but the flux for each paraben across PDMS does not vary much, approximately 2-3 folds between the different vehicles. This indicates that the vehicles (PBS, Miglyol and Capmul) did not interact with the membrane and the amount of parabens that diffuses through the membrane was solely controlled or limited by the PDMS membrane. This means that the vehicle effect cannot be tested using PDMS membrane because PDMS exerts a rate-limiting effect of drug flux. When compared drug release from Capmul® and PBS through Visking, the vehicle effect became apparent (up to 10 times different). In this case, it was apparent Visking was less-rate limiting than PDMS. Being the thinner and more porous membrane, the Visking allowed more solutes passing through. When Visking was employed as model membrane it was observed that the the Capmul released less parabens compared to the PBS despite parabens are more soluble in Capmul. This shows that the vehicle was a factor controlling the paraben release.

Futherwork can be carried out to look upon the partition coefficient between the parabens and Miglyol and Capmul, which might help explained on the differences in paraben flux from the two oily phases.

6.5 Conclusions

The conclusions from this study were:-

1. Methylparaben, ethylparaben, propylparaben and butylparaben diffusion from saturated solution across PDMS, Visking (cellulose) and Biodyne (nylon) has been investigated.
2. Among the three model membranes, Biodyne was the least rate-limitng, followed by visking membrane and PDMS showed rate-controlling effect and it is not suitable to be used for testing vehicle effect.

3. A highly lipophilic drug such as butylparaben may form hydrophobic interaction with the membrane polymer. The hydrophobicity of the drug has great influence on hydrophobic dense PDMS membrane but lesser extend on porous membranes.
4. It was also concluded that porous membranes were better in revealing the formulation effect compared to non-porous membrane.

CHAPTER VII

INVESTIGATION OF IBUPROFEN SATURATED SODIUM ALGINATE GEL AND ITS LYOPHILISED WAFER

7.1 Introduction

The alginates are high molecular weight linear copolymers (~ 5×10^5) derived from seaweed and it are normally presented as sodium salts, called sodium alginate. The alginate polymers are a family of linear unbranched polysaccharides which contain varying amount of 1,4'-linked β-D-mannuronic acid (M) and α-L-guluronic acid (G) residues. The structure of alginate is shown in Figure 7.0. The residues arranged in a pattern of blocks of varying sequence along the chain with difference proportion M and G depending on the algae species of which the alginate is obtained.

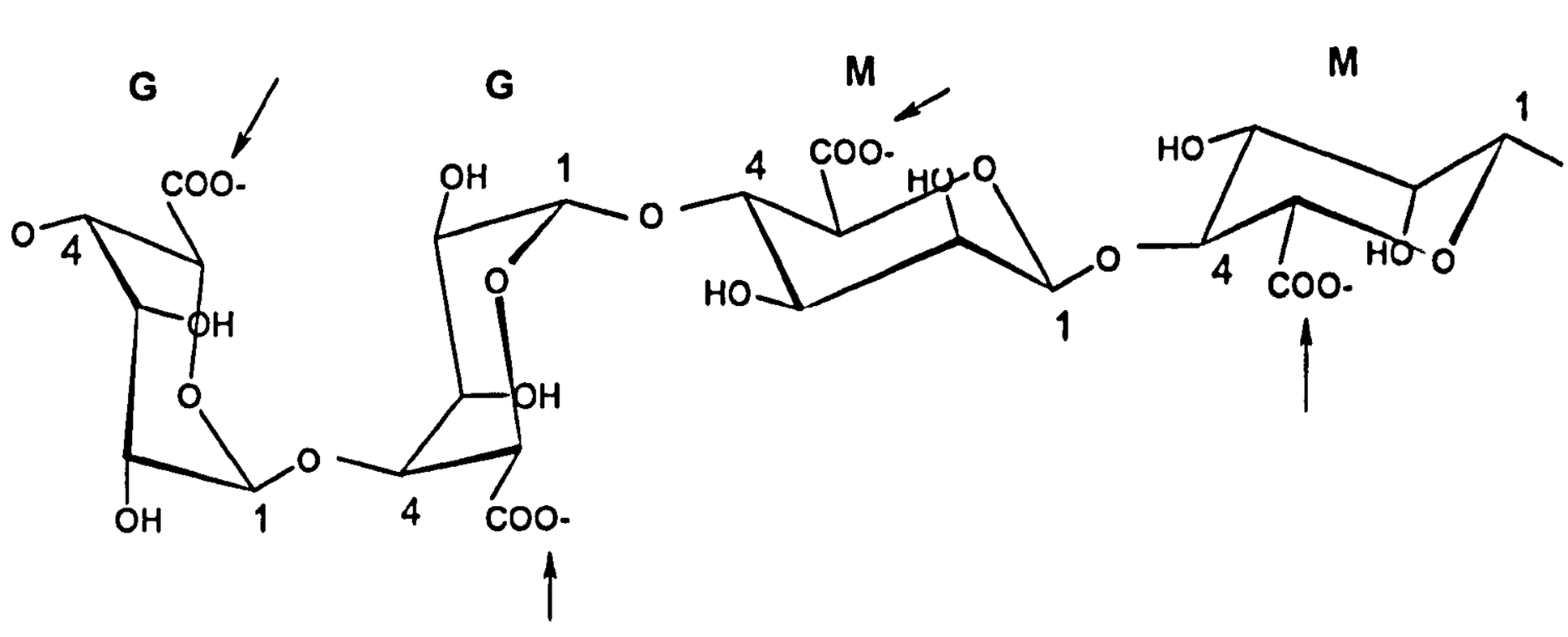

Figure 7.0: Sodium alginate structural unit containing α-(1,4)-L-guluronic acid and (G) β-(1,4)-D mannuronic acid (M) residues. The arrows show potential sites for bonding with water molecules.

Sodium alginate is water soluble and it can form viscous gel. Sodium alginate is an anionic polymer when the carboxyl groups on the uronic acid residues (pKa ~3.5) are dissociated in water. At low concentrations (<5 % w/v), the sodium alginate chains are ionised and do not form gels. As such, divalent cations such as Ca^{2+} and Ba^{2+} are added to induce gelation. But at high concentrations (≥ 5% w/v), sodium alginate polyanionic chains begin to entangle and swell. The chain entanglements form three-dimensional porous network which further entrap water molecules. The entangled sodium alginate chains are held together by H-bonding and hydrophobic interactions, but repel each other due to the charged groups on the polymer chain [Draget *et al.*, 2005]. This increases the chain extension thus produce a stable viscous hydrogel. Sodium alginate hydrogel stability is influenced by several factors such as pH, temperature and the presence of free radicals. Extremely high or low pH depolymerises the alginates via disruption of the glycosidic linkages [Haug *et al.*, 1963]. Free radical degrades alginate mainly by oxidative-reductive depolymerisation reactions caused by contamination of reducing agents such as polyphenols from the brown algae [Smidsrød *et al.*, 1967]. The depolymerisation reactions are also accelerated with temperature. Hence sterile filtering at ambient temperature rather than autoclaving of alginate solutions is generally recommended as a sterilisation method in order to reduce the polymer breakdown but maintain the mechanical strength of the final gel.

The alginates are shown to be useful in various applications. Conventionally, sodium alginate is used extensively in the food and beverages industry as a thickening agent, gelling agent and colloidal stabiliser. It is also an important material for wound dressings and dental impressions due to its biocompatibility, hydrophilicity and relatively low cost. Recently, alginate hydrogels have attracted much attention in tissue engineering as a scaffold for cell reconstruction or regeneration [Wang et al., 2003; Hashimoto et al., 2005]. Alginate hydrogels possess several unique properties which are desirable to create a favourable microenvironment for cell growth. These include high porosity, an open interconnected

porous network for enhancement of diffusion rate of nutrients, as well as relatively low toxicity and biodegradability [Hashimoto et al., 2005]. Alginate wafers (sometimes known as sponges) produced via lyophilisation of alginate gels were first prepared by Shapiro and Cohen [Shapiro and Cohen, 1997] for cell culture and transplantation. Later, drug delivery investigators explored these wafers as novel drug delivery vehicle for wound treatment [Lai et al., 2003; Boateng, 2005; Matthews et al., 2005]. Matthews and co-workers [Matthews et al., 2005] showed that these sodium alginate wafers instantaneously adhered to moist surfaces, transforming them from glassy porous solids to highly viscous gels when hydrated. The incorporated drug is thought to release from the formulation as gelation occurs. Using a dissolution test, alginate studies showed slow release behaviour [Lai et al., 2003] and the rate of substance release can be controlled via controlling the gel viscosity [Matthews et al., 2005] indicating that the wafers are potential as a drug controlled-release vehicle for suppurating wound.

7.1.1 Aims of study

Incorporation of drug into a wound dressing is relatively a relatively new pharmaceutical convention. There is no recommended procedure for wound dressing drug release testing. The aim of this work was to investigate the suitability of Franz cell as the evaluation of drug release from a model wound dressing (i.e. a wafer) using ibuprofen as a model drug. In the first instance, preliminary work was carried out in attempt to investigate the ibuprofen saturated sodium alginate gel characteristics using rheology, thermal and microscopic techniques. Secondly, the drug release from the lyophilised ibuprofen saturated wafers as well as the ibuprofen saturated gel using the validated Franz cell and methodology in our laboratory was investigated.

7.2 Method

7.2.1 Preparation of ibuprofen saturated sodium alginate gels

This work used ibuprofen saturated solution which was prepared in 0.1M sodium hydroxide (the method of saturated solution preparation was described in Chapter 5). Sodium alginate (SA) gel preparation methods were adapted from Matthews and colleagues [Matthews *et al.*, 2005]. 5 g of SA beads were slowly dissolved in 100 mL of ibuprofen saturated solution at 25 °C to make a 5% w/v sodium alginate gel using an overhead stirring. The gel was then allowed to stand at room temperature to eliminate trapped air bubbles for at least 24 hour prior to analysis and testing. For the preliminary studies, the positive and negative control gel were prepared using the same method above with the SA dissolved in water (distilled water, pH 5.5, adjusted to pH 7 using dropwise 0.1M hydrochloric acid) and 0.1M sodium hydroxide respectively. All the gels were stored at 25 ° C.

7.2.2 Freeze-drying procedure

This was the general freeze-drying programmed steps for the production of lyophilised wafers (Table 7.1).

Table 7.1: Freeze-drying steps for gel lyophilisation

Step	Temperature (°C)	Time held (min)
Freezing	-70	30
Drying (primary)	-60	60
	-40	60
	-20	120
	-10	540
	0	120
	5	120
	10	120
Drying (secondary)	20	120

The whole process took 21.5 hours to complete. The lyophilised wafers were stored in glass dessicator with silica beads to prevent the re-hydration of samples from the moisture in the air.

7.2.3 Preliminary studies

In preliminary studies, the apparent viscosity, water content and thermal transition of ibuprofen saturated SA gel were investigated and compared to that with the positive (SA in distilled water) and negative (SA in 0.1M sodium hydroxide) control gels.

7.2.3.1 Rheological measurements

Rheological measurements of ibuprofen saturated SA gel and the positive and negative control gels were undertaken on a Carrimed CSL 100 rheometer with cone and plate geometry at 25 °C. Two cones of diameter 4 and 6 cm with integral solvent trapping (containing water) were used depending on the apparent viscosities of the samples at the shear rates used. The shear rate was increased from 0.3 to 500 s^{-1} in 3 minutes followed by a constant shear rate decrease to 0.3 s^{-1}. To help minimize water evaporation, the cone was covered with anti-evaporation unit throughout the whole shear cycle. All measurements were carried out at least once. The shape of the flow curves and apparent viscosities of the gels at 500 s^{-1} were compared and contrasted. Flow curves were obtained by plotting shear rate (1/s) versus shear stress (Pa) and the apparent viscosities (η_{app}) were derived from the loop apex.

7.2.3.2 Differential scanning calorimetry (DSC)

The thermal properties of ibuprofen saturated SA gel, positive and negative control gel were analysed with DSC. Firstly, the sample and reference pans were weigh-matched. (The pan type used was aluminium standard 40 μL which has a maximum boiling point of 600°C.) Approximately 30 mg of gel was loaded carefully into the sample pan. The sample pan was

hermetically sealed. The accurate mass of gel was obtained by the difference from the weights of the empty and filled pans/lid set. The sample and reference material were placed in separate pans and the temperature of each pan increased at a predetermined rate from 10 °C to 80 °C, at 10 °C per minute.

7.2.3.3 Thermogravimetric analysis (TGA)

The TGA was employed to determine the weight loss with temperature (water content present in the gels) in positive and negative control gels. Approximately 20 mg of samples were loaded into 70 µl alumina crucibles (unconvered) and subjected to 30 - 150 °C at 2 °C/ min. The percentage of weight loss was integrated from the thermogram using the TA computer software (Star^e v 8.10).

7.2.3.4 Lyophilised wafers microscopic analysis

The lyophilised wafers prepared from ibuprofen saturated SA gel, and the positive and negative control gels were observed under polarised light at low magnification. To prepare the wafer on the microscope slides, a drop of gel was placed at the centre of a clean microscope slide and cover slip was lowered gently above the sample, with one edge touching the slide first. Slight pressure was applied onto the cover slip to flatten the gel so a thin layer was formed between the two pieces of glass. The sample was confined only within the cover slip. Immediately after the preparation, the slides were placed in the freeze-drier and lyophilised [Rouse *et al.*, 2006].

7.2.4 Ibuprofen drug release from gels and wafers

7.2.4.1 Preparation of wafers in donor

For Franz cells experiment, the wafers were prepared *in situ*. Firstly, the bottom opening of a donor cell was sealed with parafilm. The donor cell was positioned upright. Using a 2 mL

plastic pipette (with the tip cut off), the gel (~1 g) was then gently filled into the donor cell. The gel was loaded carefully to ensure that the spread evenly above the parafilm with no trapped air bubble. The donor top was quickly sealed with parafilm and the film was pierced to allow the elimination of water vapour during freeze-drying process. The exact weight of gel was determined by weighing the donor cell before and after gel loading. The donor cells with gels were then transferred into the freeze-drier for lyophilisation. It was crucial that the donor was kept upright throughout the whole process. Lyophilisation of gels was undertaken using the freeze drying steps described in section 7.2.2. After lyophilisation, the weight of the donor cell was weighed again to determine the amount water required for gel reconstitution in Franz cell studies (see below).

7.2.4.2 Franz cell drug release

The wafers in the donor Franz cells were prepared *in situ*. The permeation profiles of ibuprofen from gels and wafers were evaluated using *in vitro* Franz cells. The least rate-limiting synthetic membrane to ibuprofen, Nuclepore (0.1 μm pore size) was employed (see Chapter 5). The de-aerated 0.1M sodium hydroxide was the receptor fluid and maintained at 37°C. The receptor chamber was stirred continuously at 200 rpm. For the gel, after the Franz cell was assembled, the ibuprofen saturated SA gel formulation (~1g) was gently placed directly on top of the synthetic membrane in the donor chamber. For the wafers, after lyophilisation in the donor, the parafilm at the bottom of the donor cells was removed and the donor was quickly assembled (wafer adhered to donor wall) with the synthetic membrane and a receptor half-filled with receptor fluid. The exact amount of water loss after freeze-drying (determined by weighing donor cells before and after freeze-drying) was pipetted into the wafers in each donor. The hydrated wafers were left in the donor for 10 min for gel reconstitution. The time of drug release only began when the receptor was topped up with receptor fluid of 37 °C. Aliquots were extracted every 15 min for 3 hours and 30 min there

after till 7 hours. 2 mL of the solution in the receptor was removed for UV determination and replaced immediately with an equal volume of fresh 0.1M sodium hydroxide of the same temperature. A minimum of six Franz cells were performed for each formulation. The average cumulative mass drug release from gels and wafers was plotted against time and the drug flux was derived from the linear portion of the graphs.

7.3 Results

7.3.1 Gel appearance

Sodium alginate gels in water (positive control) and 0.1M sodium hydroxide (negative control) appeared as muddy brown. The negative control gel was more mobile than the positive control gels. The negative control gel also liberated a foul seaweed odour. Ibuprofen saturated SA gel appeared as muddy brown gel suspended with white solids.

7.3.2 Preliminary studies

7.3.2.1 Rheological measurements

The flow curves of 5% w/v SA gel prepared in (i) 0.1M sodium hydroxide, (ii) water and (iii) saturated ibuprofen solution in sodium hydroxide were shown in Figure 7.1 below. All the gels exhibited the shear-thinning, pseudoplastic flow behaviour typical of entangled linear macromolecular systems. The apparent viscosities (at 500 s^{-1}) were obtained at the flow curves apex were 0.40, 1.05 and 1.19 s^{-1} for negative control gel, ibuprofen saturated SA gel and positive control gel respectively.

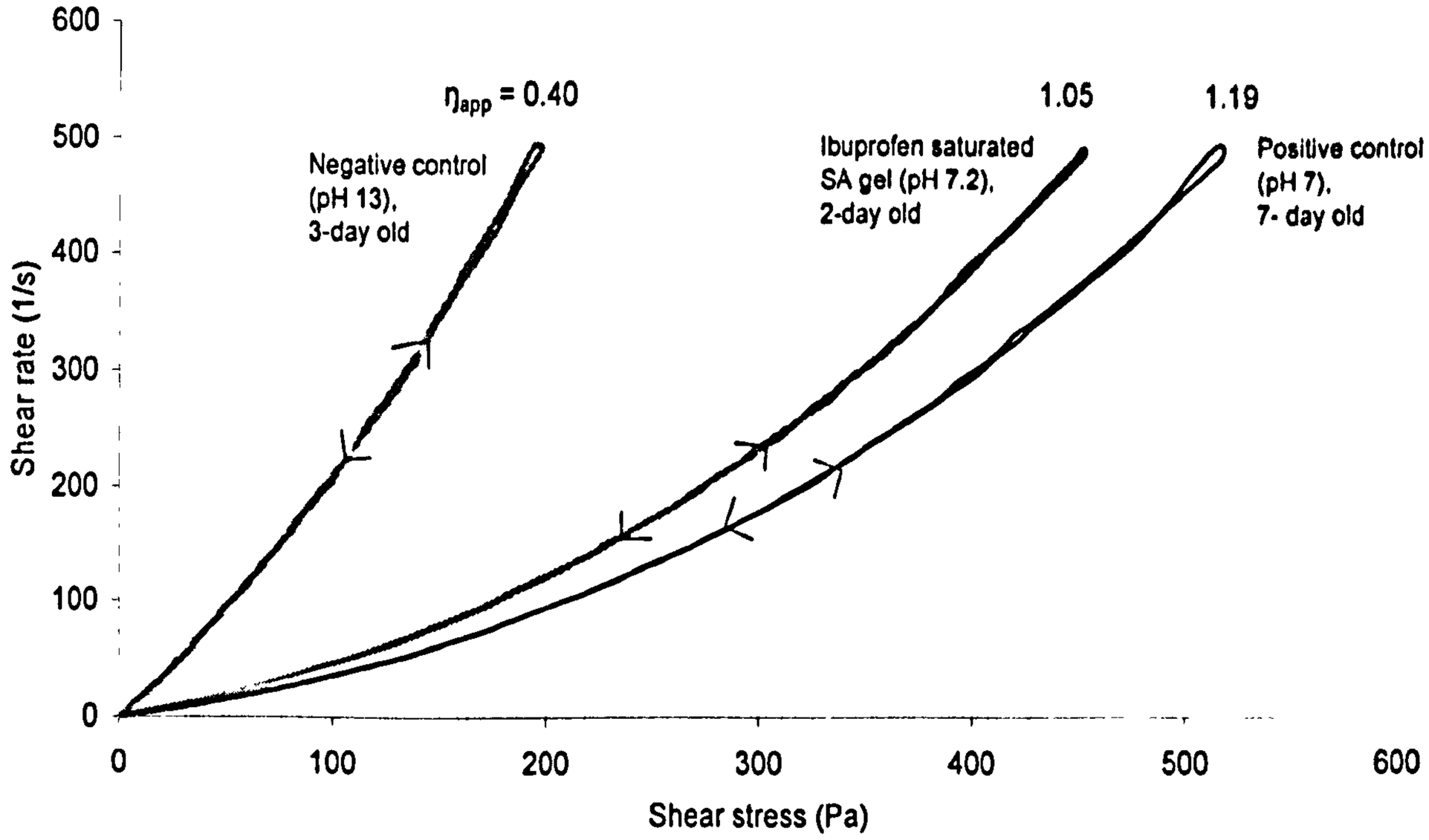

Figure 7.1: Flow curves of SA gels (1-week old). Apparent viscosities (η_{app}) at 500 s^{-1} were showed at the apex of each flow curve.

7.3.2.2 Differential Scanning Calorimetry (DSC)

The gels DSC endotherm peaks are shown in Figure 7.2 (a) below. While Figure 7.2 (b) shows the endotherm (melting point) of the ibuprofen solid. The DSC of ibuprofen saturated SA gel produced an endotherm peak at 61.3 °C. The positive control gel had two vague endotherms, at 39.3 and 50.5 °C; whilst the negative gel had a sharp endotherm peak at 49.4 °C. The summary of the DSC peaks were shown in Table 7.2.

Table 7.2: Summary of DSC endotherms of gels and ibuprofen solids.

Sample	Endotherm Peak (°C)	Remarks
Positive control gel	39.3, 50.5	Vague peaks
Negative control gel	49.4	Distinct, sharp peak
Ibuprofen saturated gel	61.3	Distinct, sharp peak
Ibuprofen solids	78.4	Sharp peak

(a)

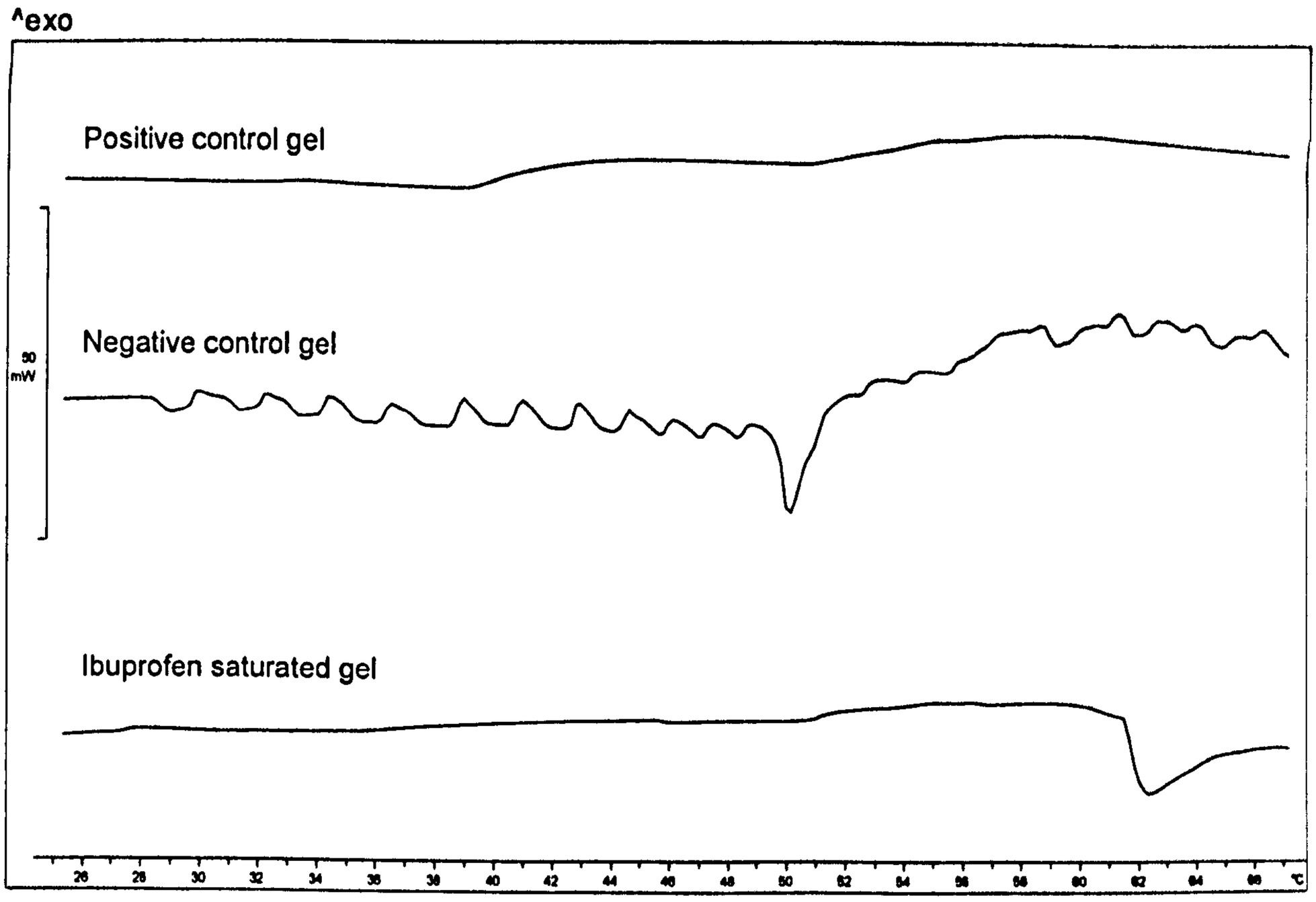

(b)

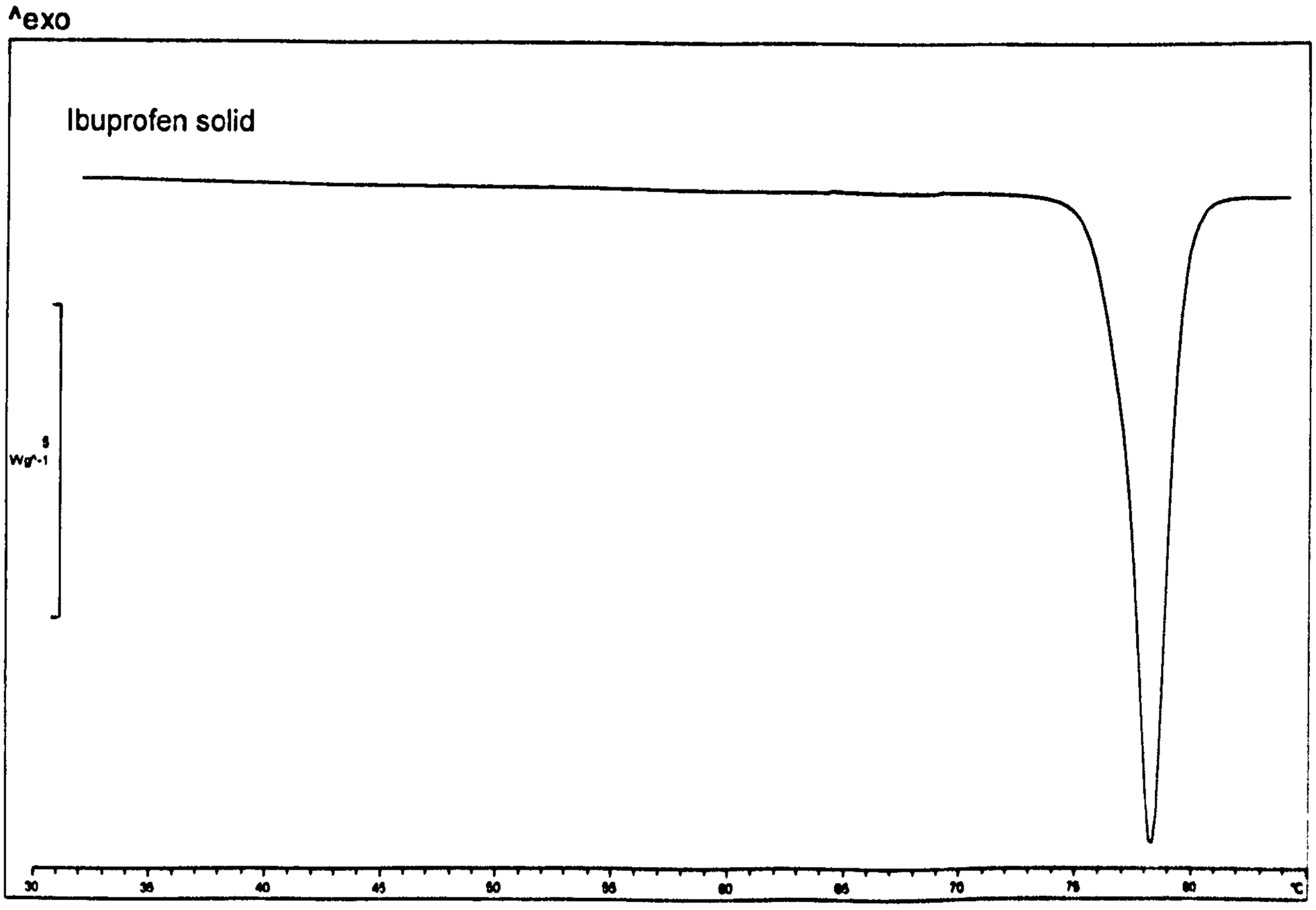

Figure 7.2: DSC endotherm of (a) SA gels and (b) ibuprofen (crystalline)

7.3.2.3 Thermogravimetric analysis (TGA)

The TGA endotherms for positive and negative control gels are shown in Figure 7.3 (a) while Figure 7.3 (b) shows the first integration of Figure 7.3 (a).

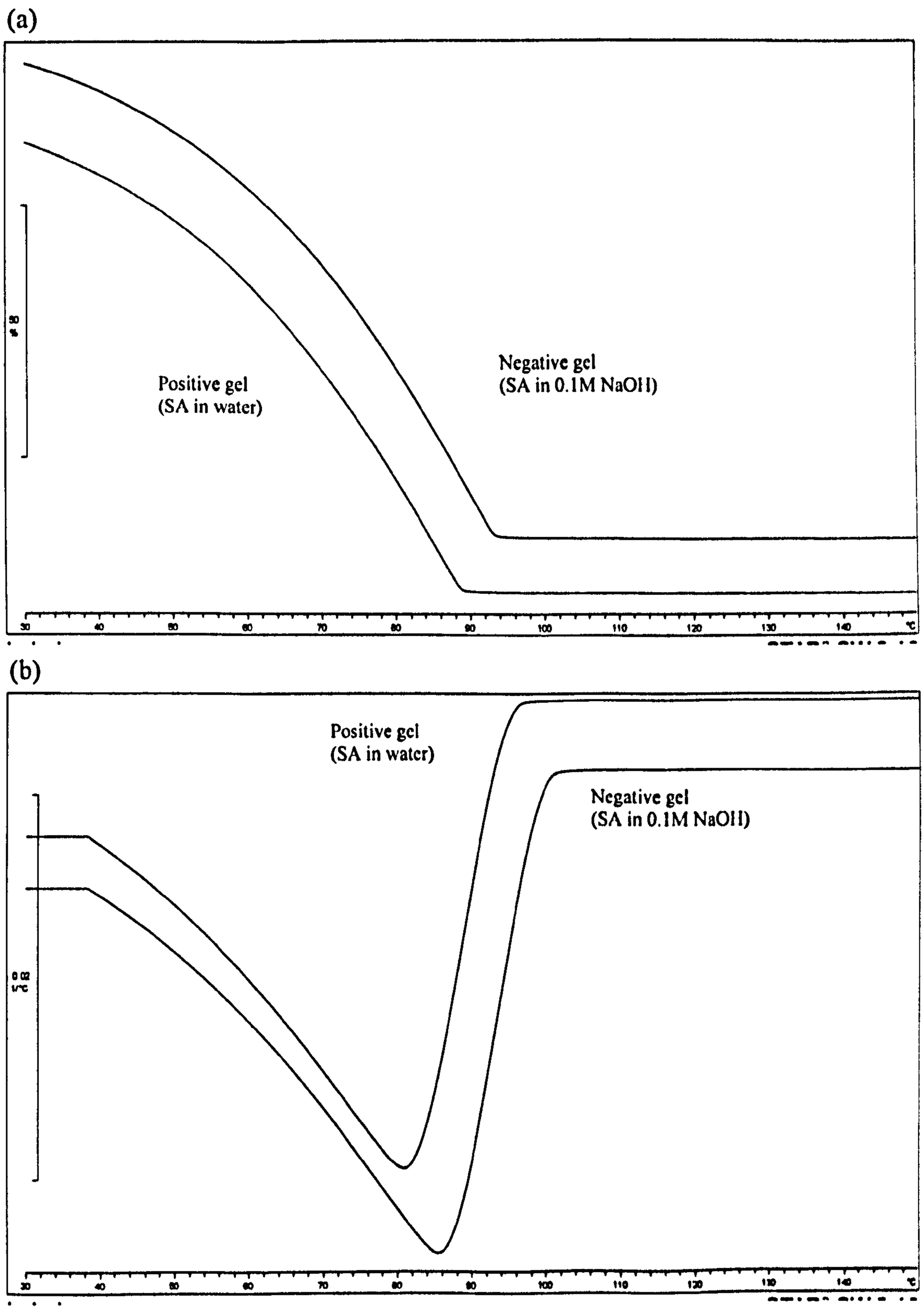

Figure 7.3: TGA plots for negative and positive control SA gels (a) and their first integration (b).

The total water (%) contained in positive and negative control gels determined using TGA is shown in Table 7.3 below.

Table 7.3: Total water loss and bound water measured in 5% w/v SA gels.

Gel		Gel moisture content (%)
Negative control	5% w/v SA gel (in 0.1M NaOH)	94.57
Positive control	5% w/v SA gel (in water)	89.83

7.3.2.4 Microscopy

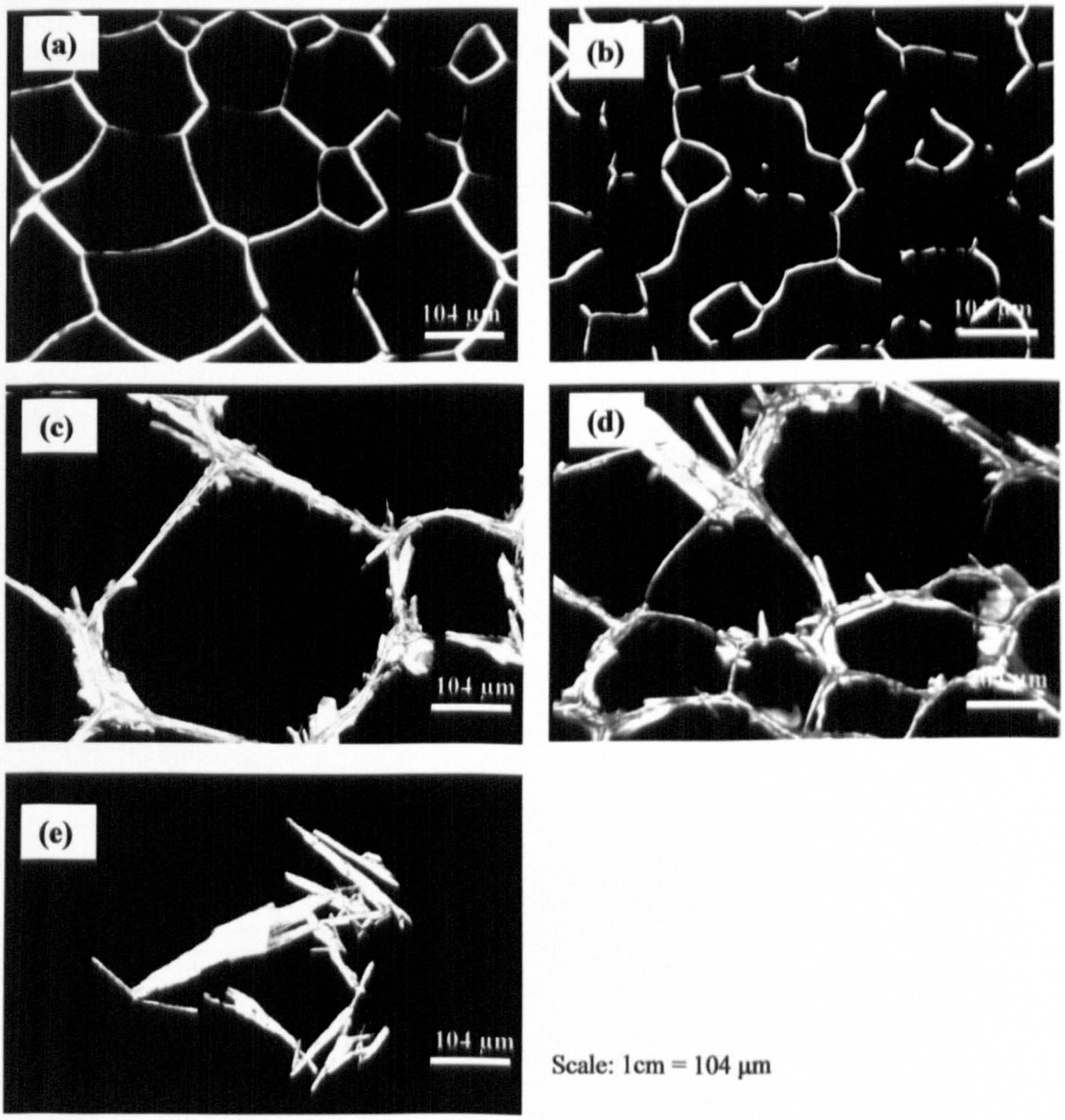

Scale: 1cm = 104 µm

Figure 7.4: Microscopic pictures of lyophilised wafers under polarised light. (a) 5% w/v SA gel prepared in water (Control). (b) 5% w/v SA gel prepared in 0.1M sodium hydroxide. (c) Ibuprofen saturated 5% w/v SA gel prepared in 0.1M sodium hydroxide – fresh preparation. (d) Same preparation as (c) but the gel was 1-week old. (e) ibuprofen crystals.

The lyophilised wafers observed under polarised microscope are shown in Figure 7.4. These microscope views are in fact a good representation of showing gel two-dimensional

structures. All the lyophilised samples had crystalline straight chains forming a porous network. The lyophilised positive control SA gel showed a well defined, interconnecting 'web-like' structures (Fig. 7.4 (a)); but the 'web' became less evident when SA wafers was prepared in 0.1M sodium hydroxide (Fig. 7.4 (b)); the network was less 'continuous' and 'short filaments' were observed. In the saturation of ibuprofen, crystal solids were found concentrated along the cross-linkages, as seen in Fig 7.4 (c). When the same gel was examined after 1 week, crystal growth was observed. Figure 7.4(e) was a view of ibuprofen crystals.

7.3.3 Franz cell studies

After freeze-drying, the wafer appeared as brown glassy sponges deposited at the lower end of the donor cell. Before the drug release from wafers was carried out, the wafers (prepared *in situ*) in the donor cell was reconstituted into gel via adding the calculated amount of water loss from freeze-drying process. Figure 7.5 shows a typical image of donor with reconstituted gel.

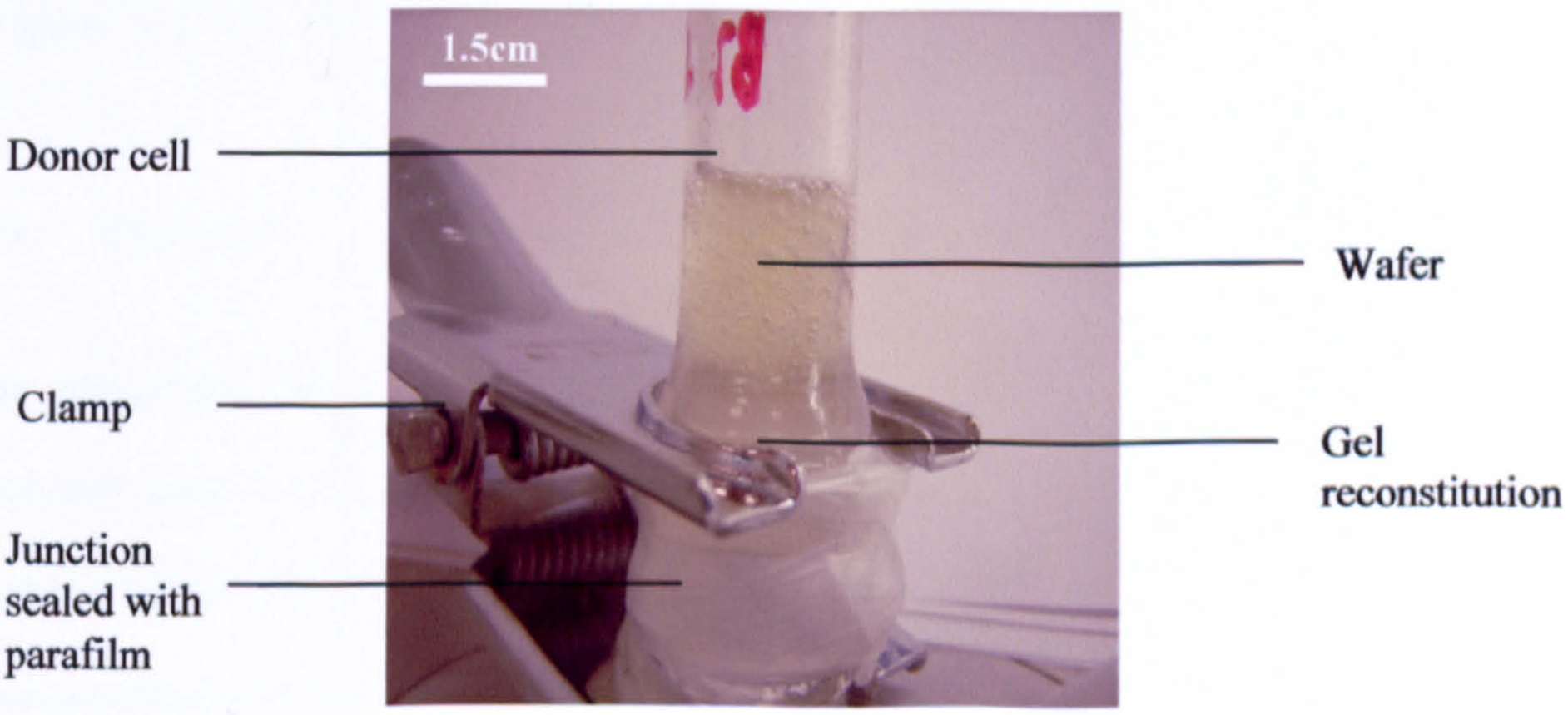

Figure 7.5: Gel reconstitution (after 15 min) from wafer in Franz cell donor.

The ibuprofen cumulative drug release from gel and wafers are shown in Figure 7.6 below. The ibuprofen flux from gel was 2.55 mg/cm^2/h but was lower from wafer, i.e. 1.54 mg/cm^2/h (both CV < 5%).

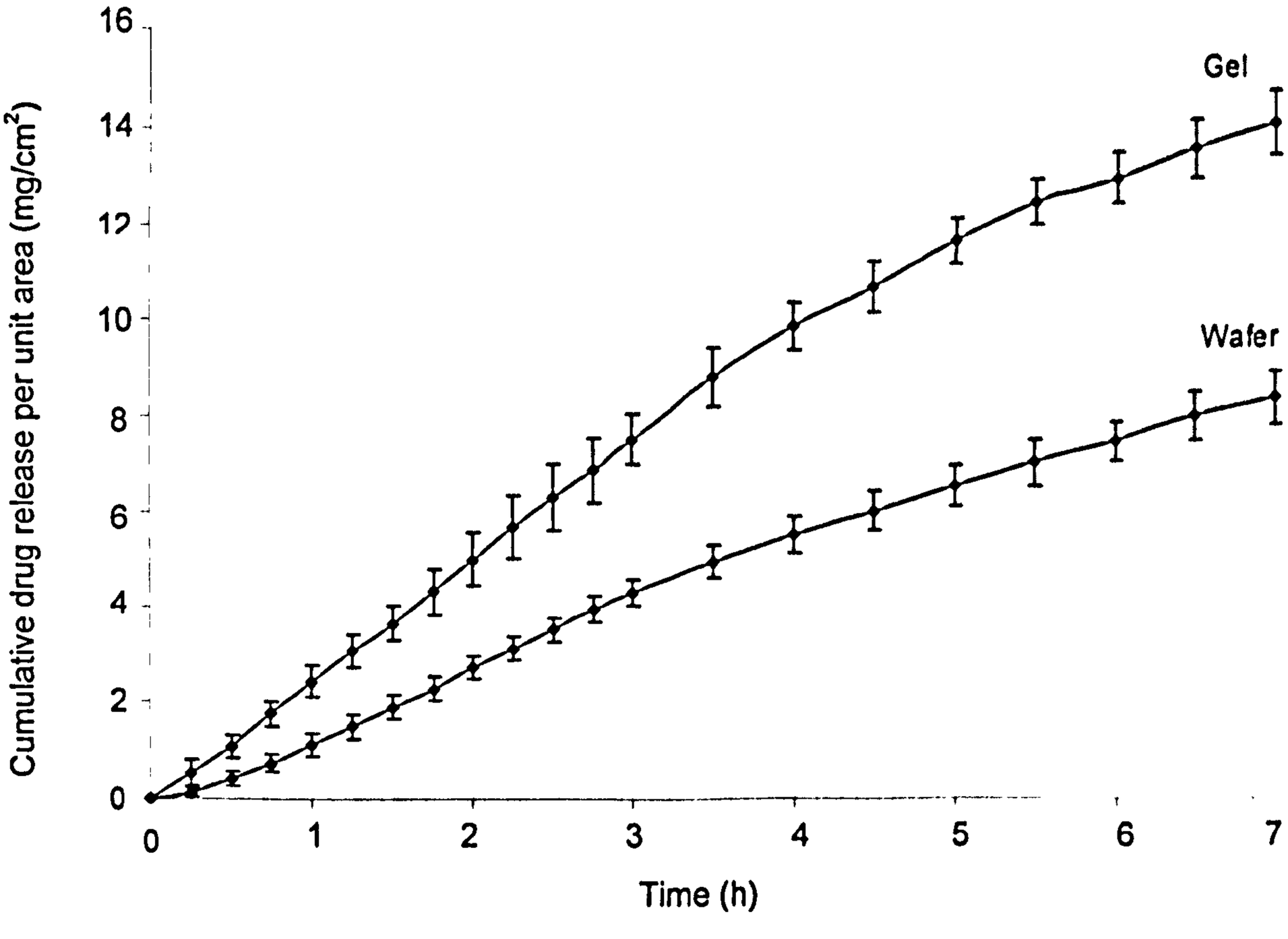

Figure 7.6: Cumulative ibuprofen drug release from 5% SA gel and wafer (n = 6).

7.4 Discussion

By convention, the preparation of a medicated gel generally involves first dispersing the polymer into a suitable liquid medium; then the incorporation of a drug into the semisolid vehicle follows. In this study, the polymer was dispersed into the 0.1M sodium hydroxide pre-saturated with drug (i.e. ibuprofen saturated solution), not directly into the 0.1M sodium hydroxide because the preliminary gel studies showed that the latter did not produce a stable gel. The rheological data revealed the SA in 0.1M sodium hydroxide (negative control gel, pH 13) was three times less viscous compared to the positive control gel, SA prepared in

water (pH 7). The instability of SA gel in the alkaline medium was also supported by TGA evidence, where the SA polymer in negative control gel contained larger amount of free water compared to the positive control gel. This indicates that the SA gel lost its viscous characteristics in alkaline medium but not in neutral solutions. It was reported that as a function of pH, the alginates degradation is at its minimum at nearly neutral pH and increases in both directions [Haug and Larsen, 1963]. The increased instability at pH <5 is explained by a acid hydrolysis, whereas reaction responsible for the degradation at pH 10 and above is the β-alkoxy elimination [Haug and Larsen, 1963; Haug *et al.*, 1963], i.e. breakage of the glycosidic bond. In inherent to this, the freeze-dried wafer of the negative control gels showed the disrupted network; indicating the SA fails to form a stable gel in 0.1M sodium hydroxide, such as in water.

Ibuprofen is a weak acid (pKa 4.5); when it was saturated in 0.1M sodium hydroxide, the ibuprofen neutralised the alkaline medium and produced a neutral solution. Since the SA polymer is stable in a neutral medium, so theoretically, the SA polymer was able to form stable gel in the ibuprofen saturated solution. The evidence of stable gel was shown by the micrographs, where the ibuprofen saturated gel presented a continuous web-like structure similar to the positive control gel. The gel prepared in the ibuprofen saturated solution (pH 7.2) also showed similar apparent viscosities as positive control gel (pH 7), showing that the SA polymer was not broken down in the ibuprofen saturated solution.

From the DSC plots, the small peaks (from 27 to 48.5 °C) observed in negative control gel was due to the continuous condensation of water below the pan lid and dripping back into the sample, because there was large amount of free water present in the gel. The sharp endotherm (49.4 °C) observed thereafter was the energy absorbed for the dissociation of physical bonds held between the residues causing the disentanglements of the alginate

polymeric chains. On the contrary, the DSC plots of positive control gel and ibuprofen saturated gel did not show such distinct peak, indicating there the gels were rather stable upon heating. Nevertheless, if observed carefully, there were vague endotherm peaks at about 51°C in these gels which shows that there might be a small degree of polymer dissociation but this was considered to be a minor event. The peak occurred at 61.3 °C for ibuprofen saturated gel was believed to be the shift in melting point of ibuprofen (pure ibuprofen Mp: 78 °C). The decreased in melting point might due to the interaction of ibuprofen with the polymer. The lyophilised ibuprofen saturated gel micrographs observed under polarised light demonstrated that ibuprofen had interacted with the polymer, where the ibuprofen crystals were found concentrated along the polymer chains. The ibuprofen may have interacted with the gel possibly via hydrophobic interaction. And this was an interesting observation because the SA cross-linkages might act as a 'reservoir' for hydrophobic drugs. When the same gel was again lyophilised after a week, apparent crystal growth was observed on the polymer chain, indicating that the crystals were indeed ibuprofen crystals. The ibuprofen saturated gel was also appeared to be of similar apparent viscosities compared to the positive control SA gel alone, with values of 1.05 and 1.19 Pa.s (at 500 s^{-1}) respectively. On the first impression it may seem like the high viscosity may be attributed presence of ibuprofen crystals, but the micrographs also shows that the presence of ibuprofen may have stabilised the gel via interacting with each other.

Till today, little work has been done assessing drug release from wound dressing wafers or sponges. The drug release from wafer for wound dressing has been undertaken using dissolution apparatus which designed for oral dosage form drug release [Lai *et al.*, 2003] and also on a diffusion cell for examining drug permeation across palatal mucosa [Boateng, 2005]. However, these methods were adapted from oral dissolution drug release guidelines and could not served as a standard procedure for wound drug application.

This work introduced the Franz cell as the recommended test for wound formulation *in vitro* testing and this method may have offered several advantages. Firstly, the donor compartment of Franz cell kept the formulation below body temperature (~33°C), a similar temperature to wound and skin lesion hence creating a more realistic condition for *in vitro* investigation for wound. While the dissolution apparatus maintains the whole system at 37 °C, which is not the realistic condition if drug formulation is applied onto a wound or skin. Temperature was particularly important because it has influence on the reconstituted gel consistency (wafer absorbed moist from moisture of the wound and air) which in turn affects the rate of drug released from the matrix. On top of that, the wafers in the donor cell are applied on a wet surface (wetted membrane), which resembled a suppurating wound. Because wafers are fragile glassy material, extra caution is required while handling the wafers. This had led to another advantage of using Franz cell, in which the wafers can be prepared in the donor (made of glass). No cutting or trimming of the wafers for fitting the wafer into the donor is required, which avoid the risk of damaging the fragile matrix.

The Franz cell ibuprofen drug release studies showed that wafers release drug at a slower rate compared to its gel; no lag time was observed for both formulations. Since the thermodynamic activities in the vehicles were the same (saturated formulation), this indicated that wafers as a drug vehicle acted as a rate-limiting factor in controlling the ibuprofen drug release. The different in drug release observed was solely controlled via the formulations. In the gel, the dissolved ibuprofen was present in the free bulk solvent within the porous gel network as well as along the polymer chain as observed previously. The ibuprofen release from gel took place via diffusion across the bulk solvent within the porous matrix and diffused into the receptor down the concentration gradient. As the ibuprofen molecules were depleted from the bulk solution, the ibuprofen deposited onto the polymer would redissolved into the bulk solution and became readily available for diffusion. As for

the wafers, the glassy sponges were presented dry in the donor. But they were left to reconstitute into gel in the donor in order for the gelation to take place as well as to prevent the fluid absorption from the receptor compartment during the course of study. The wafers absorbed water leading to relaxation (hydration of glassy polymer to a soft rubber), swelling to form a thick gel and gradual dissolution of the gel to form a viscous solution. The gel formation was thought to be the additional step in wafer which caused the slower release of the drug by viscous resistance to diffusion compared to gel.

7.5 Conclusions

1. The rheology, thermal and microscopy preliminary investigations concluded that sodium alginate did not form a stable gel in 0.1M sodium hydroxide due to polymer degradation. A stable ibuprofen saturated gel was produced via the addition of SA into 0.1M sodium hydroxide pre-saturated with ibuprofen.
2. Ibuprofen was deposited on the cross linkages of sodium alginate suggested that a hydrophobic drug can interact with the alginate polymer chains possibly via hydrophobic interactions.
3. Franz cell was proved to be a suitable apparatus for examining wafer drug release and the slow drug release compared to gel suggested that the wafer could act as a potential controlled-release formulation.

CHAPTER VIII

GENERAL DISCUSSION AND CONCLUSIONS

Today, Franz diffusion cells are employed with excised skin or synthetic substitutes for both *in vivo* correlation investigations and/or dosage form quality assessment. Nevertheless, large result variations occur in Franz cell investigations. Previous studies have shown that large variations occur with natural skin due to biological variation; however, such variation should not occur with synthetic membranes. Synthetic membranes composed of uniform flat sheets of chemically pure polymers should be inert when used as a support rather than a barrier. Recently a world wide multi-laboratory in vitro study showed up to 10% intra-laboratory and 35% inter-laboratory variations in drug flux when PDMS (polydimethylsiloxane) was used as the model membrane [Chilcott et al., 2005]. This is a very serious issue because it not only reflects the poor consistency *in vitro* data not just within a laboratory, but also between laboratories world wide. We are not aware of any effort to rectify this problem. Nevertheless, our work implied that the poor results within laboratories may be due to un-validated apparatus and methodology. The factors identified in our laboratory included diffusion cell dimensions, stirring equipment efficiency, choice of stirring bar, and temperature control. Simple validation steps, such as physical measurement, visual observation, temperature validation were undertaken to minimise the apparatus variations. Using a synthetic membrane (Visking) and a commercial gel, our study demonstrated that drug flux variations were decreased (CV reduced from 26% to 4%) after using validated Franz cells and equipment. Using this validated equipment, the Chilcott experiment was repeated and the drug flux CV was less than 5%. It was concluded that the validation of equipment and methodology is essential prior to conducting a drug diffusion cell experiment. These factors are critical when the diffusion cells are custom-made because custom made apparatus are usually manufactured under less stringent conditions and are more likely to be variable.

Validation data should be presented as an evidence of apparatus robustness and reliability whichever type of diffusion cells is used. In addition, the validation procedure should be carried out in the laboratory from time to time as a 'good laboratory practice' to ensure the apparatus is always at its good conditions.

There were several membrane factors associated with synthetic membranes when different membranes were tested in our Franz cell studies. The preparation of excised stratum corneum, from fresh to storage and handing, before it is mounted onto the Franz cell, requires a laborious procedure. Although synthetic membranes are structurally much simpler and easy to handle compared to skin, proper membrane treatment is also very important. The stratum corneum can swell in water so often the investigator pre-saturates the stratum corneum in the receptor fluid prior to Franz cell studies. The hydration effect on the synthetic membranes were tested via soaking several synthetic membranes (Visking, Cuprophan, AN69 and Biodyne) in water and the weight gained by the membranes observed over 24 hours. We found that that some synthetic membranes, especially the cellulose membranes, if left in the water for a sufficient period of time, could absorb water up to several times their original mass. It was also noticed that the water weight gained was the most apparent if the membrane is hydrophilic in nature, e.g. Cuprophan membrane water weight gained up to 900% after 24 hour. Membrane hydration changes the membrane thickness as well as displacing air from the membrane pores. If an untreated membrane is used, not only will the membrane swell and alter the drug diffusional pathlength, it will also absorb fluids from both compartments and become saturated with a mixture of both donor and receptor solvents. Hence, the maximum absorption of a synthetic membrane is required before the test and our studies showed that 12 hours of hydration was sufficient for full hydration of most synthetic membranes.

Membrane excipients are added into the synthetic membranes such as membrane plasticiser and softener to maintain membrane suppleness and prevent brittleness. For Franz cell experiment, the plasticisers must be removed prior to full membrane performance as they may influence diffusion and/or analysis. Many investigators do not report washing or cleaning the membrane prior to the experiment, and appear to simply use the membrane after removing from packaging, while those who washed the membrane via soaking for several hours appear to assume that the membrane was clean and do not report whether they have checked whether all the membrane additives are properly removed. One example of a plasticizer, glycerin is known to be present in high amounts in cellulose membranes (Visking and Cuprophan) and polyacrylonitrile AN69 membrane. In our studies, a colorimetric assay using periodic acid Schiff (PAS) reagent was developed for glycerin detection in these membranes. To test the effect of glycerin upon drug release, two ibuprofen drug release tests from saturated solution were undertaken using AN69 (glycerin content 40-50%) membranes. In the first test, the AN69 membranes were cleaned using our standard washing procedure, while in the second test the AN69 membranes were used as received. The standard membrane washing procedure in our laboratory was devised as follows: the membranes were soaked in the receptor solution at least 12 hours at 37°C, then the membranes were gently rinsed in excess of fresh receptor solution at least twice prior to the Franz cell experiment. The PAS assay effectively showed that all the glycerin in the membrane had been removed (sensitivity up to 3.12×10^{-4} % w/v), which also indicated that our standard membrane washing procedure was effective. The drug release studying also showed that the glycerin contributed to results variability. The CV for the cleaned membrane was 5.7 % while membrane with glycerin was 13.2 %. The presence of glycerin may block pores, or leach into the receptor and interfere with subsequent analysis. Hence if a membrane of high excipient content is used, it is crucial to have an assay for that particular excipient, such as the PAS assay for glycerin, to check whether the membrane washing was effective.

An initially unexpected phenomenon was observed in Franz cells with synthetic membranes, i.e. there was a net movement of receptor fluid flow from the receptor into the donor (osmosis). In our study, a simple test was carried out to investigate this phenomenon. Ibuprofen saturated solution was placed in the donor, the receptor was filled with 0.1M sodium hydroxide (standard receptor fluid), and Cuprophan was employed as the model membrane. All the openings including the donor top and receptor arm were occluded with parafilm. After 7 hours, an increased in donor level with a corresponding 'bulge' of the parafilm at the donor top indicated that solvent had moved *from the receptor into the donor* compartment via osmosis. We also tested several types of synthetic membranes and osmosis was most evident with hydrophilic membranes like Cuprophan. Osmosis can be effectively curbed if the osmotic pressure is balanced by the addition of tonicity agents. The amount of tonicity agent required can be predicted from the van't Hoff equation. To examine the effect of osmosis on drug flux, drug release from ibuprofen saturated solution was conducted before and after the addition of tonicity agent. The results showed that the ibuprofen flux had increased by four times after the tonicity agent was used. The continual water movement into the donor cells by osmosis may have disturbed the concentration gradient, which in turn led to retardation of the drug diffusion process. Osmosis is a natural process but this is not desirable in Franz cell experiment because it dilutes the donor content and changes the thermodynamic activity. Moreover, if semisolid dosage forms are used, osmosis may disrupt the semisolid structure and changes the vehicle properties. This phenomenon has not been highlighted in the literature. Investigators may fail to spot osmosis if the donor is left unoccluded or only a small amount (< 500 μL) of donor volume is used. We showed that osmosis influences drug flux. Osmosis in the Franz cell is particularly crucial if a cellulose membrane is employed because the incident of osmosis demonstrated to be high. If so, this may also suggest that hydrophilic membranes such as Cuprophan should be avoided in Franz

cell studies. Henceforth, the validation of osmosis would become an essential compulsory procedure in addition to a series of validation procedure prior to Franz cell experiment.

Since the recommendation by the FDA of the use synthetic membranes with Franz cells as a promising tool for topical dosage forms assessment, many types of synthetic membranes have been employed as model membranes. Although there is no strict standards for in vitro research regarding formulation comparison using synthetic membranes, generally the criteria of selection of an 'appropriate' membrane being recently defined [Flynn *et al.*, 1999]. These include (1) minimal diffusional resistance between the donor and the receptor, (2) little interaction with the vehicle, (3) do not bind to the drug, and (4) easy to obtain and commercially available. Nevertheless, many synthetic membranes today possess such properties, so investigators still enjoy the freedom of choosing the most 'appropriate' membrane. It is generally understood that the synthetic membrane in quality control acts as a support only to prevent the mixing of the formulation and the receptor medium. Membranes with pores are often chosen because they are assumed to offer no diffusional resistance due to the fact that the drug released from the vehicle would directly dissolve in the fluid in the pores and be carried into the receptor medium via the concentration gradient. From our study, we have screened twelve types of porous synthetic membranes. Most of the membranes employed in this study were commercially available membranes and some are derived from other applications. Using ibuprofen as the model drug, the flux measured grouped the 12 membranes into two categories, i.e. high-flux (8 – 18 mg/cm^2/h) and low-flux (1.4 – 3 mg/cm^2/h). Riboflavin, a hydrophilic drug, also showed similar membrane groupings. Despite being porous, it was apparent that all the membranes examined performed differently. Some of the synthetic membranes were shown to be more rate-limiting to ibuprofen compared to the others. It was noticed that the high flux membranes were mostly of the polymeric type while low flux membranes were cellulose-type

membranes. This shows that synthetic microfiltration membranes are in fact a better membrane candidate for quality control compared to the cellulose-based membrane. The dissimilarity in drug flux produced was due to the physical characteristics of the membrane such as membrane porosity and tortuosity. A diversity of synthetic membranes varying in pore size, thickness, and chemical nature are described in the literature and this makes comparison between experiments difficult. Membrane tortuosity may play a vital role in determining drug flux because our study shows that the least tortuous the membrane pore, the higher the flux. Apart from the requirements stated by the FDA, additional factors should be considered when choosing a membrane, i.e. the membrane should be within the 'high flux' category, membrane tortuosity close to 1, high porosity (>60%) and that the membrane should not contain any filler or support.

Although the riboflavin shows the same membrane groupings to that of ibuprofen, the riboflavin drug flux within the low flux membranes is different to that of ibuprofen. The influence of log P of the drug may play a role. Ibuprofen and riboflavin possess extreme log P values of 3.4 and -1.4 respectively. The parabens show increasing log P values with an increasing number of hydrocarbon groups. The drug release of four parabens, i.e. methyl-, ethyl-, propyl- and butylparaben from saturated solution into the three membranes (Visking, Biodyne and PDMS) were investigated. From the membrane partition coefficients and flux measurements, it was proposed that the butylparaben may have hydrophobic interactions with Biodyne (hydrophobic) membranes. This must be added into the consideration when choosing a synthetic membrane. If a very lipophilic drug such as butylparaben (log P close to 4) is used, it is advisable not to choose a membrane which may promote drug interactions.

Lyophilised wafers are potential dosage forms for wound healing. In our studies, the wafers were made from sodium alginate. The ibuprofen saturated wafers were produced by adding

the alginate polymers into the 0.1M sodium hydroxide saturated with ibuprofen. The preliminary evidences of rheology, thermal analysis and microscopy showed that the sodium alginate gel formed a stable three-dimensional gel network in ibuprofen saturated solution, but not in the 0.1M sodium hydroxide alone. High pH was thought to be the main determinant factor for the destabilisation of the gel. The presence of ibuprofen drug appears to stabilise the polymer gel network, which was clearly observed microscopically under crossed polars. The fact that the wafers showed a slow, steady release of ibuprofen drug shed light onto designing a wound healing dressing with drug controlled-release effect. Using the validated Franz cell and equipment, the Franz cells were shown to be a suitable tool for examining drug release from the wafer. The Franz cells are shown not only to be useful for testing conventional semisolid dosage forms, but also for testing drug release from novel topical dosage forms such as the alginate wafers.

In summary, the validation of Franz cells and experimental variables eliminated the source of result variability. Not all the synthetic membranes are suitable for topical formulation quality assessment. The considerations of choosing a membrane should include the membrane properties as well as the drug log P. And finally, the validated Franz cells were shown to be a suitable method for testing a variety of formulations.

Appendix

Riboflavin degradation studies in model receptor fluid (0.1M NaOH).

(c.f. Chapter 5, p.154)

50 mL of 0.05 M of riboflavin solution in 0.1M sodium hydroxide was prepared. The concentration of the solution was measured using UV spectrophotometer on the day of preparation. The solution was stored in a tight screw glass transparent jar on an open bench at room temperature. The concentration of the solution was determined again at day 2, 3 and 7. The riboflavin concentration was plotted over 7 days was shown in Figure A. The riboflavin degradation was approximately half its original concentration after one week of storage. This showed that the riboflavin degrades in alkaline solution with time.

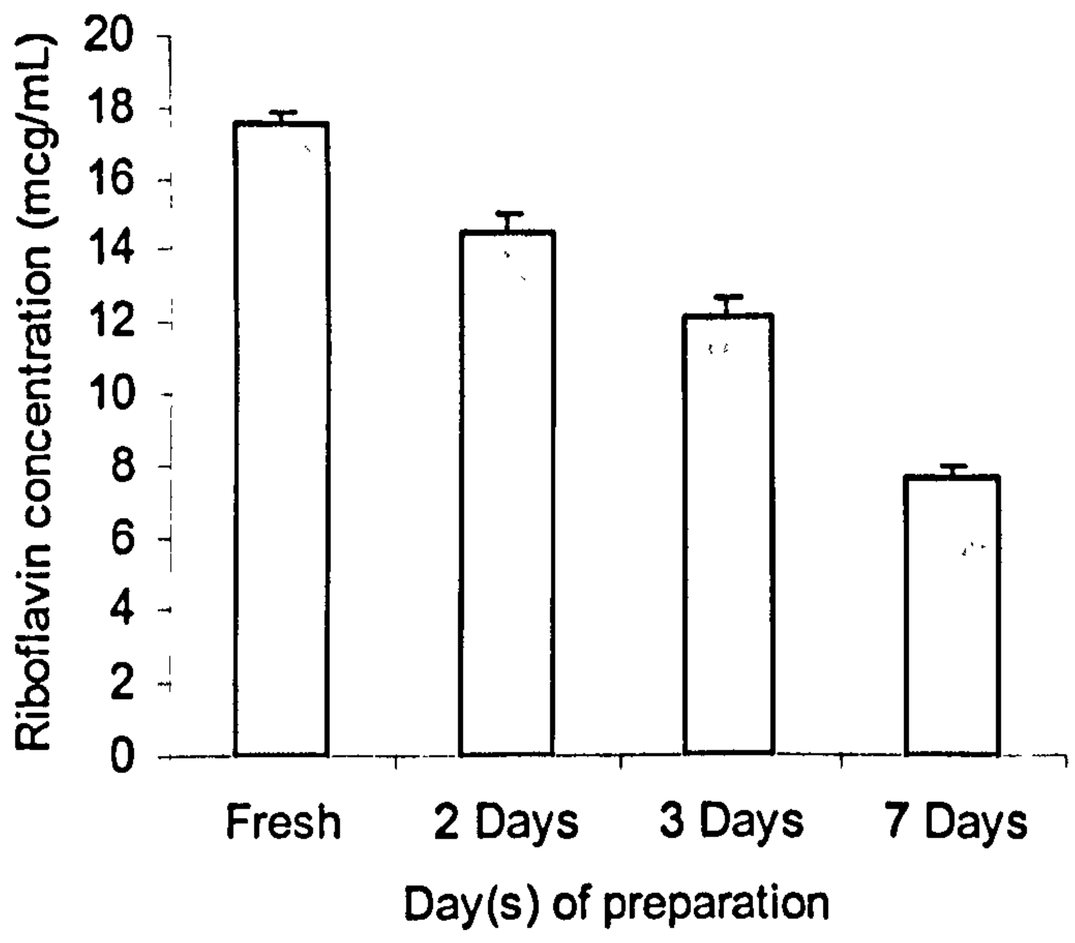

Figure A: Riboflavin in 0.1M sodium hydroxide concentration plot over 7 days (n=3).

References

ABITEC Corp., Product Information. Capmul: Your Clear Solution. Abitec Group USA.

Abraham M. H., Chanda H. S., Mitchell R. C., (1995). The factors that influence skin penetration of solutes. J Pharm Pharmacol, 47, 8-16.

Adami G., Larese F., Venier M., Barbieri B., Lo Coco F., Reisenhofer E., (2006). Penetration of benzene, toluene and xylenes contained in gasoline thorugh human abdominal skin *in vitro*. Toxic in vitro, 20, 1321-1330.

Addicks W. J., Flynn G. L., Weiner N., (1987). Validation of a flow-through diffusion cell for use in transdermal research. Pharm Res, 4, 337-341.

Advanced Instrument. The Advanced Osmoster Model 3D3 User Guide. Massachusettes, USA.

Akomeah F., Nazir T., Martin G. P., Brown M. B., (2004). Effect of heat on the percutaneous absorption and skin retention of three model penetrants. Eur J Pharm Sci, 21, 337-345.

Astley J. P., Levine M., (1976). Effect of dimethyl sulfoxide on permeability of human skin in vitro. J Pharm Sci, 65, 210-215.

Auner B. G., Valenta C., (2004). Influence of phloretin on the skin permeation of lidocaine from semisolid preparations. Eur J Pharm Biopharm, 57, 307-312.

Avdeef A., Box K. J., Comer J. E., Gilges M., Hadley M., Hibbert C., Patterson W., Tan K. Y., (1999). PH-metric log P 11. pKa determination of water-insoluble drugs in organic solvent-water mixtures. J Pharm Biomed Anal, 20, 631-641.

Baddiley J., Buchanan J. G., Handschumacher R. E., Prescott J. F., (1956). Chemical studies in the biosynthesis of purine nucleotides. Part 1. The preparation of N-glycylglycosylamines. J Chem Soc (London), 2818-2823.

Badkar A., Talluri K., Tenjarla S. N., Jaynes J., Banga A. K., (2000). *In vitro* release testing of a peptide gel. Pharm Tech, 24, 44-52.

Baker R. W., (2004a). Membrane transport theory. In: Membrane technology and application, Baker R. W. (Ed), Vol. 2nd, England, J. Wiley, 15-84.

Baker R. W., (2004b). Overview of membrane science and technology. In: Membrane technology and application, Baker R. W. (Ed), Vol. 2nd, England, J. Wiley, 1-14.

Baker R. W., (2004c). Reverse osmosis. In: Membrane technology and application, Baker R. W. (Ed), Vol. 2nd, England, J. Wiley, 191-236.

Barnes H. A., Hutton J. F., Walters K., (1989). Normal Stresses. In: An introduction to rheology, Barnes H. A., Hutton J. F., Walters K. (Ed), New York, Elsevier science, 55-74.

Barry B. W., (1983). Methods for studying percutaneous absorption. In: Dermatological formulations. Percutaneous absorption., Barry B. W. (Ed), New York, Marcel Dekker, Inc, 234-280.

Barry B. W., (2002). Drug delivery routes in skin: a novel approach. Adv Drug Deliv Rev, 54, S31-S40.

Barry B. W., Harrison S., Dugard P. H., (1985). Correlation of thermodynamic activity and vapour diffusion through human skin for the model compound, benzyl alcohol. J Pharm Pharmacol, 37, 84-90.

Bashford C. L., (1987). UV Spectrophotometer. In: Spectrophotometry and spectrofluorimetry, Bashford C. L., Harris D. A. (Ed), Oxford, IRL Press, 13-47.

Bellomo R., Ronco C., (2001). An Introduction to continuous renal replacement therapy. In: Altlas of hemodialysis, Bellomo R., Baldwin I., Ronco C., Thomas G. (Ed), Vol. 1, London, Bailliere Tindall, 1-10.

Bierenbaum H. S., Isaacson R. B., Druin M. L., Plovan S. G., (1974). Microporous polymeric films. Ind Eng Chem Proc Res Dev, 13, 2-9.

Bin T., Kulshreshtha A. K., Al-Shakhshir R., Hem S. L., (1999a). Adsorption of benzalkonium chloride by filter membranes: mechanism and effect of formulaion processing parameters. Pharm Dev Tech, 4, 151-165.

Bin T., McCrosky L., Kulshreshtha A. K., Hem S. L., (1999b). Adsorption of esters of p-hydroxybenzoic acid by filter membranes: Mechanism and effect of formulation and processing parameters. Pharm Dev Tech, 5, 95-104.

Boateng J. S., (2005). Development of formulations for delivery of drugs to wounds. Ph.D. Thesis thesis, University of Strathclyde, Glasgow, UK.

Bonferoni M. C., Rossi S., Ferrari F., Caramella C., (1999). A modified Franz diffusion cell for simultaneous assessment of drug release and washability of mucoadhesive gels. Pharm Dev Tech, 4, 45-53.

Bouwstra J., Gooris G., Spek J. v. d., Lavrijsen S., Bras W., (1994). The lipid and protein structure of mouse stratum corneum: a wide and small angle diffraction study. Biochim Biophys Acta, 1212, 183-192.

Bronaugh R. L., Stewart R. F., (1985). Methods for percutaneous absorption studies IV. The flow through diffusion cell. J Pharm Sci, 74, 64-67.

Brown M. B., Hanpanitcharoen M., Martin G. P., (2000). An *in vitro* investigation into the effect of glycosaminoglycans on the skin partitioning and deposition of NSAIDs. Int J Pharm, 225, 113-121.

Chattaraj S., Kanfer I., (1995). Release of acyclovir from semisolid dosage forms: a semi-automated procedure using a simple plexiglass flow-through cell. Int J Pharm, 125, 215-222.

Chattaraj S., Kanfer I., (1996). 'The insertion cell': a novel approach to monitor drug release from semi-solid dosage forms. Int J Pharm, 133, 59-63.

Chenoweth D. E., Cheung A. K., Henderson L. W., (1983). Anaphylatoxin formation during hemodialysis: Effects of different dialyzer membranes. Kidney Int, 24, 764-769.

Chilcott R. P., Barai N., Beezer A. E., Brain S. I., Brown M. B., Bunge A. L., Burgess S. E., Cross S., Dalton C. H., Dias M., Farinha A., Finnin B. C., Gallagher S. J., Green D. M., Gunt H., Gwyther R. L., Heard C. M., Jarvis C. A., Kamiyama F., Kasting G. B., Ley E. E., Lim S. T., McNaughton G. S., Morris A., Nazemi M. H., Pellett M. A., Plessis J. D., Quan Y. S.,

Raghavan S. L., Roberts M., Romonchuk W., Roper C. S., Schenk D., Simonsen L., Simpson A., Traversa B. D., Trottet L., Watkinson A., Wilkinson S. C., Williams F. M., Yamamoto A., Hadgraft J., (2005). Inter- and intra-laboratory variation of *in vitro* diffusion cell measurements: An international multi-centre study using quasi-standardised methods and materials. J Pharm Sci, 94, 632-638.

Cho Y. J., Choi H. K., (1998). Enhancement of percutaneous absorption of ketoprofen: effect of vehicles and adhesive matrix. Int J Pharm, 169, 95-104.

Clarys P., Alewasters K., Jadoul A., Brel A., Manadas R. O., Preat V., (1998). *In vitro* percutaneous penetration through hairless rate skin: in fluence of temperature, vehicle, penetration enhancers. Eur J Pharm Biopharm, 46, 279-283.

Clement P., Laugel C., Marty J.-P., (2000). Influence of three synthetic membranes on the release of caffeine from concentrated w/o emulsions. J Controlled Release, 66, 243-254.

Clowes H. M., Scott R. C., R H. J., (1994). Skin absorption: flow-through or static diffusion cells. Toxic *in vitro*, 8, 827-830.

Cooper E., Iqbal A., Bartlett C., Marriott C., Whitefield P. J., Brown M. B., (2004). A comparison of topical formulations for the prevention of human schistosomiasis. J Pharm Pharmacol, 56, 957-962.

Corbo M., (1995). Techniques for conducting *in vitro* release studies on semisolid formulations. Disso Tech, 2, 3-6.

Corbo M., Schults T. W., K W., van Buskirk G. A., (1993). Development and validation of *in vitro* release testing methods for semisolid formulations. Pharm Tech, 9, 112-128.

Cordoba-Diaz M., Nova M., Elorza B., Cordoba-Diaz D., Chantres J. R., Cordoba-Borrego M., (2000). Validation protocol of an automated in-line flow-through diffusion equipment for *in vitro* permeation studies. J Controlled Release, 69, 357-367.

Cronin M. T. D., Dearden J. C., Moss G. P., Murray-Dickson G., (1998). Investigation of the mechanism of flux across human skin in vitro by quantitative structure-permeability relationship. Eur J Pharm Sci, 7, 325-330.

Dempski R. E., Portnoff J. B., Wase A. W., (1969). In vitro release and in vivo penetration studies of a topical steroid from non-aqueous vehicles. J Pharm Sci, 58, 572-582.

Dias M., Farinha A., Faustino E., Hadgraft J., Pais J., Toscano C., (1999). Topical delivery of caffeine from some commercial formulations. Int J Pharm, 182, 41-47.

Dias M., Raghavan S. L., Hadgraft J., (2001). ATR-FTIR spectroscopic investigation on the effect of solvents on the permeation of benzoic acid and salicylic acid through silicone membranes. Int J Pharm, 216, 51-59.

Diembeck W., Beck H., Benech-Kieffer F., Courtellemont P., Dupuis J., Lovell W., Paye M., Spengler J., Steiling W., (1999). Test guidelines for *in vitro* assessment of dermal absorption and percutaneous penetration of cosmetic ingredients. Food Chem Toxicol, 37, 191-205.

Draget K. I., Smidsrød O., Skjak-Bræk G., (2005). Alginates from algae. In: Polysaccharides and polyamides in the food industry. Properties, production and patents., Steinbuchel A., Rhee S. K. (Ed), Vol. 1, Weinheim, Wiley-VCH, 1-30.

EC, (2004). European Commission. Health and consumer protection directorate, directorate E. Guidance document on dermal absorption. Sanco/222/2000 rev. 7.

Eccleston G. M., (1990). Multiple-phase oil-in-water emulsions. J Soc Cosmet Chem, 41, 1-22.

Eccleston G. M., (1997). Functions of mixed emulsifiers and emulsifying waxes in dermatological lotions and creams. Colloids Surf A Physicochem Eng Asp, 123, 169-182.

Elias P. M., (1983). Epidermal lipids, barrier function, and desquamation. J Invest Dermatol, 80 Suppl, 44s-49s.

FDA-SUPAC-SS, (1997). Guidance for Industry. SUPAC-SS Non-sterile Semisolid Dosage Forms. Scale-up and Postapproval Changes: Chemistry, Manufacturing and Controls. In vitro Release Testing and In Vivo Bioequivalence Documentation.

Fenske D. B., Thewalt J. L., Bloom M., Kitson N., (1994). Models of stratum corneum intercellular membranes: ^{2}H NMR of macroscopically oriented multilayers. Biophys J, 67, 1562-1573.

Ferry J. D., (1936). Ultrafilter membranes and ultrafiltration. Chem Rev, 18, 373.

Fleischner R. L., Alter H. W., Furman S. C., Price P. B., Walker R. M., (1972). Particle track etching. Science, 172, 225-263.

Flynn G. L., Shah V. P., Tenjarla S. N., Corbo M., DeMagistris D., Feldmann T. G., Franz T. J., Miran D. R., Pearce D. M., Sequiera J. A., Swarbrick J., Wang C. T., Yacobi A., Zatz J. L., (1999). Assessment of value and applications of *in vitro* testing of topical dermatological drug products. Pharm Res, 16, 1325-1330.

Franz T. J., (1975). Percutaneous absorption. On the relevance of *In vitro* data. J Invest Dermatol, 64, 190-195.

Franz T. J., (1978). The finite dose technique as a valid in vitro model for the study of percutaneous absorption. Curr Probl Dermatol, 7, 58-68.

Franz T. J., (1983). Review: Kinetics of Cutaneous Drug penetration. Int J Dermatol, 22, 499-505.

Friend D., Catz P., Heller J., Okagaki M., (1989). Transdermal delivery of Levonorgestrel IV: Evaluation of membranes. J Pharm Sci, 78, 477-481.

Friend D. R., (1992). *In vitro* skin permeation techniques. J Control Release, 18, 235-248.

Frum Y., Bonner M. C., Eccleston G. M., Meidan V. M., (2007). The influence of drug partition coefficient on follicular penetration: *In vitro* human skin studies. Eur J Pharm Sci, 30, 280-287.

Gale E. F., Folkes J. P., (1965). The Incorporation of glycerol and lysine into the lipid fraction of staphyloccoccus aureus. Biochem J, 94, 390-400.

Gallagher S. J., L T., Carter T. P., Heard C. M., (2003a). Effects of membrane type and liquid/liquid phase boundary on *in vitro* release of Ketoprofen from gel formulations. J Drug target, 11, 373-379.

Gallagher S. J., Trottet L., Heard C. M., (2003b). Ketoprofen: release from, permeation across and rheology of simple gel formulations that simulate increasing dryness. Int J Pharm, 268, 37-45.

Gay C. L., Guy R. H., Golden G. M., Mak V. H., Francoeur M. L., (1994). Characterization of low-temperature (i.e., < 65 degrees C) lipid transitions in human stratum corneum. J Invest Dermatol, 103, 233-239.

Giordano F., Bettini R., Donini C., Gazzaniga A., Caira M. R., Zhang G. G., Grant D. J., (1999). Physical properties of parabens and their mixtures: *solubility in water, thermal* behavior, and crystal structures. J Pharm Sci, 88, 1210-1216.

Grubauer G., Feingold K. R., Harris R. M., Elias P. M., (1989). Lipid content and lipid type as determinants of the epidermal permeability barrier. J Lipid Res, 30, 89-96.

Gummer C. L., Hinz R. S., Maibach H. I., (1987). The skin penetration cell: a design update. Int J Pharm, 40, 101-104.

Guzek D. B., Kennedy A. H., McNeil S. C., Wakshull E., Potts R. O., (1989). Transfermal drug transport and metabolism I: Comparison of in vitro and in vivo results. Pharm Res, 6, 33-39.

Hadgraft J., (2001). Skin, the final frontier. Int J Pharm, 224, 1-18.

Haigh J. M., Smith E. W., (1994). The selection and use of natural and synthetic membranes for *in vitro* diffusion experiments. Eur J Pharm Sci, 2, 311-330.

Halary J. L., Noel C., Monnerie L., (1980). Analysis of transport phenomena in cellulose diacetate membranes III. General relationships between hydration and dialysis coefficients of unilayer membranes. Polymer Bulletin, 2, 89-96.

Hansch C., Leo A., Hoekman D., (1995). Exploring QSAR - Hydrophobic, Electronic, and Steric Constants. American Chemical Society Washington, pp 368.

Hashimoto T., Suzuki Y., Suzuki K., Nakashima T., Tanihara M., Ide C., (2005). Peripheral nerve regeneration using non-tubular alginate gel crosslinked with covalent bonds. J Mater Sci Mater Med, 16, 503-509.

Hatanaka T., Inuma M., Morimoto Y., (1990). Prediction of skin permeability of drugs. 1. Comparison with artificial membrane. Chem Pharm Bull, 38, 3452-3459.

Hatanaka T., Inuma M., Sugibayashi K., Morimoto Y., (1992). Prediction of skin permeability of drugs .2. Development of composite membrane as a skin alternative. Int J Pharm, 79, 21-28.

Haug A., Larsen B., (1963). The solubility of alginate at low pH. Acta Chem Scand, 17, 1653-1662.

Haug A., Larsen B., Smidsrød O., (1963). The degradation of alginates at different pH values. Acta Chem Scand, 17, 1466-1468.

He P., Davis S., Illum L., (1998). In vitro evaluation of the mucoadhesive properties of chitosan microspheres. . Int J Pharm, 166, 75-68.

Heard C. M., Johnson S., Moss G., Thomas C. P., (2006). *In vitro* transdermal delivery of caffeine, theobromine, theophylline and catechin from extract of Guarana, *Paullinia Cupana* Int J Pharm, 317, 26-31.

Henis J. M. S., Tripodi M. K., (1980). A novel approach to gas separation using composite hollow fibers membranes. Sep Sci Tech, 15, 1059-1063.

Hoang V. D., (2005). The influence of excipient composition and functionality on the microstructure of fatty alcohol. Ph. D. Thesis thesis, University of Strathclyde, Glasgow.

Hoffman A., (2002). Hydrogels for biomedical applications. Adv Drug Deliv Rev, 43, 3-12.

Hollein M. E., Hammond M., Slater C. S., (1993). Concentration of dilute acetone-water solution using pervaporation. Sep Sci Tech, 28, 1043-1056.

Htchkiss R. D., (1948). The microchemical reaction resulting in the staining of polysaccharide structures in fixed tissue preparations. Arch Biochem, 16, 131-141.

Hoes D., Guy R., Hadgraft J., Heylings J., Hoeck U., Kemper F., Maibach H. I., Marty J.-P., Merk H., Parra J., Rekkas D., Rondelli I., Schaefer H., Tauber U., Verbiese N., (1996). Methods for assessing percutaneous absorption. In ECVAM Workshop report 13: Alternatives to laboratory animals. 24, 81-106.

Huang X. F., Tanojo H., Lenn J., Deng C., Krochmal L., (2005). A novel foam vehicle for delivery of topical corticosteroids. J Am Acad Dermatol, 53, S26-S38.

Illel B., Schaefer H., Wepierre J., Doucet O., (1991). Follicles play an important role in percutaneous absorption. J Pharm Sci, 80, 424-427.

Jetzer W. E., Huq A. S., Ho N. F. H., Flynn G. L., Duraiswamy N., Condie L., Jr., (1986). Permeation of mouse skin and silicone rubber membranes by phenols: relationship to in vitro partitioning. J Pharm Sci, 75, 1098-1103.

Kao J., Hall J., Helman G., (1988). *In vitro* percutaneous absorption in mouse skin: influence of skin appendages. Toxicol Appl Pharmacol, 94, 93-103.

Kasting G. B., Filloon T. G., Francis W. R., Meredith M. P., (1994). Improving the sensitivity on *in vitro* skin penetration experiments. Pharm Res, 11, 1747-1756.

Kaukonen A., Boyd B., Charman W., Porter C., (2004). Drug solubilisation behavior duing *in vitro* digestion of suspension formulations of poorly water-soluble drugs in triglyceride lipids. Pharm Res, 21, 254-260.

Khan G. M., Frum Y., Sarheed O., Eccleston G. M., Meidan V. M., (2005). Assessment of drug permeability distribution in two different model skins. Int J Pharm, 303.

Kundu S. C., Cameron A. P., Meltzer N. M., (1993). Development and validation of method for determination of *in vitro* release of retinoic acid for creams. Drug Dev Ind Pharm, 19, 125-138.

Lai H. L., Khalil A., Craig D. Q. M., (2003). The preparation and characterisation of drug-loaded alginate and chitosan sponges. Int J Pharm, 251, 175-181.

Li J. B., Rahn P. C., (1993). Automated dissolution testing of topical drug formulation using Franz cells and HPLC analysis. Pharm Tech, July, 44-54.

Liaw J., Lin Y.-C., (2000). Evaluation of poly(ethylene oxide)-poly(propylene oxide)-poly(ethylene oxide) (PEO-PPO-PEO) gel as a release vehicle for percutaneous fentanyl. J Controlled Release, 68, 273-282.

Liebenberg W., Engelbrecht E., Wessels A., Devarakonda B., Yang W., De Villers M. M., (2004). A comparative study of the release of active ingredients from semisolid cosmeceutical measured with Franz, enhancer or flow-through cell diffusion apparatus. J Food Drug Anal, 12, 19-28.

Loeb S., Sourirajan S., (1963). Sea water for demineralisation by means of an osmotic membrane. American Chemical Society, Washington, D.C., pp 117-132.

Lonsdale H. K., Merten U., Riley R. L., (1965). Transport properties of cellulose acetate osmotic membrane. J Appl Polym Sci, 9, 1341-1362.

Marriott C., (2000). Rheology and the flow of fluids. In: Pharmaceutics. The science of dosage form design, Aulton M. E. (Ed), London, Chuchill Livingstone, 17-37.

Matsuura T., (1994). Membrane material. CRC Press, Inc., pp 11-46.

Matsuzaki K., Imaoka T., Asano M., Miyajima K., (1993). Development of a model membrane systme using stratum corneum lipids for estimation of drug skin permeability. Chem Pharm Bull, 41, 575-579.

Matthews K. H., Stevens H. N. E., Auffret A. D., Humphrey M. J., Eccleston G. M., (2005). Lyophilised wafers as a drug delivery system for wound healing containing methylcellulose as a viscosity modifier. Int J Pharm, 289, 51-62.

Megrab N. A., Williams A. C., Barry B. W., (1995). Oestradiol permeation through human skin and silastic membrane: effects of propylene glycol and supersaturation. J Controlled Release, 36, 277-294.

Mettler Toledo. DSC 822^e Module Operating Instructions. Mettler Toledo Star^e System. Leicester, UK.

Mettler Toledo. TGA/SDTA851^e Module Operating Instructions. Mettler Toledo Star^e system, Leicester, UK

Meuwissen M. E., Janssen J., Cullander C., Junginger H. E., Bouwstra J. A., (1998). A cross-section device to improve visualization of fluorescent probe penetration into the skin by confocal laser scanning microscopy. Pharm Res, 15, 352-356.

Morell J. L. P., Claramonte M. D. C., Vialard A. P., (1996). Validation of a release diffusion cell for topical dosage forms. Int J Pharm, 137, 49-55.

Mulder M., (1996). Introduction. In: Basic principles of membrane technology, Mulder M. (Ed), Vol. 1, Dordrecht, Kluwer Academic Publishers, 1-20.

Ogiso T., Hirota T., Masahiro I., Hino T., Tadatoshi T., (1998). Effect of temperature on percutaneous absorption of terodiline and relationship between penetration and fluidity of stratum corneum lipids. Int J Pharm, 176, 63-72.

Ohara N., Takayama K., Nagai T., (1995). Combined effect of d-limonene pretreatment and temperature on the rat skin permeation of lipophilic and hydrophilic drugs. Biol Pharm Bull, 18, 439-442.

Pellett M. A., Castellano S., Hadgraft J., Davis A. F., (1997). The penetration of supersaturated solutions of piroxicam across silicone membranes and human skin *in vitro*. J Controlled Release, 46, 205-214.

Porter C., Kaukonen A., Taillardat-Bertschinger A., (2004). Us of *in vitro* lipid digestion data to explain the *in vivo* performance of triglycerine-based oral lipid formulations of poorly-water soluble drugs: Studies with halofantrine. J Pharm Sci, 93, 1110-1121.

Potts R. O., Guy R. H., (1992). Predicting skin permeability. Pharm Res, 9, 663-669.

Proniuk S., Dixon S. E., Blanchard J., (2001). Investigation of the utility of an *in vitro* release test for optimizing semisolid dosage forms. Pharm Dev Technol, 6, 469-476.

Richards J. H., (2000). Solution and their properties. In: Pharmaceutics. The science of dosage form design, Aulton M. E. (Ed), London, Churchill Livingstone, 38-49.

Rouse J. J., Whateley T. L., Thomas M., Eccleston G. M., (2006). Controlled drug delivery to the lung: Influence of hyaluronic acid solution conformation on its absorption to hydrophobic drug particles. Int J Pharm, 330, 175-182.

Roy S. D., Manoukian E., Combs D., (1995). Absorption of transdermally delivered ketorolac acid in humans. J Pharm Sci, 84, 49-52.

Santhanam A., Miller M. A., Kasting G. B., (2004). Absorption and evaporation of N, N-dimethyl-m-toluamide from human skin *in vitro*. Toxicol Appl Pharmacol, 204, 81-90.

Santoyo S., Arrelano A., Ygartua P., Martin C., (1996). *In vitro* percutaneous absorption of piroxicam through synthetic membranes and abdominal rat skin. Pharm Acta Helv, 71, 141-146.

Scheuplein R., (1978). The Skin as a barrier, vol. 5. Academic Press, London, pp 1669-1692.

Scheuplein R., Blank I., (1971). Permeability of the skin. Physiol Rev, 51, 702-747.

Scheuplein R., Ross L. W., (1974). Mechanism of percutaneous absorptioin. V. Percutaneous absorption of solvent deposited solids. J Invest Dermatol, 62, 353-360.

Scheuplein R. J., (1967). Mechanism of percutaneous absorption. II. Transient diffusion and the relative importance of various routes of skin penetration. J Invest Dermatol, 48, 79-88.

Schwarb F. P., Imanidis G., Smith E. W., Haigh J. M., Surber C., (1999). Effect of concentration and degree of saturation of topical fluocinonide formulations on *in vitro* membrane transport and in vivo availability on human skin. Pharm Res, 16 909-915.

Shah V., Elkins J., (1995). *In vitro* release from corticosteroid ointments. J Pharm Sci, 84, 1139-1140.

Shah V., Elkins J., Hanus J., Noorizadeh C., Skelly J., (1991a). *In vitro* release of Hydrocortisone from topical preparations and automated procedure. Pharm Res, 8, 55-59.

Shah V., Elkins J., Schuirman D., Pelsor F., Shrivastava S., DeCamp W., Schwartz P., Williams R., (1998a). Application of *in vitro* release methods to assure product performance of semisolid dosage forms before and after certain post-approval changes. Disso Tech, 5, 5-11.

Shah V., Elkins J., Williams R., (1993). *In vitro* drug release measurement for topical glucocorticoid creams. Pharmacopeial Forum, 19, 5048-5060.

Shah V., Elkins J., Williams R., (1999). Evaluation of the test system used for *in vitro* release of drugs for topical dermatological drug products. Pharm Dev Technol, 4, 377-385.

Shah V., Flynn G. L., Guy R., Maibach H., Schaefer H., Skelly J., Wester R., Yacobi A., (1991b). Workshop report. In vivo percutaneous penetration/absorption, Washington D.C. 1989. Pharm Res, 8, 1071-1075.

Shah V. P., (2005). IV-IVC for topically applied preparations - a critical evaluation. Eur J Pharm Biopharm, 60, 309-314.

Shah V. P., Elkins J. S., Lam S. Y., Skelly J. P., (1989). Determination of *in vitro* drug release from hydrocortisone creams. Int J Pharm, 53, 53-39.

Shah V. P., Flynn G. L., Yacobi A., Maibach H. I., Bon C., Fleischer R. L., Franz T. J., Kaplan S. A., Kawamoto J., Lesko L. J., Marty J.-P., Pershing L. K., Schaefer H., Sequiera J. A., Shrivastava S., Wilkin J., Williams R. L., (1998b). AAPS/FDA workshop report:

bioequivalence of topical dermatological dosage forms - methods of evaluation of bioequivalence. Pharm Res, 15, 167-171.

Shapiro L., Cohen S., (1997). Novel alginate sponges for cell culture and transplantation. Biomaterials, 18, 583-590.

Siewert M., Dressman J., Brown C. K., Shah V. P., (2003). FIP/AAPS guidelines to dissolution/*In vitro* release testing of novel/special dosage forms. AAPS PharmSci Tech, 4, Article 7.

Skelly J. P., Shah V. P., Maibach H. I., Guy R. H., Wester R. C., Flynn G. L., Yacobi A., (1987). FDA and AAPS report of the workshop on principles and practices of *in vitro* percutaneous penetration studies - relevance to bioavailability and biocquivalence. Pharm Res, 4, 265-267.

Smidsrød O., Haug A., Larsen B., (1967). Oxidative-reductive depolymerisation: a note on the comparison of degradation rates of different polymers by viscosity measurements. Carbohydrate Res, 5, 482-485.

Smith E. W., Haigh J. M., (1992). In vitro diffusion cell design and validation II. Temperature, agitation and membrane effects on betamethasone 17-valerate permeation. Acta Pharm Nord, 4, 171-178.

Smith J. C., Irwin W. J., (2000). Ionisation and the effect of absorption enhancers on transport of salicylic acid through silastic rubber and human skin. Int J Pharm, 210, 69-82.

Snowman J. W., (1997). Freeze dryers. In: Industrial drying of foods, Bakers C. G. J. (Ed), London, Blackie Academic & Professional, 137.

Southwell D., Barry B. W., (1983). Penetration enhancers for human skin: mode of action of 2-pyrrolidone and dimethylformamide on partition and diffusion of model compounds water, n-alcohols and caffeine. J Invest Dermatol, 80, 507-514.

Southwell D., Barry B. W., Woodford R., (1984). Variation in permeability of human skin within and between specimens. Int J Pharm, 18, 299-309.

Strathmann H., Kock K., (1977). The formation mechanism of phase inversion membranes. Desalination, 21, 241-255.

Swartzendruber D., Wertz P., Kitko D., Madison K., Downing D., (1989). Molecular models of the intercellular lipid lamellae in mammalian stratum corneum. J Invest Dermatol, 92, 251-257.

The Pharmaceutical Codex (1994a). The Pharmaceutical Codex: Principles and practice of pharmaceutics. Lund W. (Ed), London, Pharmaceutical Press, 134-159.

The Pharmaceutical Codex (1994b). The Pharmaceutical Codex: Principles and practice of pharmaceutics. Lund W. (Ed), 12th ed., London, Pharmaceutical Press, 518-519.

Tojo K., Chiang C. C., Chien Y. W., (1967). Drug permeation across the skin: effect of penetrant hydrophilicity. J Pharm Sci, 76 123-126.

Tojo K., Ghannam M. M., Sun Y., Chien Y. W., (1984). In vitro apparatus for controlled release studies and intrinsic rate of permeation. J Controlled Release, 1, 197-203.

Tregear R. T., (1966). The permeability of mammalian skin to ions. J Invest Dermatol, 46, 16-23.

Twist J. N., Zatz J. L., (1986). Influence of solvents on paraben permeation through idealized skin model membranes. J Soc Cosmet Chem, 37, 429-444.

van de Sandt J., Burgsteden J. A. v., Cage S., Carmichael P. L., Dick I., Kenyon S., Korinth G., Larese F., Limasset J. C., Maas W. J., Montomoli L., Nielsen J. B., Payan J. P., Robinson E., Sartorelli P., Schaller K. H., Wilkinson S. C., Williams F. M., (2004). *In vitro* predictions of skin absorption of caffeine, testosterone, and benzoic acid: a multi-centre comparison study. Regul Toxicol Pharmacol, 39, 271-281.

Vincent C.-M., Laugel C., Marty J.-P., (1999). In vitro topical delivery of non-steroidal anti-inflammatory drugs through human skin. Arzneimittelforschung, 49, 509-513.

Walter K. A., Watkinson A., Brain K. R., (1998). In vitro skin permeation evaluation: the only realistic option. Int J Cosmet Sci, 20, 307-316.

Wang L., Shelton R. M., Cooper P. R., Lawson M., Triffitt J. T., Barralet J. E., (2003). Evaluation of sodium alginate for bone marrow cell tissue engineering. Biomaterials, 24, 3475-3481.

Watkinson A. C., Brain K. R., (2002). Mathematical principles in skin permeation. J Toxicol Cutaneous Ocul Toxicol, 21, 371-402.

Watkinson A. C., Joubin H., Green D. M., Brain K. R., Hadgraft J., (1995). The influence of vehicle on permeation from saturated solutions. Int J Pharm, 121, 27-36.

Watson D. G., (2005). High performance liquid chromatography. In: Pharmaceutical analysis: A Textbook for pharmacy students and pharmaceutical chemists, Watson D. G. (Ed), 2nd ed. ed., London, Elsevier Churchill Livingstone, 267-314.

Welin-Berger K., Neelissen J. A. M., Bergenstahl B., (2001). The effect of rheological behaviour of a topical anaesthetic formulations on the release and permeation rates of the active compound. Eur J Pharm Sci, 13, 309-318.

Wells J. I., Aulton M. E., (2000). Preformulation. In: Pharmaceutics: The science of dosage form design., Aulton M. E. (Ed), London, Churchill Livingston, 223-253.

Wester R. C., Maibach H. I., (1992). Percutaneous absorption of drugs. Clin Pharmacokinet, 23, 253-266.

Williams A. C., (2003a). Experimental design. In: Transdermal and topical drug delivery, Williams A. C. (Ed), London, Pharmaceutical Press, 51-82.

Williams A. C., (2003b). Structure and function of human skin. In: Transdermal and topical drug delivery, Williams A. C. (Ed), London, Pharmaceutical Press, 1-26.

Williams A. C., (2003c). Theoretical aspects of transdermal drug delivery. In: Transdermal and topical drug delivery, Williams A. C. (Ed), London, Pharmaceutical Press, 27-50.

Wu S. T., Shiu G. K., Simmons J. E., Bronaugh R. L., Skelly J. P., (1992). In vitro release of nitroglycerin from topical products by use of artificial membranes. J Pharm Sci, 81, 1153-1156.

Young P. E., Coquilla V., Katz M., (1968). Effect of topical vehicle composition on the in vitro release of fluocinolone acetonide and its acetate ester. J Pharm Sci, 57, 921-933.

Zatz J. L., (1995). Drug release from semisolids: Effect of membrane permeability on sensitivity to product parameters. Pharm Res, 12, 786-789.

Zorin S., Kuylenstierna F., Thulin H., (1999). *In vitro* test of Nicotine's permeability through human skin. Risk evaluation and safety aspects. Am Occup Hyg, 43, 405-413.

Conference Publications from this thesis

Ng SF, Rouse JJ, Sanderson FD, Eccleston GM. Validation of Franz cell diffusion experiments and evaluation of drug release through various cellulose membranes. J Pharm Pharmacology, S53 (2005).

Ng SF, Rouse JJ, Sanderson FD, Eccleston GM. Investigation of drug diffusion thorugh various synthetic membranes utilizing validated Franz cells. The AAPSPharmSci. 7, S2, R6078 (2005).